Energy Harvesting
for Low-Power Autonomous Devices and Systems

Downloaded From: https://www.spiedigitallibrary.org/ebooks/ on 07 Mar 2022
Terms of Use: https://www.spiedigitallibrary.org/terms-of-use

Tutorial Texts Series

- *Practical Electronics for Optical Design and Engineering*, Scott W. Teare, Vol. TT107
- *Automatic Target Recognition*, Bruce J. Schachter, Vol. TT105
- *Design Technology Co-optimization in the Era of Sub-resolution IC Scaling*, Lars W. Liebmann, Kaushik Vaidyanathan, and Lawrence Pileggi, Vol. TT104
- *Special Functions for Optical Science and Engineering*, Vasudevan Lakshminarayanan and L. Srinivasa Varadharajan, Vol. TT103
- *Discrimination of Subsurface Unexploded Ordnance*, Kevin A. O'Neill, Vol. TT102
- *Introduction to Metrology Applications in IC Manufacturing*, Bo Su, Eric Solecky, and Alok Vaid, Vol. TT101
- *Introduction to Liquid Crystals for Optical Design and Engineering*, Sergio Restaino and Scott Teare, Vol. TT100
- *Design and Implementation of Autostereoscopic Displays*, Byoungho Lee, Soon-gi Park, Keehoon Hong, and Jisoo Hong, Vol. TT99
- *Ocean Sensing and Monitoring: Optics and Other Methods*, Weilin Hou, Vol. TT98
- *Digital Converters for Image Sensors*, Kenton T. Veeder, Vol. TT97
- *Laser Beam Quality Metrics*, T. Sean Ross, Vol. TT96
- *Military Displays: Technology and Applications*, Daniel D. Desjardins, Vol. TT95
- *Interferometry for Precision Measurement*, Peter Langenbeck, Vol. TT94
- *Aberration Theory Made Simple, Second Edition*, Virendra N. Mahajan, Vol. TT93
- *Modeling the Imaging Chain of Digital Cameras*, Robert D. Fiete, Vol. TT92
- *Bioluminescence and Fluorescence for* In Vivo *Imaging*, Lubov Brovko, Vol. TT91
- *Polarization of Light with Applications in Optical Fibers*, Arun Kumar and Ajoy Ghatak, Vol. TT90
- *Digital Fourier Optics: A MATLAB Tutorial*, David G. Voeltz, Vol. TT89
- *Optical Design of Microscopes*, George Seward, Vol. TT88
- *Analysis and Evaluation of Sampled Imaging Systems*, Richard H. Vollmerhausen, Donald A. Reago, and Ronald Driggers, Vol. TT87
- *Nanotechnology: A Crash Course*, Raúl J. Martin-Palma and Akhlesh Lakhtakia, Vol. TT86
- *Direct Detection LADAR Systems*, Richard Richmond and Stephen Cain, Vol. TT85
- *Optical Design: Applying the Fundamentals*, Max J. Riedl, Vol. TT84
- *Infrared Optics and Zoom Lenses, Second Edition*, Allen Mann, Vol. TT83
- *Optical Engineering Fundamentals, Second Edition*, Bruce H. Walker, Vol. TT82
- *Fundamentals of Polarimetric Remote Sensing*, John Schott, Vol. TT81
- *The Design of Plastic Optical Systems*, Michael P. Schaub, Vol. TT80
- *Fundamentals of Photonics*, Chandra Roychoudhuri, Vol. TT79
- *Radiation Thermometry: Fundamentals and Applications in the Petrochemical Industry*, Peter Saunders, Vol. TT78
- *Matrix Methods for Optical Layout*, Gerhard Kloos, Vol. TT77
- *Fundamentals of Infrared Detector Materials*, Michael A. Kinch, Vol. TT76
- *Practical Applications of Infrared Thermal Sensing and Imaging Equipment, Third Edition*, Herbert Kaplan, Vol. TT75
- *Bioluminescence for Food and Environmental Microbiological Safety*, Lubov Brovko, Vol. TT74
- *Introduction to Image Stabilization*, Scott W. Teare and Sergio R. Restaino, Vol. TT73
- *Logic-based Nonlinear Image Processing*, Stephen Marshall, Vol. TT72
- *The Physics and Engineering of Solid State Lasers*, Yehoshua Kalisky, Vol. TT71
- *Thermal Infrared Characterization of Ground Targets and Backgrounds, Second Edition*, Pieter A. Jacobs, Vol. TT70
- *Introduction to Confocal Fluorescence Microscopy*, Michiel Müller, Vol. TT69
- *Artificial Neural Networks: An Introduction*, Kevin L. Priddy and Paul E. Keller, Vol. TT68
- *Basics of Code Division Multiple Access (CDMA)*, Raghuveer Rao and Sohail Dianat, Vol. TT67
- *Optical Imaging in Projection Microlithography*, Alfred Kwok-Kit Wong, Vol. TT66
- *Metrics for High-Quality Specular Surfaces*, Lionel R. Baker, Vol. TT65
- *Field Mathematics for Electromagnetics, Photonics, and Materials Science*, Bernard Maxum, Vol. TT64
- *High-Fidelity Medical Imaging Displays*, Aldo Badano, Michael J. Flynn, and Jerzy Kanicki, Vol. TT63

(For a complete list of Tutorial Texts, see http://spie.org/publications/books/tutorial-texts.)

Downloaded From: https://www.spiedigitallibrary.org/ebooks/ on 07 Mar 2022
Terms of Use: https://www.spiedigitallibrary.org/terms-of-use

Energy Harvesting
for Low-Power Autonomous Devices and Systems

Jahangir Rastegar

Harbans S. Dhadwal

Tutorial Texts in Optical Engineering
Volume TT108

SPIE PRESS
Bellingham, Washington USA

Downloaded From: https://www.spiedigitallibrary.org/ebooks/ on 07 Mar 2022
Terms of Use: https://www.spiedigitallibrary.org/terms-of-use

Library of Congress Cataloging-in-Publication Data

Names: Rastegar, Jahangir, author. | Dhadwal, Harbans Singh, author.
Title: Energy harvesting for low-power autonomous devices and systems / Jahangir Rastegar and Harbans S. Dhadwal.
Other titles: Tutorial texts in optical engineering ; v. TT 108.
Description: Bellingham, Washington : SPIE Press, [2016] | Series: Tutorial texts in optical engineering ; volume TT 108 | Includes bibliographical references and index.
Identifiers: LCCN 2016039269 | ISBN 9781510604902 (softcover ; alk. paper) | ISBN 1510604901 (softcover ; alk. paper) | ISBN 9781510604926 (epub) | ISBN 1510604928 (epub) | ISBN 9781510604933 (Kindle) | ISBN 1510604936 (Kindle) | ISBN 9781510604919 (pdf) | ISBN 151060491X (pdf)
Subjects: LCSH: Energy harvesting. | Energy conversion. | Transducers.
Classification: LCC TK2897 .R37 2016 | DDC 621.042–dc23 LC record available at https://lccn.loc.gov/2016039269

Published by

SPIE
P.O. Box 10
Bellingham, Washington 98227-0010 USA
Phone: +1 360.676.3290
Fax: +1 360.647.1445
Email: books@spie.org
Web: http://spie.org

Copyright © 2017 Society of Photo-Optical Instrumentation Engineers (SPIE)

All rights reserved. No part of this publication may be reproduced or distributed in any form or by any means without written permission of the publisher.

The content of this book reflects the work and thought of the authors. Every effort has been made to publish reliable and accurate information herein, but the publisher is not responsible for the validity of the information or for any outcomes resulting from reliance thereon.

Printed in the United States of America.
First Printing.
For updates to this book, visit http://spie.org and type “TT108” in the search field.

Downloaded From: https://www.spiedigitallibrary.org/ebooks/ on 07 Mar 2022
Terms of Use: https://www.spiedigitallibrary.org/terms-of-use

Introduction to the Series

Since its inception in 1989, the Tutorial Texts (TT) series has grown to cover many diverse fields of science and engineering. The initial idea for the series was to make material presented in SPIE short courses available to those who could not attend and to provide a reference text for those who could. Thus, many of the texts in this series are generated by augmenting course notes with descriptive text that further illuminates the subject. In this way, the TT becomes an excellent stand-alone reference that finds a much wider audience than only short course attendees.

Tutorial Texts have grown in popularity and in the scope of material covered since 1989. They no longer necessarily stem from short courses; rather, they are often generated independently by experts in the field. They are popular because they provide a ready reference to those wishing to learn about emerging technologies or the latest information within their field. The topics within the series have grown from the initial areas of geometrical optics, optical detectors, and image processing to include the emerging fields of nanotechnology, biomedical optics, fiber optics, and laser technologies. Authors contributing to the TT series are instructed to provide introductory material so that those new to the field may use the book as a starting point to get a basic grasp of the material. It is hoped that some readers may develop sufficient interest to take a short course by the author or pursue further research in more advanced books to delve deeper into the subject.

The books in this series are distinguished from other technical monographs and textbooks in the way in which the material is presented. In keeping with the tutorial nature of the series, there is an emphasis on the use of graphical and illustrative material to better elucidate basic and advanced concepts. There is also heavy use of tabular reference data and numerous examples to further explain the concepts presented. The publishing time for the books is kept to a minimum so that the books will be as timely and up-to-date as possible. Furthermore, these introductory books are competitively priced compared to more traditional books on the same subject.

When a proposal for a text is received, each proposal is evaluated to determine the relevance of the proposed topic. This initial reviewing process has been very helpful to authors in identifying, early in the writing process, the need for additional material or other changes in approach that would serve to strengthen the text. Once a manuscript is completed, it is peer reviewed to ensure that chapters communicate accurately the essential ingredients of the science and technologies under discussion.

It is my goal to maintain the style and quality of books in the series and to further expand the topic areas to include new emerging fields as they become of interest to our reading audience.

James A. Harrington
Rutgers University

Downloaded From: https://www.spiedigitallibrary.org/ebooks/ on 07 Mar 2022
Terms of Use: https://www.spiedigitallibrary.org/terms-of-use

Downloaded From: https://www.spiedigitallibrary.org/ebooks/ on 07 Mar 2022
Terms of Use: https://www.spiedigitallibrary.org/terms-of-use

Contents

Downloaded From: https://www.spiedigitallibrary.org/ebooks/ on 07 Mar 2022
Terms of Use: https://www.spiedigitallibrary.org/terms-of-use

Downloaded From: https://www.spiedigitallibrary.org/ebooks/ on 07 Mar 2022
Terms of Use: https://www.spiedigitallibrary.org/terms-of-use

Downloaded From: https://www.spiedigitallibrary.org/ebooks/ on 07 Mar 2022
Terms of Use: https://www.spiedigitallibrary.org/terms-of-use

Downloaded From: https://www.spiedigitallibrary.org/ebooks/ on 07 Mar 2022
Terms of Use: https://www.spiedigitallibrary.org/terms-of-use

Preface

Energy harvesting is an energy-to-energy conversion technology involving processes that generate electrical energy from other sources of energy such as mechanical, thermal, chemical, solar, and radio frequency. Use of mechanical and solar energy represents the most developed technologies and offers solutions over a broad range of energy levels. Solar cells are used to power wrist watches, calculators, and road signs, whereas mechanical-energy-harvesting solutions based on piezoelectric transducers are being used to harvest energy from sources such as vibration or shock loading. Radio-frequency-based harvesters, for example, are finding use in converting ambient electromagnetic energy to power sensor nodes. Conversion of thermal gradients to electrical energy is another promising technology.

This book is restricted to the generation of small amounts of electrical energy on a local scale and for conversion of mechanical potential and kinetic energy to electrical energy. Persons interested in learning more about the fundamental concepts of energy harvesting will find the treatment of relevant topics readable with little prerequisite requirement of engineering topics. This book will be of particular interest to application engineers from diverse disciplines and industries. It provides a fundamental view of the scope of the energy-harvesting technology as well as the trade-offs and limitations for practical systems.

The book will be of interest to those who want to know the potentials as well as shortcomings of energy-harvesting technologies. It is particularly useful for energy-harvesting system design because it provides a systematic approach to: selection of the proper transduction mechanisms, methods of interfacing with a host system, and electrical energy collection and conditioning options.

The book is divided into five chapters. Chapter 1 briefly describes the various energy-conversion processes currently being used in the generation of electrical energy from sources such as solar, radio frequency, thermoelectric, and energy from human activity.

Chapter 2 describes the three primary types of transducers typically used for converting mechanical energy to electrical energy, that is, piezoelectric, electromagnetic, and electrostatic. Magnetostrictive-based transducers are also briefly introduced.

Downloaded From: https://www.spiedigitallibrary.org/ebooks/ on 07 Mar 2022
Terms of Use: https://www.spiedigitallibrary.org/terms-of-use

Chapter 3 presents an in-depth analysis of the interfacing mechanisms used for coupling the host system to the energy harvester for effective transfer of mechanical kinetic and/or potential energy to the transducer.

Chapter 4 addresses collection and conditioning circuits needed to extract the generated electrical energy for delivery to a load. The theme of chapters 2, 3, and 4 shows the connection between the three components of an energy-harvesting system, namely, the host interfacing mechanism, the transducer, and the collection and conditioning circuit.

In addition to the design of efficient energy harvesters, this book also discusses how certain types of energy harvesters can be configured to provide self-powered sensing capabilities. Additional circuitry not requiring any external power may also provide further enhancement by including logic functionality. Case studies with particular emphasis on shock-loading-based energy harvesting and sensory applications are presented in Chapter 5.

An extensive list of references is provided to direct the reader to appropriate literature for more in-depth material not covered in the book.

We thank James Harrington, SPIE *Tutorial Text* Series Editor, for encouraging us to write the book and Tim Lamkins, SPIE Press Manager, for his editorial suggestions and support. We very much appreciate the effort, patience, and guidance provided by Nicole Harris, our editor at SPIE.

Jahangir Rastegar
Harbans S. Dhadwal
New York
December 2016

Downloaded From: https://www.spiedigitallibrary.org/ebooks/ on 07 Mar 2022
Terms of Use: https://www.spiedigitallibrary.org/terms-of-use

Chapter 1
Energy Harvesting

1.1 Introduction

The generation of electrical energy involves an energy-to-energy conversion process such as mechanical-to-electrical (ME), chemical-to-electrical (CE), solar-to-electrical (SE), radio frequency-to-electrical (RFE), and thermal-to-electrical (TE). ME conversion is used in hydroelectric and wind turbines for large-scale generation to meet the demands of cities. CE conversion is used in batteries to provide portable electrical energy. TE conversion is a technology under development. SE conversion uses solar energy to generate electrical energy. Solar farms provide electrical generation on a large industrial scale as well as for individual home owners. RFE converts electromagnetic energy in the millimeter (mm)-to-micron-wavelength range of the electromagnetic spectrum to electrical energy.

Currently, energy harvesting refers to the nonchemical generation of small amounts of electrical energy on a local scale using one of the above energy conversion principles. Among the above energy conversion processes for electrical energy harvesting, even under very low light levels, SE conversion has generally been found to be the best choice and is widely used in consumer goods and many other products. For example, SE conversion is used to power wrist watches, calculators, road signs, and in practically any other application where solar illumination is available and its space and power requirements can be met. The energy output of SE-based energy harvesters is limited by the size of the solar cell. However, in many energy-harvesting applications, a few microwatts of power may suffice and can be obtained. For 24/7 operation, storage devices such as rechargeable batteries and super-capacitors have been used.

It is, however, important to note that in many applications, the use of SE conversion is not practical, such as in enclosed environments where enough light is never available. The use of SE conversion may also be impractical due to the required size of the solar collector and its collection and storage components. Examples of such cases include self-powered and networked sensors used on machinery to monitor vibration and health in industrial plants; sensors for use inside an enclosed space such as in vehicle tires or inside a

Downloaded From: https://www.spiedigitallibrary.org/ebooks/ on 07 Mar 2022
Terms of Use: https://www.spiedigitallibrary.org/terms-of-use

machine body; or self-powering of encapsulated microelectromechanical systems (MEMS)-type sensors of various types. In many applications, the energy that has been made available for harvesting is in the form of mechanical kinetic and/or potential energy, or even impulsive loading of some form.

As a result, in many applications, energy harvesters based on converting kinetic and/or potential energy to electrical energy become the only viable option. Certain ME-based energy-harvesting devices, such as those employing piezoelectric transducers, also have the unique capability of being used as sensors, for example, for detecting and measuring acceleration or force generated due to a specific emergency event.

Today, energy harvesters may be designed to provide perpetual power for autonomous wireless sensor nodes, or pulse power for short-lived one-time use, as in initiation or emergency systems. Design of energy harvesters is determined by both the local energy source (host system) and by the interfacing mechanism, particularly for motion-based energy-harvesting systems. Available sources of energy for harvesters can be grouped into either ambient or man-made. The former category includes natural sources such as solar radiation, thermal gradients, wind, and ocean waves. Man-made sources may arise as by-products of various activities and processes, for example, background energy from radio-frequency signals generated primarily for use in telecommunication systems, or vibrational energy resulting from vehicles or large industrial systems, such as production machinery.

The choice of a particular energy source is determined by the operational environment, available energy density, and the required energy level to power the intended device. Figure 1.1 shows some of the popular energy sources and the corresponding energy density. It should be noted that, while the solar

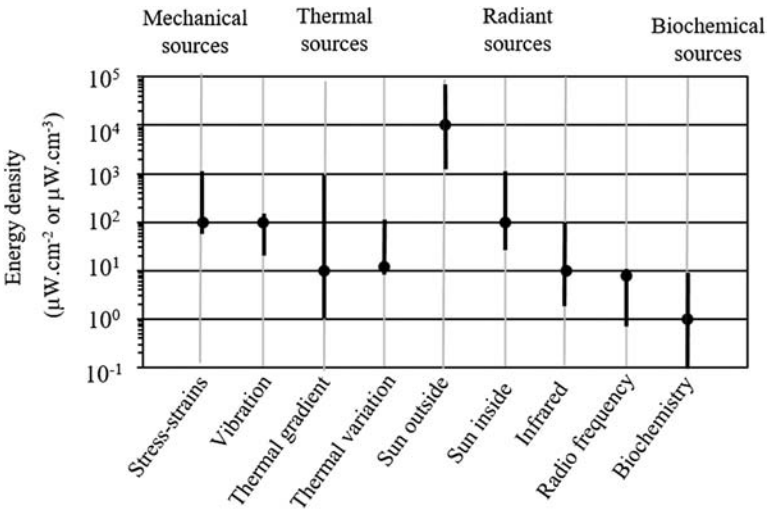

Figure 1.1 Energy densities of typical ambient energy sources.[1]

Downloaded From: https://www.spiedigitallibrary.org/ebooks/ on 07 Mar 2022
Terms of Use: https://www.spiedigitallibrary.org/terms-of-use

luminance has the highest available power density, it cannot be changed, and its availability is not always guaranteed.

The primary focus of this book is on harnessing mechanical potential and/or kinetic energy. Other sources of energy are also available, such as thermal gradient and radiated electromagnetic energy. The latter sources of energy are briefly described below. A brief description of the application of energy harvesting for self-powering implantable devices and sensors in the human body is also provided. The reader is referred to available literature for an in-depth treatment of the subject and for other sources of available energy for harvesting.

1.2 Thermal-to-Electrical-based Energy Harvesting

The thermoelectric effect[2] is used to convert temperature difference into voltage. An implementation of the effect in a loop constructed of two dissimilar conductors generates an electromotive force V_{emf} when a constant temperature gradient exists between the two common points. The generated voltage is given by

$$V_{emf} = (\alpha_1 - \alpha_2)\Delta T, \tag{1.1}$$

where α_1 and α_2 are the Seebeck coefficients for the two dissimilar conductors. The value of α may range from –100 μV/K to 1000 μV/K for common conductors.[3] Very large temperature differences are needed to produce useful operating voltages compatible with electronic integrated circuits. In order to make a useful generator, conductors are typically replaced by n- and p-type semiconductors, as illustrated in Fig. 1.2. This configuration allows heat transfer in the same direction, while the voltage difference across the n- and p-type materials is additive.

The power output of an n-p-based thermoelectric generator is proportional to the square of the temperature difference between the hot and cold surfaces and is proportional to the physical cross-sectional area of the n-p legs. For example, the generated power density at a temperature difference of 200 °C is on the order of 100 mW/cm^2.[5]

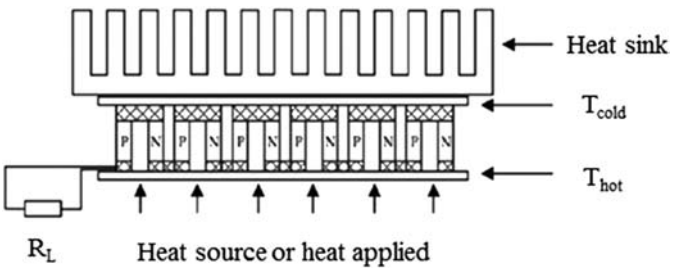

Figure 1.2 Thermoelectric-generating cell n- and p-type semiconductors.[4]

Downloaded From: https://www.spiedigitallibrary.org/ebooks/ on 07 Mar 2022
Terms of Use: https://www.spiedigitallibrary.org/terms-of-use

1.3 Solar-to-Electrical-based Energy Harvesting

The most dominant source of radiated electromagnetic energy is solar energy, which illuminates the surface of the earth at a nominal value of 1 $kW \cdot m^{-2}$. Solar energy may be harvested indoors and outdoors using photovoltaic devices. This makes solar energy the first choice for harvesting, as long as it satisfies the constraints of the devices or systems to be powered. For example, the device to be powered may not have direct solar radiation or may require uninterrupted power during daytime as well as during the night without the use of a storage device due to size or weight limitations.

Photovoltaics technology primarily targets the visible-to-near infrared part of the electromagnetic spectrum. The transducers, commonly referred to as photovoltaics or photocells, are quantum devices that directly generate electron–hole pairs from the absorption of incident photons within the depletion region of a p-n junction device. These devices are generally modeled as a current source shunted by an ideal p-n junction diode. For indoor applications, electrical energy generated will also depend on the spatial characteristics of the light source as well as the distance of the transducer from the source. For example, a 100-W incandescent bulb is expected to generate a few microwatts at the output of a 2-mm diameter photovoltaic cell placed at a distance of 2 m.

1.4 Radio-Frequency-to-Electrical-based Energy Harvesting

RFE technology harvests electromagnetic energy in the radio-frequency band from megahertz to microwave. RFE devices typically have a tuned receiving antenna for converting the received RF energy into electrical energy. The power generated by RFE harvesters is extremely low unless the receiver is in close proximity to the source and/or the receiver is very large. Some of these energy-harvesting devices use the ambient electromagnetic energy emitted by nearby sources and are finding use in autonomous sensor nodes. However, these types of harvesters cannot be placed inside conductive enclosures.

Directed radiofrequency emissions have also been used for collection by matched receiving antennas (the so-called rectenna).[6] For example, active and passive radio-frequency identification (RFID) systems use such technologies.[7]

1.5 Sources of Energy from Human Activity

Due to the recent proliferation of wearable health monitoring devices and portable electronics, considerable effort is being devoted to harnessing power from voluntary and involuntary human activities, for example, from the pulsating motion of the heart.[8,9] Table 1.1[10] compares nominal values of power available from human activity and the corresponding power needs of some typical applications. In addition to harnessing energy from human locomotion,

Downloaded From: https://www.spiedigitallibrary.org/ebooks/ on 07 Mar 2022
Terms of Use: https://www.spiedigitallibrary.org/terms-of-use

Table 1.1 Energy output from human locomotion[10]

Human Activity	Power (W)	Application	Power (W)	Possible human activity
Pushing a button	0.3	TV remote	0.1	Finger movement
Shaking	0.4	Portable radio	0.72	Finger movement/Hand crank
Squeezing a handle	3.6	Mp3 player	0.16	Hand crank
Twisting	12.6	Cell phone	2	Hand crank
Bending	20	Laptop	2	Hand crank
Pushing	20	Flash light	4	Hand crank
Turning a handle	21	Video & camcorder	6	Hand crank
Pulling	23	Notebook	10	Hand crank
Swinging	25	Television	75	Pedaling

devices to convert body heat to electrical energy through thermoelectric conversion and flexible piezoelectric materials embedded into fabrics may soon be coming to the market.

In addition to harnessing energy from human activity, there is considerable interest in attaching self-powered health-monitoring sensors directly to organs, such as the heart. The sensors may also assist the organ's function by providing electrical stimulus, as is the case with heart pacemakers. Figure 1.3 shows an example of an autonomous device mounted on a bovine heart. This heart-assist device uses a flexible piezoelectric energy harvester.[11,12]

On another note, the hidden cost of attaching an energy-harvesting device to a system such as the heart, which is optimized for a particular function, should not be underestimated or overlooked. For instance, the heart, which is a pulsating oscillator with a life cycle of over 5 billion beats has taken nature over 65 million years to perfect. It pumps blood through a circulatory system

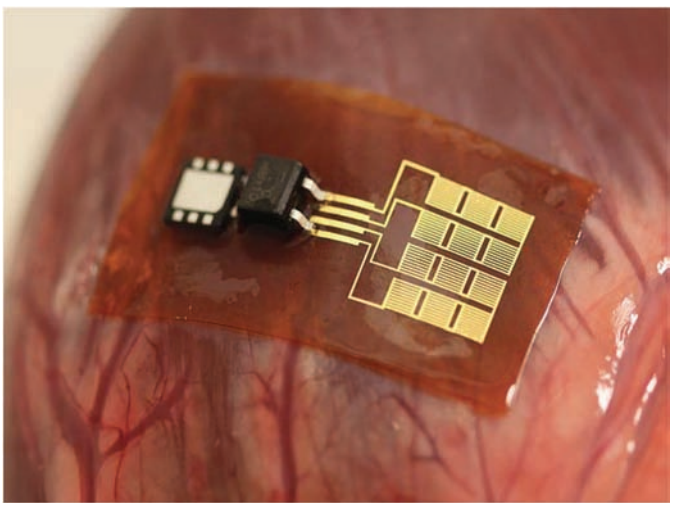

Figure 1.3 A piezoelectric energy harvester, with rectifier and microbattery, mounted on a bovine heart. (Reprinted with permission from Ref. 12.)

Downloaded From: https://www.spiedigitallibrary.org/ebooks/ on 07 Mar 2022
Terms of Use: https://www.spiedigitallibrary.org/terms-of-use

of vessels to deliver oxygen and nutrients to individual cells and removes metabolic waste.[13] Attaching an external device, no matter how small, may produce a reactive chain of events from the cardiovascular system. The long-term effects of loading the cardiovascular system are difficult to predict and will require the accumulation of clinical data over many years.

1.6 Mechanical-to-Electrical-based Energy Harvesting

This book focuses on the design of energy harvesters intended for converting mechanical kinetic and/or potential energy from a host system to electrical energy for direct consumption or storage for later use. The process of converting mechanical energy to electrical energy may be described in three distinct phases, as shown in Fig. 1.4. In the first phase, an interfacing mechanism properly transfers the mechanical energy to the transducer. In the second phase, the transducer generates electrical energy. In the third phase, the generated electrical energy is collected and conditioned to be either stored in an energy storage device such as a rechargeable battery or a capacitor or to be delivered directly to the intended electrical energy consuming device (load).

The remainder of this book is divided into four chapters. Chapter 2 describes the three primary types of transducers typically used for converting mechanical energy to electrical energy, that is, piezoelectric, electromagnetic, and electrostatic transducers. Magnetostrictive-based transducers are also briefly introduced. Chapter 3 presents an in-depth analysis of the interfacing mechanisms used for coupling mechanical kinetic and/or potential energy to the transducer for effective energy transfer. Chapter 4 addresses coupling and conditioning circuits needed to extract the generated electrical energy for delivery to the load. The theme of these chapters shows the connection between the three components of an energy-harvesting system, namely, the

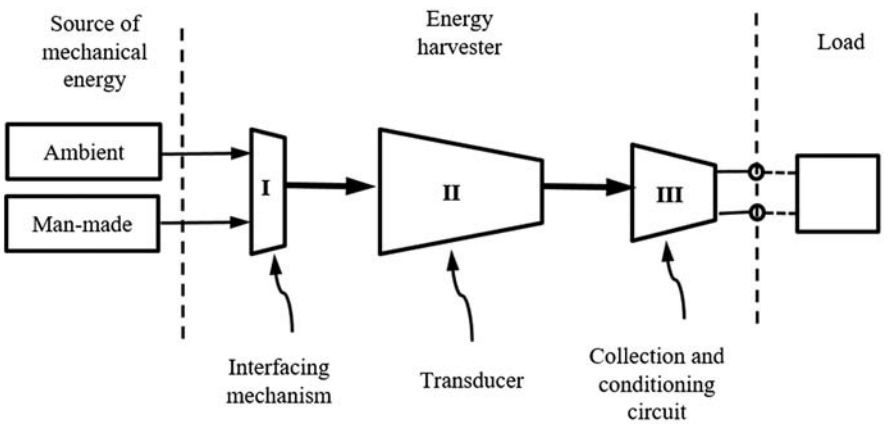

Figure 1.4 The process of harvesting electrical energy from a host system.

Downloaded From: https://www.spiedigitallibrary.org/ebooks/ on 07 Mar 2022
Terms of Use: https://www.spiedigitallibrary.org/terms-of-use

interfacing mechanism, the transducer, and the collection and conditioning circuit. Chapter 5 presents case studies of some available energy harvesting system solutions.

References

1. S. Boisseau, G. Despesse, and B. A. Seddik, "Electrostatic conversion for vibration energy harvesting," InTech Open Access Publisher, Rijeka, Croatia (2012).
2. D. M. Rowe, *Thermoelectrics Handbook: Macro and Nano*, CRC Press, Boca Raton, Florida (2010).
3. https://en.wikipedia.org/wiki/Seebeck_coefficient (accessed on November 1, 2015).
4. C. A. Gould and N. Shammas, "A review of thermoelectric MEMS devices for micropower generation, Micro Electronic and Mechanical Systems," InTech Open Access Publisher, Rijeka, Croatia, pp. 15–24 (2009).
5. P. Dziurdzia, "Modelling and simulation of thermoelectric energy harvesting processes," InTech Open Access Publisher, Rijeka, Croatia (2011).
6. G. Abadal, J. Alda, and J. Agusti, "Electromagnetic radiation energy harvesting—The rectenna based approach," InTech Open Access Publisher, Rijeka, Croatia (2014).
7. P. V. Nikitin, S. Ramamurthy, and R. Martinez, "Simple low cost UHF RFID reader," *IEEE International Conference on RFID*, pp. 126–127 (2013).
8. A. Cadei, A. Dionisi, E. Sardini, and M. Serpelloni, "Kinetic and thermal energy harvesters for implantable medical devices and biomedical autonomous sensors," *Measurement Science and Technology* **25**, 1–14 (2014).
9. P. D. Mitcheson, E. M. Yeatman, G. K. Rao, A. S. Holmes, and T. C. Green, "Energy harvesting from human and machine for wireless electronic devices," *Proc. IEEE* **96**(9), 14577–1486 (2008).
10. S. O. Ani, D. Bang, H. Polinder, J. Y. Lee, S. R. Moon, and D. H. Koo, "Human powered axial flux permanent magnet machines: review and comparison," *IEEE Energy Conversion and Exposition*, 4165–4170 (2010).
11. C. Dagdeviren, B. Yang, Y. Su, P. Tran, P. Joe, E. Anderson, J. Xia, V. Doraiswamy, B. Dehdashti, X. Feng, B. Lu, R. Poston, Z. Khalpey, R. Ghaffari, Y. Huang, M. Slepian, and J. Rogers, "Conformal piezoelectric energy harvesting and storage from motions of the heart, lung, and diaphragm," *Proc. of the National Academy of Sciences* **111**(5), 1927–1932 (2014).
12. A. Poor, "Reaping the energy harvest [resources]," *IEEE Spectrum*, **52**(4), 23–24 (2015).
13. http://www.cancerindex.org/medterm/medtm8.htm (last accessed Nov 7, 2015).

Downloaded From: https://www.spiedigitallibrary.org/ebooks/ on 07 Mar 2022
Terms of Use: https://www.spiedigitallibrary.org/terms-of-use

Downloaded From: https://www.spiedigitallibrary.org/ebooks/ on 07 Mar 2022
Terms of Use: https://www.spiedigitallibrary.org/terms-of-use

Chapter 2
Mechanical-to-Electrical Energy Conversion Transducers

2.1 Introduction

The process of harvesting mechanical energy from the environment and converting it to usable electrical energy can be illustrated as shown in the block diagram of Fig. 2.1. The input mechanical energy to be converted to electrical energy may be in the form of potential energy and/or kinetic energy. The mechanical system providing the mechanical energy for harvesting is hereinafter referred to as the "host system." The host system may be capable of providing mechanical energy in a number of ways, for example, through linear or rotatory vibration of its structure; through a rocking motion such as experienced in a boat, ship, or buoy; through random relative motion between relatively rigid machine components, such as the motion between different links of a car suspension system; or through shock loading experienced by a weapon platform during firing or target impact.

In many cases, and depending on the mechanical-to-electrical energy transducer (electrical generator) being employed, an interfacing mechanism is needed for effective transfer of mechanical energy to the energy-harvesting device. Such interfacing mechanisms may, for example, be needed to amplify force or motion, vary the input force or motion frequency, convert a shock loading impulse to oscillatory or vibratory motion, etc. The interfacing mechanism may perform more than one function depending on the application, the host system, and the transducer characteristics. For example, in many cases, the interfacing mechanism is desired to maximize the rate or amount of mechanical energy transferred to the transducer. In other cases, this mechanism is used to "condition" the available mechanical energy to make the energy transfer possible while protecting the transducer and/or the host system. An interfacing mechanism may connect the structure or a component of the host system directly to the energy-conversion transducer or indirectly via certain intermediate elements such as vibrating structures or magnetic coupling elements.

Downloaded From: https://www.spiedigitallibrary.org/ebooks/ on 07 Mar 2022
Terms of Use: https://www.spiedigitallibrary.org/terms-of-use

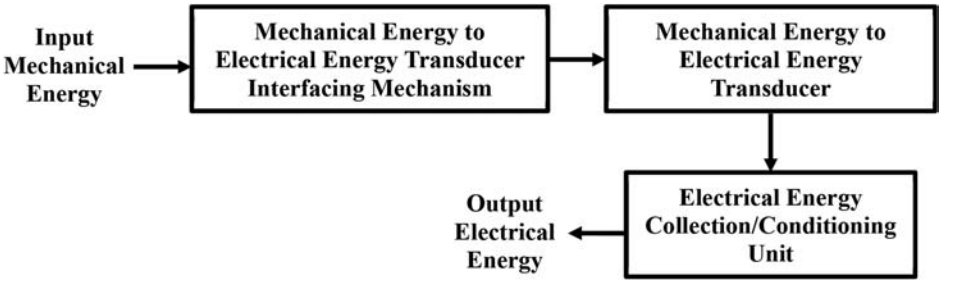

Figure 2.1 General process of electrical energy harvesting from mechanical energy.

It is therefore crucial that the energy-harvester designer be very familiar with various available transducers and their physical and mechanical-to-electrical conversion characteristics and limitations. In addition, the designer needs to understand the delicate balance between the host system and the harvesting device; the latter should not compromise the operation of the former.

The objective of the material provided in this chapter is to introduce the most currently available transducers for mechanical-to-electrical energy conversion, namely, those based on piezoelectric, electromagnetic, and electrostatic phenomena. A comprehensive list of references is provided for more-in-depth reading. Other less commonly used transducer types are also introduced. The list of transducer types and designs is by no means exhaustive, and many other special-purpose and hybrid designs have been developed or studied. It is appreciated that new transducer types and designs with different physical and performance characteristics are continuously being developed. A comparison table is provided for use as a qualitative and quick reference tool to guide the process of selecting the most suitable transducer for a particular energy-harvesting device type and application.

2.2 Piezoelectric Transducers

Piezoelectric transducers produce an electrical charge upon application of strain. This phenomenon is called the direct piezoelectric effect.[1] This effect is used in piezoelectric-based energy-harvesting devices to convert mechanical energy to electrical energy. This phenomenon was first observed by the Curie brothers in 1880,[2] and the word "piezoelectricity" was first used by Hankel[3] in 1881.[4] Early studies of the fundamentals of piezoelectricity include those provided in Refs. 5–10.

Inversely, the application of an electric field to a properly poled piezoelectric element (e.g., voltage to a piezoelectric stack) causes the piezoelectric element to deform. This phenomenon is called the inverse piezoelectric effect and is used to develop actuation devices with which electrical energy can be converted to mechanical energy.

Downloaded From: https://www.spiedigitallibrary.org/ebooks/ on 07 Mar 2022
Terms of Use: https://www.spiedigitallibrary.org/terms-of-use

When a properly poled piezoelectric element is deformed by the application of an external force, the mechanical work done by the external force is stored in the piezoelectric element as mechanical potential energy due to its elastic deformation and electrical potential energy resulting from the repelling charges of material dipoles. It is also appreciated that out of the total work done by the external force, only the portion converted to electrical potential energy is available for harvesting. During the piezoelectric element deformation, if mechanical and/or electrical losses and dynamic and nonlinearity effects are not negligible, they must also be accounted for.

The piezoelectric effect is induced in materials such as single crystals, ceramics, polymers, composites, thin films, and relaxor-type ferroelectric materials,[11] of which piezoelectric ceramics are used most in energy-harvesting devices followed by piezoelectric polymers. For this reason, the emphasis in this section is placed on piezoelectric ceramics as far as their use as transducers in energy-harvesting devices is concerned. Piezoelectric and other relevant physical characteristics of other types of piezoelectric materials are also provided. The provided information enables designers of energy-harvesting devices with the selection of proper piezoelectric types and geometries to match their specific application. An extensive list of references guides the reader for in-depth treatment of particular topics.

2.2.1 Polycrystalline piezoelectric ceramics

Piezoelectric material produces electric charges when subjected to mechanical strain. This phenomenon is due to their crystal structure, which has no center of symmetry. These crystal structures have a charge balance with separated positive and negative charges along the so-called polar axis and therefore form a dipole.[1,12–17] The polar axis is an imaginary line that runs through the center of both charges.

In a monocrystal, the polar axes of all of the dipoles lie in one direction. Polycrystals are collections of randomly oriented monocrystals that result in different regions within the material having different polar axes as shown schematically in Fig. 2.2.

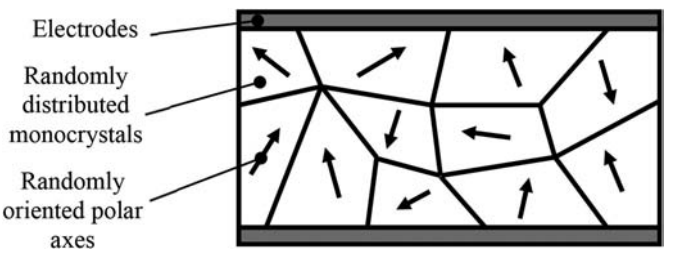

Figure 2.2 Schematic of randomly distributed and oriented monocrystals in a polycrystalline element.

Downloaded From: https://www.spiedigitallibrary.org/ebooks/ on 07 Mar 2022
Terms of Use: https://www.spiedigitallibrary.org/terms-of-use

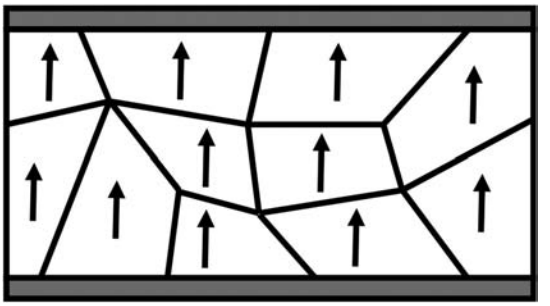

Figure 2.3 Schematic of the polarized polycrystalline element.

To produce a transducer or actuator from a polycrystalline ferroelectric ceramic, such as lead zirconate titanate (PZT), a strong electric field on the order of several kV/mm is applied to the polycrystalline element electrodes (Fig. 2.2). The electric field causes the randomly oriented polar axes to reorient the dipoles in the polycrystalline element to line up and face nearly in the same direction (Fig. 2.3).[13,17,18] During this process, the domain walls are forced to shift to allow the reorientation. When possible, the polycrystalline element is heated in an electrically nonconductive fluid such as a certain oil to assist the process. After polarization, most of the reorientations are preserved, but some polar axes shift back towards their original orientation.[18]

Once a polycrystalline element is polarized (Fig. 2.3), a change in the charge balance due to deformation as a result of an externally applied force would cause electrical energy to be transferred by electric charge carriers creating a current from one conductor to the other. Conversely, an external charge input will create an unbalance in the neutral charge state, causing mechanical stress in the polycrystalline element.[13]

The piezoelectric effect is present in natural monocrystalline materials such as quartz, tourmaline, and Rochelle salt. The piezoelectric effects of these crystals are relatively small. Polycrystalline ferroelectric ceramics such as barium titanate ($BaTiO_3$) and PZT exhibit larger strain with the application of electric field and generate higher amounts of electrical charges with the application of strain. PZT piezoceramic materials are available in many variations and are most widely used as mechanical-to-electrical energy transducers.[11,13,19–22] Special doping of PZT ceramics with, e.g., Ni, Bi, La, Nd, or Nb ions make it possible to specifically optimize their piezoelectric and dielectric parameters.[18] For example, doping of elements like Nb^{5+} or Ta^{5+} (donor) results in "soft" PZTs, for example PZT-5.[22]

PZT ceramics are commonly divided into "soft" and "hard" groups, which refers to the mobility of their dipoles and polarization and depolarization behavior.[18] Soft PZT materials have the advantage of high charge coefficient and are therefore more suitable for most actuator applications. Hard PZT materials are more stable and exhibit low dielectric and mechanical losses and

Downloaded From: https://www.spiedigitallibrary.org/ebooks/ on 07 Mar 2022
Terms of Use: https://www.spiedigitallibrary.org/terms-of-use

are therefore more suitable for continuous energy harvesting from relatively high-frequency vibration or high-frequency actuation applications.

The PZT piezoceramics are currently used primarily in actuation, energy-harvesting transducer, and sensor applications.[23,24] They can be manufactured in many geometries and with varying physical characteristics to suit the application. Characteristics of various PZT piezoceramic materials and their properties have been widely studied and reported.[18,19,25–35] In this section, the linear theory of piezoelectricity as described in ANSI/IEEE Std 176-1987, "IEEE Standard on Piezoelectricity,"[36] is used to derive a simplified mathematical model of a piezoelectric element that is subjected to an externally applied load in the direction parallel to its poling direction. The terminologies used are also from this source. In linear piezoelectricity, the equations describing elasticity are coupled to the charge equation of electrostatics by means of the piezoelectric constants.[36]

The orthogonal coordinate system used to describe the properties of a polarized piezoelectric ceramic is shown in Fig. 2.4. In this system, axis 3 is parallel to the direction of polarization. The directions 1 and 2 are physically similar and are selected arbitrarily. The axes termed 4, 5, and 6 correspond to tilting (shear) motions about axes 1, 2, and 3, respectively.

The different forms of the standard constitutive equations of piezoelectric materials under different electrical and mechanical conditions are given in the "IEEE Standard on Piezoelectricity."[36] It is noted that in these relationships, the coupling to the equations representing the dynamics of the mechanical system is not considered. Considering the present case of interest in which the piezoelectric element of Fig. 2.4 is subjected to an externally applied force F_a parallel to its poling direction as shown in Fig. 2.5, the constitutive equations can be written in the following simplified scalar form:

$$S = s^E T + d E, \tag{2.1}$$

$$D = d T + \varepsilon^T E, \tag{2.2}$$

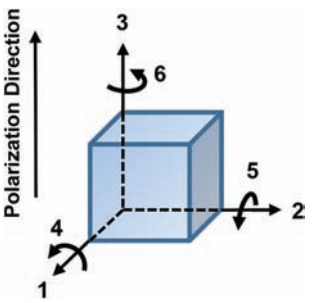

Figure 2.4 The coordinate system used to describe the properties of a polarized piezoelectric ceramic.

Downloaded From: https://www.spiedigitallibrary.org/ebooks/ on 07 Mar 2022
Terms of Use: https://www.spiedigitallibrary.org/terms-of-use

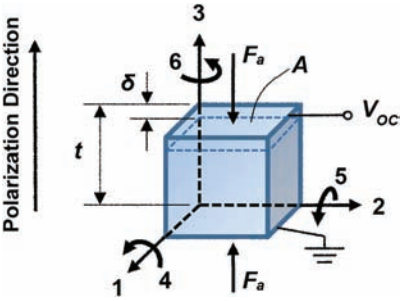

Figure 2.5 A piezoelectric element subjected to an externally applied force F_a parallel to its poling direction.

where $S = \delta/t$ is strain; s^E is a compliance coefficient at a constant electric field (m^2/N); $T = F_a/A$ is stress (N/m^2); d is the piezoelectric constant (m/V or C/N); E is electric field component (V/m); D is the electric displacement (flux density) component (C/m^2); and ε^T is dielectric permittivity at constant deformation (F/m). The top and bottom surfaces of the piezoelectric element of Fig. 2.5 are considered to be covered by charge-collecting electrodes. The open-circuit voltage V_{OC} is generated between the two electrodes. Figure 2.5 indicates a 33 mode of charge generation in which the first numeral (first index in the matrix form of the constitutive equations)[36] indicates the direction of the electric field along which the charges are to be produced for the case of a transducer or applied voltage for the case of an actuator. The second numeral (second index in the constitutive equation matrix) indicates the direction of the applied mechanical stress or strain. For example, if in Fig. 2.5 the applied force were in the direction of axis 1, the transducer would be said to be operating in a 31 mode.

By setting the electrical displacement D in Eq. (2.2) to zero, the open-circuit voltage V_{OC} is found to be

$$V_{OC} = E\,t = -(d\,T/\varepsilon^T)t = -(d\,F_a\,t)/(\varepsilon^T A). \tag{2.3}$$

The equivalent parallel plate capacitance of the piezoelectric element is given as

$$C_p = (\varepsilon^T A)/t. \tag{2.4}$$

The total work done by the applied force F_a on the piezoelectric element of Fig. 2.5 is

$$W = \tfrac{1}{2}F_a\,\delta = \tfrac{1}{2}(A/s^D\,t)\delta^2, \tag{2.5}$$

where s^D is the compliance coefficient of the piezoelectric material at constant electric displacement (m^2/N). Neglecting all mechanical and electrical losses,

Downloaded From: https://www.spiedigitallibrary.org/ebooks/ on 07 Mar 2022
Terms of Use: https://www.spiedigitallibrary.org/terms-of-use

the mechanical potential energy portion E_M of the total work (input energy) W, Eq. (2.5), can be seen to be

$$E_M = \tfrac{1}{2}(A/s^E\ t)\delta^2, \tag{2.6}$$

where $(A/s^E\ t)$ is the stiffness of the piezoelectric element of Fig. 2.5 in the direction of axis 3 at a constant electric field. The potential electrical energy portion E_E of the total input energy W is then seen to be

$$E_E = W - E_M = \tfrac{1}{2}(A/s^D\ t)\delta^2 - \tfrac{1}{2}(A/s^E\ t)\delta^2 = \tfrac{1}{2}A/t[1/s^D - 1/s^E]\delta^2. \tag{2.7}$$

The following relationships can also be shown to exist between the piezoelectric material compliance coefficients and certain piezoelectric and dielectric permittivity constants:

$$s^D = s^E - d\,g, \tag{2.8}$$

$$d = \varepsilon^T g, \tag{2.9}$$

$$\varepsilon^S/\varepsilon^T = s^D/s^E, \tag{2.10}$$

where ε^S is the dielectric permittivity at constant deformation (F/m), and g is the piezoelectric constant (m^2/C).

In the piezoelectric material, the relationship between mechanical stress and strain is given as

$$\delta/t = s^D(F_a/A). \tag{2.11}$$

The potential electrical energy portion E_E [Eq. (2.7)] can then be written as

$$\begin{aligned}
E_E &= \frac{A}{2t}\left(\frac{1}{s^D} - \frac{1}{s^E}\right)\left(s^D\, t\frac{F_a}{A}\right)^2 \\
&= \frac{A}{2t}\frac{(s^E - s^D)}{s^E\, s^D}(s^D)^2\left(\frac{F_a t}{A}\right)^2 \\
&= \frac{A}{2t}\, d\, g\, \frac{s^D}{s^E}\left(\frac{F_a t}{A}\right)^2 \\
&= \frac{A}{2t}\, d\, g\, \frac{\epsilon^S}{\epsilon^T}\left(\frac{F_a t}{A}\right)^2 \\
&= \frac{A}{2t}\epsilon^S\, \frac{d^2}{(\epsilon^T)^2}\left(\frac{F_a t}{A}\right)^2 \\
&= \frac{1}{2}\, \frac{\epsilon^S A}{t}\, \left(\frac{dF_a t}{\epsilon^T A}\right)^2.
\end{aligned} \tag{2.12}$$

Downloaded From: https://www.spiedigitallibrary.org/ebooks/ on 07 Mar 2022
Terms of Use: https://www.spiedigitallibrary.org/terms-of-use

Substituting Eqs. (2.3) and (2.4) into Eq. (2.12), the electrical potential energy portion E_E of the total input energy W is seen to be given by the expected expression for a parallel-plate capacitor:

$$E_E = \frac{1}{2} C_p V_{OC}^2. \tag{2.13}$$

Therefore, it is shown that neglecting all mechanical and electrical energy losses, the work done W [Eq. (2.5)] by the applied force F_a on the piezoelectric element of Fig. 2.5, i.e., the input mechanical energy into the piezoelectric transducer of Fig. 2.5, is divided into two distinct components. One component E_M [Eq. (2.6)] is stored in the piezoelectric element as mechanical potential energy, and the other component E_E [Eq. (2.13)] is stored in the piezoelectric element as electrical potential energy. At any given moment, an energy-harvesting device has only the latter component of the energy available for harvesting. The relative magnitudes of the two components of the stored potential energy are dependent on the relative magnitude of the compliance coefficients of the piezoelectric material at constant electric displacement s^D and at constant electric field s^E. By dividing Eqs. (2.6) and (2.7) by Eq. (2.5), the mechanical potential energy and the electrical potential energy components, E_M and E_E, respectively, of the total mechanical energy input W are derived in terms of the above compliance coefficients as

$$E_M = \frac{s^D}{s^E} W, \tag{2.14}$$

$$E_E = \left(1 - \frac{s^D}{s^E}\right) W. \tag{2.15}$$

It is noted that, to date, most piezoelectric-transducer-based energy-harvesting devices have been designed to operate as vibrating beams, and many as cantilever beam structures with base-induced vibration excitation. As a result, most piezoelectric transducer modeling efforts have concentrated on their behavior, including in Refs. 15 and 37–42. A review of many of these modeling efforts and further analysis of such piezoelectric-based energy-harvesting devices are provided in Ref. 23. Modeling efforts include those that use lumped parameters.[40,43–45] Beam-vibration-mode models together with piezoelectric constitutive equations have also been used to predict the amount of electrical energy that can be generated in vibration.[37,39,46,47] Distributed parameter and finite element models have also been used for design, geometric optimization, and analysis of performance of such energy harvesting devices.[48–54] Effects of piezoelectric nonlinearity in actuation and energy-harvesting devices have also been studied.[55–58]

Downloaded From: https://www.spiedigitallibrary.org/ebooks/ on 07 Mar 2022
Terms of Use: https://www.spiedigitallibrary.org/terms-of-use

2.2.2 Piezoelectric polymers and polymer–ceramic composites

Piezoelectric ceramics such as PZT are mostly hard and brittle. In many applications it is highly desirable to have flexible transducers for developing flexible energy harvesting devices that can undergo large deformations and stretching. Piezoelectric polymers have been developed to serve this need. The most commonly used piezoelectric polymer in such applications is polyvinylidence fluoride (PVDF). Published reports related to piezoelectric polymer material development and their electrical and mechanical properties for use as a mechanical energy to electrical energy transducer as well as for actuation and sensing include Refs. 25, 59–71.

Improvement in the performance of polymer-based flexible piezoelectric elements has also been reported through the development of piezoelectric polymer and ceramic composites.[60,65,72–74] Many other composite structures such as fibrous composites have either been developed or proposed.[11,76,77] Such composites are designed to enhance various mechanical properties of the elements and address issues such as toughness of piezoelectric ceramic transducers and actuators.

2.2.3 Single-crystal piezoelectric ceramics

Relaxor-based single crystals such as PZNT and PMNT are single-crystal ferroelectrics that exhibit high piezoelectric effect when poled. The piezoelectric properties of PMN-PT and PZN-PT single crystals poled along different crystallographic directions were reported in the late 1990s and early 2000s,[78] showing piezoelectric coefficients and electromechanical coupling factors that are significantly higher than those of PZT ceramics.[22,23,79–90] A large amount of published literature is currently available reporting studies of relaxor-based single crystals addressing issues such as their manufacture and poling, dielectric and piezoelectric properties, effects of temperature and electric field, and current and potential future applications and outlook.[79–107]

Performance of currently available single-crystal piezoelectric and polycrystalline piezoelectric ceramics, mainly various PZT ceramics, has been compared for different applications in several studies, such as those reported in Refs. 23, and 108–111. For example, different configurations of piezoelectric single-crystal PMN-PZT, polycrystalline PZT-5A, and PZT-5H ceramics were studied in unimorph cantilevered beams to determine the best design for lightweight energy harvesting.[112] The study concluded that single-crystal-based harvesters produced higher levels of electrical power than polycrystalline devices. In another study, the potentials of generating high output power using $0.71Pb(Mg_{1/3}Nb_{2/3})O_3$-$0.29PbTiO_3$ (PMN-PT) single crystals for energy harvesting is demonstrated.[113] The piezoelectric, dielectric, and loss properties of different single crystals, such as pure, Mn-doped PMN-PZ-PT, and those poled along their primary crystallographic directions

Downloaded From: https://www.spiedigitallibrary.org/ebooks/ on 07 Mar 2022
Terms of Use: https://www.spiedigitallibrary.org/terms-of-use

together with hard PZT ceramics are provided in a tabulated form in Ref. 85. Various properties of hard and soft piezoelectric ceramics and PMN-PT and PMN-PZT single crystals that affect energy-harvesting performance are also given in Ref. 23.

The conclusions reached regarding the use of piezoelectric ceramics and single crystals as transducers in energy-harvesting devices in the published literature, including in the above references, may be summarized as follows.

In contrast to polycrystalline ceramics, relaxor-PT crystals possess not only very high piezoelectric and electromechanical properties, but their properties are also highly tunable. Different piezoelectric and electromechanical properties can be achieved in relaxor-PT crystals by taking advantage of engineered domain configurations, crystal phase, orientation, and anisotropic characteristics, which are not achievable in polycrystalline ceramics.[78]

In polycrystalline ceramics, reduction in internal mechanical damping is achieved by sacrificing electromechanical couplings. In domain-engineered relaxor-PT crystal systems however, their internal mechanical damping can be improved without sacrificing their electromechanical coupling.[85]

The dielectric loss of PMNT and PZNT crystals is similar to that of hard-PZT-based piezoelectric ceramics. However, their internal mechanical damping is higher than that of hard PZT but similar to that of soft PZT.[107,114] The internal mechanical damping of relaxor-PT ferroelectric crystals can be reduced by either acceptor doping or through anisotropic domain engineering.[85]

The Curie temperatures of PMNT and PZNT single crystals are relatively low (~130 to 170 °C)[85] and may therefore limit their applications.

In conclusion, single crystals appear to present several advantages over polycrystalline ceramics for certain energy-harvesting applications. Current challenges facing single crystals for energy-harvesting applications include high fabrication cost and difficulties in growing relatively large crystals with adequate homogeneity. For these reasons, the use of expensive single crystals is generally limited to medical ultrasound imaging applications where performance considerations outweigh the materials cost.[22] It is, however, appreciated that new as well as modified single crystals and piezoelectric ceramics are continuously being developed. This includes those that are in composite form or constructed in geometries that make them particularly suitable for energy harvesting, actuation, or sensory applications.

2.2.4 Lead-free piezoelectric materials

The piezoelectric materials currently used in energy-harvesting devices are mostly lead based. There is, however, a desire and, in some cases, a requirement to use lead-free materials instead. Lead-free materials with significant piezoelectric effect for energy-harvesting devices are not currently available, but a number of promising materials are under investigation. Until recently, the piezoelectric effect of available lead-free materials has been very

Downloaded From: https://www.spiedigitallibrary.org/ebooks/ on 07 Mar 2022
Terms of Use: https://www.spiedigitallibrary.org/terms-of-use

low;[115–117] however, new lead-free piezoelectric materials are being developed with improved functional response.[22,118–122]

Smolenskii et al.[123] discovered bismuth sodium titanate ($Bi_{1/2}Na_{1/2}TiO_3$ or BNT), which is a perovskite ferroelectric. BNT is considered to be an excellent candidate material for lead-free piezoelectric ceramics because it is a ferroelectric with the Curie temperature of $T_c = 320$ °C.[121] For this reason, several studies have been done to address their manufacturing and piezoelectric properties.[120,121,124–126] Limited commercial BNT-based ceramic products are currently available, which, due to their low piezoelectric coupling factors as compared to PZT materials, are still not generally suitable for energy harvesting devices. However, considering the amount of work in this area and the rapid progress that has been made in recent years, lead-free or at least low-lead piezoelectric materials suitable for use in energy-harvesting devices might become commercially available in the near future.

In addition, for the case of mechanical-to-electrical energy transducer applications, the environmental conditions; the nature, type, and level of the input mechanical energy; the characteristics of the host system; the mechanical-to-electrical energy transducer interfacing mechanism; and the electrical energy collection, regulation electronics, and characteristics of the output storage and/or load also influence the choice of the most suitable transducer for each application. The internal damping characteristics of the transducer and the elastic elements of the vibration-based energy-harvesting device are also important and can become critical at high operating frequencies. Many of the above and related issues are addressed in the following two chapters of this book.

2.2.5 Piezoelectric materials for high-temperature applications

Mechanical-to-electrical energy transducers for energy harvesting at elevated temperatures are of interest in numerous applications such as for powering various sensors and electronic devices.[22,127–131] At elevated temperatures, transducer stability is the main concern, particularly when the device is subjected to repeated loading. High-temperature stability for several other single crystals is reported in Ref. 28, indicating that certain crystals have the potential to generate electrical energy at temperatures of up to 1000 °C.

The results of an experimental study of the output power from soft and hard PZT elements in a vibrating-beam-based energy-harvesting device is reported in Ref. 132. In this study, the output power is measured as the temperature is increased from room temperature to 150 °C. The drop in generated power is shown to be less than 6% at 75 °C and becomes increasingly larger at higher temperatures.

Wide-bandgap materials having a wurtzite structure have also been considered as promising material candidates for harvesting energy at elevated temperatures.[22,25,133,134]

Downloaded From: https://www.spiedigitallibrary.org/ebooks/ on 07 Mar 2022
Terms of Use: https://www.spiedigitallibrary.org/terms-of-use

2.2.6 Other piezoelectric material types and structures

Tailoring the microstructure of piezoelectric ceramics has been a pursued approach for enhancing their performance.[22] To date, different methods have been used to fabricate highly textured piezoelectric materials with superior properties.[135–139]

PZT–polymer composites with enhanced performance for sensors and ultrasound applications have been fabricated using various techniques.[73,140–149] The use of composites fabricated as layers of carbon/epoxy, PZT ceramic, and glass/epoxy has been reported for energy-harvesting transducers.[150] Other layered structures have been developed for MEMS energy-harvesting devices, such as epitaxial PZT thin films deposited on silicon substrate.[151,152]

Other piezoelectric materials have also been investigated for actuation as well as energy harvesting, such as those using aluminum nitride (AlN) and ZnO.[153–158] AlN has been indicated as a potential alternative to PZT since it is lead free and suitable for MEMS manufacturing processes such as sputtering. The piezoelectric coefficient of AlN is lower than that of PZT, but its dielectric constant is also lower.[153,155]

2.3 Electromagnetic Induction Transducers

Electromagnetic induction transducers function on Faraday's law, which was discovered in 1831. In such transducers, the input mechanical energy produces a time-varying magnetic flux through a conductor, usually a coil, thereby generating an electromotive force in the conductor. The magnetic flux variation is usually achieved through the relative linear or rotary motion between a coil and a permanent magnet. Magnetic flux variation may also be realized through variation in the magnetic field.[159–163] The relative motion between the coil and the permanent magnet may be the result of moving the coil relative to a fixed permanent magnet or moving the permanent magnet relative to a fixed coil. The latter method is usually preferred in energy-harvesting devices since it results in fixed output wires. The amount of power that an electromagnetic induction harvester generates is dependent on the length of the conductor, i.e., the number of turns of the coil, the strength of the magnetic field and its coil coupling, and the velocity of the coil motion in the magnetic field.

Electromagnetic generator technology is highly developed and has been used in small handheld devices to generate a small fraction of one watt as well as in power plants to generate megawatts of power. Such electrical energy generators are rotary machines and have also been used in "more traditional" energy-harvesting systems such as windmills.[164,165] However, the emphasis here is on small generators and micro-generators, and primarily those with linear, rotary or vibratory, or oscillatory input motions.

In recent years, numerous researchers have investigated, fabricated, and tested different electromagnetic-based energy-harvesting devices for various

Downloaded From: https://www.spiedigitallibrary.org/ebooks/ on 07 Mar 2022
Terms of Use: https://www.spiedigitallibrary.org/terms-of-use

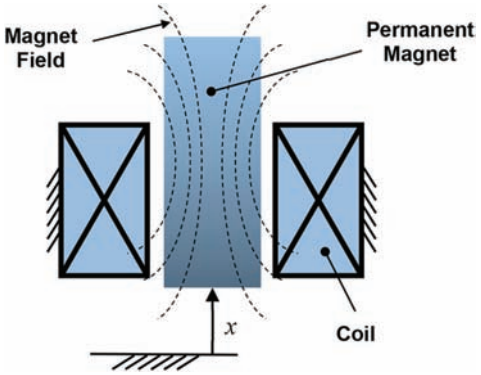

Figure 2.6 The basic model of an electromagnetic induction transducer.

applications,[20,166–175] including for powering MEMS devices.[163,169,176–191] For additional in-depth treatment, the reader is also referred to reviews provided in Refs. 11, 163, and 170. A comprehensive review of the physical and performance characteristic of several such electromagnetic-based micro-generators is summarized in a tabulated form in Ref. 11.

A typical electromagnetic-induction-type generator may be represented as shown in the schematic of Fig 2.6. In electromagnetic induction transducers (generators) used in energy-harvesting devices, the magnetic flux is usually generated by permanent magnets, and a coil is used as the conductor. The coil crosses the magnetic flux at a certain velocity, generating an induced electromotive force (emf). The strength of the magnetic flux crossing the conducting coils is dependent on the strength of the permanent magnets and the closeness of the coil to the permanent magnets.

In the schematic of the electromagnetic induction generator of Fig 2.6, the permanent magnet is positioned inside the coil and is shown to be moving relative to the generator coil, which is considered to be fixed. The time-varying position x of the permanent magnet produces a time-varying magnetic flux linked to the coil. At any given instant, the permanent magnet velocity $v = dx/dt$, where t is time, l is the total coupled (effective) coil conductor length with the corresponding crossing magnetic flux density $B(x)$ at the position x of the permanent magnet, the induced potential difference between the ends of the coil conductor [electromotive force (emf)] is[159–163,192]

$$V_{emf} = l\,B(x)v. \tag{2.16}$$

If the coupled coil consists of a wire that is wound N number of turns at a diameter D, then the effective length l is πND.

The circuit representation of an electromagnetic induction generator of the type shown in Fig. 2.6 is shown in Fig. 2.7, where R_C and L_C are the coil resistance and inductance, respectively. If the generator output, i.e., the generator coil, is connected to a resistive load R_L, the load closes the generator

Downloaded From: https://www.spiedigitallibrary.org/ebooks/ on 07 Mar 2022
Terms of Use: https://www.spiedigitallibrary.org/terms-of-use

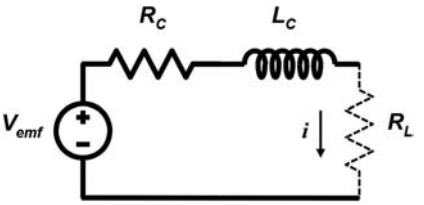

Figure 2.7 The circuit representation of an electromagnetic induction generator.

circuit as shown in Fig. 2.7, and the generated voltage V_{emf} causes a current i to flow through the circuit.

Neglecting the inductance L_C, the current i is seen to be

$$i = V_{emf}/R = l\,B\,v/R, \tag{2.17}$$

where $R = R_C + R_L$. As the permanent magnet moves with velocity v, the coil moving in the magnetic field with the induced passing current i requires an applied external mechanical force F_{input} to overcome the magnetic force (magnetic drag) exerted on the passing coil by the magnetic field.[192] The magnetic force and its overcoming mechanical force F_{input} is given as

$$F_{input} = i\,l\,B = v\,l^2B^2/R, \tag{2.18}$$

making the input mechanical power

$$P_{input} = F_{input}v = v^2\,l^2\,B^2/R. \tag{2.19}$$

From Eq. (2.17), the output electrical power, i.e., the electrical power dissipated in the resistive load R_L, can be seen to be

$$P_{output} = R_L\,i^2 = (v^2\,l^2\,B^2\,/R^2)R_L. \tag{2.20}$$

Then, as expected, the ratio of the output electrical power to input mechanical power becomes

$$P_{output}/P_{input} = R_L/R = R_L/(R_C + R_L), \tag{2.21}$$

which means that in the absence of coil inductance L_C, the only transducer loss is due to the electrical resistance of the coil of the electromagnetic induction generator.

Electromagnetic-induction-based transducers are highly reliable and, unlike piezoelectric transducers, do not exhibit structural resistance to the applied motion. The fabrication and assembly of submillimeter electromagnetic systems remain a challenge for implementation in MEMS devices.[20] In addition, the voltage generated with such devices is usually between 0.1 and 0.2 V, and transformers are usually needed to meet voltage requirements for MEMS applications.[11]

Downloaded From: https://www.spiedigitallibrary.org/ebooks/ on 07 Mar 2022
Terms of Use: https://www.spiedigitallibrary.org/terms-of-use

2.4 Electrostatic Transducers

A capacitor consists of two conductive overlaying plates that are held a certain distance apart. The gap between the two conductive plates may be vacuum, or may be filled with air or another nonconductive gas or a certain insulator (dielectric) material.

Electrostatic transducers use capacitors for which their capacitance can be mechanically varied. The mechanical work done to vary the capacitor's capacitance is then converted to electrical energy to be harvested. The capacitor's capacitance may be varied by varying the distance between the capacitor's conductive plates or by varying the extent of their overlapping surfaces.

Electrostatic transducers have long been used in audio speakers and receivers.[193,194] In recent years, and particularly due to their relative ease of implementation in MEMS devices, their application for mechanical-to-electrical energy conversion has attracted attention.[20,195–221]

In an energy-harvesting device, an electrostatic transducer may be used in two different modes to convert mechanical energy to electrical energy. In both modes of operation, the transducer capacitor is initially charged by an external source. In one mode, the capacitor charge is kept constant as the transducer converts input mechanical energy to electrical energy, which is stored in the transducer capacitor. This mode of operation is the "charge-constrained mode." In the other mode, the voltage across the capacitor's conductive plates is kept constant as the transducer converts input mechanical energy to electrical energy, which is also stored in the transducer capacitor. This mode of operation is the "voltage-constrained mode." In either mode of operation, the generated electrical energy—generally together with the initially charged electrical energy—is then extracted for direct use or storage in an electrical storage device. The transducer capacitor is then returned to its initial charged state.

The principal operation of electrostatic transducers is very simple. In the aforementioned charge-constrained mode of operation, the variable capacitance capacitor is first charged at its maximum capacitance configuration, i.e., when the conductive plates are at their minimum distance and/or at maximum overlap depending on the capacitor type. The schematic of such a variable capacitor of the former type is shown in Fig. 2.8. In the maximum

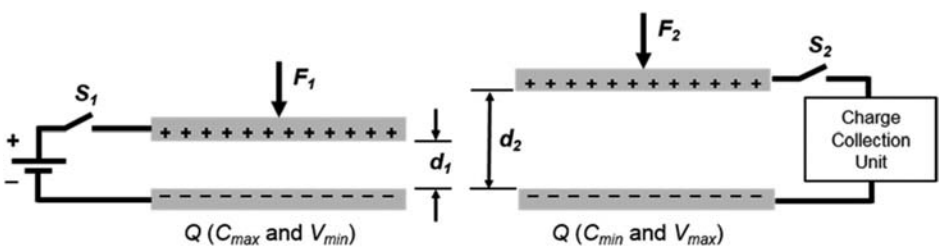

Figure 2.8 Charge-constrained mode of electrostatic transducer operation.

Downloaded From: https://www.spiedigitallibrary.org/ebooks/ on 07 Mar 2022
Terms of Use: https://www.spiedigitallibrary.org/terms-of-use

capacitance configuration [Fig. 2.8(a)], the capacitor is considered to have a capacitance of C_{max} and is charged by an external source to a certain voltage V_{min}, after which the external source is disconnected by opening the switch S_1. Now by mechanically separating the two conductive plates of the capacitor by the application of an external force F, the capacitor's capacitance is continuously decreased. In the schematic of Fig. 2.8(b), the capacitor is shown in its considered maximum conductive-plate separation at which point its capacitance is at its minimum, indicated as C_{min}. Since the total charge Q stored on the capacitor is fixed, i.e., constrained from being discharged, the capacitor voltage is increased to its maximum level V_{max} as the capacitor conductive plates are separated and the capacitance C_{min} is reached. Because the total charge Q is constant,

$$Q = C_{max} V_{min} = C_{min} V_{max}. \tag{2.22}$$

And since the electrical energy stored in a capacitor is

$$E = \tfrac{1}{2}\, C\, V^2, \tag{2.23}$$

the mechanical energy converted to electric energy is

$$E_e = \tfrac{1}{2}\, C_{min} V_{max}^2 - \tfrac{1}{2}\, C_{max} V_{min}^2 = \tfrac{1}{2}(C_{max} - C_{min}) V_{max} V_{min}. \tag{2.24}$$

It is also readily seen that the converted mechanical energy may also be written in terms of the total capacitor charge Q as

$$E_e = \tfrac{1}{2}\, Q^2 (1/C_{min} - 1/C_{max}). \tag{2.25}$$

Once the maximum voltage V_{max} has been reached, the capacitor charges are discharged into the charge collection unit shown in Fig. 2.8 by closing switch S_2.

It can also be shown from Coulomb's law that the external force F (Fig. 2.8) needed to counter the attractive force between the charges on the capacitor conductor plates is

$$F = Q^2 / 2\, \varepsilon\, A, \tag{2.26}$$

where ε is the permittivity of the material between the capacitor plate. The mechanical work E_m done by the force F as the capacitor conductive plates are separated from their minimum and maximum distances d_1 and d_2, respectively, correspond to the capacitor maximum and minimum capacitances C_{max} and C_{min}, respectively; i.e., the mechanical energy input into the electrostatic transducer therefore becomes

Downloaded From: https://www.spiedigitallibrary.org/ebooks/ on 07 Mar 2022
Terms of Use: https://www.spiedigitallibrary.org/terms-of-use

$$E_m = (d_2 - d_1)Q^2/2\,\varepsilon\,A = (Q^2/2)(d_2/\varepsilon\,A - d_1/\varepsilon\,A)$$
$$= (Q^2/2)(1/C_{min} - 1/C_{max}), \tag{2.27}$$

which as expected equals the generated electrical energy E_e [Eq. (2.25)].

In the voltage-constrained mode of operation, the variable-capacitance capacitor is connected to a constant voltage source that can maintain the capacitor at a certain voltage V. In its initial state, the capacitor is in its previously indicated maximum capacitance C_{max} state. Since the capacitor voltage V is constant, as the overlap area between the conductive capacitor plates is decreased, the capacitor capacitance decreases while the capacitor charge is decreased, thereby generating a current that can be used by an external load or stored in an electrical energy storage device. The charges remaining in the capacitor at its latter minimum capacitance C_{min} state may also be collected. The total amount of mechanical energy that is converted to electrical energy as the capacitor capacitance is varied from C_{max} to C_{min} is

$$E_e = \tfrac{1}{2}\,C_{max}V^2 - \tfrac{1}{2}\,C_{min}V^2 = \tfrac{1}{2}(C_{max} - C_{min})V^2. \tag{2.28}$$

Electrostatic transducers have been grouped into three categories:[184,203,212,222–224] (1) in-plane overlap varying, (2) in-plane gap varying, and (3) out-of-plane gap varying. Figure 2.9 illustrates the basic design of the three electrostatic transducers.[212] In the in-plane overlap varying type [Fig. 2.9(a)], the motion indicated by the double arrow causes overlapping

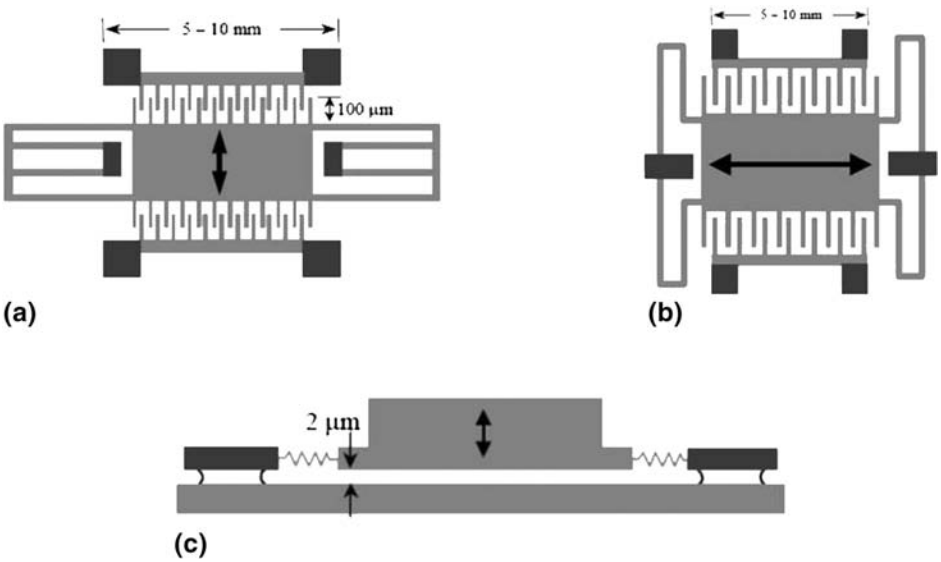

Figure 2.9 Three basic designs of an electrostatic transducer:[212] (a) in-plane overlap varying, (b) in-plane gap varying, (c) out-of-plane gap varying. The tabs on the device capacitors are shown on each meshing capacitor fingers.

Downloaded From: https://www.spiedigitallibrary.org/ebooks/ on 07 Mar 2022
Terms of Use: https://www.spiedigitallibrary.org/terms-of-use

surfaces between the two capacitor electrode fingers to vary, thereby varying the capacitor capacitance. In the in-plane gap varying type [Fig. 2.9(b)], the indicated motion causes the gap between the two capacitor electrode fingers to vary, thereby varying the capacitor capacitance. In the out-of-plane gap varying type [Fig. 2.9(c)], changes in the distance between the capacitor electrode plates causes the capacitor capacitance to vary.

The electrostatic transducers require an input charge or a constant voltage source for their operation, which must be provided by an external power source. Electrostatic transducers have been developed that use electrets to provide biasing charges for their operation. Methods have also been developed to use part of the generated electrical energy for this purpose following initial charging of the transducer. The requirement of initial charging via an external source makes electrostatic transducers not suitable for certain applications. Different approaches for the design and efficient harvesting of the generated electrical energy by electrostatic transducers are provided in the literature referenced in this chapter.[184,195–197,199,200–209,211–215,217–219,221,222,224–231]

2.4.1 Electret-based electrostatic transducers

One shortcoming of the electrostatic transducers described above is that they require an external source of input charge or constant voltage for their operation. Electrostatic transducers may however be provided with layers of electret on one or both capacitor's conductive plates to induce initial voltage. The electret-based and externally charged electrostatic transducers function similarly to convert mechanical energy to electrical energy. The main difference between the two is that the electret-based electrostatic transducers do not require any initial electrical energy to operate since the initial charges are provided directly by the transducer electret layer.[195]

Electrets are dielectric materials that have a quasi-permanent electric charge or dipole polarization.[195] The English physicist Oliver Heaviside[232] named the material "electret" as an electrostatic equivalent of a permanent magnet (**electr**icity magn**et**). Dr. Mototaro Eguchi[233] later successfully fabricated the first electret using a thermal charging method.

A review of the different types of electrets, their characteristics, and methods of manufacture are provided in Ref. 195. The most commonly used electrets in electret-based electrostatic mechanical-to-electrical energy transducers are obtained by implanting electric charges into dielectrics using different techniques.[195,234–236] These electrets include those based on Teflon™[235–243] and CYTOP™.[244–247] Many other types of electret materials and their characteristics are provided in the above references. Dielectric materials are however not perfect insulators, and the charges may dissipate over time. As a result, recent research efforts in this area have concentrated on implanted charge stability,[246,248] and materials such as Teflon and

Downloaded From: https://www.spiedigitallibrary.org/ebooks/ on 07 Mar 2022
Terms of Use: https://www.spiedigitallibrary.org/terms-of-use

silicon-dioxide-based electrets with an estimated life of over 100 years have been developed.[238,239,241,243]

Electret-based transducers convert mechanical energy to electrical energy in a manner similar to that described for externally charged electrostatic transducers, i.e., by varying the capacitance of a charged capacitor. Different designs of electret-based transducers and the use of different electret materials have been reported in the literature.[182,215,216,234,249–256]

In an electret-based mechanical-to-electrical energy transducer, the electret element maintains the transducer capacitor charge at all times without the need of an initial charging. Electrets are dielectric materials that are capable of maintaining an electric field and a surface voltage in the way that permanent magnets maintain a magnetic field. The operation of electret-based transducers may be described using the transducer of Fig. 2.10, which is intended to function in the same mode as the transducer of Fig. 2.8. Using the terminology of Boisseau,[234] the transducer consists of an electrode plate on which an electret layer is deposited. The other capacitor electrode plate, called counter-electrode, is positioned parallel to the other electrode at a certain varying distance. The gap between the counter-electrode and the electret is filled with a certain gas such as air.

Let the constant charge on the electret be indicated as Q_e and the resulting charges on the electrode and counter-electrode be Q_1 and Q_2, respectively. The sum total of induced charges Q_1 and Q_2 on the electrode and counter-electrode must equal the charge on the electret Q_e, i.e.,

$$Q_1 + Q_2 = Q_e. \tag{2.29}$$

Then, when the externally applied force F moves the counter-electrode toward the electret layer, the gap between them is decreased. If the switch S is open, since the charge Q_2 is constant, the voltage across the transducer and thereby the electrical energy stored in the transducer equivalent capacitance C_{eq} is increased. Here, C_{eq} is the capacitance between the counter-electrode and the electrode, which includes the in-series capacitance of the electret and the gap between it and the counter-electrode. As a result, and similar to the transducer

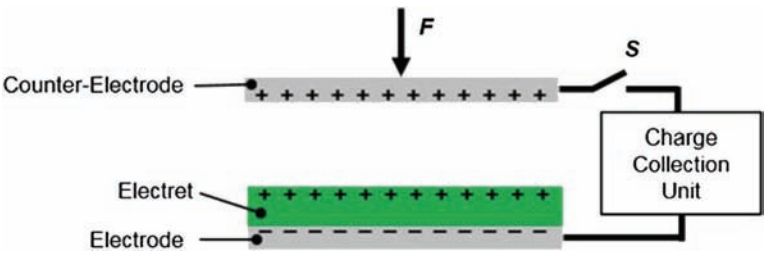

Figure 2.10 An electret-based electrostatic transducer.

Downloaded From: https://www.spiedigitallibrary.org/ebooks/ on 07 Mar 2022
Terms of Use: https://www.spiedigitallibrary.org/terms-of-use

of Fig. 2.8, the work done by force F increases the total electrical energy stored in the transducer to

$$E_{total} = \tfrac{1}{2}\, Q^2 / C_{eq}. \tag{2.30}$$

The generated electrical energy can then be discharged into the charge collection unit shown in Fig. 2.10 by closing the switch S for direct use or storage. As discussed above for the electret-free implementation, the electret-based electrostatic energy harvester can be operated by varying either the gap or the overlap area between the electrodes.

2.5 Magnetostrictive-Material-based Transducers

Magnetostrictive-material-based transducers have also been used in energy-harvesting devices. Magnetostrictive materials deform when subjected to a changing magnetic field. These materials also induce changes in the magnetic field when deformed. The latter phenomenon is known as inverse magnetostrictive, magnetoelastic, magnetomechanical, and Villari effects (after the Italian physicist who discovered it in 1865).

When used as a mechanical-to-electrical energy transducer, a time-varying strain is applied to the magnetostrictive material, thereby obtaining a time-varying magnetic field, which is then used to generate a current in a pick-up coil or solenoid positioned within the changing magnetic field. It is therefore appreciated that these transducers can generate appreciable electrical energy only if strained at high rates, which in dynamic mechanical systems indicates that the applied external or dynamic forces have to be large and long enough in duration (low enough frequency if vibrational) to allow an appreciable strain/deformation rate to be achieved.

Among the magnetostrictive materials that are currently available and have been used as mechanical-to-electrical energy transducers,[257–266] most common are the crystalline alloy Terfenol-D ($Tb_{0.3}Dy_{0.7}Fe_{1.9-2}$)[260,267] and to a lesser degree amorphous metallic glass Metglas®.[264,266,268–270]

The magnetostrictive material Metglas[268–270] has been used for mechanical-to-electrical energy transduction.[264–266] For this application, thin film Metglas material layers have been annealed under a strong transverse magnetic field in the width direction to enhance magnetomechanical coupling[268,270] and mitigate the need for a bias magnetic field to reduce the transducer size.[264,265] In this configuration, several laminated thin 18-μm Metglas (2605SC) ribbons are bonded to a copper cantilever beam and a pick-up coil is provided around the beam–Metglas laminate. Strain in the laminate due to the bending vibration of the cantilever beam induces a change in the magnetization of the Metglas laminate, generating current in the pick-up coil. Electrical energy is then extracted from the coil by an appropriate circuitry.

Downloaded From: https://www.spiedigitallibrary.org/ebooks/ on 07 Mar 2022
Terms of Use: https://www.spiedigitallibrary.org/terms-of-use

Attempts have been made to use Terfenol-D for mechanical-to-electrical energy transduction.[262,263] Such transducers developed to date are however bulky and generate very small amounts of electrical energy relative to their size and space that they occupy. Terfenol-D does however provide relatively large strains compared to piezoelectric material and has therefore been used to form piezoelectric–magnetostrictive composites. In such composites, the relatively large Terfenol-D-generated strain due to an externally applied magnetic field is used to strain piezoelectric layers to generate relatively large amount of electrical charge.[257,258,261] Such composites were originally used in magnetic field sensors.[24] When used for energy harvesting, the varying magnetic field has to be applied externally. For example, in the device described in Ref. 258, four magnets positioned on the free end of a vibrating cantilever beam are used as the external source of the varying magnetic field.

One advantage of piezoelectric-magnetostrictive composites for mechanical-to-electrical energy transduction as compared to transducer types that utilize straining magnetostrictive elements with pick-up coils is that they do not rely on the rate of change in the applied strain, i.e., the level of input mechanical power, to generate electrical energy. As a result, the former can be used at relatively low as well as high rates of mechanical energy input, while the latter can generate appreciable electrical energy only when the rate of mechanical energy input is high.

2.6 General Comparison of Different Transducers

In this section a mostly qualitative comparison is provided for use by energy-harvesting device designers as merely a guide in selecting the most suitable transducer type for an energy-harvesting device type and application. It is appreciated that many other factors that must be considered—such as limitations in size and shape; operating environment; input mechanical energy type and level; electrical energy and/or power requirement of the devices to be powered; amount of electrical energy to be generated; acceptable level of complexity in the electrical energy collection, regulation, direct usage and/or storage electronics and controls; and usually many other limiting factors—would also narrow the range of acceptable transducers. It is assumed that the designer would be following good engineering practice and that therefore issues such as mechanical and electrical overload protection and other factors to ensure structural integrity and proper operation of the selected transducer would be considered during the design process.

A number of researchers have provided comparisons between the modes of operation, basic characteristics, output, and general advantages and disadvantages of each transducer type for energy-harvesting applications.[11,20,24,163,223,224,265,271,272] A summary of general advantages and

Downloaded From: https://www.spiedigitallibrary.org/ebooks/ on 07 Mar 2022
Terms of Use: https://www.spiedigitallibrary.org/terms-of-use

Table 2.1 Comparison of different mechanical to electrical energy transducers

Type	Advantages	Disadvantages
Piezoelectric	• No external voltage source • High output voltage • Compatible with MEMS • Simple structure	• Low output current • Low toughness • Low tensile strength* • Charge leakage** • Depolarization and aging***
Electrostatic	• Easy to integrate with MEMS • High output voltage • Function well at slow and fast displacement rates • High degree of miniaturization possible	• External voltage source needed§ • Low output current • Difficult to fabricate large capacitor surfaces
Electromagnetic	• No external voltage source • High output current • Well-established technology	• Difficult to integrate with MEMS—requires permanent magnet and pick-up coil • Low output voltage • Low output energy at slow speeds • Low output energy in small size
Magnetostrictive	• No external voltage source • No depolarization problem • Highly flexible films available§§	• Difficult to integrate with MEMS—requires pick-up coil • Low output energy at slow speeds • Low output energy in small size • May need biasing magnets

*May need to be preloaded in compression if subjected to equal compressive and tensile loading.
**Makes it not suitable for applications with slow stain rates.
***Mainly for polymer and polycrystalline ceramic types at high temperature.
§Unless using charged electret.
§§Particularly, the amorphous metallic glass type (Metglas[269]).

disadvantages of each transducer type for use in energy-harvesting devices is provided in Table 2.1. Possible implications of certain shortcomings and basic methods of addressing them are also provided.

2.7 Transducer Shelf Life and Operational Life

Energy-harvesting devices must satisfy the application shelf life and operational life requirements in the relevant environment. In many applications such as in implanted devices, operational life of over 20 years is highly desirable or required. In other applications such as in emergency equipment or certain normally dormant event detection sensors, or in impact- or impulse-activated devices, the energy-harvesting transducer must have a very long shelf life, sometimes well over 20 years, and during this time it may be subjected to highly fluctuating temperatures or be subjected to other environmental elements.

Several lifetime studies have been performed and reported to date for PZT materials used for actuation purposes. Repeated mechanical and electrical cycling of piezoelectric ceramics has been shown to result in a progressive

Downloaded From: https://www.spiedigitallibrary.org/ebooks/ on 07 Mar 2022
Terms of Use: https://www.spiedigitallibrary.org/terms-of-use

degradation in performance to various degrees.[273–276] During a typical operation, the piezoelectric element of the device may experience repeated and varying mechanical loading and electric voltage inputs at varying environmental conditions such as temperature.[277] The level of performance degradation depends on the level, duration, and frequency of the input mechanical load and the electrical voltage input; the PZT material composition; and environmental conditions that affect mechanisms such as the loss of mobility in domain walls, depoling, formation of micro-cracks, and failure of the electrode-ceramic.[278,279]

Other related life cycle studies of PZT materials focused on stack configurations for actuation purposes for applications requiring long-term operation in challenging environments such as in space.[276,280–288]

From the shelf-life and operational-life cycle points of view, piezoelectric transducer degradation of performance needs to be considered. Performance degradation can be due to: depoling from thermal effects and high levels of loading and number of cycles; degradation in the material properties due to aging and environmental conditions; fatigue failure; piezoelectric creep; and many other application-specific factors that may need to be considered.

There is a relatively limited amount of information available about the shelf life, life cycle, and life cycle time of transducers under various operating and environmental conditions. The available information is primarily on PZT-based materials and mainly covers these materials being used as actuation devices and not for energy harvesting. There is therefore a great need for systematic studies to provide the needed information for the developers of energy harvesting devices using different piezoelectric materials and composites, particularly for energy harvesting devices that have to reliably operate for long periods of time, sometimes well over 20 years, and sometimes in relatively harsh environments.

References

1. A. Arnau and D. Soares, "Fundamentals of Piezoelectricity," in *Piezoelectric Transducers and Applications*, A. Arnau, Ed., Springer, Berlin, pp. 1–37 (2008).
2. P. Curie and J. Curie, "Développement, par pression, de l'électricité polaire dans les cristaux hémièdres à faces inclines," *Comptes Rendus* **91**, 294–295 (1880).
3. W. G. Hankel, "Uber die aktinound piezoelektrischen Eigenschaften des Bergkrystalles und ihre Beziehung zu den thermoelektrischen," *Abh. Sächs* **12**, 457 (1881).
4. Y. Zhang, "Piezoelectric Based Energy Harvesting on Low Frequency Vibrations of Civil Infrastructures," Ph.D. thesis, Louisiana State University (2014).

Downloaded From: https://www.spiedigitallibrary.org/ebooks/ on 07 Mar 2022
Terms of Use: https://www.spiedigitallibrary.org/terms-of-use

5. W. G. Cady, *Piezoelectricity: An Introduction to the Theory and Application of Electromechanical Phenomena in Crystals*, McGraw-Hill, New York (1946).
6. W. P. Mason, *Piezoelectric Crystals and their Applications to Ultrasonics*, Van Nostrand, New York (1950).
7. R. D. Mindlin, "On the equations of motion of piezoelectric crystals," in *Problems of Continuum Mechanics*, Society of Industrial and Applied Mathematics, Philadelphia, pp. 282–290 (1961).
8. J. Smits and W. Choi, "The constituent equations of heterogeneous bimorphs," *IEEE Transactions on Ultrasonics, Ferroelectrics, and Frequency Control* **38**(3), 256–270 (1991).
9. J. Smits, S. Dalke, and T. K. Cooney, "The constituent equations of piezoelectric bimorphs," *Sensors and Actuators* **28**, 41–61 (1990).
10. W. Voigt, *Lehrbuck der Kristallphysik*, Teubner, Leipzig (1910).
11. K. A. Cook-Chennault, N. Thambi, and A. M. Sastry, "Powering MEMS portable devices—a review of non-regenerative and regenerative power supply systems with special emphasis on piezoelectric energy harvesting systems," *Smart Materials and Structures* **17**(4), 1–33 (2008).
12. S. R. Anton and H. A. Sodano, "A review of power harvesting using piezoelectric materials (2003–2006)," *Smart Materials and Structures* **16**(10), 1–21 (2007).
13. R. Calio, U. B. Rongala, D. Camboni, M. Milazzo, C. Stefanini, G. de Petris, and C. M. Oddo, "Piezoelectric energy harvesting solutions," *Sensors* **14**, 4755–4790 (2014).
14. E. Fukada and I. Yasuda, "On the piezoelectric effect of bone," *Journal of The Physical Society of Japan* **12**, 1158–1162 (1957).
15. T. Ikeda, *Fundamentals of Piezoelectricity*, Oxford University Press, Oxford, UK (1990).
16. B. Jaffe, *Piezoelectric Ceramics*, Vol. **3**, Academic Press, London, UK (1971).
17. The Piezoelectric Effect, www.aurelienr.com/electronique/piezo/piezo.pdf (accessed on May 31, 2015).
18. PI Ceramic GmbH, http://piceramic.com/piezo-technology/fundamentals.html (accessed on May 31, 2015).
19. A. Arnau, Ed., *Piezoelectric Transducers and Applications*, Springer, New York (2004).
20. S. P. Beeby, M. J. Tudor, and N. M. White, "Energy harvesting vibration sources for microsystems applications," *Measurement Science and Technology* **17R**, 175–195 (2006).
21. S. Chalasani and J. Conrad, "A survey of energy harvesting sources for embedded systems," *IEEE SoutheastCon 2008*, 442–447 (2008).
22. Q. Xu and T. Kobayashi, Eds., *Advanced Materials for Clean Energy*, CRC Press, Boca Raton, Florida (2015).

Downloaded From: https://www.spiedigitallibrary.org/ebooks/ on 07 Mar 2022
Terms of Use: https://www.spiedigitallibrary.org/terms-of-use

23. A. Erturk and D. Inman, *Piezoelectric Energy Harvesting*, John Wiley & Sons, Ltd. (2011).
24. T. Kazmierski and S. Beeby, *Energy Harvesting Systems. Principles, Modeling and Applications*, Springer, Science+Media, LLC (2011).
25. C. R. Bowen, H. A. Kim, P. M. Weaver, and S. Dunn, "Piezoelectric and ferroelectric materials and structures for energy harvesting applications," *Energy and Environmental Science* **7**, 25–44 (2014).
26. M. J. Hoffmann, H. Kungl, J. T. Reszat, and S. Wagner, *Polar Oxides*, Wiley-VCH Verlag GmbH & Co. KGaA, Weinheim, Germany, pp. 137–150 (2005).
27. R. A. Islam and S. Priya, "Realization of high-energy density polycrystalline piezoelectric ceramics," *Applied Physics Letters* **88**, 032903 (2006).
28. B. Jaffe, W. R. Cook, and H. Jaffe, *Piezoelectric Ceramics*, Academic, New York (1971).
29. H. Kim, Y. Tadesse, and S. Priya, "Piezoelectric Energy Harvesting," in *Energy Harvesting Technologies*, S. Priya and D. J. Inman, Eds., Springer, New York, pp. 3–39 (2009).
30. A. J. Moulson and J. M. Herbert, *Electroceramics: Materials, Properties, Applications*, Second Edition, Wiley, London (2003).
31. B. Noheda, J. A. Gonzalo, L. E. Cross, R. Guo, S. E. Park, D. E. Cox, and G. Shirane, "Tetragonal-to-monoclinic phase transition in a ferroelectric perovskite: The structure of $PbZr_{0.52}Ti_{0.48}O_3$," *Phys. Rev. B* **61**, 8687–8695 (2000).
32. W. F. Rao and Y. U. Wang, "Microstructures of coherent phase decomposition near morphotropic phase boundary in lead zirconate titanate," *Applied Physics Letters* **90**, 041915 (2007).
33. K. Uchino, "The Development of Piezoelectric Materials and the New Perspective," in *Advanced Piezoelectric Materials: Science and Technology*, K. Uchino, Ed., Woodhead Publishing, Philadelphia, pp. 1–82 (2010).
34. K. Uchino, *Ferroelectric Devices*, Second Ed., CRC Press, Boca Raton, Florida (2009).
35. C. N. Xu, M. Akiyama, K. Nonaka, and T. Watanabe, "Electrical power generation characteristics of PZT piezoelectric ceramics," *IEEE Transactions on Ultrasonics, Ferroelectrics and Frequency Control* **45**, 1065–1070, (1998).
36. ANSI/IEEE Std 176-1987, "IEEE Standard on Piezoelectricity," IEEE Ultrasonic, Ferroelectrics, and Frequency Control Society (1987).
37. J. Ajitsaria, S. Y. Choe, D. Shen, and D. J. Kim, "Modeling and analysis of a bimorph piezoelectric cantilever beam for voltage generation," *Smart Materials and Structures* **16**, 447–454 (2007).
38. A. Erturk, "Electromechanical Modeling of Piezoelectric Energy Harvesters," Ph.D. thesis, Virginia Polytechnic Institute and State University (2009).

Downloaded From: https://www.spiedigitallibrary.org/ebooks/ on 07 Mar 2022
Terms of Use: https://www.spiedigitallibrary.org/terms-of-use

39. F. Lu, H. P. Lee, and S. P. Lin, "Modeling and analysis of micro piezoelectric power generators for micro-electromechanical-systems application," *Smart Materials and Structures* **13**, 57–63 (2004).
40. S. Roundy and P. K. Wright, "A piezoelectric vibration based generator for wireless electronics," *Smart Materials and Structures* **13**, 1131–1144 (2004).
41. H. A. Sodano and D. J. Inman, "Estimation of electric charge output for piezoelectric energy harvesting," *Journal of Strain Analysis* **40**(2), 49–58 (2004).
42. E. B. Tadmore and G. Kosa, "Electromechanical coupling correction for piezoelectric layered beams," *Journal of Microelectromechanical Systems* **12**, 899–906 (2003).
43. F. M. Daqaq, J. M. Renno, J. R. Farmer, and D. J. Inman, "Effects of system parameters and damping on an optimal vibration-based energy harvester," *Proc. 48th AIAA/ASME/ASCE/AHS/ASC Structures, Structural Dynamics, and Materials Conference*, 22–26 April 2007, Honolulu, Hawaii, pp. 1–11 (2007).
44. N. E. duToit, B. L. Wardle, and S. Kim, "Design consideration for MEMS-scale piezoelectric mechanical vibration energy harvesters," *Journal of Integrated Ferroelectrics* **71**, 121–160 (2005).
45. N. G. Stephen, "On energy harvesting from ambient vibration," *Journal of Sound and Vibration* **293**, 409–425 (2006).
46. S. N. Chen, G. J. Wang, and M. C. Chien, "Analytical modeling of piezoelectric vibration-induced micro power generator," *Mechatronics* **16** 387–397 (2006).
47. J. H. Lin, X. M. Wu, T. L. Ren, and L. T. Liu, "Modeling and simulation of piezoelectric MEMS energy harvesting device," *Integrated Ferroelectrics* **95**, 128–141 (2007).
48. C. De Marqui, Jr., A. Erturk, and D. J. Inman, "An electromechanical finite element model for piezoelectric energy harvester plates," *Journal of Sound and Vibration* **237**, 9–25 (2009).
49. N. G. Elvin and A. A. Elvin, "A general equivalent circuit model for piezoelectric generators," *Journal of Intelligent Material Systems and Structures* **20**(1), 3–9 (2009).
50. N. G. Elvin and A. A. Elvin, "A coupled finite element—circuit simulation model for analyzing piezoelectric energy generators," *Journal of Intelligent Material Systems and Structures* **20**, 587–595 (2009).
51. A. Erturk and D. J. Inman, "An experimentally validated bimorph cantilever model for piezoelectric energy harvesting from base excitations," *Smart Materials and Structures* **18**, 025009 (2009).
52. A. Erturk and D. J. Inman, "A distributed parameter electromechanical model for cantilevered piezoelectric energy harvesters," *Journal of Vibration and Acoustics* **130**, 041002 (2008).

Downloaded From: https://www.spiedigitallibrary.org/ebooks/ on 07 Mar 2022
Terms of Use: https://www.spiedigitallibrary.org/terms-of-use

53. C. J. Rupp, A. Evgrafov, K. Maute, and M. L. Dunn, "Design of piezoelectric energy harvesting systems: a topology optimization approach based on multilayer plates and shells," *Journal of Intelligent Material Systems and Structures* **20**, 1923–1939 (2009).
54. Y. Yang and L. Tang, "Equivalent circuit modeling of piezoelectric energy harvesters," *Journal of Intelligent Material Systems and Structures* **20**, 2223–2235 (2009).
55. E. Crawley and K. Lazarus, "Induced strain actuation of isotropic and anisotropic plates," *AIAA Journal* **29**, 944–951 (1991).
56. E. Crawley and E. Anderson, "Detailed models for the piezoelectric actuation of beams," *Journal of Intelligent Material Systems and Structures* **1**, 4–25 (1990).
57. S. C. Stanton, A. Erturk, B. P. Mann, and D. J. Inman, "Nonlinear piezoelectricity in electroelastic energy harvesters: modeling and experimental identification," *Journal of Applied Physics* **108**, 074903 (2010).
58. U. von Wagner and P. Hagedorn, "Piezo-beam subjected to weak electric field: experiments and modeling of nonlinearities," *Journal of Sound and Vibration* **256**, 861–872 (2002).
59. J. Chang, M. Dommer, C. Chang, and L. Lin, "Piezoelectric nanofibers for energy scavenging applications," *Nano Energy* **1**(3), 356–371 (2012).
60. Y. Choi, M. J. Yoo, H. W. Kang, H. G. Lee, S. Han, and S. Nahm, "Dielectric and piezoelectric properties of ceramic-polymer composites with 0-3 connectivity type," *Journal of Electroceramics* **30**, 30–35 (2013).
61. J. Fang, H. Niu, H. Wang, X. Wang, and T. Lin, "Enhanced mechanical energy harvesting using needleless electrospun poly(vinylidene fluoride) nanofiber webs," *Energy and Environmental Science* **6**, 2196–2202 (2013).
62. E. Guzman, J. Cugnoni, T. Gmür, P. Bonhôte, and A. Schorderet, "Survivability of integrated PVDF film sensors to accelerated ageing conditions in aeronautical/aerospace structures," *Smart Materials and Structures* **22**(6), 065020 (2013).
63. H. Kawai, "The piezoelectricity of poly (vinylidene fluoride)," *Japanese Journal of Applied Physics* **8**(7), 975–976 (1969).
64. S. R. Khaled, D. Sameoto, and S. Evoy, "A review of piezoelectric polymers as functional materials for electromechanical transducers," *Smart Materials and Structures* **23**, 033001 (2014).
65. R. E. Newnham, D. P. Skinner, and L. E. Cross, "Connectivity and piezoelectric-pyroelectric composites," *Materials Research Bulletin* **13**, 525–536 (1978).
66. E. L. Nix and I. M. Ward, "The measurement of the shear piezoelectric coefficients of polyvinylidene fluoride," *Ferroelectrics* **67**, 137–141 (1986).
67. K. Omote, H. Ohigashi, and K. Koga, "Temperature dependence of elastic, dielectric, and piezoelectric properties of single crystalline films

Downloaded From: https://www.spiedigitallibrary.org/ebooks/ on 07 Mar 2022
Terms of Use: https://www.spiedigitallibrary.org/terms-of-use

of vinylidene fluoride trifluoroethylene copolymer," *Journal of Applied Physics* **81**(6), 2760–2769 (1997).
68. Y. Qi and M. C. McAlpine, "Nanotechnology-enabled flexible and biocompatible energy harvesting," *Energy and Environmental Science* **3**, 1275–1285 (2010).
69. Q. M. Zhang, V. Bharti, and G. Kavarnos, "Poly (Vinylidene Fluoride) (PVDF) and its Copolymers," in *Encyclopedia of Smart Materials*, M. Schwartz, Ed., Vol. **1–2**, John Wiley & Sons, pp. 807–825 (2002).
70. Q. Zhang, J. Lu, F. Saito, and M. Baron, "Mechanochemical solid-phase reaction between polyvinylidene fluoride and sodium hydroxide," *Journal of Applied Polymer Science* **81**(9), 2249–2252 (2001).
71. Q. M. Zhang, V. Bharti, and X. Zhao, "Giant electrostriction and relaxor ferroelectric behavior in electron-irradiated poly (vinylidene fluoride-trifluoroethylene) copolymer," *Science* **280**(5372), 2101–2104 (1998).
72. K. H. Lam and H. L. W. Chan, "Piezoelectric and pyroelectric properties of 65PMN-35PT/P(VDF-TrFE) 0–3 composites," *Composites Science and Technology* **65**, 1107–1111 (2005).
73. R. E. Newnham, "Composite electroceramics," *Annual Review of Materials Research* **16**, 47–68 (1986).
74. W. Nhuapeng and T. Tunkasiri, "Properties of 0-3 lead zirconate titanate-polymer composites prepared in a centrifuge," *Journal of the American Ceramic Society* **85**, 700–702 (2002).
75. W. A. Smith and B. A. Auld, "Modeling 1-3 composite piezoelectrics: thickness-mode oscillations," *IEEE Transactions on Ultrasonics, Ferroelectrics, and Frequency* **38**(1), 40–47 (1991).
76. F. Mohammadi, A. L. Kholkin, B. Jadidian, and A. Safari, "High-displacement spiral piezoelectric actuators," *Applied Physics Letter*s 75, 2488–90 (1999).
77. A. Safari, V. F. Janas, and A. Bandyopadhyay, "Development of fine-scale piezoelectric composites for transducers," *AIChE Journal* **43**, 2849–56 (1997).
78. S. Zhang and F. Li, "High performance ferroelectric relaxor-$PbTiO_3$ single crystals: status and perspective," *Journal of Applied Physics* **111**, 031301, 1–50 (2012).
79. H. Fu and R. E. Cohen, "Polarization rotation mechanism for ultrahigh electromechanical response in single-crystal piezoelectrics," *Nature* **403**, 281–283 (2000).
80. X. Huo, S. Zhang, G. Liu, R. Zhang, J. Luo, R. Sahul, W. Cao, and T. Shrout, "Elastic, dielectric and piezoelectric characterization of single domain PIN-PMN-PT: Mn crystals," *Journal of Applied Physics* **12**, 124113 (2012).

Downloaded From: https://www.spiedigitallibrary.org/ebooks/ on 07 Mar 2022
Terms of Use: https://www.spiedigitallibrary.org/terms-of-use

81. S. E. Park and W. Hackenberger, "High performance single crystals piezoelectrics: applications and issues," *Current Opinion in Solid State & Materials Science* **6**, 11–18 (2002).
82. S. E. Park and T. R. Shrout, "Ultrahigh strain and piezoelectric behavior in relaxor based ferroelectric single crystals," *Journal of Applied Physics* **82**, 1804–1811 (1997).
83. S. E. Park and T. R. Shrout, "Relaxor based ferroelectric single crystals for electro-mechanical actuators," *Material Research Innovations* **1**, 20–25 (1997).
84. Z. Ye, Ed., *Handbook of Advanced Dielectric, Piezoelectric and Ferroelectric Materials—Synthesis, Characterization and Applications*, Woodhead, Cambridge, UK (2008).
85. S. J. Zhang and T. R. Shrout, "Relaxor-PT single crystals: observations and developments," *IEEE Transactions on Ultrasonics, Ferroelectrics, and Frequency* **57**(10), 2138–2146 (2010).
86. S. J. Zhang, J. Luo, D. W. Snyder, and T. R. Shrout, "High performance, high temperature piezoelectric crystals," in *Handbook of Advanced Dielectric, Piezoelectric and Ferroelectric Materials – Synthesis, Characterization and Applications*, Z. G. Ye, Ed., Woodhead, Cambridge, UK, pp. 130–157 (2008).
87. R. Zhang, B. Jiang, W. Jiang, and W. Cao, "Complete set of elastic, dielectric, and piezoelectric coefficients of $0.93Pb(Zn_{1/3}Nb_{2/3})O_3$-$0.07PbTiO_3$ single crystal poled along [011]," *Applied Physics Letters*, **93**, 242908 (2006).
88. R. Zhang, B. Jiang, and W. Cao, "Superior d^*_{32}, and k^*_{32} coefficients in $0.955Pb(Zn_{1/3}Nb_{2/3})O_3$-$0.045PbTiO_3$, and $0.92Pb(Zn_{1/3}Nb_{2/3})O_3$-$0.08PbTiO_3$ single crystals poled along [011]," *Journal of Physics and Chemistry of Solids*, **65**, 1083–1086 (2004).
89. S. J. Zhang, L. Lebrun, D. Y. Jeong, C. A. Randall, Q. M. Zhang, and T. R. Shrout, "Growth and characterization of Fe-doped $Pb(Zn_{1/3}Nb_{2/3})O_3$–$PbTiO_3$ single crystals," *Journal of Applied Physics* **93**, 9257–9262 (2003).
90. R. Zhang, B. Jiang, and W. W. Cao, "Elastic, piezoelectric, and dielectric properties of multidomain $0.67Pb(Mg_{1/3}Nb_{2/3})O_3$-$0.33PbTiO_3$ single crystal," *Journal of Applied Physics* **90**, 3471–3475 (2001).
91. A. Amin, "Electromechanical properties of high coupling single crystals under large electric drive and uniaxial compression," *IEEE Transactions on Ultrasonics, Ferroelectrics, and Frequency* **52**(10), 1632–1637 (2005).
92. W. W. Cao, "Full-set material properties and domain engineering principles of ferroelectric single crystals," in *Handbook of Advanced Dielectric, Piezoelectric and Ferroelectric Materials—Synthesis, Characterization and Applications*, Z. G. Ye, Ed., Woodhead, Cambridge, UK, 235–265 (2008).

Downloaded From: https://www.spiedigitallibrary.org/ebooks/ on 07 Mar 2022
Terms of Use: https://www.spiedigitallibrary.org/terms-of-use

93. H. Cao, V. H. Schmidt, R. Zhang, W. Cao, and H. Luo, "Elastic, piezoelectric, and dielectric properties of $0.58Pb(Mg_{1/3}\ Nb_{2/3})O_3$-$0.42PbTiO_3$ single crystal," *Journal of Applied Physics* **96**, 549–554 (2004).
94. J. Chen and R. Panda, "Review: Commercialization of piezoelectric single crystals for medical imaging applications," *IEEE International Ultrasonics Symposium,* 235–240 (2005).
95. M. Davis, "Picturing the elephant: Giant piezoelectric activity and the monoclinic phases of relaxor ferroelectric single crystals," *Journal of Electroceramics* **19**(1), 25–47 (2007).
96. M. Davis, "Phase Transitions, Anisotropy and Domain Engineering: The Piezoelectric Properties of Relaxor-Ferroelectric Single Crystals," Ph.D. dissertation, Swiss Federal Institute of Technology (EPFL), Lausanne, Switzerland (2006).
97. S. X. Dong, L. Yan, D. Viehland, X. N. Jiang, and W. S. Hackenberger, "A piezoelectric single crystal traveling wave step motor for low temperature application," *Applied Physics Letters* **98**(15), 153504 (2008).
98. J. Kuwata, K. Uchino, and S. Nomura, "Phase transitions in the $Pb(Zn_{1/3}Nb_{2/3})O_3$-$PbTiO_3$ system," *Japanese Journal of Applied Physics* **21**, 1298–1302 (1982).
99. F. Li, S. J. Zhang, Z. Xu, Z. Y. Wei, and T. R. Shrout, "Critical property in relaxor-PT single crystals—Shear piezoelectric response," *Advanced Functional Materials* **21**(11), 2118–2128 (2011).
100. T. Q. Liu, "Electromechanical Behavior of Relaxor Ferroelectric Crystals," Ph.D. dissertation, Georgia Institute of Technology (2004).
101. S. F. Liu, S. E. Park, T. R. Shrout, and L. E. Cross, "Electric field dependence of piezoelectric properties for rhombohedral $0.955Pb(Zn_{1/3}Nb_{2/3})O_3$-$0.045PbTiO_3$ single crystals," *Journal of Applied Physics* **85**, 2810–2814 (1999).
102. S. Wada, S. Suzuki, T. Noma, T. Suzuki, M. Osada, M. Kakihana, S. E. Park, L. E. Cross, and T. R. Shrout, "Enhanced piezoelectric property of barium titanate single crystals with engineered domain configurations," *Japanese Journal of Applied Physics* **38**, 5505–5511 (1999).
103. S. Wada, S. E. Park, L. E. Cross, and T. R. Shrout, "Engineered domain configuration in rhombohedral PZN-PT single crystals and their ferroelectric related properties," *Ferroelectrics* **221**, 147–155 (1999).
104. G. S. Xu, K. Chen, D. F. Yang, and J. B. Li, "Growth and electrical properties of large size PIN-PMN-PT crystals prepared by the vertical Bridgman technique," *Applied Physics Letters* **90**(3), 032901 (2007).
105. S. J. Zhang, F. Li, J. Luo, R. Sahul, and T. R. Shrout, "Relaxor-$PbTiO_3$ single crystals for various applications," *IEEE Trans. on Ultrasonics Ferroelectrics, and Frequency Control* **60**(8), 1572–1580 (2012).

Downloaded From: https://www.spiedigitallibrary.org/ebooks/ on 07 Mar 2022
Terms of Use: https://www.spiedigitallibrary.org/terms-of-use

106. S. J. Zhang, G. Liu, W. H. Jiang, J. Luo, W. W. Cao, and T. R. Shrout, "Characterization of single domain PIN-PMN-PT crystals with monoclinic phase," *Journal of Applied Physics* **110**(6), 064108 (2011).
107. S. J. Zhang, S. M. Lee, D. H. Kim, H. Y. Lee, and T. R. Shrout, "Characterization of Mn-modified $Pb(Mg_{1/3}Nb_{2/3})$ O_3-$PbZrO_3$-Pb-TiO_3 single crystals for high power broad bandwidth transducers," *Applied Physics Letters* **93**(12), 122908 (2008).
108. M. A. Karami, O. Bilgen, D. J. Inman, and M. I. Friswell, "Experimental and analytical parametric study of single-crystal unimorph beams for vibration energy harvesting," *IEEE Transactions on Ultrasonics, Ferroelectrics, and Frequency Control* **58**(7), 1508–1520 (2011).
109. M. A. Karami and D. J. Inman, "Parametric study of zigzag microstructure for vibrational energy harvesting," *Journal of Microelectromechanical Systems* **21**(1), 145–160 (2011).
110. M. A. Karami and D. J. Inman, "Analytical modeling and experimental verification of the vibrations of the zigzag microstructure for energy harvesting," *Journal of Vibration and Acoustics* **133**(1), 011002 (2011).
111. P. Rakbamrunga, M. Lallart, D. Guyomar, N. Muensita, C. Thanachayanont, C. Lucatd, B. Guiffard, L. Petit, and P. Sukwisuta, "Performance comparison of PZT and PMN–PT piezoceramics for vibration energy harvesting using standard or nonlinear approach," *Sensors and Actuators* **163**(2), 493–500 (2010).
112. M. A. Karami and D. J. Inman "Electromechanical modeling of the low-frequency zigzag micro-energy harvester," *Journal of Intelligent Material Systems and Structures* **22**(3), 271–282 (2011).
113. B. Ren, Y. Y. Zhang, Q. H. Zhang, X. B. Li, W. N. Di, X. Y. Zhao, H. S. Luo, and S. Wing, "Energy harvesting using multilayer structure based on $0.71Pb(Mg_{1/3}Nb_{2/3})O_3$–$0.29PbTiO_3$ single crystal," *Applied Physics Material Science and Processing* **100**(1), 125–128 (2010).
114. S. J. Zhang, N. P. Sherlock, R. J. Meyer, Jr., and T. R. Shrout, "Crystallographic dependence of loss in domain engineered relaxor-PT single crystals," *Applied Physics Letters* **94**(16), 162906 (2009).
115. Y. Saito, H. Takao, I. Tani, T. Nonoyama, K. Takatori, T. Homma, T. Nagaya, and M. Nakamura, "Lead-free piezoceramics," *Nature* **432**, 84–87 (2004).
116. T. R. Shrout and S. J. Zhang, "Lead-free piezoelectric ceramics – alternatives for PZT," *Journal of Electroceramics* **19**, 111–124 (2007).
117. D. Maurya, M. Murayama, and S. Priya, "Synthesis and characterization of $Na_2Ti_6O_{13}$ whiskers and their transformation to $(1 - x)$ $Na_{0.5}Bi_{0.5}TiO_{3-x}BaTiO_3$ ceramics," *Journal of the American Ceramic Society* **94**(9), 2857–2871 (2011).
118. D. Maurya, M. Murayama, A. Pramanick, W. T. Reynolds, K. An, and S. Priya, "Origin of high piezoelectric response in A-site disordered

Downloaded From: https://www.spiedigitallibrary.org/ebooks/ on 07 Mar 2022
Terms of Use: https://www.spiedigitallibrary.org/terms-of-use

morphotropic phase boundary composition of lead-free piezoelectric $0.93(Na_{0.5}Bi_{0.5})TiO_3$–$0.07BaTiO_3$," *Journal of Applied Physics* **113**, 114101 (2013).
119. D. Maurya, A. Pramanick, K. An, and S. Priya, "Enhanced piezoelectricity and nature of electric-field induced structural phase transformation in textured lead-free piezoelectric $Na_{0.5}Bi_{0.5}TiO_3$-$BaTiO_3$ ceramics," *Applied Physics Letters* **100**, 172906 (2012).
120. H. Nagata, M. Yoshida, Y. Makiuchi, and T. Takenaka, "Large piezoelectric constant and high curie temperature of lead-free piezoelectric ceramic ternary system based on bismuth sodium titanate-bismuth potassium titanate-barium titanate near the morphotropic phase boundary," *Japanese Journal of Applied Physics* **42**(12), 7401–7403 (2003).
121. P. Pookmanee, G. Rujijanagul, S. Ananta, R. B. Heimann, and S. Phanichphant, "Effect of sintering temperature on microstructure of hydrothermally prepared bismuth sodium titanate ceramics," *Journal of the European Ceramic Society* **24**, 517–520 (2004).
122. L. Zheng, X. Yi, S. Zhang, W. Jiang, B. Yang, R. Zhang, and W. Cao, "Complete set of material constants of $0.95(Na_{0.5}Bi_{0.5})TiO_3$-$0.05BaTiO_3$ lead-free piezoelectric single crystal and the delineation of extrinsic contributions," *Applied Physics Letters* **103**, 122905 (2013).
123. G. A. Smolenskii, V. A. Isupov, A. I. Agranovskaya, and N. N. Krainik, "New ferroelelectrics of complex composition," *Soviet Physics - Solid State* **2**, 2651–2654 (1961).
124. A. Herabut and A. Safari, "Processing and electromechanical properties of $(Bi_{0.5}Na_{0.5})_{1-1.5X}$ $LaXTiO_3$ ceramics," *Journal of the American Ceramic Society* **80**, 2954–2958 (1997).
125. H. Nagata and T. Takenaka, "Lead-free piezoelectric ceramics of $(Bi_{1/2}Na_{1/2})TiO_3$-$KNbO_3$-$1/2(Bi_2O_3.Sc_2O_3)$ system," *Japanese Journal of Applied Physics* **37**, 5311–5314 (1998).
126. T. Takenaka, K. Sakata, and O. Toda, "Piezoelectric properties of $(Bi_{1/2}Na_{1/2})TiO_3$-based ceramics," *Ferroelectrics* **106**, 375–380 (1990).
127. B. W. Barron, G. Li, and G. H. Haertling, "Temperature dependent characteristics of CERAMBOW actuators," *Proc. of the 10th IEEE International Symposium on the Application of Ferroelectrics* **1**, East Brunswick, New Jersey, pp. 305–308 (1996).
128. V. Bedekar, J. Oliver, S. Zhang, and S. Priya, "Comparative study of energy harvesting from high temperature piezoelectric single crystals," *Japanese Journal of Applied Physics* **48**, 091406 (2009).
129. Z. Chang, S. Sherrit, X. Bao, and Y. Bar-Cohen, "Design and analysis of ultrasonic horn for USDC (Ultrasonic/Sonic Driller/Corer)," *Proc. SPIE* **5388**, 320–326 (2004) [doi: 10.1117/12.540000].
130. S. Sherrit, "Smart material/actuator needs in extreme environments in space," *Proc. SPIE* **5761**, 335–346 (2005) [doi: 10.1117/12.606475].

Downloaded From: https://www.spiedigitallibrary.org/ebooks/ on 07 Mar 2022
Terms of Use: https://www.spiedigitallibrary.org/terms-of-use

131. S. Sherrit, X. Bao, Y. Bar-Cohen, and Z. Chang, "Resonance analysis of high temperature piezoelectric materials for actuation and sensing," *Proc. SPIE* **5388**, 411–420 (2004) [doi: 10.1117/12.540102].
132. B. S. Kim, J. H. Park, H. Ahn, D. Liu, and D. J. Kim, "Temperature effects on output power of piezoelectric vibration energy harvesters," *Microelectronics Journal* **42**, 988–991 (2011).
133. D. Damjanovic, "Materials for high temperature piezoelectric transducers," *Current Opinion in Solid State & Materials Science* **3**(5), 469–473 (1998).
134. M. Minary, R. A. Bernal, I. Kuljanishvili, V. Parpoil, and H. D. Espinosa, "Individual GaN nanowires exhibit strong piezoelectricity in 3D," *Nano Letters* **12**(2), 970–976 (2011).
135. G. L. Messing, S. Trolier-McKinstry, E. M. Sabolsky, C. Duran, S. Kwon, B. Brahmaroutu, P. Park, H. Yilmaz, P. W. Rehrig, K. B. Eitel, E. Suvaci, M. Seabaugh, and K. S. Oh, "Templated grain growth of textured piezoelectric ceramics," *Critical Reviews in Solid State and Materials Sciences* **29**, 45–96 (2004).
136. Y. Yan, Y. Zhou, and S. Priya, "Enhanced electromechanical coupling in $Pb(Mg_{1/3}Nb_{2/3})O_3$-$PbTiO_3$ C radially textured cylinders," *Applied Physics Letters* **104**, 012910 (2014).
137. Y. Yan, K. H. Cho, D. Maurya, A. Kumar, S. Kalinin, A. Khachaturyan, and S. Priya, "Giant energy density in [001]-textured Pb $(Mg_{1/3}Nb_{2/3})$ O_3-$PbZrO_3$-$PbTiO_3$ piezoelectric ceramics," *Applied Physics Letters* **102**(4), 042903 (2013).
138. Y. Yan, K. H. Cho, and S. Priya, "Piezoelectric properties and temperature stability of Mn-doped $Pb(Mg_{1/3}Nb_{2/3})$-$PbZrO_3$-$PbTiO_3$ textured ceramics," *Applied Physics Letters* **100**, 132908 (2012).
139. Y. Yan, Y. Wang, and S. Priya, "Electromechanical behavior of [001]-textured Pb $(Mg_{1/3}Nb_{2/3})O_3$-$PbTiO_3$ ceramics," *Applied Physics Letters* **100**, 192905 (2012).
140. M. Allahverdi, S. C. Danforth, M. Jafari, and A. Safari, "Processing of advanced electroceramic components by fused deposition technique," *Journal of the European Ceramic Society* **21**, 1485–1490 (2001).
141. A. Bandyopadhyay, R. K. Panda, V. F. Janas, M. K. Agarwala, S. C. Danforth, and A. Safari, "Processing of piezocomposites by fused deposition technique," *Journal of the American Ceramic Society* **80**, 1366–1372 (1997).
142. J. Cesarano III and P. Calvert, "Freeforming objects with low-binder slurry," U.S. Patent No. 6,027,326 (2000).
143. V. F. Janas and A. Safari, "Overview of fine-scale piezoelectric ceramic/polymer composite processing," *Journal of the American Ceramic Society* **78**, 2945–2955 (1995).
144. R. E. Newnham, "Composites electroceramics," *Ferroelectrics* **68**, 1–32 (1986).

Downloaded From: https://www.spiedigitallibrary.org/ebooks/ on 07 Mar 2022
Terms of Use: https://www.spiedigitallibrary.org/terms-of-use

145. R. E. Newnham, L. J. Bowen, K. A. Klicker, and L. E. Cross, "Composite piezoelectric transducers," *Materials Science and Engineering* **2**, 93–106 (1980).
146. K. Rittenmyer, T. Shrout, W. A. Schulze, and R. E. Newnham, "Piezoelectric 3–3 composites," *Ferroelectrics* **41**, 189–195 (1982).
147. J. E. Smay, J. Cesarano III, B. A. Tuttle, and J. A. Lewis, "Directed colloidal assembly of linear annular lead zirconate titanate array," *Journal of the American Ceramic Society* **87**(2), 293–295 (2004).
148. W. A. Smith and A. A. Shaulov, "Composite piezoelectrics: basic research to a practical device," *Ferroelectrics* **87**, 309–20 (1988).
149. J. F. Tressler, S. Alkpu, A. Dogan, and R. E. Newnham, "Functional composites for sensors, actuators and transducers," *Composites Part A* **30A**, 477–82 (1999).
150. C. M. T. Tien and N. S. Goo, "Use of a piezocomposite generating element in energy harvesting," *Journal of Intelligent Materials Systems and Structures* **21**(14), 1427–1436 (2010).
151. D. Isarakorn, A. Sambri, P. Janphuang, D. Briand, S. Gariglio, J. M. Triscone, F. Guy, J. W. Reiner, C. H. Ahn, and N. F. de Rooij, "Epitaxial piezoelectric MEMS on silicon," *Journal of Micromechanics and Microengineering* **20**, 055008 (2010).
152. A. Sambri, D. Isarakorn, A. Torres-Pardo, S. Gariglio, P. Janphuang, D. Briand, O. Stephan, J. W. Reiner, J. M. Triscone, N. F. de Rooij, and C. H. Ahn, "Epitaxial Piezoelectric $Pb(Zr_{0.2}\ Ti_{0.8})O_3$ thin films on silicon for energy harvesting devices," *Smart Materials Research* **2012**, 426048 (2012).
153. R. Andosca, T. G. McDonald, V. Genova, S. Rosenberg, J. Keating, C. Benedixen, and J. Wu, "Experimental and theoretical studies of MEMS piezoelectric vibrational energy harvesters with mass loading," *Sensors and Actuators A* **178**, 76–87 (2012).
154. R. Elfrink, T. M. Kamel, M. Goedbloed, S. Matova, D. Hohlfeld, Y. V. Andel, and R. V. Schaijk, "Vibration energy harvesting with aluminum nitride-based piezoelectric devices," *Journal of Micromechanics and Microengineering* **19**(9), 094005 (2009).
155. L. M. Miller, "Micro-scale Piezoelectric Vibration Energy Harvesting: From Fixed-Frequency to Adaptable-Frequency Devices," Ph.D. thesis, University of California, Berkley (2012).
156. G. Piazza, "Piezoelectric Aluminum Nitride Vibrating RF MEMS for Radio Front-End Technology," Ph.D. dissertation, University of California, Berkeley (2005).
157. P. J. Stephanou, "Piezoelectric Aluminum Nitride MEMS Resonators for RF Signal Processing," Ph.D. dissertation, University of California, Berkeley (2006).

Downloaded From: https://www.spiedigitallibrary.org/ebooks/ on 07 Mar 2022
Terms of Use: https://www.spiedigitallibrary.org/terms-of-use

158. J. Y. Zhang, Z. P. Cao, and H. Kuwano, "Fabrication of low-residual-stress AlN thin films and their application to microgenerators for vibration energy harvesting," *Japanese Journal of Applied Physics* **50**(9), 09ND18 (2011).
159. B. Amin, *Induction Motors: Analysis and Torque Control (Power Systems)*, Springer, New York (2010).
160. N. Ida, *Engineering Electromagnetics*, Third Edition, Springer, New York (2010).
161. K. K. Kim, F. Cottone, S. Goyal, and J. Punch, "Energy scavenging for energy efficiency in networks and applications," *Bell Labs Technical Journal* **15**(2), 7–29 (2010).
162. D. Spreemann and T. Manoli, *Electromagnetic Vibration Energy Harvesting Devices: Architectures, Design, Modeling and Optimization, Springer Series in Advanced Microelectronics*, Springer, New York (2014).
163. A. C. Waterbury, "Vibration Harvesting Using Electromagnetic Transduction," Ph.D. thesis, University of California, Berkeley (2011).
164. *Basic AC Electrical Generators*, American Society of Power Engineers, Inc., Lawrenceburg, Indiana, http://www.asope.org/pdfs/AC_Electrical_Generators_ASOPE.pdf.
165. H. Yoshihide, *Handbook of Power System Engineering*, John Wiley & Sons, Hoboken, New Jersey (2007).
166. R. Amirtharajah and A. P. Chandrakasan, "Self-powered signal processing using vibration-based power generation," *IEEE Journal of Solid-State Circuits* **33**, 687–95 (1998).
167. S. P. Beeby and T. O. Donnell, "Electromagnetic Energy Harvesting," in *Energy Harvesting Technologies*, S. Priya and D. J. Inman, Eds., Springer, New York, pp. 129–161 (2009).
168. N. N. H. Ching, G. M. H. Chan, W. J. Li, H. Y. Wong, and P. H. W. Leong, "PCB integrated micro-generator for wireless systems," *Proc. International Symposium on Smart Structures and Microsystems*, August 2000, pp. 19–21 (2000).
169. M. El-hami, R. Glynne-Jones, N. M. White, M. Hill, S. Beeby, E. James, A. D. Brown, and J. N. Ross, "Design and fabrication of a new vibration-based electromechanical power generator," *Sensors Actuators A* **92**, 335–44 (2001).
170. F. Henningsen and A. Josefsson, "Design and Verification of Vibration Energy Harvester," M.S. thesis, Chalmers University of Technology, Goteborg, Sweden (2014).
171. A. M. Hedayetullah, "Analysis of Piezoelectric Energy Harvesting for Bridge Health Monitoring Systems," Doctoral dissertation, University of Wales, Cardiff, Wales, UK (2010).

Downloaded From: https://www.spiedigitallibrary.org/ebooks/ on 07 Mar 2022
Terms of Use: https://www.spiedigitallibrary.org/terms-of-use

172. L. Mateu and F. Moll, "Review of energy harvesting techniques and applications for microelectronics," *Proc. SPIE* **5837**, 359–373 (2005) [doi: 10.1117/12.613046].
173. L. M. Miller, "Vibration Energy Harvesting from Wideband and Time-Varying Frequencies," in *Micro Energy Harvesting*, D. Briand, E. Yeatman, and S. Roundy, Eds., Wiley-VCH, Weinheim, Germany, pp. 223–244 (2015).
174. K. Sasaki, Y. Osaki, J. Okazaki, H. Hosaka, and K. Itao, "Vibration-based automatic power-generation system," *Micro- and Nanosystems Information Storage and Processing Systems* **11**, 965–969 (2005).
175. C. B. Williams and R. B. Yates, "Analysis of a micro-electric generator for microsystems," *Sensors Actuators A* **52**, 8–11 (1996).
176. S. P. Beeby, R. N. Torah, M. J. Tudor, P. Glynne-Jones, T. O'Donnell, C. R. Saha, and S. Roy, "A micro electromagnetic generator for vibration energy harvesting," *Journal of Micromechanics and Micro-engineering* **17**, 1257–1265 (2006).
177. N. N. H. Ching, H. Y. Wong, W. J. Li, P. H. W. Leong, and Z. Wen, "A laser-micromachined vibrational to electrical power transducer for wireless sensing systems," *Sensors and Actuators A* **97–98**, 685–690 (2002).
178. P. Glynne-Jones, M. J. Tudor, S. P. Beeby, and N. M. White, "An electromagnetic, vibration-powered generator for intelligent sensor systems," *Sensors and Actuators A* **110**, 344–449 (2004).
179. E. Koukarenko, S. P. Beeby, M. J. Tudor, N. M. White, T. O'Donnell, T. Saha, S. Kulkani, and S. Roy, "Microelectromechanical systems vibration powered electromagnetic generator for wireless sensor applications," *Microsystem Technologies* **12**(11), 1071–1077 (2006).
180. H. Kulah and K. Najafi, "Energy scavenging from low-frequency vibrations by using frequency up-conversion for wireless sensor applications," *IEEE Sensors Journal* **8**(3), 261–268 (2008).
181. H. Kulah and K. Najafi, "An electromagnetic micro power generator for low-frequency environmental vibrations," *Micro Electro Mechanical Systems—17th IEEE Conference on MEMS (Maastricht)*, pp. 237–240 (2004).
182. M. Mizuno and D. Chetwynd, "Investigation of a resonance microgenerator," *Journal of Micromechanics and Microengineering* **13**, 209–216 (2003).
183. C. T. Pan and T. T. Wu, "Development of a rotary electromagnetic microgenerator," *Journal of Micromechanics and Microengineering* **17**, 120–8 (2007).
184. S. J. Roundy, "Energy Scavenging for Wireless Sensor Nodes with a Focus on Vibration to Electricity Conversion," Ph.D. dissertation, University of California, Berkeley (2003).

Downloaded From: https://www.spiedigitallibrary.org/ebooks/ on 07 Mar 2022
Terms of Use: https://www.spiedigitallibrary.org/terms-of-use

185. C. R. Saha, T. O'Donnell, H. T. Loder, S. P. Beeby, and M. J. Tudor, "Optimization of an electromagnetic energy harvesting device," *IEEE Transactions on Magnetics* **42**(10), 3509–3511 (2006).
186. C. Serre, A. Perez-Rodriguez, N. Fondevilla, J. R. Morante, J. Montserrat, and J. Esteve, "Vibrational energy scavenging with Si technology electromagnetic inertial microgenerators," *Microsystem Technologies* **13**, 1449–661 (2007).
187. C. Shearwood and R. B. Yates, "Development of a resonant electromagnetic micro-generator," *Electronic Letters* **33**(22), 1883–1884 (1997).
188. S. R. Snarski, R. G. Kasper, and A. B. Bruno, "Device for electromagnetohydrodynamic (EMHD) energy harvesting," *Proc. SPIE* **5417**, 147–161 (2004) [doi: 10.1117/12.545170].
189. T. von Buren and G. Troster, "Design and optimization of a linear vibration-driven electromagnetic micro-power generator," *Sensors and Actuators A* **135**, 765–75 (2007).
190. C. B. Williams, C. Shearwood, M. A. Harradine, P. H. Mellor, T. S. Birch, and R. B. Yates, "Development of an electromagnetic micro-generator," *IEE Proc. - Circuits Devices and Systems* **148**(6), 337–42 (2001).
191. C. B. Williams, A. Pavic, R. S. Crouch, and R. C. Wood, "Feasibility study of vibration-electric generator for bridge vibration sensors," *Proc. 16th International Modal Analysis Conference (IMAC)* **32**, 1111–1117 (1998).
192. R. D. Knight, *Physics for Scientists and Engineers: A Strategic Approach*, Pearson Addison Wesley, Boston (2008).
193. J. Borwick, *Loudspeaker and Headphone Handbook*, Butterworth and Co., London (1988).
194. W. P. Mason, *Electromechanical Transducers and Wave Filters*, D. Van Nostrand Company, New York (1942).
195. S. Boisseau, G. Despesse, and B. A. Seddik, "Electrostatic conversion for vibration energy harvesting," *INTECH Open Access Publisher* (2012).
196. Y. Chiu and V. F. G. Tseng, "Capacitive vibration-to-electricity energy converter with integrated mechanical switches," *Proc. Power MEMS*, 121–124 (2007).
197. G. Despesse, T. Jager, J. Chaillout, J. Leger, A. Vassilev, S. Basrour, and B. Chalot, "Fabrication and characterization of high damping electrostatic micro devices for vibration energy scavenging," *Proc. of Design, Test, Integration and Packaging of MEMS and MOEMS*, 386–390 (2005).
198. A. Harb, "Energy harvesting: state-of-the-art," *Renewable Energy* **36**, 2641–2654 (2011).
199. D. Hoffmann, B. Folkmer, and Y. Manoli, "Fabrication, characterization and modeling of electrostatic micro-generators," *Journal of Micromechanics and Microengineering* **19**, 094001 (2009).

Downloaded From: https://www.spiedigitallibrary.org/ebooks/ on 07 Mar 2022
Terms of Use: https://www.spiedigitallibrary.org/terms-of-use

200. M. E. Kiziroglou, C. He, and E. M. Yeatman, "Flexible substrate electrostatic energy harvester," *Electronics Letters* **45**, 166–167 (2010).
201. I. Kuehne, A. Frey, G. Eckstein, U. Schmid, and S. Haging, "Design and analysis of a capacitive vibration to electrical energy converter with built-in voltage," *Proc. of the 36th European Solid-State Device Research Conference*, 138–141 (2006).
202. S. Meninger, J. Mur-Miranda, J. Lang, A. Chandrakasan, A. Slocum, M. Schmidt, and R. Amirtharajah, "Vibration to electric energy conversion," *IEEE Transactions on Very Large Scale Integration Systems* **9**, 64–76 (2001).
203. S. Meninger, "A Low Power Controller for a MEMS Based Energy Converter," M.Sc. thesis, Massachusetts Institute of Technology (1999).
204. P. Miao, P. Mitcheson, P. D. Holmes, A. S. Yeatman, E. M. Green, T. C., and B. H. Stark, "MEMS inertial power generators for biomedical applications," *Microsystem Technologies* **12**, 1079–1083 (2006).
205. P. Miao, P. Micheson, A. Holmes, E. Yeatmam, T. Green, and B. Stark, "MEMs inertial power generators for biomedical applications," *Proc. Design, Test, Integration and Packaging of MEMS and MOEMS*, 295–298 (2005).
206. P. D. Mitcheson, P. Miao, B. H. Stark, E. M. Yeatman, A. S. Holmes, and T. C. Green, "MEMS electrostatic micropower generator for low frequency operation," *Sensors and Actuators A* **115**(2-3), 523–529 (2004).
207. P. D. Mitcheson, T. C. Green, E. M. Yeatman, and A. S. Holmes, "Architectures for vibration-driven micropower generators," *IEEE/ASME Journal of Microelectromechanical Systems* **13**(3), 429–440 (2004).
208. M. Miyazaki, H. Tanaka, G. Ono, T. Nagano, N. Ohkubo, T. Kawahara, and K. Yano, "Electric-energy generation using variable-capacitive resonator for power-free LSI: efficiency analysis and fundamental experiment," *International Symposium on Low Power Electronics and Design (ISLPED)*, 193–198 (2003).
209. Y. Naruse, N. Matsubara, K. Mabuchi, M. Izumi, and S. Suzuki, "Electrostatic micro power generation from low frequency vibration such as human motion," *Journal of Micromechanics and Microengineering* **19**, 094002 (2009).
210. J. A. Paradiso, "Systems for human-powered mobile computing," *Proc. of the 43rd Annual Conference on Design Automation*, 645–650 (2006).
211. S. Roundy, P. K. Wright, and J. M. Rabaey, *Energy Scavenging for Wireless Sensor Networks with Special Focus on Vibrations*, Kluwer Academic Publishers, Boston, Massachusetts (2004).
212. S. Roundy, P. Wright, and K. Pister, "Micro-electrostatic vibration-to-electricity converters," *ASME International Mechanical Engineering Congress and Exposition (IMECE)*, 1–10 (2002).

Downloaded From: https://www.spiedigitallibrary.org/ebooks/ on 07 Mar 2022
Terms of Use: https://www.spiedigitallibrary.org/terms-of-use

213. B. H. Stark, P. D. Mitcheson, P. Miao, T. C. Green, E. M. Yeatman, and A. S. Holmes, "Converter circuit design, semiconductor device selection and analysis of parasitics for micropower electrostatic generators," *IEEE Transactions on Power Electronics* **21**(1), 27–37 (2006).
214. B. H. Stark and T. C. Green, "Comparison of SOI power device structures in power converters for high-voltage, low-charge electrostatic microgenerators," *IEEE Transactions on Electron Devices* **52**(7), 1640–1648 (2005).
215. T. Sterken, P. Fiorini, K. Baert, G. Borghs, and R. Puers, "Novel design and fabrication of a MEMS electrostatic vibration scavenger," *Power MEMS Conference*, 18–21, Kyoto, Japan (2004).
216. T. Sterken, K. Baert, R. Puers, and S. Borghs, "Power extraction from ambient vibration," *Proc. of 3rd Workshop on Semiconductor Sensors and Actuators*, 680–683, Veldhoven, Netherlands (2002).
217. R. Tashiro, N. Kabei, K. Katayama, F. Tsuboi, and K. Tsuchiya, "Development of an electrostatic generator for a cardiac pacemaker that harnesses the ventricular wall motion," *International Journal of Artificial Organs* **5**(4), 239–245 (2002).
218. R. Tashiro, N. Kabei, K. Katayama, Y. Ishizuka, F. Tsuboi, and K. Tsuchiya, "Development of an electrostatic generator that harnesses the motion of a living body," *JSME International Journal Series C* **43**, 916–922 (2000).
219. E. O. Torres and G. A. Rincon-Mora, "Electrostatic energy-harvesting and battery charging CMOS system prototype," *IEEE Transactions on Circuits and Systems I* **56**(9), 1938–1948 (2009).
220. R. J. M. Vullers, R. van Schaijk, I. Doms, C. Van Hoof, and R. Mertens, "Micropower energy harvesting," *Solid State Electronics* **53**, 648–693 (2009).
221. B. C. Yen and J. H. Lang, "A variable capacitance vibration-to-electric energy harvester," *IEEE Transactions on Circuits and Systems* **53**(2), 288–295 (2006).
222. S. Roundy, "On the effectiveness of vibration-based energy harvesting," *Journal of Intelligent Material Systems and Structures* **16**, 809–823 (2005).
223. S. Roundy, E. S. Leland, J. Baker, E. Carleton, E. Reilly, E. Lai, B. Otis, J. M. Rabaey, P. K. Wright, and V. Sundararajan, "Improving power output for vibration-based energy scavengers," *IEEE Pervasive Computing Magazine* **4**(1), 28–36 (2005).
224. S. J. Roundy, P. K. Wright, and J. Rabaey, "A study of low level vibrations as a power source for wireless sensor nodes," *Computer Communications* **26**, 1131–1144 (2003).
225. R. Amirtharajah, S. Meninger, J. O. Mur-Miranda, A. P. Chandrakasan, and J. Lang, "A micropower programmable DSP powered using a

Downloaded From: https://www.spiedigitallibrary.org/ebooks/ on 07 Mar 2022
Terms of Use: https://www.spiedigitallibrary.org/terms-of-use

MEMS-based vibration-to-electric energy converter," *IEEE International Solid State Circuits Conference*, 362–363 (2000).
226. R. Amirtharajah, "Design of Low Power VLSI Systems Powered by Ambient Mechanical Vibration," Ph.D. thesis, Massachusetts Institute of Technology (1999).
227. A. Chandrakasan, R. Amirtharajah, R. J. Goodman, and W. Rabiner, "Trends in low power digital signal processing," *Proc. of the 1998 IEEE International Symposium on Circuits and Systems*, 604–607 (1998).
228. M. I. Haller and T. Khuri-Yakub, "A surface micromachined electrostatic ultrasound air transducer," *IEEE Ultrasonics Symposium*, 1241–1244 (1994).
229. W. Ma, M. Wong, and L. Ruber, "Dynamic simulation of an implemented electrostatic power micro-generator," *Proc. Design, Test, Integration and Packaging of MEMS and MOEMS*, 380–585 (2005).
230. S. Meninger, J. O. Mur-Miranda, R. Amirtharajah, A. P. Chandrakasan, and J. Lang, "Vibration-to-electric conversion," *Proc. International Symposium on Low Power Electronics and Design (ISLPED)*, 48–53 San Diego, California (1999).
231. M. Miyazaki, H. Tanaka, G. Ono, T. Nagano, N. Ohkubo, and T. Kawahara, "Electric-energy generation through variable-capacitive resonator for power-free LSI," *IEICE Transactions on Electronics* **E87C**, 549–55 (2004).
232. O. Heaviside, "Electromagnetic induction and its propagation. Electrization and electrification. Natural electrets," *The Electrician* **XIV**, Aug 7, pp. 230–231 (1885).
233. M. Eguchi, "On dielectric polarization," *Proc. of the Physico-Mathematical Society of Japan* **3**(1), 326–331 (1919).
234. S. Boisseau, G. Despesse, T. Ricart, E. Defay, and A. Sylvestre, "Cantilever-based electret energy harvesters," *Smart Materials and Structures* **20**, 105013 (2011).
235. J. A. Giacometti, S. Fedosov, and M. M. Costa, "Corona charging of polymers: recent advances on constant current charging," *Brazilian Journal of Physics* **29**, 269–279 (1999).
236. K. Ikezaki, M. Miki, and J. I. Tamura, "Thermally stimulated currents from ion-injected Teflon-FEP film electrets," *Japanese Journal of Applied Physics* **20**, 1741–1747 (1981).
237. P. Gunther, H. Ding, and R. Gerhard-Multhaupt, "Electret properties of spin-coated Teflon-AF films," *Proc. Electrical Insulation and Dielectric Phenomena*, 197–202 (1993).
238. R. Kressmann, G. Sessler, and P. Gunther, "Space-charge electrets," *Transactions on Dielectrics and Electrical Insulation* **3**, 607–623 (1996).
239. P. Kotrappa, "Long term stability of electrets used in electret ion chambers," *Journal of Electrostatics* **66**, 407–409 (2008).

Downloaded From: https://www.spiedigitallibrary.org/ebooks/ on 07 Mar 2022
Terms of Use: https://www.spiedigitallibrary.org/terms-of-use

240. G. M. Sessler, Ed., *Electrets*, Third Edition (in Two Volumes)," Laplacian Press, Morgan Hill, California (1999).
241. H. Amjadi, "Charge storage in double layers of thermally grown silicon dioxide and APCVD silicon nitride," *IEEE Transactions on Electrical Insulation* **6**, 852–857 (1999).
242. P. Gunther, "Charging, long-term stability and TSD measurements of SiO_2 electrets," *Transactions on Electrical Insulation* **24**(3), 439–442 (1989).
243. V. Leonov, P. Fiorini, and C. Van Hoof, "Stabilization of positive charge in SiO_2/Si_3N_4 electrets," *IEEE Transactions on Dielectrics and Electrical Insulation* **13**(5), 1049–1056 (2006).
244. K. Kashiwagi, K. Okano, Y. Morizawa, and Y. Suzuki, "Nano-cluster-enhanced high-performance perfluoro-polymer electrets for micro power generation," *Proc. Power MEMS* 169–72 (2010).
245. D. Rychkov and R. Gerhard, "Stabilization of positive charge on polytetrafluoroethylene electret films treated with titanium-tetrachloride vapor," *Applied Physics Letters* **98**, 122901 (2011).
246. Y. Sakane, Y. Suzuki, and N. Kasagi, "The development of a high-performance perfluorinated polymer electret and its application to micro power generation," *Journal of Micromechanics and Microengineering* **18**, 104011 (2008).
247. R. Schwödiauer, G. Neugschwandtner, S. Bauer-Gogonea, S. Bauer, and T. Rosenmayer, "Dielectric and electret properties of nanoemulsion spin-on polytetrafluoroethylene films," *Applied Physics Letters* **76**, 2612 (2000).
248. Q. Chen, "TFE electret negative charge stability after RF plasma treatment," *Journal of Physics D: Applied Physics* **35**(22), 2939–2944 (2002).
249. Y. Arakawa, Y. Suzuki, and N. Kasagi, "Micro seismic power generator using electret polymer film," *Proc. of Power MEMS*, 187–190, Kyoto, Japan (2004).
250. H. Lo and Y. C. Tai, "Parylene-based electret power generators," *Journal of Micromechanics and Microengineering* **18**, 104006 (2008).
251. F. Peano and T. Tambosso, "Design and optimization of a MEMS electret-based capacitive energy scavenger," *Journal of Microelectromechanical Systems* **14**, 435–529 (2005).
252. T. Sterken, P. Fiorinil, G. Altena, C. Van Hoof, and R. Puers, "Harvesting energy from vibrations by micromachined electret generator," *International Solid-State Sensors, Actuators and Microsystems Conference*, 129–132, Lyon, France (2007).
253. T. Sterken, P. Fiorini, K. Baert, R. Puers, and G. Borghs, "An electret-based electrostatic μ-generator," *Proc. 12th International Conference on Solid State Sensors, Actuators, and Microsystems*, 1291–1294 (2003).
254. T. Sterken, K. Baert, R. Puers, G. Borghs, and R. Mertens, "A new power MEMS component with variable capacitance," *Proc. Pan-Pacific Microelectronics Symposium*, 27–34 (2003).

Downloaded From: https://www.spiedigitallibrary.org/ebooks/ on 07 Mar 2022
Terms of Use: https://www.spiedigitallibrary.org/terms-of-use

255. Y. Suzuki, D. Miki, M. Edamoto, and M. Honzumi, "A MEMS electret generator with electrostatic levitation for vibration-driven energy-harvesting applications," *Journal of Micromechanics and Microengineering* **20**, 104002 (2010).
256. Z. Yang, J. Wang, and J. Zhang, "A high-performance micro electret power generator based on microball bearings," *Journal of Micromechanics and Microengineering* **21**, 065001 (2011).
257. A. Byrashev, W. P. Robbins, and B. Ziaie, "Low frequency wireless of microsystems using piezoelectric-magnetostrictive laminate composites," *Sensors and Actuators A: Physical* **114**, 244–249 (2004).
258. X. Dai, Y. Wen, P. Li, and G. Zhang, "Modeling, characterization and fabrication of vibration energy harvester using Terfenol-D/PZT/Terfenol-D composite transducer," *Sensors and Actuators A: Physical* **156**, 350–358 (2009).
259. M. J. Dapino, "On magnetostrictive materials and their use in adaptive structures," *Structural Engineering and Mechanics* **17**(3-4), 303–329 (2004).
260. E. Du Tremolet de Lacheisserie, *Magnetostriction: Theory and Applications of Magnetoelasticity*, CRC Press, Boca Raton, Florida (1993).
261. J. Huang, R. C. O'Handley, and D. Bono, "New, high-sensitivity, hybrid magnetostrictive/electroactive magnetic field sensors," *Proc. SPIE* **5050**, 229–237 (2003) [doi: 10.1117/12.484257].
262. M. E. Staley, "Development of a Prototype Magnetostrictive Energy Harvesting Device," M.S. thesis, University of Maryland, College Park (2005).
263. M. E. Staley and A. B. Flatau, "Characterization of energy harvesting potential of Terfenol-D and Galfenol," *Proc. SPIE* **5764**, 630–640 (2005) [doi: 10.1117/12.604871].
264. L. Wang and F. G. Yuan, "Vibration energy harvesting by magnetostrictive material," *Smart Materials and Structures* **17**, 045009 (2008).
265. L. Wang, "Vibration Energy Harvesting by Magnetostrictive Material for Powering Wireless Sensors," Ph.D. thesis, North Carolina State University (2007).
266. L. Wang and F. G. Yuan, "Energy harvesting by magnetostrictive material (MsM) for powering wireless sensors in SHM," *Proc. SPIE* **6529**, 652941 (2007) [doi: 10.1117/12.716506].
267. ETREMA Products, Inc., Ames, Iowa. www.etrema.com (accessed on May 31, 2015).
268. S. W. Meeks and J. C. Hill, "Piezomagnetic and elastic properties of metallic-glass alloys $Fe_{6\ 7}Co_{1\ 8}B_{1\ 4}Si_1$, and $Fe_{8\ 1}B_{13.5}Si_{3.5}C_2$," *Journal of Applied Physics* **54**, 6584–6593 (1983).
269. Metglas, Inc., Conway, South Carolina. www.metglas.com (accessed on May 31, 2015).

Downloaded From: https://www.spiedigitallibrary.org/ebooks/ on 07 Mar 2022
Terms of Use: https://www.spiedigitallibrary.org/terms-of-use

270. C. Modzelewski, H. T. Savage, L. T. Kabacoff, and A. E. Clark, "Magnetomechanical coupling and permeability in transversely annealed Metglas 2605 alloys," *IEEE Transactions on Magnetics* **17**, 2837–2839 (1981).
271. J. R. Farmer, "A Comparison of Power Harvesting Techniques and Related Energy Storage Issues," M.S. thesis, Virginia Polytechnic Institute and State University (2007).
272. G. Poulin, E. Sarraute, and F. Costa, "Generation of electrical energy for portable devices: comparative study of an electromagnetic and a piezoelectric system," *Sensors and Actuators A: Physical* **116**(3), 461–471 (2004).
273. M. G. Cain, M. Stewart, and M. G. Gee, "Degradation of piezoelectric materials," National Physical Laboratory Management Ltd., Teddington, Middlesex, UK, NPL Rep. SMMT (A) **148** (1999).
274. M. D. Hill, G. S. White, and C. S. Hwang, "Cyclic damage in lead zirconate titanate," *Journal of the American Ceramic Society* **79**(7), 1915–1920 (1996).
275. H. H. A. Krueger and D. Berlincourt, "Effects of high static stress on the piezoelectric properties of transducer materials," *Journal of the Acoustical Society of America* **33**, 1339–1344 (1961).
276. B. Zickgraf, G. A. Schneider, and F. Aldinger, "Fatigue behavior of multilayer piezoelectric actuators," *IEEE International Symposium on the Applications of Ferroelectrics*, 325–328 (1994).
277. S. R. Platt, S. Farritor, and H. Haider, "On low-frequency electric power generation with PZT ceramics," *IEEE/ASME Transactions on Mechatronics* **10**, 240–252 (2005).
278. F. Lowrie, M. Cain, and M. Stewart, "Time dependent behavior of piezoelectric materials," National Physical Laboratory Management Ltd., Teddington, Middlesex, UK, NPL Rep. SMMT (A) **151** (1999).
279. G. Yang, S. F. Liu, W. Ren, and B. K. Mukherjee, "Effects of uniaxial stress on the piezoelectric, dielectric, and mechanical properties of lead zirconate titanate piezoceramics," *Ferroelectrics* **262**, 1181–1186 (2001).
280. M. Badescu, S. Sherrit, X. Bao, J. Aldrich, Y. Bar-Cohen, and C. Jones, "Extended life PZT stack test fixture," *Proc. SPIE* **6929**, 692908 (2008) [doi: 10.1117/12.776483].
281. L. S. Bowen, T. Shrout, W. A. Shulze, and J. V. Biggers, "Piezoelectric properties of internally electroded PZT multilayers," *Ferroelectrics* **27**(1), 59–62 (1980).
282. M. Goldfarb and N. Celanovic, "Modeling piezoelectric stack actuators for control of micromanipulation," *IEEE Control Systems Magazine* **17**(3), 69–79 (1997).
283. Physik Instrumente (PI) GmbH & Co. KG, "Reliability & Lifetime of Multilayer Piezo Actuators," PI, Karlsruhe, Germany (2010).

Downloaded From: https://www.spiedigitallibrary.org/ebooks/ on 07 Mar 2022
Terms of Use: https://www.spiedigitallibrary.org/terms-of-use

284. S. M. Pilgrim, A. E. Bailey, M. Massuda, F. C. Poppe, and A. P. Ritter, "Fabrication and characterization of PZT multilayer actuators," *Ferroelectrics* **160**, 305–316 (1994).
285. S. Sherrit, X. Bao, C. M. Jones, J. B. Aldrich, C. J. Blodget, J. D. Moore, J. W. Carson, and R. Goullioud, "Piezoelectric multilayer actuator life test," *IEEE Transactions on Ultrasonics, Ferroelectrics and Frequency Control* **58**(4), 820–828 (2006).
286. S. Sherrit, C. M. Jones, J. B. Aldrich, C. Blodget, X. Bao, M. Badescu, and Y. Bar-Cohen, "Multilayer piezoelectric stack actuator characterization," *Proc. SPIE* **6929**, 692909 (2008) [doi: 10.1117/12.776396].
287. S. Sherrit, C. M. Jones, J. B. Aldrich, C. Blodget, X. Bao, M. Badescu, and Y. Bar-Cohen, "Multilayer piezoelectric stack actuator characterization," *Proc. Earth and Space Conf. ASCE*, Long Beach, California, March 2–4 (2008).
288. S. A. Wise and M. W. Hooker, "Characterization of multilayer piezoelectric actuators for use in active isolation mounts," *NASA Technical Brief* **4742**, Langley, Virginia (1997).

Downloaded From: https://www.spiedigitallibrary.org/ebooks/ on 07 Mar 2022
Terms of Use: https://www.spiedigitallibrary.org/terms-of-use

Chapter 3
Mechanical-to-Electrical Energy Transducer Interfacing Mechanisms

3.1 Introduction

Harvesting electrical energy from mechanical energy of a mechanical (host) system involves the use of transducers (electrical generators) such as those introduced in Chapter 2. In almost all cases an appropriate interfacing ("conditioning") mechanism is needed for effective integration of the transducer with the source of mechanical energy, i.e., the host system. Such interfacing or conditioning mechanisms may for example be needed to amplify force or displacement or to increase or decrease input displacement or frequency of an input oscillatory motion. Hereinafter, the term *interfacing mechanism* is intended to refer to those devices that are used to transfer mechanical energy to the transducer, while in some cases performing certain motion and/or force conditioning action. In addition, *motion* is intended to refer to translational as well as rotational motions. The term "force" is used to also indicate couple, moment, and torque when appropriate. The transfer of mechanical energy to a transducer may be direct or through other intermediate elements in which the mechanical energy may, for example, be stored in the form of potential or kinetic energy and when needed (or a threshold is reached) be released to the transducer for conversion to electrical energy.

A host system may provide mechanical energy for harvesting in the form of kinetic energy, potential energy, or a combination of both. For example, the "GravityLight," (declared as one of "The 25 Best Inventions of the Year 2013" by Time Magazine), harvests potential energy stored in a descending mass to generate electrical energy. The mechanical energy stored in a moving vehicle at the time of braking is in the form of kinetic energy, and a regenerative braking system converts it to electrical energy. In a mass–spring system vibrating at its natural frequency, the kinetic energy is converted to

Downloaded From: https://www.spiedigitallibrary.org/ebooks/ on 07 Mar 2022
Terms of Use: https://www.spiedigitallibrary.org/terms-of-use

potential energy, and vice versa, during each cycle of vibration; depending on the type of transducer that is used, only one of the forms of mechanical energy is usually converted to electrical energy (harvested). For example, if an electromagnetic-type transducer is used, mechanical energy is harvested only when it is in the form of kinetic energy. On the other hand, if the spring pressure on a piezoelectric element is used to generate electrical energy, mechanical energy of the vibrating mass–spring element is harvested only when it is in the form of potential energy.

Potential energy is stored in a mechanical system either due to elastic deformation of flexible elements such as springs or structure of the system, or in a mass element displaced (raised) against the gravitational field of the earth. For example, the work done to compress a spring is stored in the spring element as potential energy while accounting for losses due to internal damping of the spring material and other damping and/or friction losses during the spring compression. Similarly, the work done on a mass element to raise it a certain distance against the gravity-field-induced force is the potential energy that is stored in the mass element. The kinetic energy is the amount of work that has been done on an object to accelerate it from rest to its linear and/or rotational velocity state relative to the inertial reference frame.

As indicated in the previous chapter, piezoelectric, electromagnetic and electrostatic, and to a lesser degree magnetostrictive are the foremost motion-based transducers for generating electrical energy. When used in an energy-harvesting device to convert mechanical energy to electrical energy, each one of the above transducers demands a different interfacing/conditioning mechanism for their efficient operation. In many cases and depending on the characteristics of the mechanical-energy-providing host system, each transducer type and design may require a different interfacing mechanism for proper operation and without interfering with the operation of the host system. For these reasons, a wide range of interfacing mechanisms are needed to cover all possible applications.

The choice of interfacing methods and mechanisms is dependent on the characteristics and limitations imposed by the host system as well as the transducer type and design. The choice also depends on the criteria with which the effectiveness of the energy-harvesting device is to be measured for a given application. For example, from a mechanical-to-electrical energy conversion point of view, the criterion may be the amount of electrical power that the energy-harvesting device can provide when a continuous flow of mechanical energy is available to the device. However, when only one or relatively infrequent bursts of mechanical energy is available, the optimal energy-harvesting device may be the one that captures the maximum amount of available mechanical energy and stores it as potential and/or kinetic energy and converts it to electrical energy over a relatively long period of time. On the other hand, if the electrical energy generated by the same infrequent bursts

Downloaded From: https://www.spiedigitallibrary.org/ebooks/ on 07 Mar 2022
Terms of Use: https://www.spiedigitallibrary.org/terms-of-use

of mechanical energy is to be used directly, for example to generate heat in a resistive filament, the available mechanical energy may have to be converted to electrical energy as soon as it becomes available. In other words, even for the same host system, the optimal performance of the energy-harvesting device is dependent on the electrical load, that is, the system/device to be powered. In each case a different interfacing mechanism is generally needed to achieve effective overall performance of the system consisting of the energy-harvesting device as well as the powered device.

Thus, the designer should consider the host system, the interfacing mechanism, the system or device to be powered, and the electrical energy collection and conditioning electronics, which may include various sensors, processing units, driving software, and storage devices, as an integral system. Hereinafter in this book, the system consisting of all the above components, as well as driving software if any, is referred to as the "integrated system."

In this chapter, the reader is introduced to different basic methods and types of mechanisms for interfacing host systems to different types and designs of transducers for powering a given system or device type without being specific to any particular host or powered system. It is appreciated that the presented interfacing mechanisms and host system or device types to be powered are by no means exhaustive, particularly considering the fact that new applications and transducers are constantly being developed. The method of classifying interfacing mechanisms should however serve as a guide for their placement in the proper category. In addition, the systematic method being presented for selecting proper transducers and their host-system-interfacing mechanisms for effective overall system performance is general and should be expandable to include new components and applications.

In the process of selecting transducer type and design and a mechanism for interfacing it to the host system for powering a specific system or device, the designer must determine which of the following factors must be considered for proper operation of the integrated system:

- If the host system provides mechanical energy in the form of either potential energy or kinetic energy:
  - Is the potential energy due to the gravitational field or due to elastic deformation of certain structure—and the type of deforming structure, e.g., a helical or linear or torsional spring or bending flexure, etc.?
  - What are the maximum and minimum force/torque/moment and displacement/rotation levels that the host system can provide?
  - What is the level of kinetic energy that the host system can provide?
- If the host system provides a nearly continuous periodic oscillatory translational or rotational motion or vibration:
  - The frequency content and range of its variation and power distribution;

Downloaded From: https://www.spiedigitallibrary.org/ebooks/ on 07 Mar 2022
Terms of Use: https://www.spiedigitallibrary.org/terms-of-use

  - Whether the motion is a simple harmonic, and its frequency and variations—if any;
  - The type(s) of oscillatory motion, i.e., translational, rotational or their combination.
- If the host system provides continuous and nearly random translational and/or rotational oscillatory motion or vibration:
  - The characteristics of the available oscillatory motion(s) in terms of motion amplitudes (displacement, velocity, and acceleration), forces/torques/moments, and frequency distribution.
- For continuous and nearly periodic oscillatory motions of the host system:
  - Does the range of vibration frequencies allow direct excitation of a vibration-based energy-harvesting device in resonance and transfer of a significant portion of the available mechanical energy to that system?
  - If not, is the range of frequencies of the oscillatory motions of the host system relatively low or high (as will be discussed in detail later in this and the next chapter)?
- If the host system provides a continuous but relatively slow motion or a relatively low frequency oscillatory motion:
  - The characteristics of the available continuous or oscillatory motion in terms of speed, frequency, type of motion, range of motion, and any motion and/or force/torque/moment limitations that must be considered to prevent interference with the proper operation of the host system.
- The force/torque/moment limitations that must be considered so that the energy-harvesting device does not interfere with the proper operation of the host system.
- The total amount of mechanical energy that the host system can provide for extraction and conversion to electrical energy as a function of time without interfering with its proper operation.
- The percentage of the available mechanical energy that has to be harvested to satisfy the power-consuming system or device needs.
- Any limitations on the effects of the energy-harvesting device on the operation of the host system, such as its dynamics, motion pattern, precision, and the like.
- Any potentially positive effect that the energy-harvesting system can provide to the host system, such as damping certain unwanted modes of vibration or serving as an integrated sensor to enhance the performance of the host system controls or to control the energy harvesting level and rate.
- Any size, shape, or weight limitations for the energy harvesting system.
- If the mechanical energy provided by the host system is in the form of relatively short-duration impulse(s) such as short-duration force, torque, pressure, acceleration, or the like:

Downloaded From: https://www.spiedigitallibrary.org/ebooks/ on 07 Mar 2022
Terms of Use: https://www.spiedigitallibrary.org/terms-of-use

  - If the impulse event occurs only once, i.e., if it is a so-called one-shot event such as those occurring during a car accident impact, munitions explosion, or gun firing or target impact; the impulse profile and its variations.
  - If the impulse events consist of continuously occurring, relatively short-duration impulses that are regularly or randomly spaced in time; the minimum and maximum time spacing(s), and the impulse profile and its variations.
- Can the energy-harvesting device be provided with external sources of power?
- Can the energy-harvesting device be provided with internal or external processing capability?

It is appreciated that in addition to the above factors, others may also have to be considered depending on a specific application. In addition, the main purpose of the above list is to provide designers with the types of constraints that may have to be considered while searching for the best transducer and host-system-interfacing mechanism and other components of the energy-harvesting device for a particular application. The provided classification of the characteristics of the mechanical energy that the host system can provide is also not unique and universally accepted but should provide a quick guide for the formulation of the energy-harvesting device design requirements and constraints that must be considered.

It is also noted that most energy-harvesting devices have nonlinear behavior due to their kinematics, their motion-limiting elements, their transducer and structural dynamics, as well as in most cases their electrical energy collection and regulation electronics. It is therefore critical for the designer to consider the effects of such nonlinearities on the overall design of the energy-harvesting device and their possible interference with the proper operation of the host system. The development and use of linearized models is always useful as an initial step, but in many cases, particularly when attempting to maximize energy-harvesting device performance, all significant nonlinearities must be considered before embarking on generally costly and time-consuming prototyping and testing efforts.

In the following sections, the basic interfacing mechanisms that are particularly suitable for different transducer types and designs are described. The designs consider the nature of the mechanical energy provided by the host system as well as the system or device to be powered. An attempt is also made to address the consequences of the previously indicated limitations on the proper choice of interfacing mechanisms.

For each transducer type and design, interfacing mechanisms are categorized in groups based primarily on the characteristics of the mechanical energy provided by the host system. Some overlap is inevitable, and the reader must view the categorization as a basic guide for the selection of a suitable

Downloaded From: https://www.spiedigitallibrary.org/ebooks/ on 07 Mar 2022
Terms of Use: https://www.spiedigitallibrary.org/terms-of-use

interfacing mechanism, noting that in many applications, due to the limitations imposed on the overall system, a sub-optimal mechanism may be more suitable. The mechanical energy provided by the host system falls primarily into the following three basic categories:

1. Mechanical energy in the form of potential energy or kinetic energy of rotating elements;
2. Mechanical energy to be extracted from a continuous oscillatory (vibratory) motion;
3. Mechanical energy to be extracted from relatively short-duration "pulses" of force or torque, pressure, or linear or rotary motions, with the distinctive characteristic of being either a single event or multiple events but spaced significantly far from each other.

The electrical energy collection and conditioning electronics as well as the characteristic of the device to be powered or the storage device type and capacity, etc., are also factors to be considered and will be addressed in Chapter 4.

3.2 Interfacing Mechanisms for Piezoelectric-based Transducers

Piezoelectric transducers generate electrical charges when strained. The applied strain may be tensile/compressive or shearing. The amount of allowable tensile, compressive, and shear strain is dependent on the material type and the transducer design. A review of piezoelectric materials and their mechanical and electrical characteristics is provided in Chapter 2 with an extensive list of references for more in-depth reading.

3.2.1 Interfacing mechanisms for potential energy sources and continuous rotations

Piezoelectric elements cannot be used to continuously convert potential energy to electrical energy. For example, the potential energy stored in elastic elements such as linear, torsional power springs, or the potential energy due to raising of a mass in the gravitational field as in a grandfather clock, can only be converted to electrical energy using an appropriate interfacing mechanism. This is also the case if the mechanical energy provided by the host system is in the form of a continuous rotation of an object such as a flywheel. In both cases, the available mechanical energy may be used to directly strain a piezoelectric element to generate a charge, but only once.

Rotary-type electromagnetic transducers (generators) are generally best for direct conversion of mechanical energy from continuous rotary motion provided by the host system. Speed-increasing gearing may also be used when the host system speed is relatively low. This is also the case when potential

Downloaded From: https://www.spiedigitallibrary.org/ebooks/ on 07 Mar 2022
Terms of Use: https://www.spiedigitallibrary.org/terms-of-use

energy has to be converted to electrical energy over a relatively long period of time, such as for the case of the electrical generator of the aforementioned GravityLight device. The available potential and kinetic energy can, however, be "conditioned" for conversion to electrical energy by piezoelectric transducers using a two-stage (or similarly operating multistage) interfacing mechanism.[1–11] Multistage interfacing mechanisms may also be used in applications where the mechanical energy provided by the host system is due to oscillatory or vibratory motions. Such cases are discussed later in this section.

The functioning of two-stage interfacing mechanisms for transferring potential or kinetic energy to a piezoelectric-type transducer may be illustrated by the schematic of Fig. 3.1. Here, the wheel is considered to be turning continuously at a certain rate that might be time varying. The wheel is provided with certain means, in this case one or more engagement teeth, to intermittently transfer its kinetic energy to one or more secondary vibrating elements, in the present case in the form of potential energy stored in their elastic elements. The consequent vibration of the secondary vibrating elements can then be transformed into electrical energy via provided piezoelectric transducers. In practice, to reduce mechanical losses due to friction between the engagement teeth and the vibrating element, properly oriented magnets may be arranged at the engaging surfaces, as described in Refs. 3 and 8, to perform the same function without friction losses.

In the schematic of Fig. 3.1, two secondary vibrating element types are presented. It is appreciated that countless other such vibrating-element designs with essentially one or more significant modes of vibration may be used for this purpose. The one to the right is a vibrating element that is in the form of a cantilevered beam with one piezoelectric layer that is intermittently deflected and released by the engagement teeth provided on the rotating wheel. As a

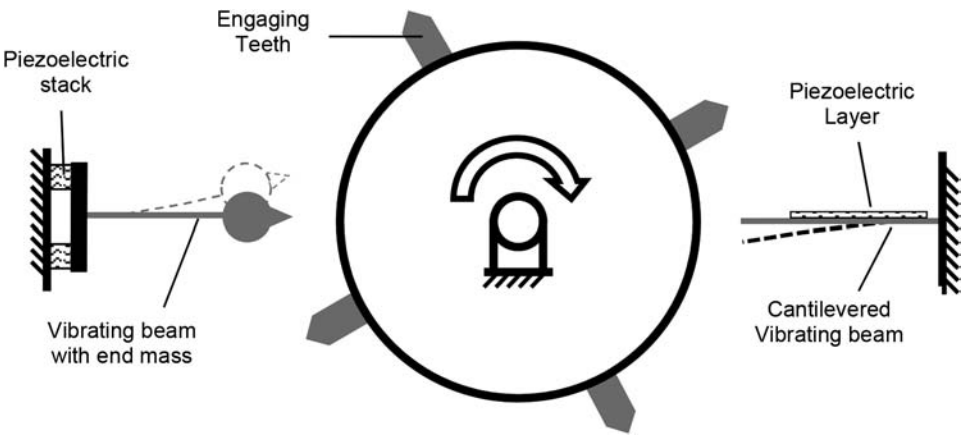

Figure 3.1 The functioning of a two-stage interfacing mechanism.

Downloaded From: https://www.spiedigitallibrary.org/ebooks/ on 07 Mar 2022
Terms of Use: https://www.spiedigitallibrary.org/terms-of-use

result, during each engagement, kinetic energy is transferred from the rotating wheel (the first stage of this two-stage interfacing mechanism) to the secondary cantilever vibrating beam (the second stage of the two-stage interfacing mechanism). Such cantilevered-beam types of energy-harvesting devices—with one or two piezoelectric layers (uniform or bimorph) and in certain cases with a tip mass in different geometries attached to a host structure to be excited in vibration from the beam base—have dominated studies of energy-harvesting devices, particularly due to their relative ease of implementation in MEMS and similar devices, e.g., see Refs. 12–36. In Fig. 3.1, the cantilevered beam to the left is shown to be provided with an end mass—generally to reduce the natural mode of vibration—that could also be included on the cantilevered beam to the right.

In the schematic of Fig. 3.1, two distinct types of secondary vibratory element types are shown. The basic functional difference between the two secondary vibratory elements is the manner in which the potential-energy-storing elastic element—in both cases the cantilevered beam elements—and the straining piezoelectric members are configured. In the vibrating element to the right, the piezoelectric member is configured in parallel with the equivalent spring element of the vibrating cantilevered beam as shown in the model of Fig. 3.2. In this configuration and considering a single mode of vibration, piezoelectric member strain and beam deformation are proportional. In the model of Fig. 3.2, k_s and m_e are the effective vibrating beam and piezoelectric member spring and mass, respectively, for the considered first mode of vibration, k_p is the effective spring rate (constant) of the piezoelectric material for the considered mode of vibration, and the forces F_{es} represent the electrostatic forces that resist the piezoelectric member strain due to the generated charges. The piezoelectric member strain resisting forces F_{es} are present as long as the generated charges are not removed, i.e., collected by the electronics unit of the energy-harvesting device.

In the secondary vibrating element to the left in Fig. 3.1, the piezoelectric members are effectively configured in series with the equivalent spring element

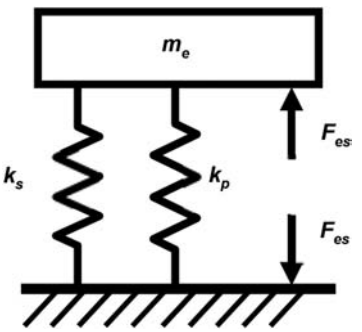

Figure 3.2 Mass–spring and piezoelectric-induced electrostatic force model of the secondary vibrating element on the right in Fig. 3.1.

Downloaded From: https://www.spiedigitallibrary.org/ebooks/ on 07 Mar 2022
Terms of Use: https://www.spiedigitallibrary.org/terms-of-use

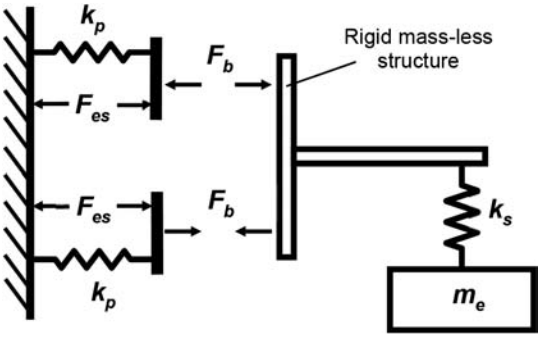

Figure 3.3 Mass–spring and piezoelectric-induced electrostatic force model of the secondary vibrating element on the left in Fig. 3.1.

of the vibrating cantilevered beam as shown in the equivalent model of Fig. 3.3. In this configuration, the reaction couple at the base of the vibrating beam is transferred to the two symmetrically positioned piezoelectric members as shown by the reaction forces. The piezoelectric elements are preferably of stacked type and axially strained (Fig. 2.5).

In the model of Fig. 3.3, k_s and m_e are the effective spring rate and mass of the vibrating beam and its base structure, respectively, for the considered first mode of vibration, and F_b is the magnitude of the forces that form a couple balancing the moment generated by the spring k_s force acting at the tip of the rigid and mass-less structure of the device. Equal and opposite reaction forces are applied to the piezoelectric members, which are modeled as springs with an effective spring rate k_p due to the member axial elasticity and the strain-resisting forces F_{es} representing the generated electrostatic forces that resist the piezoelectric member strain due to the generated charges. The forces F_{es} are present as long as the generated charges are not removed (harvested) by the energy-harvesting device.

It is appreciated that the basic in-series design of the secondary vibratory element of Fig. 3.3 may be implemented in numerous other configurations. In fact, the potential-energy storage (elastic) element of the secondary vibratory element does not have to be a cantilevered beam and may be formed by helical or any other type of spring (elastic) elements, or may even be an integral part of the harvester structure.

The basic design illustrated in Fig. 3.3 is intended for use to describe the functionality of the secondary vibratory element and to compare it with the in-parallel version of Fig. 3.2. In this regard, the in-series design shown schematically in Fig. 3.3 has several design and operational advantages over the in-parallel design of Fig. 3.2. Firstly, by providing mechanical stops for the structure of the device against the ground, the piezoelectric members can be protected against overstraining. Secondly, the brittle piezoelectric members can be protected from excessive tensile loading by preloading them in compression (see Section 3.2.3 and Chapter 5 for a more detailed discussion

Downloaded From: https://www.spiedigitallibrary.org/ebooks/ on 07 Mar 2022
Terms of Use: https://www.spiedigitallibrary.org/terms-of-use

on methods of protecting generally fragile piezoelectric elements from excessive compressive and tensile loading). Thirdly, in general, significantly more potential energy may be stored in elastic element(s) of in-series secondary vibratory elements than those of in-parallel designs. This is the case since relatively large amounts of potential energy may be stored in the elastic elements of an in-series device and harvested over many cycles of its mass–spring vibration. Fourthly, because the piezoelectric members are deployed in the 33 mode and may in general be designed with relatively small cross-sections and long lengths, in many applications they can be designed to generate larger amounts of charges with the available mechanical energy during each cycle of beam vibration. The main shortcoming of in-series secondary vibratory elements is their relatively more complex construction and the challenges of their implementation in microscale energy-harvesting devices.

In Fig. 3.1 the model of the basic design of a rotary two-stage interfacing mechanism for transferring kinetic energy stored in a rotating wheel to a secondary vibratory element is illustrated. Potential energy stored in an elastic (spring) element or a mass in the gravitational field may be similarly transferred to such secondary vibratory elements. This can be simply done by using the potential energy to cause the rotation of a wheel that serves as the first stage of the interfacing mechanism, for example, through a wound cable attached to the falling mass or a pulling spring, and possibly with speed-reducing gearing to match the rate of potential energy availability to the rate of its conversion to electrical energy by the transducer(s). Alternatively, the engagement teeth (Fig. 3.2) may be directly attached to a cable/belt attached to the falling mass to directly engage and transfer potential mechanical energy to the secondary vibratory elements.

Two-stage interfacing mechanisms may be similarly used to transfer potential and/or kinetic energy to almost any transducer type and design, as is discussed in the following sections of this chapter. Two-stage interfacing mechanisms are particularly suitable for harvesting very slow oscillatory motions as described in detail in Section 3.2.3.2. Briefly, the following features of the present two-stage interfacing mechanisms make them particularly beneficial in the design of highly effective energy-harvesting devices for a number of applications, in addition to those with potential energy or continuously rotating sources of mechanical energy:

- Since potential energy is transferred directly to the secondary vibratory element, the efficiency of the energy-harvesting device can be optimized by proper selection of the frequency of the natural mode of vibration of the secondary vibratory element.
- The performance of the resulting energy-harvesting device is independent of the host system's frequency of vibration (oscillatory motion), which may be widely varying over time.

Downloaded From: https://www.spiedigitallibrary.org/ebooks/ on 07 Mar 2022
Terms of Use: https://www.spiedigitallibrary.org/terms-of-use

– The energy-harvesting device may use multiple secondary vibratory elements, thereby allowing it to harvest the available mechanical energy at relatively high rates.
– Using the proper number of engagement teeth on the first stage of the interfacing mechanism and by optimal positioning of the secondary vibratory elements, the transferred potential energy can be harvested over several cycles of vibration of the secondary element, thereby increasing the overall efficiency of the energy-harvesting device.
– Using in-series secondary vibratory elements, a relatively large amount of potential energy can be transferred to their elastic potential-energy storage component, and electrical energy can be harvested over a significantly longer period of time over several cycles of vibration of the secondary element.

3.2.2 Interfacing mechanisms for continuous oscillatory translational and rotational motions

In this section, possible interfacing mechanisms for input mechanical energy from continuous translational and/or rotational oscillatory motions of host systems are described. The oscillatory motions are considered to be continuous; i.e., they continue past the point in time at which the energy-harvesting system achieves its steady state condition.

Continuous oscillatory motions provided by host systems to energy-harvesting devices may be grouped into the following three categories:

1. Continuous periodic simple harmonic oscillatory motions;
2. Continuous periodic multiple-harmonic oscillatory motion; or
3. Continuous random oscillatory motions.

For each of the above three categories, the oscillatory motions may also be broadly divided into the following two subcategories:

- "Low-frequency" continuous oscillatory motions—referring to applications in which resonant excitation of vibration-based energy-harvesting devices is not practical—usually due to the resulting size/weight of the device;
- "High-frequency" oscillatory motions—applications in which resonant excitation of vibration-based energy-harvesting devices is practical. Frequencies above which mechanical systems do not usually respond due to their "low-pass" filtering characteristics are intended to be excluded from discussion.

Here, the terms "low-frequency" and "high-frequency" are used solely for the lack of better words and as a qualitative indication of the practicality of a vibration-based harvester that is excited in resonance. An energy-harvesting

Downloaded From: https://www.spiedigitallibrary.org/ebooks/ on 07 Mar 2022
Terms of Use: https://www.spiedigitallibrary.org/terms-of-use

device is considered to be practical if its size and weight are within the overall system limitations and do not interfere with the proper operation of the host system.

In the following sections, interfacing mechanisms for the above three categories of translational and/or rotational oscillatory motions are discussed. For each category, the motions that are "low-frequency" and "high-frequency" as described above are also considered. Unless indicated, it is also assumed that the energy-harvesting device cannot be "grounded" to the base/foundation structure of the host system relative to which the present continuous oscillatory motions takes place.

3.2.2.1 Should a vibration-based energy-harvesting device be designed for excitation at resonance?

When selecting the type and design of a vibration-based energy-harvesting device that is to be attached to the structure of a host system that undergoes continuous oscillatory translational and/or rotational motions, the first question is whether it should be designed to be excited in resonance. It is noted that in certain applications the objective is to generate as much electrical energy as possible, which requires maximizing the amount of electrical energy generated during each cycle of the host system oscillation. Maximizing the amount of generated electrical energy may however not be the main goal in the design of an energy-harvesting device.

Two very distinct vibration-based energy-harvesting-device types are generally available: (1) those that are excited at their one or more natural modes of vibration and (2) those that are not excited at any of their natural modes of vibration. Neither of the two vibration-based energy-harvesting device types is optimal for every application. The most appropriate choice is generally dependent on the characteristics of the host system and the limitations that it imposes, as well as the characteristics and power requirements of the system or device to be powered. These include the following:

- Whether the frequency of the oscillatory motion of the host system is fixed within a relatively narrow range or it is widely varying;
- The amount of mechanical energy that the host system can make available for harvesting without affecting its proper operation;
- The limitations on the size and weight of the energy harvesting device;
- The amount of electrical energy that has to be generated for the given application— an amount that the host system must obviously be capable of providing.

In general, it can be said that vibration-based energy-harvesting devices that are to be excited in resonance by the host system translational and/or rotational oscillatory motions provide best performance per unit volume if the

Downloaded From: https://www.spiedigitallibrary.org/ebooks/ on 07 Mar 2022
Terms of Use: https://www.spiedigitallibrary.org/terms-of-use

amount of mechanical energy that can be converted to electrical energy is significantly larger than the amount of electrical energy that has to be generated by the energy-harvesting device. Here, performance is used in terms of the potential amount of electrical energy that can be generated during each cycle of device vibration (power output) per unit of energy-harvesting device volume.

The efficiency of vibration-based harvesters operating at resonance in converting the available mechanical energy to electrical energy is not high for the following obvious reasons. If the mechanical energy available during each cycle of host system oscillation were to be transferred to the energy-harvesting device and were converted to electrical energy, then no mechanical energy would be left to accumulate in the vibration-based harvesting device in resonance. In such a case, even wide variations in the frequency of the host system oscillatory motion would have little effect on the harvester output—not considering its effects on losses due to structural damping, friction, transducer, and electrical energy collection electronics inefficiencies, etc.

Now consider the case in which the amount of mechanical energy that has to be transferred to the energy-harvesting device to generate the required amount of electrical energy for a given application is less than the available mechanical energy from the host system. In such cases, mechanical energy can be transferred and accumulated in the vibration-based energy harvester most efficiently at resonance, achieving larger amplitude vibrations of the harvester's vibrating element(s), and thereby applying larger strains (forces/torques/flexural moment) to the harvester transducer. As a result, larger amounts of electrical energy can be produced with a relatively smaller energy-harvesting device, thereby potentially resulting in larger generated power per unit volume. Such options may also become relevant if the peak acceleration levels of the host system oscillatory motion and overall harvester size constraints limit the maximum levels of piezoelectric member strain energy for efficient electrical energy generation and harvesting without the resonant accumulation of mechanical energy in the vibrating element of the harvester, particularly considering the quadratic nature of the relationship between piezoelectric transducer strain and the generated electrical energy.

Many applications in which energy-harvesting devices are considered to be used fall in the latter category in which the host system can provide a significantly larger amount of mechanical energy than is required by the energy-harvesting device. In the following sections, interfacing mechanisms for vibration-based energy harvesting devices that are to be excited from the base input motion in resonance are discussed first for host system oscillatory motions that are periodic with single or multi-harmonic content. Host system motions that are random in frequency and amplitude, including pulsed one-shot or multiple pulsed inputs that occur randomly or are far apart, are addressed in Sections 3.2.4 and 3.2.5.

Downloaded From: https://www.spiedigitallibrary.org/ebooks/ on 07 Mar 2022
Terms of Use: https://www.spiedigitallibrary.org/terms-of-use

3.2.3 Interfacing mechanisms for periodic oscillatory translational and rotational motions of the host system

Mechanical energy provided by host systems through periodic oscillatory translational or rotational motion for conversion to electrical energy needs to be first examined to determine if it should be categorized as relatively "high-frequency" or "low-frequency" as previously defined, i.e., whether it can be used for direct base excitation of a practical vibratory system in resonance. In general, what determines the practicality of exciting a vibrating system in resonance is the limitations on the size and mass of the harvester that can be accommodated by the host system, noting that the lower the excitation frequency the larger the equivalent mass and/or the softer the springs need to be in the construction of the harvester vibratory member.

3.2.3.1 "High-frequency" periodic oscillatory motions of the host system

If a vibration-based energy-harvesting device that can be excited by the periodic oscillatory motion of the host system is considered to be practical, then either one of the in-series or in-parallel vibratory element types shown in Figs. 3.2 and 3.3, respectively, may be used. The base of the vibratory element is then attached directly to the host system, and the frequency of its natural mode of vibration is designed to match the frequency of the fundamental harmonic of the host system periodic oscillatory motion or one of its significant harmonics. No motion or force-modifying interfacing mechanism is therefore required.

Cantilevered-type energy-harvesting devices of various designs are the most widely studied and were discussed in Section 3.2; several references were provided for further reading on their possible designs, modeling, and testing performance results. Cantilevered-type devices of the type shown in in Fig. 3.2 provide piezoelectric members that are strained in parallel with the device elastic element, thereby presenting the previously indicated shortcomings for certain applications but having the advantage of being relatively easy to implement in MEMS and other similar micro-generators.

In-series energy-harvesting devices such as the type shown in Fig. 3.3 are more challenging to miniaturize but can usually generate larger amounts of electrical energy since they can accommodate larger piezoelectric elements and achieve more-uniform strain patterns in the 33 mode. Such in-series harvesting devices may also be designed with axially vibrating mass–spring systems. The schematic of the basic design of such an axially vibrating mass–spring system with an in-series piezoelectric element that is strained in the 33 mode is shown in Fig. 3.4 (left) together with its lumped model (right). If the piezoelectric element is of a relatively brittle type, it is preferably preloaded in compression so that it is not subjected to excessive tensile loading. Examples of methods to provide compressive preloading for axially strained piezoelectric elements are discussed in more detail in Chapter 5. The level of

Downloaded From: https://www.spiedigitallibrary.org/ebooks/ on 07 Mar 2022
Terms of Use: https://www.spiedigitallibrary.org/terms-of-use

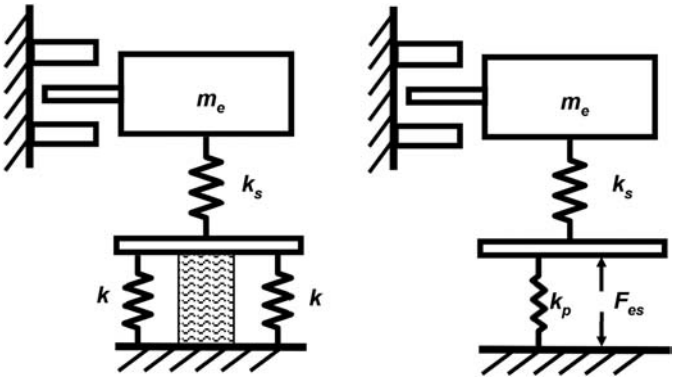

Figure 3.4 Schematic and model of the basic design of an axially vibrating energy-harvesting device with overload protection.

piezoelectric element compressive as well as tensile deformation may also be limited by constraining the deformation of the vibrating unit spring by the provided stops. In practice, the stop-engaging member is preferably provided with relatively stiff springs, such as Belleville washers as described in Chapter 5, to minimize introduction of impulsive forces as the stops are engaged.

In Fig. 3.4, k_s and m_e are the effective spring rate and mass of the vibrating element of the generator, respectively, k_p is the effective axial spring rate of the piezoelectric element, and F_{es} represents the electrostatic forces that resist the piezoelectric element member strain due to the generated charges. The springs k are used to preload the piezoelectric element in compression as needed to limit its tensile loading (not shown in the model to the right). The piezoelectric member strain resisting force F_{es} is present as long as the generated charges are not removed, i.e., collected by the energy harvesting device electronics. In Fig. 3.4, the ground indicates the structure of the host system to which the energy-harvesting device is attached.

3.2.3.2 "Low-frequency" periodic oscillatory motions of the host system

If a vibration-based energy-harvesting device that can be excited in resonance by the oscillatory motion of the host system is not considered to be practical, as was previously discussed due to the low frequency of its otherwise periodic oscillatory motion, the oscillatory motion is considered to be at "low-frequency." As a result, the host system cannot transfer a significant amount of mechanical energy to the energy-harvesting device for conversion to electrical energy. In such cases, the interfacing mechanism and/or its operating environment has to be configured to produce appropriate higher harmonic motions with significant amplitudes to make it possible to excite the natural mode of a properly designed vibration-based energy-harvesting device in resonance.

Downloaded From: https://www.spiedigitallibrary.org/ebooks/ on 07 Mar 2022
Terms of Use: https://www.spiedigitallibrary.org/terms-of-use

Here, the interfacing mechanisms to be considered are limited to those with a single degree-of-freedom and constructed with passive elements. The basic methods may, however, be readily expanded to multiple-degrees-of-freedom systems. For the sake of simplicity, the dynamics of the interfacing mechanisms is considered to be decoupled from that of the vibration-based generator of the energy-harvesting device. The output of the interfacing mechanism is therefore input to the vibration-based generator. When designing such energy-harvesting devices, the coupling of the dynamics of the two systems must be considered.

A quick look at the equation of motion of a vibrating mechanical system that is subjected to a certain "low-frequency" input motion clearly indicates the range of possible methods for achieving a higher harmonic system response. To this end, consider the simple lumped one degree-of-freedom mass–spring–damper model of Fig. 3.5, where m, k, and c are the vibrating mass, spring rate, and viscous dampers, respectively; $f(t)$ is the externally applied time-varying force; t is time; y is the motion of the device base, i.e., the host system structure, which is shown as the ground; and x is the position of the mass relative to the base structure. The schematic of the linkage to the left represents a one-degree-of-freedom (mass-less) mechanism that constrains the motion of the system mass in the x direction. The equation of motion of the system is readily seen to be

$$m\ddot{x} + c\dot{x} + kx = F(y,t) + f(t). \tag{3.1}$$

In the Fig. 3.5 the vibrating mass–spring–damper system is considered to be attached to a host system that is undergoing a certain, in this case oscillatory, motion. On the right-hand side of the equation of motion [Eq. (3.1)], the term $F(y, t)$, which is related to the motion of the host system in the direction of mass vibration x and the externally applied forcing function $f(t)$, does not obviously affect the natural motion of the system.

In the model of Fig. 3.5 the vibrating system parameters are lumped, and its equation of motion is described by the ordinary differential [Eq. (3.1)].

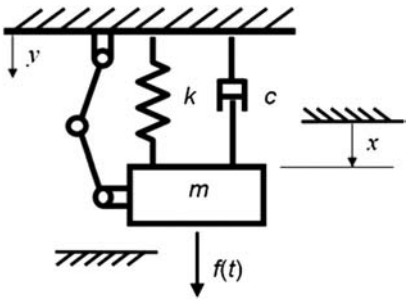

Figure 3.5 Model of a simple mass–spring–damper vibrating system attached to a host system.

Downloaded From: https://www.spiedigitallibrary.org/ebooks/ on 07 Mar 2022
Terms of Use: https://www.spiedigitallibrary.org/terms-of-use

The system is considered to represent an interfacing mechanism that is attached at the base (ground) to a host system, and its output motion $x(t)$ is used to transfer mechanical energy to an energy-harvesting device such as the vibration-based cantilevered beam with piezoelectric layers of Fig. 3.1.

If the motion of the interfacing mechanism is subjected to other constraints such as those due to provided displacement range-limiting stops (Fig. 3.5) or by a linkage mechanism constraining the motion of the mass m to a certain motion pattern, the equation of motion must be supplemented with the relationships describing such constraints. For example, for the case of displacement limiting stops, the constraint is

$$x^L \leq x \leq x^U, \tag{3.2}$$

where x^L and x^U are the lower and upper limits, respectively, of the possible mass displacement. The interaction of the interfacing mechanism with the provided motion constraints must obviously be considered when analyzing the dynamic behavior of the interfacing mechanism and the energy-harvesting device.

Now consider the case in which the base of the interfacing mechanism of Fig. 3.5 is subjected to a relatively low frequency, oscillatory motion by the host system. The output motion of the interfacing mechanism, i.e., the motion that is to transfer mechanical energy to a vibration-based energy-harvesting device, would contain higher harmonics of the input motion only if:

- Either the differential equation describing the natural motion of the system, i.e., the left-hand side of the Eq. (3.1), is nonlinear; or
- Forcing functions with the desired frequency content are provided.

The equation of motion of the interfacing mechanism may be rendered nonlinear by constructing the mechanism with nonlinear kinematics, or by providing it with nonlinear spring and/or damping elements. The kinematic nonlinearity may, for example, be provided by including stops to limit the range of motion, or by constraining motion to a certain path through the use of linkage-type mechanisms.

The forcing function on the right-hand side of Eq. (3.1) is seen to have two components. If the differential equation describing the natural motion of the system, i.e., the left-hand side, is linear and no motion constraints are present, the steady state response of the system to the forcing functions $F(y, t)$ and $f(t)$ has the same harmonic content as the forcing functions. The transient response of the system also contains the frequency of the natural mode of vibration of the interfacing mechanism. In the present case, since the forcing function $F(y, t)$ due to the oscillatory motion of the host system is considered to be low frequency, the steady state response to it is also low frequency and not suitable for exciting a vibration-based energy-harvesting element in resonance. It is also noted that since the objective of using energy-harvesting

Downloaded From: https://www.spiedigitallibrary.org/ebooks/ on 07 Mar 2022
Terms of Use: https://www.spiedigitallibrary.org/terms-of-use

devices is to generate electrical energy, the use of externally powered means of applying the forcing function $f(t)$ is generally ruled out.

Here, the dynamics of the interfacing mechanism is assumed not to affect that of the host system or the energy-harvesting member. The former assumption is usually valid since the energy-harvesting device together with its interfacing mechanism is generally small compared to the size of the host system, and a small fraction of its available mechanical energy is harvested. The latter assumption, however, is usually not totally valid, and the dynamics of the energy-harvesting device must be considered when analyzing the overall behavior of the interfacing mechanism, and vice versa.

Thus, if a vibration-based energy-harvesting device that can be excited in resonance by oscillatory motions of the host system (where the base of the interfacing mechanism is still considered to be attached directly to the oscillating host system) is not considered to be practical, several transducer-interfacing mechanism options are available. The following mechanisms may be used to transfer a significant amount of mechanical energy from the host system to the energy-harvesting device for conversion to electrical energy:

1. Two-stage interfacing mechanism types;
2. Interfacing mechanisms with a direct oscillatory motion frequency-increasing feature;
3. Interfacing mechanisms with nonlinear behavior to generate higher frequency harmonics; or
4. Provision of a position-dependent external force.

The second interfacing type of mechanism above is a specific case with nonlinear kinematics that can directly double the frequency of the input motion, as described later in this section. A certain level of overlapping is seen between the first and third types of interfacing mechanisms listed above.

It is noted that in many mechanical systems, low-frequency oscillations are not in the hundreds or sometimes not even in the tens of cycles per second and may even be one cycle in several seconds, such as is the case in ocean waves or rocking motions of a ship. The frequency content and amplitudes of the input oscillatory motions or input forcing functions may also vary widely. In most mechanical systems, oscillatory motions with several hundred cycles per second are rare, and those in the thousands of cycles per second are exceptionally rare.[37–39]

3.2.3.2.1 Two-stage interfacing mechanisms

The objective of a two-stage interfacing mechanism is to "condition" the input low-frequency oscillatory motions of the host system for effective transfer of mechanical energy to vibration-based energy-harvesting devices for conversion to electrical energy. Two-stage interfacing mechanisms are particularly effective if the frequency of the oscillatory motion of the host system is highly

Downloaded From: https://www.spiedigitallibrary.org/ebooks/ on 07 Mar 2022
Terms of Use: https://www.spiedigitallibrary.org/terms-of-use

variable. Two-stage interfacing mechanisms may be constructed to operate based on the following two methods: (1) during each cycle of host system oscillation, mechanical energy is intermittently transferred to secondary vibratory elements (similar to the method of Section. 3.2); and (2) during each cycle of host system oscillation, mechanical energy is transferred to a potential- or kinetic-energy storage element, and when a predetermined threshold is reached, the stored mechanical energy is released to the provided generator for conversion to electrical energy.

The first method is very similar to the two-stage interfacing mechanisms described in Section 3.2, except that in this case the engaging teeth (Fig. 3.1) are oscillating back and forth, each time transferring a certain amount of mechanical energy to the secondary vibrating element(s). An example of such a host system with low-frequency oscillatory motion is a platform such as a ship or buoy undergoing rocking motion due to the ocean waves. Human and animal locomotion and rocking motions encountered in most vehicles and machinery are other examples of such host systems that provide low-frequency oscillatory motions that can be used to harvest electrical energy.

The basic idea of two-stage interfacing mechanisms for low-frequency oscillatory motions is described in Refs. 6, 10, and 11, and is best illustrated by Fig. 3.6, where the interfacing mechanism consists of a sliding mass that is released to slide downwards when the rocking host system, to which the energy-harvesting device is fixed, rocks at angle α. A simple release mechanism may consist of a very shallow blocking element over which the sliding mass can slide when the threshold angle α has been reached. One or more secondary vibratory elements are provided to receive a portion of the potential energy stored in the sliding mass and convert it to electrical energy. The secondary vibratory elements in Fig. 3.6 are the cantilevered type such as the one shown in Fig. 3.1, but any other type may obviously be used.

Such a two-stage interfacing mechanism may also be constructed as a simple pendulum as shown in Fig. 3.7. If the rocking motion is symmetrical

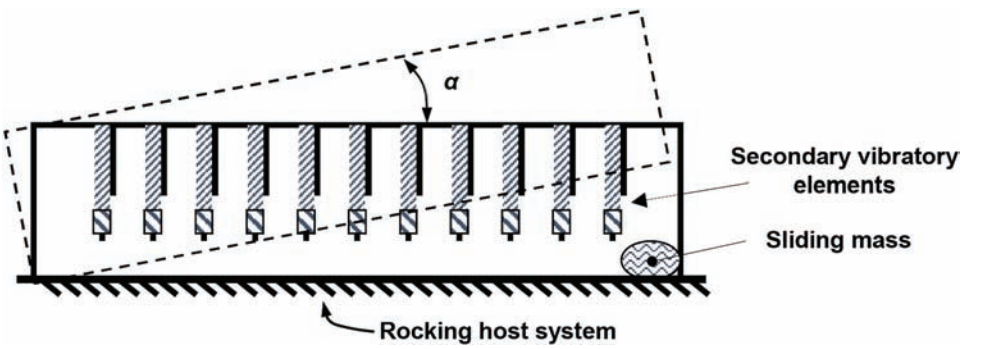

Figure 3.6 A two-stage interfacing mechanism depicting the basic method of transferring mechanical energy from the low-frequency rocking oscillation of a host system.

Downloaded From: https://www.spiedigitallibrary.org/ebooks/ on 07 Mar 2022
Terms of Use: https://www.spiedigitallibrary.org/terms-of-use

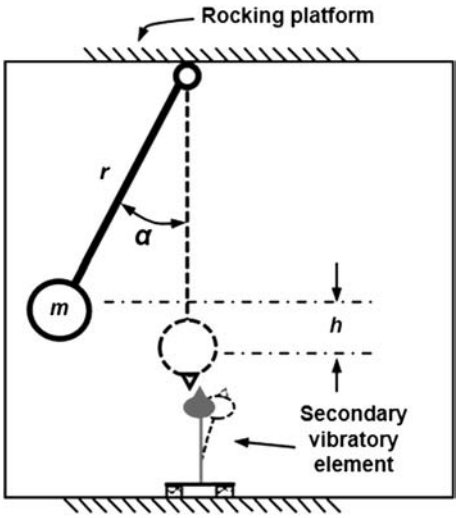

Figure 3.7 A two-stage interfacing mechanism for a host system undergoing rocking motions.

with respect to the direction of gravity and has an amplitude of α, then during each cycle of host-system rocking motion and assuming no losses, the available mechanical energy for harvesting is $E_M = 2mgh = 2mgr\ (1 - \cos\alpha)$, where m is the pendulum mass, g is the gravitational acceleration, and r is the length of the pendulum arm, which is considered to be mass-less. As expected, larger amounts of mechanical energy can be made available using a longer pendulum and/or a larger mass or both.

During each cycle of the rocking motion of the host system, the pendulum teeth twice engage the tip of the secondary vibratory element where it transfers a portion of its mechanical energy for conversion to electrical energy. In Fig. 3.7, one of the two secondary vibrating elements shown in Fig. 3.1 is being used. Any other type of secondary vibratory element, for example, the vibration-based generator shown in Fig. 3.4, which is similarly excited but in the axial direction, may also be used. Friction-type engagement teeth may also be replaced with the previously described permanent magnets to minimize related losses.[3,8]

Other examples of two-stage interfacing mechanisms are presented in Refs. 40–42 and shown in Fig. 3.8. In the example of Fig. 3.8, the interfacing mechanism (driving beam) is provided with stops, in this case, two secondary vibrating elements (generating beams). The interfacing mechanism base is attached to the host system and intermittently transfers mechanical energy to the secondary vibrating elements (generators) upon each impact. A shortcoming of the impact (impulse) mode of mechanical energy transfer to secondary vibrating elements in comparison to the aforementioned permanent magnet type of engagement mechanism is a considerable amount of

Downloaded From: https://www.spiedigitallibrary.org/ebooks/ on 07 Mar 2022
Terms of Use: https://www.spiedigitallibrary.org/terms-of-use

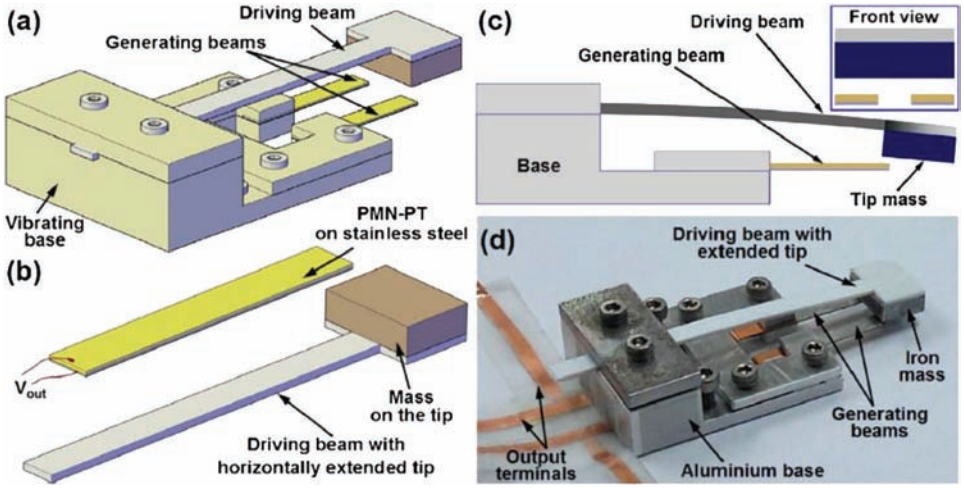

Figure 3.8 A two-stage interfacing mechanism transferring mechanical energy to the secondary vibrating elements upon each impact. (Reprinted with permission from Ref. 42.)

mechanical energy loss due to each impact. In addition, the level of transferred mechanical energy usually varies from one impact to the next.

It is worth noting that the mechanical energy to be transferred from the first stage of a two-stage interfacing mechanism may be transferred to a nonvibrating secondary element such as a flywheel with engagement teeth similar to those of Fig. 3.1, which would in turn engage an element-generating electrical energy such as the secondary vibratory elements mentioned above. Such intermediate mechanical-energy storage elements may be necessary in cases where the energy to be transferred is relatively large, the period of host system oscillation is relatively long, or the flywheel engages the vibration-based generators several times during each cycle of host system oscillation.

The second method of constructing two-stage interfacing mechanisms uses the oscillatory motion of the host system to store mechanical potential or kinetic energy in a certain energy-storage device and releases it when enough mechanical energy has been stored for effective conversion to electrical energy. As an example, a torsion (power) spring may be wound using a pendulum-type mechanism with a ratchet, similar to mechanical self-winding watches, or a one-way clutch. The potential energy stored in the power spring may then be released after a threshold level has been reached to intermittently excite a secondary vibratory element as was described in Section 3.2 [e.g., to rotate a wheel with teeth (Fig. 3.1)]. Different mechanisms may be used to perform the power spring winding and releasing functions.[43] When a power spring is used to store potential energy, rotary electromagnetic transducers (generators) are generally more suitable since the released potential energy can be used to continuously rotate such a transducer at relatively high speed, as long as the generally larger size can be accommodated. This type of interfacing mechanism

Downloaded From: https://www.spiedigitallibrary.org/ebooks/ on 07 Mar 2022
Terms of Use: https://www.spiedigitallibrary.org/terms-of-use

is of particular interest when the mechanical energy available during each cycle of host system oscillation is too small for direct harvesting.

A MEMS-scale two-stage device—in which the secondary vibrating element is a piezoelectric beam with sharp probes that translates against ridges provided on the base of the device that is attached to the host system—is presented in Ref. 44. Other similar two-stage energy-harvesting devices are described in Refs. 36 and 45–48.

3.2.3.2.2 *Interfacing mechanisms for direct doubling of input oscillatory motion frequency*

Kinematic nonlinearity in the interfacing mechanism may be used to excite a secondary vibratory element at frequencies higher than the host system frequency of oscillation, thereby making a more effective and more realistically sized energy-harvesting device practical. For a host system providing a periodic motion, the effect of kinematic nonlinearity of the interfacing mechanism is to generate harmonics of the input motion. The frequency of the available oscillatory motion to the secondary vibratory element is thereby increased. In most interfacing mechanisms the output motion contains the fundamental frequency of the input motion, and in general the generated higher harmonics of the output motion have relatively small amplitudes and energy content. As a result, only a fraction of the mechanical energy available from the host system can be transferred to the secondary vibratory system in resonance.

However, a class of interfacing mechanisms has been found that can be used to double the output fundamental frequency.[49–56] This class of mechanisms has been referred to as "motion-doubling" mechanisms. These mechanisms are designed to undergo oscillatory motions about their kinematic singularities as described below and may be cascaded to increase the input fundamental frequency by a factor of 2^n, where $n = 1, 2, \ldots$, even though each doubling similarly reduces the amplitude of output motion, thereby making an increase larger than $2\times$ or $4\times$ impractical in most applications.

This class of motion-doubling linkage mechanisms are fully described in Ref. 56 and for energy-harvesting application in Ref. 50. Briefly, consider the so-called slider-crank mechanism of Fig. 3.9. The link O_AA is the rocking input link, and the slider c motion is the mechanism output. The input and the coupler link AB are in their singular position when in $O_AA'B'$ configuration. The input link undergoes a periodic rocking motion that is symmetric about its singular position O_AA'. This periodic motion is a simple harmonic with a frequency ω described as

$$\theta = \theta_1 \sin(\omega t), \tag{3.3}$$

where θ_1 is the amplitude of the input link oscillation about its singular position, and t is time. In Fig. 3.9 the position of the slider is indicated by s.

Downloaded From: https://www.spiedigitallibrary.org/ebooks/ on 07 Mar 2022
Terms of Use: https://www.spiedigitallibrary.org/terms-of-use

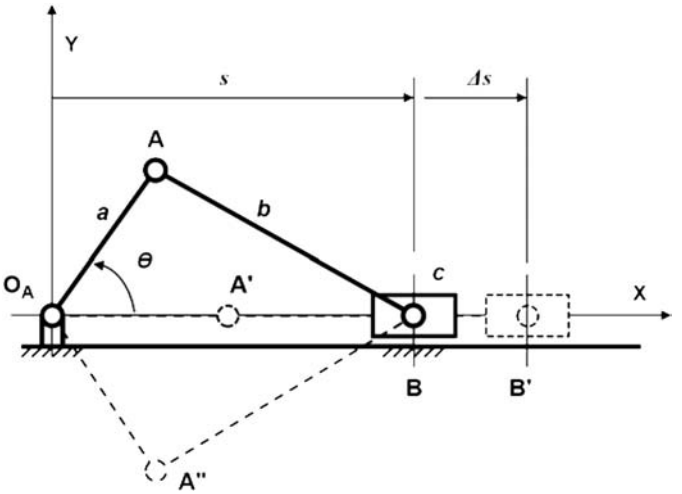

Figure 3.9 A motion-doubling mechanism undergoing symmetric input link oscillation about its singular position O_AA'.

During one cycle of its rocking motion, the input link rotates clockwise from its position O_AA, passes through its singular position to position O_AA'' during the first half of its motion cycle, and rotates counterclockwise back to position O_AA during the second half of its motion cycle. It is noted that during this one cycle of input link rotation, slider c is translated a distance Δs from point B to B′ as the input link is rotated from position O_AA to its singular position and is then translated back to the point B as the input link continues to rotate to the position O_AA''. The cycle of back-and-forth translation of slider c is repeated as the input link rotates back to its position O_AA. Therefore, during one cycle of input link oscillation, slider c undergoes two cycles of back-and-forth translation. Thus, for the simple harmonic oscillation [Eq. (3.3)] of the input link, position s of slider c becomes

$$s = s_0 + s_1 \sin(2\omega t), \tag{3.4}$$

where s_0 is the position of slider c at $\theta = 0$ and s_1 is the amplitude of the output (slider) motion. The fundamental frequency of the translational oscillatory motion of the slider is obviously doubled to 2ω and contains harmonics of this (fundamental) frequency due to the nonlinearity of the kinematics of the mechanism motion. A close examination of the motion of the above mechanism shows that one cycle of output slider motion occurs in one branch of the mechanism input–output relationship and the second cycle in another branch.[56]

Motion-doubling (frequency-doubling) mechanisms may be constructed from almost any linkage mechanism. Any such mechanism may then be used

Downloaded From: https://www.spiedigitallibrary.org/ebooks/ on 07 Mar 2022
Terms of Use: https://www.spiedigitallibrary.org/terms-of-use

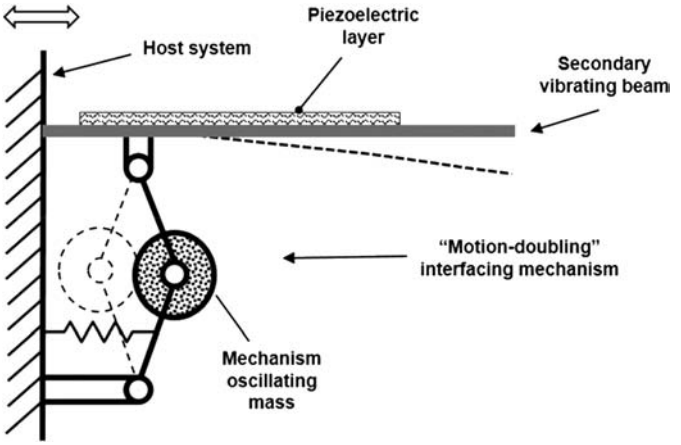

Figure 3.10 An example of a two-stage energy-harvesting device with a frequency-doubling interfacing mechanism and a cantilevered secondary vibratory element.

as an interfacing mechanism to excite a secondary vibratory element at twice the frequency of oscillation of the host system. A simple example of a two-stage energy-harvesting system with a frequency-doubling interfacing mechanism and a cantilevered-beam-type secondary vibratory element is shown in Fig. 3.10.

The interfacing mechanism is constructed with two links that oscillate about their singular positioning, which is reached when the two links are collinear. The input (low-frequency) oscillatory motion of the host system indicated by the double arrow causes the interfacing mechanism with the provided mass and spring to vibrate about the mechanism's singular positioning. The provided spring is preferably biased to position the mechanism in its singular positioning in the absence of the host system vibratory motion. Then, similar to the mechanism of Fig. 3.9, during each cycle of host system oscillation, the mechanism joint attached to the cantilevered secondary vibratory element applies two cycles of bending displacements to the beam, thereby exciting it at double the frequency of the oscillation of the host system.

One simple implementation of the frequency-doubling interfacing mechanism of Fig. 3.10 is achieved by replacing the two links of the mechanism with a cable with the mechanism oscillating mass attached at its center as shown in Fig. 3.11. The balancing spring shown in Fig. 3.11 may be needed to allow the oscillating cable to be preloaded in tension with minimal bending loading of the cantilevered energy-harvesting beam.

The frequency-doubling interfacing mechanism of the type shown in the schematic of Fig. 3.11 has been used in the development of energy-harvesting devices for a number of applications.[49–51] The frequency-doubling interfacing mechanisms may be cascaded to further double the frequency of the host

Downloaded From: https://www.spiedigitallibrary.org/ebooks/ on 07 Mar 2022
Terms of Use: https://www.spiedigitallibrary.org/terms-of-use

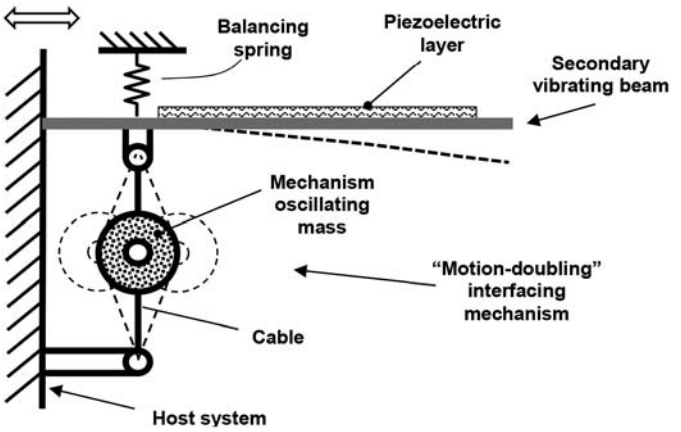

Figure 3.11 An implementation of the interfacing mechanism of Fig. 3.10.

system oscillatory motion. Interfacing mechanisms may be used with almost any type of secondary vibratory elements.

3.2.3.2.3 Interfacing mechanisms to generate higher frequencies of the input oscillatory motions

This section describes general methods of developing interfacing mechanisms with inherent nonlinear behavior for the purpose of generating higher-frequency harmonics of the host system oscillatory motions. The currently available and proposed methods may be categorized as follows:

1. Methods based on the kinematic (geometric) nonlinearity of the interfacing mechanisms;
2. Methods based on integrating "motion constraints" into interfacing mechanisms for added or enhanced kinematic nonlinearity;
3. Methods based on integrating nonlinear spring or damping elements with the interfacing mechanism;
4. Methods providing position-dependent external forcing functions.

Most linkage-type mechanisms with rotational joints undergoing relatively large motion exhibit kinematics (geometry)-based nonlinear dynamic behavior.[57–61] Kinematics-based input–output motion nonlinearity of linkage mechanisms may be used to generate higher harmonics of the input motion. As an interfacing mechanism, such linkage mechanisms may be used to transmit host system oscillatory motion to a vibration-based energy-harvesting device with higher-frequency content. The vibration-based energy-harvesting device may, for example, be a cantilevered type and be excited by the interfacing linkage mechanism as shown in Fig. 3.10. The output of the interfacing linkage mechanism may also be used to excite other vibrating mass–spring-type energy-harvesting devices such as the one shown in Fig. 3.4 from the base.

Downloaded From: https://www.spiedigitallibrary.org/ebooks/ on 07 Mar 2022
Terms of Use: https://www.spiedigitallibrary.org/terms-of-use

When designing machinery with such linkage mechanisms, an attempt is made to minimize the content and amplitudes of the generated higher-frequency harmonics to avoid excitation of the natural modes of vibration of the machine.[58–60] In the present energy-harvesting applications, interfacing-linkage-type mechanisms can be similarly designed in order to maximize the amplitudes of those output motion harmonics that are close to the natural mode(s) of vibration of the vibration-based energy-harvesting device. For linkage mechanism types and their design and analysis, the reader is referred to general textbooks on the subject, such as Ref. 62.

It is noted that many mechanisms used for generating higher-frequency oscillatory motions—and in fact most interfacing mechanisms—routinely use so-called "living joints." Living joints indicate structural flexibilities that allow for the desired gross motion of the relatively rigid segments of the interfacing mechanism and are generally preferred since they minimize friction and can lead to significantly smaller mechanisms. Living joints are also essential and readily implemented in MEMS and other miniaturized devices. The inherent elasticity provided by living joints and the device structure may also be used to eliminate the need for stabilizing or biasing springs.

One basic method of enhancing kinematic nonlinearity is the provision of motion constraints in the form of impact-generating stops in the path of natural motion of an interfacing mechanism. For example, by providing a stop in the path of a link or an oscillating mass of the motion-doubling mechanism of Fig. 3.10, the intermittent engagement of the interfacing mechanism with the provided stops introduces an impulsive force that can excite a wide range of modes of vibration of the secondary vibratory element used for electrical energy generation. Motion constraints in the form of a "rack" placed transversely near the tip of a vibrating beam that would pluck the beam as it vibrates have also been used to make a sudden change in the state of the vibrating system.[63]

Similar motion constraints may be provided to generate varieties of dynamic effects that can be utilized to transfer mechanical energy to secondary energy-harvesting devices, and as long as the host system can transfer mechanical energy to the interfacing mechanism, the secondary vibratory element (generator) can harvest the energy at resonance.

The other method of generating or enhancing nonlinear behavior of an interfacing mechanism of a vibration-based energy-harvesting device is to provide the mechanism with a nonlinear spring, a viscous damping element, or a Coulomb damping element. In general, damping elements may not be a good choice if they can be avoided since they dissipate a portion of the available mechanical energy. Nonlinear spring elements on the other hand do not dissipate mechanical energy, except for the internal damping of their material, and may be used to broaden the natural modes of vibration of the affected system.[64,65]

Downloaded From: https://www.spiedigitallibrary.org/ebooks/ on 07 Mar 2022
Terms of Use: https://www.spiedigitallibrary.org/terms-of-use

3.2.3.2.4 Provision of position-dependent external forcing functions

The above methods presented in this section are intended to provide the means of rendering the dynamics of the natural motion of the interfacing mechanism [Eq. (3.1)] nonlinear. As a result, the interfacing mechanism output motion would contain higher harmonics of the input motion provided by the host system. The higher harmonics of the interfacing mechanism output are in turn intended to excite a properly designed vibration-based energy-harvesting device in resonance.

It is noted that Eq. (3.1) represents the equation of motion of the interfacing mechanism of the energy-harvesting device, the output of which is input to a vibration-based (piezoelectric) generator. In cases in which the vibration-based generator is directly attached to the host structure, Eq. (3.1) can still be used to describe its dynamics in which y and x are the host system displacement and the deformation of the generator elastic element, respectively. For example, in the cantilevered beam generator shown in Fig. 3.1 and the model in Fig. 3.2, the deformation x would represent the amplitude of the first mode of vibration of the cantilevered beam.

An interfacing mechanism or a vibration-based generator attached directly to the structure of the host system undergoing low-frequency oscillatory motion may also be forced to undergo higher-frequency vibrations by the provision of passive position-dependent external forcing functions. Considering this forcing function to be $f_{ex}(x)$, the equation of motion [Eq. (3.1)] becomes

$$m\ddot{x} + c\dot{x} + kx = F(y,t) + f_{ex}(x). \tag{3.5}$$

The function $f_{ex}(x)$ may be linear or nonlinear. If it is linear, then its effect is similar to the spring constant k. If the function is nonlinear, the interfacing mechanism (or the vibration-based generator directly attached to the host system) is forced to respond to the sum of the applied external forces, i.e., right-hand side of Eq. (3.5), with the component corresponding to the external force $f_{ex}(x)$ containing higher harmonics of the host system motion. If the interfacing mechanism has nonlinear dynamics, the nonlinear function $f_{ex}(x)$ may be used to enhance the nonlinear behavior of the system, thereby increasing the harmonic content and amplitudes of the higher-harmonic components of the output motion, i.e., the input to the vibration-based energy-harvesting device.

One widely studied method for providing position-dependent external forcing functions is the use of one or more magnets to generate a magnetic field to apply position-dependent forces to vibration-based energy-harvesting devices that have interacting magnets or certain magnetizable elements. Various arrangements of magnets and magnetizable elements on the vibrating elements and the base structure of the vibrating element have been used. For

Downloaded From: https://www.spiedigitallibrary.org/ebooks/ on 07 Mar 2022
Terms of Use: https://www.spiedigitallibrary.org/terms-of-use

example, these arrangements have been used to construct vibrating systems that are bistable or tristable, or that exhibit other similar behaviors.[66–82]

It is appreciated that the magnetic field generated by permanent magnets may be used to apply position-dependent forces to an interfacing mechanism attached to a host system undergoing oscillatory motion or may be used to apply the position-dependent force directly to a vibration-based energy-harvesting device as has mostly been done in the aforementioned references.

The characteristics and dynamic behavior of vibration-based energy-harvesting devices with position-dependent external forces can be described by examining the basic system shown in the schematic of Fig. 3.12. For the sake of simplicity, a cantilevered-beam-type vibration-based energy-harvesting device similar to the one shown in Fig. 3.10 is attached directly to the host system without an intermediate interfacing mechanism. The host system oscillates in the direction shown by the double arrows at a frequency that is significantly lower than that of the natural mode of vibration of the beam. The tip mass is made of iron. Several permanent magnets are positioned on the base structure of the energy harvester along the path of oscillation of the iron tip mass. The permanent magnet spacings *a*, *b*, and *c* may be the same or different and, as described below, have a significant effect on the vibration of the device.

In the system of Fig. 3.12, the permanent magnets generate a magnetic field, through which the tip iron mass undergoes oscillatory motion as the host system applies an oscillatory motion to the base of the cantilevered beam, as indicated by the double arrow. During each passing of the tip iron mass through the established magnetic field, the net attracting force applied to the tip mass undergoes a minimum–maximum variation depending on the tip position relative to the permanent magnets. The (lateral) component of the force in the direction of the tip mass vibration acts to accelerate or decelerate the mass

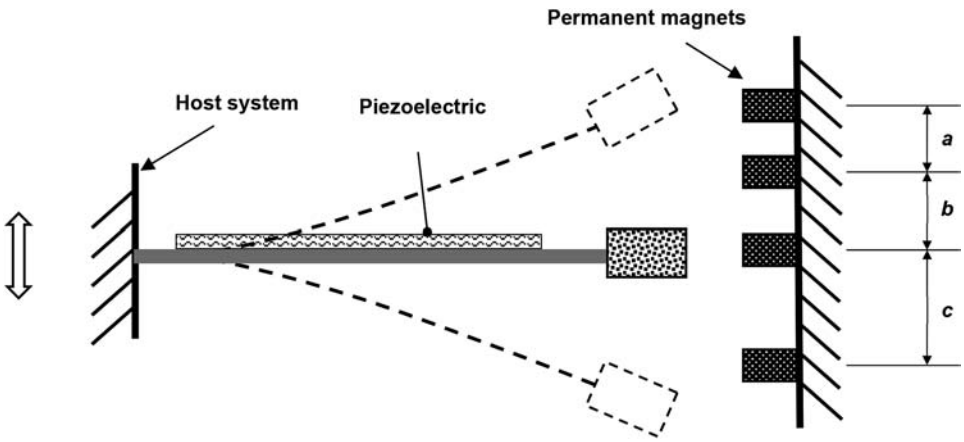

Figure 3.12 A vibration-based energy-harvesting device with position-dependent permanent-magnet-based external-force sources.

Downloaded From: https://www.spiedigitallibrary.org/ebooks/ on 07 Mar 2022
Terms of Use: https://www.spiedigitallibrary.org/terms-of-use

motion depending on the direction of its vibratory motion. The longitudinal component of the applied force generally has a slight stiffening effect on the cantilever beam, the effect of which is not considered in this discussion.

Here, it is assumed that the attracting force applied by each permanent magnet is not high enough to hold the mass attracted to a single permanent magnet and that the host system displacement causes the cantilevered beam and its tip mass to vibrate across the provided permanent magnets and their generated magnetic field.

If the permanent magnets are spaced at equal distances with respect to the vibrating beam tip, and if the tip mass travels past the magnets at a constant speed, then the lateral component of the attracting force acting on the tip mass exhibits a minimum–maximum variation profile with a first-order approximation of a sinusoidal function with a frequency that is dependent on the velocity of the passing tip mass. The faster the velocity of the passing tip the higher the frequency of the sinusoidal function. If the permanent magnets are not positioned at equal distances, the first-order approximation of the attractive force acting on the tip mass contains several frequencies depending on the spacing of the permanent magnets. In general, the tip mass velocity includes a combination of frequencies of the natural mode of vibration of the cantilever beam and the oscillatory motion of the host system in the absence of the permanent magnets, thereby resulting in added motion harmonics due to the added position-dependent external force with the provided permanent magnets.

The introduction of high-frequency oscillatory motions to the energy-harvesting device by the introduction of the position-dependent component $f_{ex}(x)$ (in the case of the system of Fig. 3.12, a cantilevered beam with piezoelectric transducer) ensures excitation of the beam at the generated high frequencies. The frequencies of the generated excitations also vary due to their dependence on the tip velocity. In particular, if several permanent magnets are used and are irregularly positioned, then the range of higher-frequency excitations is increased. As a result, the number of cycles of energy-harvesting device (cantilevered-beam) oscillation per cycle of host system oscillation can be significantly increased, and thereby the electrical energy that the harvesting device can generate is similarly increased.

It is appreciated that the positions of maximum attractive force appearing in the aforementioned attractive force profiles indicate points at which the cantilevered beam and the permanent magnet system can be at their minimum potential energy state, and thereby at a stable configuration state. As previously indicated, this characteristic of such systems with permanent-magnet-generated magnetic fields and with magnitizeable or permanent magnet tip mass have been configured to generate bistable or tristable systems or systems with a multiple-stable configuration.[66–82] If a permanent magnet is used instead of the iron mass at the tip of the bending beam (Fig. 3.12), and if the magnets are

Downloaded From: https://www.spiedigitallibrary.org/ebooks/ on 07 Mar 2022
Terms of Use: https://www.spiedigitallibrary.org/terms-of-use

positioned in repulsive configuration, then the above stable configurations are at the points of minimum-repulsive beam tip positions. Other permanent-magnet and magnitizeable, or permanent-magnet tip mass configurations, are also possible and would generally provide similar stable configurations.

It is also appreciated that the external force profile generated by the established magnetic field is expected to have significantly high-order terms and have a significant effect on the vibration of the cantilevered beam. The purpose of the present simplification is to illustrate the basic characteristics of the behavior of the energy-harvesting device in the presence of the externally applied position-dependent forces generated by the permanent magnets. In addition, important insight is provided that can assist the designer to develop higher-performance concepts and maximize harvester performance. For more detailed modeling and experimental results, the reader is referred to the provided references.

In the system of Fig. 3.12, the force applied to the tip of the vibrating beam by the permanent-magnet-generated magnetic field is dependent on the position of the beam tip in the magnetic field. The applied force may also be made dependent on the velocity of the beam tip in the magnetic field by providing a coil (connected to an electric load) close to the tip, in effect forming an electromagnetic generator.

3.2.3.2.5 *Methods to develop relatively small and lightweight structures with low natural frequencies*

The natural frequency of a vibration-based energy-harvesting device can be lowered by either increasing the effective mass or decreasing effective stiffness. However, by increasing the effective mass the device becomes heavy and relatively large. In general, the natural frequency of a vibrating structure decreases more rapidly by increasing its size as compared to its mass due to faster reduction of its stiffness. For example, in a cantilevered-beam-type vibration-based energy-harvesting device, doubling the tip mass results in a drop in the natural frequency of the beam by a factor of around 1.4. However, by doubling the length of the beam and assuming no change in its effective mass, the natural frequency is dropped by a factor of around 2.8, i.e., at twice the rate. The effective spring rate of the beam can also be reduced by a factor of 2.8 by reducing its thickness by one-half and by a factor of 1.4 by reducing its width. It is therefore readily seen that to achieve low natural frequency in a cantilevered-beam-type energy-harvesting device, the best beam geometry is a thin, long beam with a tip mass. The beam must however be wide enough to achieve stable vibration with minimal twisting.

As a result, attempts have been made to achieve longer effective lengths by using a so-called meandering piezoelectric beam[14] or by using a zig-zag structure.[83–85] Such techniques make it possible to achieve longer effective

Downloaded From: https://www.spiedigitallibrary.org/ebooks/ on 07 Mar 2022
Terms of Use: https://www.spiedigitallibrary.org/terms-of-use

lengths while maintaining a smaller footprint, thereby resulting in a natural frequency reduction of more than an order of magnitude.

3.2.4 Interfacing mechanisms for oscillatory translational and rotational motions with highly varying frequencies and random motions

In some applications, the host systems exhibit oscillatory motions that are essentially simple harmonic motions with relatively fixed frequencies. Such applications are however very few, and in the majority of host systems of interest, the oscillatory motions contain more than one significant harmonic that may vary over time. In many other applications, host system oscillatory motions are more or less random, particularly when the host system is subjected to random input forcing functions, such as in the case of a vehicle traveling on a road.

In general, the bandwidth of vibration-based energy-harvesting devices that are designed for single-mode excitation is narrow. When the frequency of the input oscillatory motion of the host system is known and relatively fixed, such vibration-based energy-harvesting devices would obviously exhibit good performance. However, if the input frequency is varying beyond the bandwidth of such vibration-based energy-harvesting devices, then a broader-bandwidth energy-harvesting device is needed.

One approach for increasing the bandwidth of vibration-based energy-harvesting devices has been the use of multiple transducers with slightly different natural frequencies to provide overlapping bandwidths.[86–89] In most such energy-harvesting devices, transducers have been of the cantilevered type. In Ref. 89 it is also shown that by elastically connecting the cantilevered beams, a broader frequency response can be obtained.

In certain applications, the host system exhibits oscillatory motions with multiple frequencies with significant amplitudes. If the multiple frequencies are fixed or vary within a very narrow range, then a vibration-based energy-harvesting device with multiple transducers, such as those described in Refs. 32 and 86–89, may be effective. It should however be noted that at any given point in time only a limited number of vibration-based generators would be effectively generating electrical energy. A survey of many of the different methods for the design of broadband vibration-based energy-harvesting devices and their advantages and disadvantages for different applications is provided in Ref. 32.

When the oscillatory motions of the host system are highly varying and even random but provide excitation frequencies within a relatively limited range, then multiple-transducer harvesters may prove effective.[32,86–89] Other options to consider include the use of position-dependent external-force-generating permanent magnets as described in Section 3.2.3.2.4. The use of kinematic nonlinearity, nonlinear spring, or damping elements is generally not

Downloaded From: https://www.spiedigitallibrary.org/ebooks/ on 07 Mar 2022
Terms of Use: https://www.spiedigitallibrary.org/terms-of-use

as effective since these only cause generation of harmonics of the input host system oscillatory motions, particularly when the input frequencies vary over a very wide range.

When the oscillatory motions of the host system are highly varying, particularly when the oscillatory motions are relatively slow, energy-harvesting devices using the two-stage interfacing mechanisms described in Section 3.2.3.2.1 are the most effective. The shortcoming of two-stage energy-harvesting devices, however, is the challenges of their implementation in MEMS-scale devices. Another option for such cases is the use of mechanical stops as described in Section 3.2.3.2.1 to apply short-duration impulses to the vibratory element(s) of the vibration-based energy-harvesting device for effective transfer of mechanical energy. The shortcomings of the latter approach are the relatively high levels of energy loss during each impact and the challenges of its implementation in MEMS-scale devices.

3.2.5 Interfacing mechanisms for energy harvesting from short-duration force and accelerating/decelerating pulses

In some applications, the energy-harvesting device is intended to generate electrical energy from impulsive loading. Such impulsive loading may, for example, be due to impact of an object with the host system, impact of the host with an object, pressure-wave or short-duration acceleration or deceleration shock loading due to detonation of explosives such as in munitions, and the like. The distinguishing characteristic of such energy-harvesting device input loading and related motions is their short duration and generally large amplitudes. The host system may provide a single or multiple pulses that are significantly far apart with minimal interaction between their effects. The energy-harvesting device and its electrical energy collection electronics must therefore be capable of addressing issues such as transducer physical damage protection, efficient transfer of available mechanical energy to the energy-harvesting device, efficient collection of the generated short-duration charges, and other application-specific issues.

Energy-harvesting devices developed to date for generating electrical energy from shock loading, such as from shock loading induced by firing setback acceleration in munitions or due to impact type of shock loading, may be divided into two basic groups.

The first group includes those devices in which the short-duration (shock) loading is applied directly to the piezoelectric transducer to generate electrical energy. In some cases, the pulse duration is a small fraction of a millisecond and thereby poses efficient collection and storage challenges. In some applications, such as in many impact or munitions firing applications, the shock loading occurs only once. Such devices are referred to as one-shot energy-harvesting power sources or generators.[90–92]

Downloaded From: https://www.spiedigitallibrary.org/ebooks/ on 07 Mar 2022
Terms of Use: https://www.spiedigitallibrary.org/terms-of-use

The second group includes those devices in which interfacing mechanisms are used to transfer mechanical energy made available by the input shock loading to a mechanical energy storage device. The stored mechanical energy is then converted to electrical energy using an appropriately designed transducer such as piezoelectric elements. For example, the interfacing mechanism may consist of a mass–spring system in which the input shock loading is stored as mechanical potential energy in its spring element and/or as mechanical kinetic energy in its mass element. Following the shock loading, the mass–spring system begins to vibrate. The mechanical energy of vibration is then converted to electrical energy using piezoelectric elements. The natural frequency of the mass–spring system must be selected taking into consideration the duration of the impact loading event and the rate at which electrical energy has to be generated.

The energy-harvesting devices belonging to the first group can generally convert a very small fraction of the total available mechanical energy to electrical energy. However, due to their relatively small size compared to the energy-harvesting devices of the second group, they are used in applications with limited available space and when only small amounts of electrical energy is required to be generated. Such devices are also used in applications in which the magnitude of the generated voltage pulse is important rather than the total amount of generated electrical energy, such as in impact level detection or pyrotechnic initiation devices.

The earliest published literature related to the first group appear to be related to extracting electrical energy from the impact of dropping a steel ball onto piezoelectric transducers for storage in capacitors and rechargeable batteries.[93,94] Similar dropping-ball-induced impact pulsed loading of piezoelectric elements are described in Refs. 95–98. Studies of impact compressive loading of piezoelectric elements positioned between the impacting head of an object housing and a loading mass during impact with relatively hard surfaces to generate very short-duration electrical energy pulses are provided in Refs. 99–104. Electrical energy generation based on the impact of dropping weights on piezoelectric elements is also presented in Ref. 105.

In another approach, Ref. 106 presents interfacing mechanisms that can be used to lock the generated strain in compressively loaded piezoelectric elements of energy-harvesting devices when the device is subjected to impulsive (shock) loading due to firing acceleration in munitions or during target impact.

A simple interfacing mechanism for the second group of energy-harvesting devices is the mass–spring system shown in Fig. 3.13. The system consists of an equivalent mass m and a spring with a rate k. As a result of shock loading due to an externally applied force to the mass m or when the device platform is subjected to an acceleration pulse a (such as during firing setback acceleration in munitions), the spring and the mass elements are provided with an initial

Downloaded From: https://www.spiedigitallibrary.org/ebooks/ on 07 Mar 2022
Terms of Use: https://www.spiedigitallibrary.org/terms-of-use

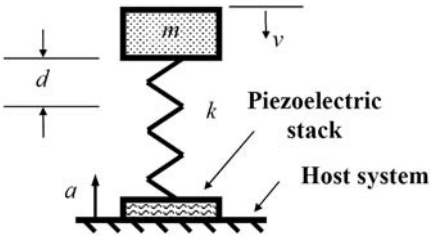

Figure 3.13 A mass–spring interfacing mechanism of an energy-harvesting device for storing mechanical energy from shock loading.

deflection d and velocity v, respectively. An initial potential energy (1/2) kd^2 and kinetic energy (1/2) mv^2 is thereby stored in the mass–spring system. Following the shock loading, the mass–spring system begins to vibrate. A piezoelectric transducer (preferably, a stack type operating in the 33 mode) may then be provided between the base of the spring element and the structure of the host system to convert the mechanical energy stored in the mass–spring interfacing mechanism to electrical energy.

In practice, particularly when high levels of shock loadings are involved, the piezoelectric element has to be protected from excessive tensile as well as compressive loading as described, for example, in Refs. 92 and 107–109, and later in Chapter 5. The mass element is also preferably an integral part of the elastic element of the mass–spring interfacing mechanism.

The frequency of the natural mode of vibration of the mass–spring system must be selected to allow effective transfer of mechanical energy and to provide the generated electrical energy at the desired rate. It is also noted that since a significant amount of mechanical energy can be stored in a properly designed mass–spring-based interfacing mechanism, such energy-harvesting devices can generate significantly larger amounts of electrical energy over several cycles of vibration of the mass–spring system than a single piezoelectric transducer can generate when subjected to the same shock-loading event.

An example of another related type of energy-harvesting device that is referred to as piezoelectric-based "mechanical reserve power source" is shown in the schematic of Fig. 3.14. This power source functions similarly to chemical reserve batteries such as thermal batteries and liquid reserve batteries with the difference that mechanical energy is stored in them in the form of potential energy. Upon activation of the power source, the released mechanical energy is converted to electrical energy by the piezoelectric transducer. Several designs of such mechanical reserve power sources using compressive-, tensile-, torsional-, or bending-type springs are described in Ref. 110. In the example of Fig. 3.14, a mass–spring vibrating element is mounted over a piezoelectric stack. The power source is attached to the structure of the host system. Prior to activation, the spring element is preloaded in compression and is kept in this state by preload retention members (solid lines). The preload retention members are also

Downloaded From: https://www.spiedigitallibrary.org/ebooks/ on 07 Mar 2022
Terms of Use: https://www.spiedigitallibrary.org/terms-of-use

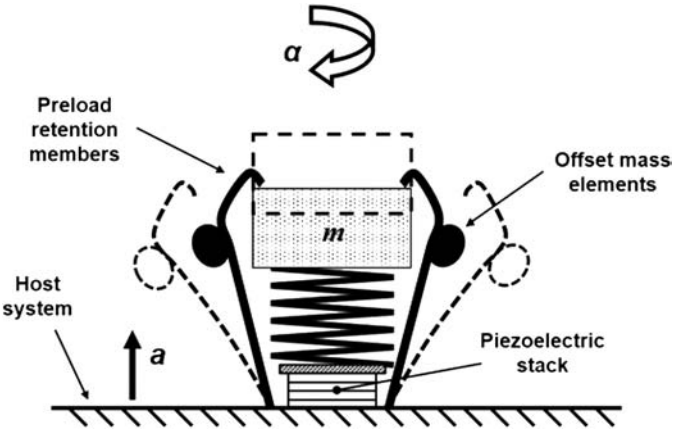

Figure 3.14 A schematic of a linear acceleration pulse or spin-activated piezoelectric-based mechanical reserve power source—U.S. Patent number 8,183,746.[110]

provided with an "offset mass element," which tends to apply a bending moment that releases the preloaded mass–spring element (dashed lines) when the host system is subjected to an acceleration a in the direction indicated by the arrow or a rotary acceleration α, thereby activating the power source and allowing electrical energy to be generated by the vibrating mass–spring system.

3.3 Interfacing Mechanisms for Electromagnetic-based Transducers

In electromagnetic induction transducers the input mechanical energy is used to vary magnetic flux through a conductor, usually a coil, to generate electrical current in the conductor connected to a load. The magnetic flux variation is usually achieved via relative linear or rotary motion between a coil and a permanent magnet. The relative motion between the coil and the permanent magnet is preferably the result of moving the permanent magnet relative to a fixed coil since it results in fixed output wires. The amount of power that an electromagnetic induction transducer generates is dependent on the length of the conductor, i.e., the number of turns of the coil when it is wound, the strength of the magnetic field and its coil coupling, and the velocity of the coil motion in the magnetic field.

A review of electromagnetic transducers and their characteristics is provided in Chapter 2 with an extensive list of references for more in-depth reading. As indicated, electromagnetic generator technology is highly developed and has been used to generate electrical power ranging from a small fraction of one watt to megawatts. In almost all such applications, electrical energy is generated through rotary motion to achieve high relative velocities that are continuous, and when possible constant, for efficient electrical energy generation and to minimize mechanical as well as electrical

Downloaded From: https://www.spiedigitallibrary.org/ebooks/ on 07 Mar 2022
Terms of Use: https://www.spiedigitallibrary.org/terms-of-use

losses. The emphasis in this section is on small and micro-generators, primarily with linear or rotary vibratory or oscillatory input motions.

Electromagnetic transducers, particularly their continuously rotating versions, are difficult to implement in micro-scales and even very small scales due to transducer coils as well as permanent magnet component limitations. For this reason, they have been studied mostly for use in relatively large energy-harvesting devices. In addition, as indicated in Chapter 2, electromagnetic transducers (generators) are not efficient in converting mechanical energy to electrical energy at low relative velocities of transducer coil in the established magnetic field. For this reason, they may have to be provisioned with speed-increasing gearings in applications such as windmills.

The electromagnetic transducers of a continuously rotating type are generally more efficient than vibration-based types, particularly when relatively high rotary speeds can be achieved. It is also noted that vibration-based generators exhibit significant mechanical energy losses due to internal damping of their elastic members. Internal damping losses are proportional to the strain rates in the device elastic (spring) members. However, to increase the generator efficiency, the vibration amplitude and frequency must be increased. This would however also increase mechanical energy losses due to internal damping of the device elastic members. These issues make the design of highly efficient vibration-based electromagnetic energy-harvesting devices challenging.

In the remaining part of this section, mechanisms for interfacing electromagnetic transducers to host systems undergoing different types of motions are described. Similar to the case of piezoelectric-based devices described in Section 3.2, interfacing mechanisms are intended to effectively transfer mechanical energy to the electromagnetic transducer of the energy-harvesting device for conversion to electrical energy.

3.3.1 Interfacing mechanisms for rotary input motions

When input motion from the host system is continuous and rotary, the need for an interfacing mechanism is dependent mainly on the input speed. If the input speed is high enough for efficient conversion to electrical energy with a rotary electromagnetic transducer, the host system may be directly coupled to the transducer. Otherwise, interfacing mechanisms may need to be considered.

When the input speed provided by the host system is relatively low, the commonly used solution for efficient operation requires speed-increasing gearing. Such gearing mechanisms have long been used in windmills, but attempts are being made to avoid their use due to high operating costs. Electromagnetic generators for efficient operation at speeds on the order of 5–10 rpm are possible in the absence of space limitations. However, at speeds approaching fractions of one rpm, direct coupling to electromagnetic

Downloaded From: https://www.spiedigitallibrary.org/ebooks/ on 07 Mar 2022
Terms of Use: https://www.spiedigitallibrary.org/terms-of-use

generators for efficient operation is not practical with currently available technology.

For very low input speeds or when the input speed is highly varying over time or even intermittent or reversing, the following two basic interfacing mechanism types may be used for effective transfer of mechanical energy from the host system to electromagnetic transducers for efficient conversion to electrical energy:

1. The interfacing mechanism transfers mechanical energy from the host system via its rotary motion to a mechanical potential energy storage device. Then when a predetermined threshold is reached, the stored mechanical energy is released to the provided generator for conversion to electrical energy. The generator is preferably provided with an appropriately sized flywheel to allow for a smooth and effective transfer of mechanical energy and efficient generator operation. The potential mechanical energy storage device is preferably a power spring, and the indicated release threshold is selected to achieve the desired generator input speed. The potential energy from the power spring is preferably first transferred to a flywheel, which is in turn connected to the electromagnetic generator.
2. Another approach is to use a two-stage interfacing mechanism similar to that shown in the schematic of Fig. 3.1 but using a vibration-based electromagnetic generator instead of a piezoelectric-based generator. Such vibration-based generators are described later in this section. It is, however, appreciated that in both of the above cases, the energy-harvesting device may be considered to be grounded, i.e., attached to the foundation of the host system, or attached to the host system.

3.3.2 Interfacing mechanisms for continuous oscillatory translational and rotational motions

Interfacing mechanisms appropriate for extracting mechanical energy from translational or rotational motions of a host system for transfer to an electromagnetic transducer may be categorized as follows based on the characteristics and magnitudes of the oscillatory motions and the transducer type:

1. If the translational or rotational oscillatory motion of the host system is fast enough to provide high enough translational or rotational speeds, and if the energy-harvesting device and its transducer can be grounded, the energy-harvesting device transducer may be connected directly to the host system with an appropriate coupling member. For rotary oscillatory motions, the transducer is preferably of rotary type. For translational oscillatory motions, the transducer may be a linear type similar to linear motors or may be a rotary type coupled to the host

Downloaded From: https://www.spiedigitallibrary.org/ebooks/ on 07 Mar 2022
Terms of Use: https://www.spiedigitallibrary.org/terms-of-use

system as a so-called slider-crank mechanism, in which the host system serves as the slider and the transducer shaft as the crank, connected to the host system with a coupling link. The dimensions of the slider-crank mechanism links can be selected to provide the transducer a range of rotary speeds at which it can efficiently generate electrical energy.

2. For the host system oscillatory motions described above, if the energy-harvesting device and its transducer cannot be grounded, the harvesting device has to be directly attached to the host system. Mechanical energy must then be transferred from the translational or rotational oscillatory motion of the host system to the transducer via an appropriate interfacing mechanism. Similar to piezoelectric-based energy-harvesting devices, the following cases need to be considered:
   a. If the frequency of oscillatory motion of the host system is not very high, a two-stage interfacing mechanism similar to the pendulum-type mechanism described in Section 3.2.3.2 may be used to wind a torsion (power) spring. The potential energy stored in the power spring may then be released after a threshold level has been reached to directly rotate the shaft of a rotary electromagnetic generator or to rotate a wheel with teeth as shown in Fig. 3.1 to intermittently excite a secondary vibratory element, which in the present case uses an electromagnetic transducer to generate electrical energy. When using a rotating generator, the potential energy is preferably transferred to a flywheel, which may be integral to the generator rotor, for efficient conversion to electrical energy over several rotation cycles.
   b. When using vibration-based electromagnetic transducers, the interfacing mechanisms similar to those described in Sections 3.2.2–3.2.4 for piezoelectric-based transducers may be employed, depending on the frequencies of the host system oscillatory motions and whether the frequencies are relatively fixed or time varying.

The development of various relatively small vibration-based electromagnetic energy-harvesting devices has been reported.[111–123] The implementation of electromagnetic-based transducers is more challenging at MEMS scale and has been the subject of several efforts (e.g., Refs. 114–120).

Both linear and rotational electromagnetic transducers may be used as secondary vibrating elements in two-stage energy-harvesting devices. Schematics of such linearly and rotationally vibrating systems are shown in Figs. 3.15 and 3.16, respectively. A linearly vibrating electromagnetic generator may also be configured similarly to the piezoelectric-based mass–spring generator shown in Fig. 3.13 or the flexible vibrating-beam-type generators of Fig. 3.1, with a permanent-magnet- and coil-based transducer replacing the piezoelectric transducer.

Downloaded From: https://www.spiedigitallibrary.org/ebooks/ on 07 Mar 2022
Terms of Use: https://www.spiedigitallibrary.org/terms-of-use

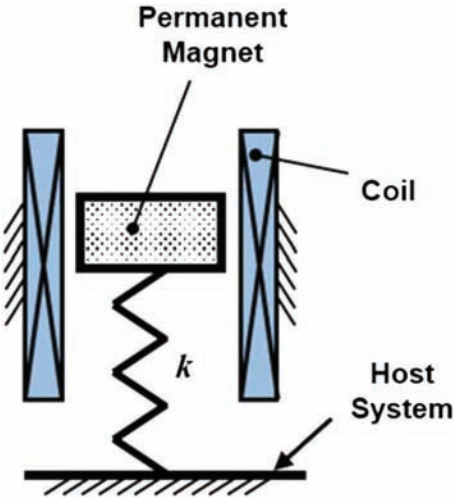

Figure 3.15 A schematic of a linear vibratory electromagnetic generator.

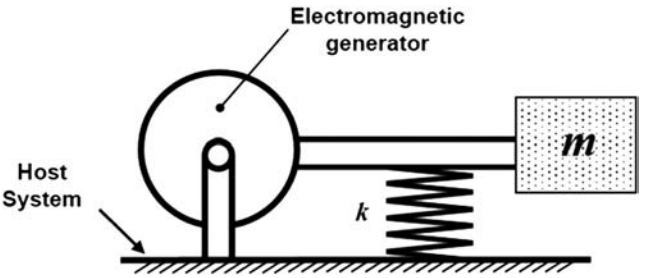

Figure 3.16 A schematic of a rotary vibratory electromagnetic generator.

In the generator of Fig. 3.15, the mass of the mass–spring element preferably consists of or is provided with at least one permanent magnet and is attached to the generator structure by a spring element. The generator coils are fixed to the structure of the generator. The vibratory motion of the permanent magnets produces a time-varying flux linked to the coil. An electrical potential difference is thereby induced between the ends of the coil conductor [electromotive force (emf)], providing electrical energy that can be collected as described in Chapter 4. It is appreciated that the permanent magnet of the generator in Fig. 3.15 may be attached to the tip of a vibrating beam to allow similar vibratory motion of the permanent magnet between the generator coil(s). The configuration of the coil elements may have to be modified to allow for vibratory motion of the permanent magnet(s) close to the coils. The replacement of the helical spring shown in Fig. 3.15 with such a vibrating-beam-type elastic element does not affect the basic operation of the generator.

The vibratory generator shown schematically in Fig. 3.16 functions similarly but in rotational mode. The rotary electromagnetic generator is

Downloaded From: https://www.spiedigitallibrary.org/ebooks/ on 07 Mar 2022
Terms of Use: https://www.spiedigitallibrary.org/terms-of-use

provided with an off-set mass and linear or torsional spring element to form a vibrating mass–spring system. The rotational vibration of the mass–spring element directly, or through a speed-increasing gearing or linkage mechanism, rotates the rotor of the generator, thereby generating electrical energy to be collected.

3.3.3 Interfacing mechanisms for energy harvesting from short-duration force and acceleration pulses

When the energy-harvesting device is intended to generate electrical energy from a host system that is subjected to impulsive loading such as due to the events described in Section 3.2.5, the interfacing mechanisms described in that section for piezoelectric-based transducers may be similarly used for electromagnetic transducers. In such applications, the impulse loading or acceleration pulse is also used to transfer mechanical potential and/or kinetic energy to the device spring and mass of a mass–spring vibrating system such as those shown in Figs. 3.15 and 3.16. The transferred mechanical energy is then converted to electrical energy as the mass–spring system vibrates via the provided electromagnetic transducer.

The mechanical reserve power source shown in Fig. 3.14 may similarly be designed to operate with an electromagnetic generator. Such reserve power sources can be designed to generate a significant amount of electrical energy to power emergency equipment such as emergency sensors and transmitters or to operate certain electronic devices. Such reserve power sources have the advantage of having very long shelf life of well over 20–30 years when packaged in a hermetically sealed housing.

3.4 Interfacing Mechanisms for Electrostatic- and Magnetostrictive-based Transducers

The modes of operation of electrostatic and magnetostrictive transducers are generally similar to those of piezoelectric and electromagnetic transducers, respectively. For this reason, their proper interfacing mechanisms are generally similar to those described for piezoelectric and electromagnetic transducers and are briefly described below.

As the output energy of electrostatic transducers is a function of the displacement between the electrodes or the overlap area between the electrodes, the interfacing techniques described above for piezoelectric harvesters are directly applicable to these transducers. This is particularly the case for those described for vibration-based piezoelectric energy-harvesting devices. In the case of magnetostrictive transducers, the output energy is a function of the displacement rate; thus, the interfacing techniques described above for electromagnetic harvesters are directly applicable to such transducers.

Downloaded From: https://www.spiedigitallibrary.org/ebooks/ on 07 Mar 2022
Terms of Use: https://www.spiedigitallibrary.org/terms-of-use

References

1. R. Murray and J. Rastegar, "Novel two-stage electrical energy generators for highly-variable and low-speed linear or rotary input motions," *ASME 2009 Design Engineering Technical Conference, DETC2009-87526*, pp. 789–796–540, San Diego, California (2009).
2. R. Murray and J. Rastegar, "Novel two-stage electrical energy generators for low and variable speed rotary machinery," *ASME 2013 Conference on Smart Materials, Adaptive Structures and Intelligent Systems*, SMASIS2013-3217, V002T07A024, Snowbird, Utah (2013).
3. J. Rastegar, T. Spinelli, and R. Murray, "Electrical generators for low-frequency and time-varying rocking and rotary motions," U.S. Patent Number 8,410,667 (2013).
4. J. Rastegar and R. Murray, "Electrical generators for use in unmoored buoys and the like platforms with low-frequency and time-varying oscillatory motions," U.S. Patent Number 8,134,281 (2012).
5. J. Rastegar and R. Murray, "Novel two-stage piezoelectric-based electrical energy generators for low and variable speed rotary machinery," *Proc. SPIE* **7288**, 72880B (2009) [doi: 10.1117/12.815764].
6. J. Rastegar, "Electrical generators for low-frequency and time-varying rocking and rotary motion," U.S. Patent Number 7,821,183 (2010).
7. R. Murray and J. Rastegar "Novel two-stage piezoelectric-based ocean wave energy harvesters for moored or unmoored buoys," *Proc. SPIE* **7288**, 72880E (2009) [doi: 10.1117/12.815852].
8. J. Rastegar and R. Murray, "Novel two-stage piezoelectric-based electrical energy generators for low and variable speed rotary machinery," *Proc. SPIE* **7288**, 72880B (2010) [doi: 10.1117/12.815764].
9. J. Rastegar and R. Murray, "Novel two-stage electrical energy generators for highly-variable and low-speed linear or rotary input motions," *ASME 2008 Design Engineering Technical Conference*, DETC2008-49646, pp. 533–540, Brooklyn, New York (2008).
10. J. Rastegar and R. Murray, "Novel vibration-based electrical energy generators for low and variable speed turbo-machinery," *Proc. SPIE* **6527**, 65270Z (2007) [doi: 10.1117/12.715017].
11. J. Rastegar, C. Pereira, and H.-L. Nguyen, "Piezoelectric-based power sources for harvesting energy from platforms with low frequency vibration," *Proc. SPIE* **6171**, 617101 (2006) [doi: 10.1117/12.657464].
12. K. Adachi and T. Tanaka, "An experimental power generation evaluation of cantilever type of piezoelectric vibration energy harvester," *ASME Conf. Smart Materials, Adaptive Structures and Intelligent Systems*, 281–289 (2009).
13. J. Baker, S. Roundy, and P. Wright, "Alternative geometries for increasing power density in vibration energy scavenging for wireless

Downloaded From: https://www.spiedigitallibrary.org/ebooks/ on 07 Mar 2022
Terms of Use: https://www.spiedigitallibrary.org/terms-of-use

sensor networks," *Proc. 3rd Int. Energy Conversion Engineering Conf.*, AIAA-2005-5617, San Francisco, California (2005).
14. D. F. Berdy, P. Srisungsitthisunti, B. Jung, X. Xu, J. F. Rhoads, and D. Peroulis, "Low-frequency meandering piezoelectric vibration energy harvester," *IEEE Transactions on Ultrasonics, Ferroelectrics and Frequency Control* **59**(5), 846–858 (2012).
15. R. Calio, U. B. Rongala, D. Camboni, M. Milazzo, C. Stefanini, G. de Petris, and C. M. Oddo, "Piezoelectric energy harvesting solutions," *Sensors* **14**, 4755–4790 (2014).
16. A. Erturk and D. Inman, *Piezoelectric Energy Harvesting*, John Wiley & Sons, Ltd., Hoboken, New Jersey (2011).
17. M. Goldfarb and L. D. Jones, "On the efficiency of electric power generation with piezoelectric ceramic," *ASME Journal of Dynamic Systems, Measurement, and Control* **121**, 566–571 (1999).
18. Y. Hu, F. Y. Zhang, C. Xu, L. Ling, R. L. Snyder, and Z. L. Wang, "Self-powered system with wireless data transmission," *Nano Letters* **11**, 2572–2577 (2011).
19. Y. B. Jeon, R. Sood, J. Jeong, and S. Kim, "MEMS power generator with transverse mode thin film PZT," *Sensors and Actuators A: Physical* **122**(1), 16–22 (2005).
20. T. Johnson, D. Charnegie, W. Clark, M. Buric, and G. Kusic, "Energy harvesting from mechanical vibration using piezoelectric cantilever beams," *Proc. SPIE* **6169**, 61690D (2006) [doi: 10.1117/12.659466].
21. A. Kasyap, J. Lim, D. Johnson, S. Horowitz, T. Nishida, K. Ngo, M. Sheplak, and L. Cattafesta, "Energy reclamation from a vibrating piezoceramic composite beam," *Proc. of 9th International Congress on Sound and Vibration 271 Orlando*, Florida (2002).
22. S. B. Kim, J. J. Park, H. Ahn, D. Liu, and D. J. Kim, "Temperature effects on output power of piezoelectric vibration energy harvesters," *Microelectronics Journal* **42**, 988–991 (2011).
23. H. S. Kim, J. J. Kim, and J. Kim, "A review of piezoelectric energy harvesting based on vibration," *International Journal of Precision Engineering and Manufacturing* **12**(6), 1129–1141 (2011).
24. H. Kim, V. Bedekar, R. A. Islam, W. H. Lee, D. Leo, and S. Priya, "Laser-machined piezoelectric cantilevers for mechanical energy harvesting," *IEEE Transactions on Ultrasonics, Ferroelectrics and Frequency Control* **55**(9), 1900–1905 (2008).
25. H. Kim, S. Priya, H. Stephanou, and K. Uchino, "Consideration of impedance matching techniques for efficient piezoelectric energy harvesting," *IEEE Transactions on Ultrasonics, Ferroelectrics and Frequency Control* **54**, 1851–1859 (2007).
26. E. Lefeuvre, A. Badel, C. Richard, L. Petit, and D. Guyomar, "A comparison between several vibration-powered generators for

Downloaded From: https://www.spiedigitallibrary.org/ebooks/ on 07 Mar 2022
Terms of Use: https://www.spiedigitallibrary.org/terms-of-use

standalone systems," *Sensors and Actuators A: Physical* **126**(2), 405–416 (2006).
27. L. M. Miller, "Micro-scale Piezoelectric Vibration Energy Harvesting: From Fixed-Frequency to Adaptable-Frequency Devices," Ph.D. thesis, University of California, Berkley (2012).
28. E. Murimi and M. Neubauer, "Piezoelectric energy harvesting: an overview," *Proc. of the 2012 Mech. Eng. Conf. on Sustainable Research and Innovation 4*, 117–121 (2004).
29. S. Priya and D. J. Inman, *Energy Harvesting Technologies*, Springer, New York (2009).
30. H. A. Sodano and D. J. Inman, "Estimation of electric charge output for piezoelectric energy harvesting," *Journal of Strain Analysis* **40**(2), 49–58 (2004).
31. H. A. Sodano, D. J. Inman, and G. Park, "A review of power harvesting from vibration using piezoelectric materials," *The Shock and Vibration Digest* **36**(3), 197–205 (2004).
32. J. Twiefel and H. Westermann, "Survey on broadband techniques for vibration energy harvesting," *Journal of Intelligent Material Systems and Structures* **24**(11), 1291–1302 (2013).
33. Z. L. Wang and J. Song, "Piezoelectric nanogenerators based on zinc oxide nanowire arrays," *Science* **312**, 242–246 (2006).
34. C. B. Williams and R. B. Yates, "Analysis of a micro-electric generator for microsystems," *Sensors and Actuators A: Physical* **52**, 8–11 (1996).
35. T. B. Xu, E. J. Siochi, J. H. Kang, L. Zuo, W. Zhou, X. Tang, and X. Jiang, "Energy harvesting using a PZT ceramic multilayer stack," *Smart Materials and Structures 22*, 065015 (2013).
36. Y. Zhang, "Piezoelectric Based Energy Harvesting on Low Frequency Vibrations of Civil Infrastructures," Ph.D. thesis, Louisiana State University (2014).
37. N. E. duToit, B. L. Wardle, and S. Kim, "Design consideration for MEMS-scale piezoelectric mechanical vibration energy harvesters," *Journal of Integrated Ferroelectrics* **71**, 121–160 (2005).
38. E. K. Reilly, L. M. Miller, R. Fain, and P. K. Wright, "A study of ambient vibrations for piezoelectric energy conversion," *9th Int. Workshop on Micro and Nanotechnology for Power Generation and Energy Conversion Applications*, 312–315 (2009).
39. S. Roundy, P. K. Wright, and J. M. Rabaey, *Energy Scavenging for Wireless Sensor Networks with Special Focus on Vibrations*, Kluwer Academic Publishers, Boston (2004).
40. H. Liu, C. J. Tay, C. Quan, T. Kobayashi, and C. Lee, "Piezoelectric MEMS energy harvester for low-frequency vibrations with wideband operation range and steadily increased output power," *Journal of Microelectromechanical Systems* **20**(5), 1131–1142 (2011).

Downloaded From: https://www.spiedigitallibrary.org/ebooks/ on 07 Mar 2022
Terms of Use: https://www.spiedigitallibrary.org/terms-of-use

41. H. Liu, C. Lee, T. Kobayashi, C. J. Tay, and C. Quan, "Investigation of piezoelectric MEMS-based wideband energy harvesting system with assembled frequency-up-conversion mechanism," *Procedia Engineering* **25**, 725–728 (2011).
42. M. A. Halim and J. Y. Park, "Theoretical modeling and analysis of mechanical impact driven and frequency up-converted piezoelectric energy harvester for low-frequency and wide-bandwidth operation," *Sensors and Actuators A* **208**, 56–65 (2014).
43. J. Rastegar and R. Murray "Dynamo-type lanyard operated event detection and power generators," U.S. Patent Number 9,112,390 (2015).
44. D. G. Lee, G. P. Carman, D. Murphy, and C. Schulenburg, "Novel micro vibration energy harvesting device using frequency up conversion," *Proc. 14th Int. Conf. on Solid State Sensors, Actuators and Microsystems (IEEE Transducer 07)*, pp. 871–874 (2007).
45. L. Gu and C. Livermore, "Impact-driven, frequency up-converting coupled vibration energy harvesting device for low frequency operation," Smart Material and Structures 20, 045004 (2011).
46. M. Han, Y. C. Chan, W. Liu, S. Zhang, and H. Zhang, "Low frequency PVDF piezoelectric energy harvester with combined d31 and d33 operating modes," *Proc. 8th IEEE Intern. Nano/Micro Engineered and Molecular Systems Conference*, 440–443 (2013).
47. P. Janphuang, R. Lockhart, D. Briand, and N. F. de Rooij, "On the optimization and performance of a compact piezoelectric impact MEMS energy harvester," *MEMS 2014*, San Francisco, California, 429–432 (2014).
48. P. Janphuang, D. Isarakorn, D. Briand, and N. F. de Rooij, "Energy harvesting from a rotating gear using an impact type piezoelectric mems scavenger," *16th International Solid-State Sensors, Actuators and Microsystems Conference (TRANSDUCERS)*, Beijing, China, 735–738 (2011).
49. J. Rastegar, "*Energy harvesting from input impulse with motion doubling mechanism for generating power from mortar tube firing impulses and other inputs*," U.S. Patent Number 8,912,710 (2014).
50. J. Rastegar and R. Murray, "Development of high-efficiency piezoelectric-based energy-harvesting power sources using motion-doubling mechanisms," *ASME 2013 Conference on Smart Materials, Adaptive Structures and Intelligent Systems*, SMASIS2013-3225, Snowbird, Utah (2013).
51. J. Rastegar, R. Murray, and C. Pereira, "Novel motion-doubling mechanism for improved piezoelectric energy-harvesting performance," *Proc. SPIE* **8341**, 83411M (2012) [doi: 10.1117/12.915411].
52. J. Rastegar and D. Feng, "Novel motion-doubling linkage mechanisms for vehicle suspension – performance simulation results," *ASME Design*

Downloaded From: https://www.spiedigitallibrary.org/ebooks/ on 07 Mar 2022
Terms of Use: https://www.spiedigitallibrary.org/terms-of-use

Engineering Technical Conference, DETC2007-3583, 251–256, Las Vegas, Nevada (2007).
53. J. Rastegar, K. Jorabchi, and H. Park, "Enhancement of the vehicle suspension performance using motion-doubling linkage mechanisms," *ASME Design Engineering Technical Conference*, DETC2006-99504, 735–740, Philadelphia, Pennsylvania (2006).
54. J. Rastegar and J. Zhang, "Reduction of induced vibration using motion-doubling linkage mechanisms," *ASME Design Engineering Technical Conference*, DETC2006-99704, 759–764, Philadelphia, Pennsylvania (2006).
55. J. Rastegar and J. Zhang, "Special cases of input speed doubling linkage mechanisms and their dynamics advantage," *ASME Design Engineering Technical Conference*, DETC2004-57341, 885–891, Salt Lake City, Utah (2004).
56. J. Rastegar, J. Zhang, and L. Hua, "On the existence of special cases of input speed doubling linkage mechanisms," *ASME 2003 International Design Engineering Technical Conference*, DETC2003/DAC-48832, 1207–1211, Chicago, Illinois (2003).
57. B. Fardanesh and J. Rastegar, "A new model-based tracking controller for robot manipulators using trajectory pattern inverse dynamics," *IEEE Transactions on Robotics and Automation* **8**(2), 279–285 (1992).
58. J. Rastegar and L. Yuan, "A systematic method for kinematics synthesis of high-speed mechanisms with optimally integrated smart materials," *ASME Journal of Mechanical Design* **124**(1), 14–20 (2001).
59. J. Rastegar, Q. Tu, and F. Tangerman, "Trajectory synthesis and inverse dynamics formulation for minimal vibrational excitation for flexible structures based on trajectory patterns," *American Control Conference*, San Francisco (1993).
60. Q. Tu and J. Rastegar, "Trajectory pattern method based trajectory synthesis and inverse dynamics formulation for minimal vibrational excitation for flexible structures," *ASME Mechanisms Conference*, Irvine, California (1996).
61. Q. Tu, J. Rastegar, and J. R. Singh, "Trajectory synthesis and inverse dynamics model formulation and control of tip motion of a high performance flexible positioning system," *Mechanism and Machine Theory* **29**(7), 959–968 (1994).
62. A. G. Erdman, G. N. Sandor, and S. Kota, Mechanism Design, Analysis and Synthesis, 4th Edition, Prentice-Hall (2001).
63. R. M. Tieck, G. P. Carman, and D. G. E. Lee, "Electrical energy harvesting using a mechanical rectification approach," *Proc IMECE*, 547–553 (2006).

Downloaded From: https://www.spiedigitallibrary.org/ebooks/ on 07 Mar 2022
Terms of Use: https://www.spiedigitallibrary.org/terms-of-use

64. M. F. Daqaq, "On intentional introduction of stiffness nonlinearities for energy harvesting under white Gaussian excitations," *Nonlinear Dynamics* **69**(3), 1063–1079 (2012).
65. R. Ramlan, M. Brennan, B. Mace, and I. Kovacic, "Potential benefits of a non-linear stiffness in an energy harvesting device," *Nonlinear Dynamics* **59**, 545–558 (2010).
66. B. Anderson and A. Wickenheiser, "Performance analysis of frequency up-converting energy harvesters for human locomotion," *Proc. SPIE* **8341**, 834102 (2012) [doi: 10.1117/12.915277].
67. F. Cottone, H. Vocca, and L. Gammaitoni, "Nonlinear energy harvesting," *Physical Review Letters 102*, 080601 (2009).
68. M. F. Daqaq, "Transduction of a bistable inductive generator driven by white and exponentially correlated Gaussian noise," *Journal of Sound and Vibration* **330**(11), 2554–2564 (2011).
69. M. F. Daqaq, "Response of uni-modal duffing-type harvesters to random forced excitation," *Journal of Sound and Vibration* **329**(18), 3621–3631 (2010).
70. A. Erturk and D. J. Inman, "Broadband piezoelectric power generation on high-energy orbits of the bistable Duffing oscillator with electromechanical coupling," *Journal of Sound and Vibration* **330**(10), 2339–2353 (2011).
71. M. Ferrari, V. Ferrari, M. Guizetti, B. Ando, S. Baglio, and C. Trigona, "A single-magnet nonlinear piezoelectric converter for enhanced energy harvesting from random vibrations," *Sensors and Actuators A: Physical* **172**(1), 287–292 (2011).
72. L. Gammaitoni, I. Neri, and H. Vocca, "Nonlinear oscillator for vibration energy harvesting," *Applied Physics Letters 94*, 164402 (2009).
73. R. L. Harne and K. W. Wang, "A review of recent research on vibration energy harvesting via bistable systems," *Smart Materials and Structures 22*, 023001 (2013).
74. R. Masana and M. F. Daqaq, "Relative performance of a vibratory energy harvester in mono-and bi-stable potentials," *Journal of Sound and Vibration* **330**(24), 6036–6052 (2011).
75. C. R. McInnes, D. G. Gorman, and M. P. Cartmell, "Enhanced vibration energy harvesting using nonlinear stochastic resonance," *Journal of Sound and Vibration* **318**(4-5), 655–662 (2008).
76. S. P. Pellegrini, N. Tolou, M. Schenck, and J. L. Herder, "Bistable vibration energy harvesters: a review," *Journal of Intelligent Material Systems and Structures* **24**(11), 1303–1312 (2013).
77. S. C. Stanton, C. C. McGehee, and B. P. Mann, "Nonlinear dynamics for broadband energy harvesting: Investigation of a bistable piezoelectric inertial generator," *Physica D: Nonlinear Phenomena* **239**(10), 640–653 (2010).

Downloaded From: https://www.spiedigitallibrary.org/ebooks/ on 07 Mar 2022
Terms of Use: https://www.spiedigitallibrary.org/terms-of-use

78. H. Vocca, I. Neri, F. Travasso, and L. Gammaitoni, "Kinetic energy harvesting with bistable oscillators," *Appl. Ennery* **97**, 771–776 (2012).
79. A. M. Wickenheiser and E. Garcia, "Broadband vibration-based energy harvesting improvement through frequency up-conversion by magnetic excitation," *Smart Materials and Structures 19*, 065020 (2010).
80. S. Zhou, J. Cao, D. J. Inman, J. Lin, S. Liu, and Z. Wang, "Broadband tristable energy harvester: Modeling and experiment verification," *Applied Energy* **133**, 33–39 (2014).
81. S. Zhao and A. Erturk, "On the stochastic excitation of monostable and bistable electrostatic power generators: relative advantage and tradeoffs in a physical system," *Applied Physics Letters 102*, 103902 (2013).
82. S. Zhou, J. Cao, A. Erturk, and J. Lin, "Enhanced broadband piezoelectric energy harvesting using rotatable magnets," *Applied Physics Letters 102*, 173901 (2013).
83. M. A. Karami and D. J. Inman, "Parametric study of zigzag microstructure for vibrational energy harvesting," *Journal of Microelectromechanical Systems* **21**(1), 145–160 (2011).
84. M. A. Karami and D. J. Inman, "Analytical modeling and experimental verification of the vibrations of the zigzag microstructure for energy harvesting," *Journal of Vibration and Acoustics* **133**(1), 011002 (2011).
85. M. A. Karami and D. J. Inman, "Electromechanical modeling of the low-frequency zigzag micro-energy harvester," *Journal of Intelligent Material Systems and Structures* **22**(3), 271–282 (2011).
86. D. Castagnetti, "Experimental modal analysis of fractal-inspired multi-frequency piezoelectric energy converters," *Proc. ASME SMASIS*, SMASIS2001-4913, 259–266 (2011).
87. M. Ferrari, V. Ferrari, M. Guizzetti, D. Marioli, and A. Taroni, "Piezoelectric multifrequency energy converter for power harvesting in autonomous microsystems," *Sensor and Actuators A* **142**, 329–335 (2008).
88. M. C. Malkin and C. L. Davis, "Multi-frequency piezoelectric energy harvester," U.S. Patent number 6858970 B2 (2005).
89. Z. Yang and J. Yang, "Connected vibrating piezoelectric bimorph beams as a wide-band piezoelectric power harvester," *Journal of Intelligent Material Systems and Structures* **20**, 569–574 (2009).
90. J. Rastegar, D. Feng, and C. Pereira, "Efficient methods of harvesting energy from ultra-short duration shock loading," *ASME 2014 Conference on Smart Materials, Adaptive Structures and Intelligent Systems*, SMASIS2014-7657, V002T07A020, Newport, Rhode Island (2014).
91. J. Rastegar, D. Feng, and C. Pereira, "Piezoelectric-based event sensing and energy-harvesting power sources for thermal battery initiation in gun-fired munitions," *Proc. SPIE* **9115**, 91150D (2014) [doi: 10.1117/12.2053205].

Downloaded From: https://www.spiedigitallibrary.org/ebooks/ on 07 Mar 2022
Terms of Use: https://www.spiedigitallibrary.org/terms-of-use

92. J. Rastegar, D. Haarhoff, C. Pereira, and H.-L. Nguyen, "Piezoelectric-based energy harvesting power sources for gun-fired munitions," *Proc. SPIE* **6174**, 61740X (2006) [doi: 10.1117/12.657441].
93. M. Umeda, K. Nakamura, and S. Ueha, "Energy storage characteristics of a piezo-generator using impact induced vibration," *Japanese Journal of Applied Physics* **36**(5B), 3146–3151 (1997).
94. M. Umeda, K. Nakamura, and S. Ueha, "Analysis of transformation of mechanical impact energy to electrical energy using a piezoelectric vibrator," *Japanese Journal of Applied Physics* **35**(5B), 3267–3273 (1996).
95. A. A. Basari, A. Sosuke, S. Sakamoto, S. Hashimoto, B. Homma, K. Suto, H. Okada, H. Okuno, K. Kobayashi, and S. Kumagai, "Evaluation on mechanical impact parameters in piezoelectric power generation," *IEEE 10th Asian Control Conference (ASCC)*, 16 (2015).
96. B. Cavallier, H. Nouira, E. Foltete, L. Hirsinger, and S. Ballandras, "Energy storage capacity of vibrating structure: application to a shock system," *Proc. of Symposium on Design, Test, Integration and Packaging of MEMS/ MOEMS DTIP0*, Montreux, Switzerland, 391–393 (2005).
97. S. Ju and C. H. Ji, "Indirect impact based piezoelectric energy harvester for low frequency vibration," *18th International Conference on Solid-State Sensors, Actuators, and Microsystems (TRANSDUCERS)*, 21–25 June, Anchorage, Alaska, 1913–1916 (2015).
98. C. N. Xu, M. Akiyama, K. Nonaka, and T. Watanabe, "Electrical power generation characteristics of PZT piezoelectric ceramics," *IEEE Transactions on Ultrasonics, Ferroelectrics and Frequency Control* **45**, 1065–1070 (1998).
99. T. G. Engel, J. E. Becker, and W. C. Nunnally, "Energy conversion and high power pulse production using miniature magnetic flux compressors," *IEEE Transactions on Plasma Sciences* **28**(5), 1342–1346 (2000).
100. T. G. Engel, C. Keawboonchuay, and W. C. Nunnally, "Energy conversion and high power pulse production using miniature piezoelectric compressors," *IEEE Transactions on Plasma Sciences* **28**(5), 1338–1341 (2000).
101. T. G. Engel, W. C. Nunnally, J. Becker, R. Rahman, and C. Keawboonchuay, "Research progress on compact kinetic-to-electrical energy convertors," *IEEE Pulsed Power Conference* **2**, 1287–1290 (1999).
102. C. Keawboonchuay and T. G. Engel, "Scaling relationships and maximum peak power generation in a piezoelectric pulse generator," *IEEE Transactions on Plasma Sciences* **32**, 1879–1885 (2004).
103. C. Keawboonchuay and T. G. Engel, "Maximum power generation in a piezoelectric pulse generator," *IEEE Transactions on Plasma Sciences* **31** (1), 123–128 (2003).

Downloaded From: https://www.spiedigitallibrary.org/ebooks/ on 07 Mar 2022
Terms of Use: https://www.spiedigitallibrary.org/terms-of-use

104. C. Keawboonchuay and T. G. Engel, "Factors affecting maximum power generation in a piezoelectric pulse generator," *IEEE Pulsed power Conference, Digest of Technical Papers* **1**, 327–330 (2003).
105. T. Funasaka, M. Furuhata, Y. Hashimoto, and K. Nakamura, "Piezoelectric generator using a $LiNbO_3$ plate with an inverted domain," *IEEE International Ultrasonics Symposium*, 959–962 (1999).
106. J. Rastegar, R. Murray, C. Pereira, and H.-L. Nguyen, "Novel impact-based peak-energy locking piezoelectric generators for munitions," *Proc. SPIE* **6527**, 65270X (2007) [doi: 10.1117/12.715475].
107. J. Rastegar, R. Murray, C. Pereira, and H.-L. Nguyen, "Energy-harvesting power sources for very high-G gun-fired munitions," *Proc. SPIE* **7643**, 76430D (2010) [doi: 10.1117/12.847777].
108. J. Rastegar, R. Murray, C. Pereira, and H.-L. Nguyen, "Integrated event sensing and energy-harvesting power sources for gun-fired munitions," *Proc. SPIE* **7288**, 72880Z (2009) [doi: 10.1117/12.815513].
109. J. Rastegar, R. Murray, C. Pereira, and H.-L. Nguyen, "Novel piezoelectric-based energy-harvesting power sources for gun-fired munitions," *Proc. SPIE* **6527**, 65270Y (2007) [doi: 10.1117/12.715009].
110. J. Rastegar, "Methods and apparatus for mechanical reserve power sources for gun-fired munitions, mortars, and gravity dropped weapons," U.S. Patent Number 8,183,746 (2012).
111. F. Henningsen and A. Josefsson, "Design and verification of vibration energy harvester," M.S. thesis, Chalmers University of Technology, Goteborg, Sweden (2014).
112. A. C. Waterbury, "Vibration harvesting using electromagnetic transduction," Ph.D. thesis, University of California, Berkeley (2011).
113. K. A. Cook-Chennault, N. Thambi, and A. M. Sastry, "Powering MEMS portable devices – a review of non-regenerative and regenerative power supply systems with special emphasis on piezoelectric energy harvesting systems," *Smart Materials and Structures* **17**(4), 1–33 (2008).
114. S. P. Beeby, R. N. Torah, M. J. Tudor, P. Glynne-Jones, T. O'Donnell, C. R. Saha, and S. Roy, "A micro electromagnetic generator for vibration energy harvesting," *Journal of Micromechanics and Microengineering* **17**, 1257–1265 (2006).
115. H. Kulah and K. Najafi, "An electromagnetic micro power generator for low-frequency environmental vibrations," *Micro Electro Mechanical Systems—17th IEEE Conference on MEMS* 237–240 (2004).
116. C. T. Pan and T. T. Wu, "Development of a rotary electromagnetic microgenerator," *Journal of Micromechanics and Microengineering* **17**, 120–8 (2007).
117. C. Serre, A. Perez-Rodriguez, N. Fondevilla, J. R. Morante, J. Montserrat, and J. Esteve, "Vibrational energy scavenging with Si

Downloaded From: https://www.spiedigitallibrary.org/ebooks/ on 07 Mar 2022
Terms of Use: https://www.spiedigitallibrary.org/terms-of-use

technology electromagnetic inertial microgenerators," *Microsystem Technologies* **13**, 1449–661 (2007).
118. C. Shearwood and R. B. Yates, "Development of a resonant electromagnetic micro-generator," *Electronic Letters* **33**(22), 1883–1884 (1997).
119. S. R. Snarski, R. G. Kasper, and A. B. Bruno, "Device for electromagnetohydrodynamic (EMHD) energy harvesting," *Proc. SPIE* **5417**, 147–161 (2004) [doi: 10.1117/12.545170].
120. C. B. Williams, C. Shearwood, M. A. Harradine, P. H. Mellor, T. S. Birch, and R. B. Yates, "Development of an electromagnetic microgenerator," *IEE Proc. - Circuits Devices and Systems* **148**, 337–42 (2001).

Downloaded From: https://www.spiedigitallibrary.org/ebooks/ on 07 Mar 2022
Terms of Use: https://www.spiedigitallibrary.org/terms-of-use

Chapter 4
Collection and Conditioning Circuits

4.1 Introduction

In the previous chapters, four commonly used transducers for converting mechanical energy to electrical energy are described, that is, piezoelectric, electrostatic, electromagnetic, and magnetostrictive transducers. In all cases, external mechanical energy is converted to electrical energy and is available at the output of the transducer for collection, conditioning, and delivery to the load. A collection and conditioning (CC) circuit is needed to ensure that the energy demands of the load are satisfied over the entire operating range. In case of sporadic availability of input mechanical energy, an intermediate storage capability may be needed to accumulate the energy to a suitable level.

In general, the complexity of the CC circuit is dependent both on the output energy and the voltage/current characteristics of the transducer, and on the energy demands of the load. All transducers considered here produce a time-varying voltage or current, but none are ideal sources; thus, CC circuits are required for each specific system configuration. The time-varying features of the transducer output can be separated into oscillatory, or pulsed periodic, or pulsed sporadic, or even a single pulse. In the latter cases, the peak pulse amplitude as well as duration need to be considered, while for oscillatory outputs, their temporal profile as well as their periodic features must also be considered.

In addition to the transducer output energy consideration, the intended use (load) of the harvester needs to be an integral part of any CC circuit design. All loads, either passive or active, can be expressed in terms of their input impedance, which may or may not be time dependent. These include discrete components such as resistors, inductors, and capacitors. Electronic loads, comprising either discrete circuit components

Downloaded From: https://www.spiedigitallibrary.org/ebooks/ on 07 Mar 2022
Terms of Use: https://www.spiedigitallibrary.org/terms-of-use

or integrated circuits or microprocessors, have high input resistance kilohms (kΩ) and an input capacitance of a few picofarads (pF). Motors present an inductive load, while bridging wires used in initiation systems are resistive and flash lamps are time-dependent resistive loads. The latter type falls into the category of high-energy-demand loads, which can be serviced by event-driven storage elements on the output side of the conditioning circuit. However, while knowledge of loading is important to the design of the CC circuit, it may be possible to exclude loading effects by isolating the transducer output side of the CC circuit (buffering) from the load. Most contemporary designs attempt to do just that but require added circuit complexity and in some cases external energy sources to power the active components.

In general, an optimal CC circuit is a nonlinear matching network that ensures that the energy demands of the load are satisfied under the specified operating conditions. While coupling efficiency between the transducer and the load has become a comparative metric between diverse platforms, it is not relevant to the design of the CC circuit, which is constrained only by the need to satisfy the load demand, given the available transducer output energy. Figure 4.1 shows an energy-based approach for selecting an appropriate CC circuit design. For practical energy harvesters, a CC circuit with a low component count and lower complexity (fewer or no switching devices) is the preferred solution, even though it may not be the most efficient.

In view of the relative energy constraints discussed above, CC circuit designs may be categorized into the following two groups:

1. **Basic Energy-Harvesting Circuits:** If the transducer output energy is considerably greater than the energy demand of the load, then a standard circuit design using rectifier diodes and either a large capacitor or

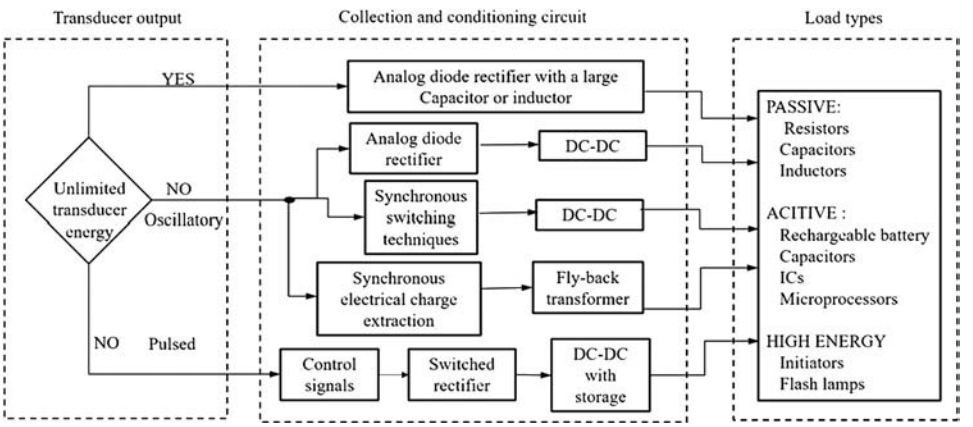

Figure 4.1 Collection and conditioning circuit design approach based on energy considerations.

Downloaded From: https://www.spiedigitallibrary.org/ebooks/ on 07 Mar 2022
Terms of Use: https://www.spiedigitallibrary.org/terms-of-use

inductor will suffice. The output of this circuit is characterized by either an ideal voltage or current source and can drive any load. The voltage level at the output of the transducer can be changed to match the load requirements either through a passive DC-to-DC converter at the output of the rectifier or through a transformer at the output of the transducer.

2. **Circuits to Maximize Harvested Energy:** If the transducer output energy is not considerably greater than the energy demand of the load, then two CC circuit design paths are possible: circuit designs that are suitable where the output of the transducer is oscillatory, and designs where the transducer output is pulsed. These two CC circuit design paths may be described briefly as follows:

   – The first path for oscillatory transducer output leads to three CC circuit design branches, with increasing circuit complexity due to the lower energy levels at the output of the transducer (Fig. 4.1). In the latter cases, the CC circuits have to be more efficient. Improvement in efficiency is achieved through the use of complex electronic-switching arrangements. The first CC circuit design, which has been referred to as the standard energy-harvesting circuit (for example, Ref. 1), uses a rectifier diode bridge to convert the AC transducer output to a DC signal. A DC-to-DC converter changes the voltage level as required by the load. The second CC circuit design uses a synchronous-switched-for-harvesting (SSH) technique, which increases the collection efficiency. A DC-to-DC converter is used to isolate the load from the transducer as in the standard circuit. The third CC circuit design, referred to as synchronous electric-charge extraction (SECE), uses electronic switching, which increases the efficiency by synchronizing energy collection with the phase of the energy-producing portion of the harvester cycle. Furthermore, a flyback transformer approach isolates the transducer from the load, thereby making it possible to charge rechargeable batteries, supercapacitors, or capacitors. In general, electronic switching circuits are active, requiring either an external voltage source or some self-starting feature in the CC circuit.
   – The second path leads to CC circuit designs that are suited for transducers driven by pulsed input, which leads to an energy pulse at the output of the transducer. The output energy pulse is characterized by its amplitude profile. Depending on the application, the generated electrical energy may be used directly or may be accumulated in a storage device.

Conditioning circuit designs have evolved with respect to particular harvester types; as a result, there is considerable overlap and repetition of the corresponding electronic solutions. The remainder of this chapter is organized according to these similarities and, subsequently, the particular CC circuit

Downloaded From: https://www.spiedigitallibrary.org/ebooks/ on 07 Mar 2022
Terms of Use: https://www.spiedigitallibrary.org/terms-of-use

design topology is described in terms of the dominant transducer technologies. Specific variants of the generic CC circuit are highlighted for the particular transducer types. It should be noted that piezoelectric and electrostatic harvesters are modeled primarily as current sources, while the electromagnetic and magnetostrictive transducers are considered to be voltage sources. The reader is referred to the references for transducer-specific development of CC circuits; for piezoelectric devices with oscillatory output (see Refs. 1–17; for impulse driven piezoelectric devices see Refs. 18–34; for electrostatic harvesters see Refs. 35–36; for electromagnetic harvesters see Refs. 37–40; and for magnetosrtictive harvesters see Refs. 41–44.

Design of collection circuits requires knowledge of the temporal characteristics of the transducer output. In general, the characteristics of the mechanisms interfacing the host system to the transducer are not required for the design of the CC circuits unless they can be used to provide certain sensory information to enhance the efficiency of circuits. However, precise knowledge of the transducer output profile is needed to efficiently collect the generated electrical energy and condition it for a particular load type. For example, in the case of a piezoelectric transducer, the energy is preferably extracted at the extremum values of the electrical potential energy (PE), whereas, for electromagnetic transducers, the generated electrical energy may be extracted continuously.

Piezoelectric transducers have dominated small energy-harvesting devices for use in remote sensors and the like. For this reason their CC circuits are described in more detail. Electromagnetic transducers are also widely used but are difficult to implement in MEMS and other small devices, and their CC circuits are well-known technologies and for this reason are described in less detail following the section on piezoelectric CC circuits. The CC circuits for electrostatics- and magnetostrictive-based harvesters are addressed next.

4.2 Collection and Conditioning Circuits for Piezoelectric Transducers

4.2.1 Direct rectification and conditioning methods

If the output energy of the transducer is enough not to require highly efficient CC circuits, then a simple rectifying circuitry such as a four-diode bridge may be used. For example, a typical circuit shown in Fig. 4.2 becomes appropriate when

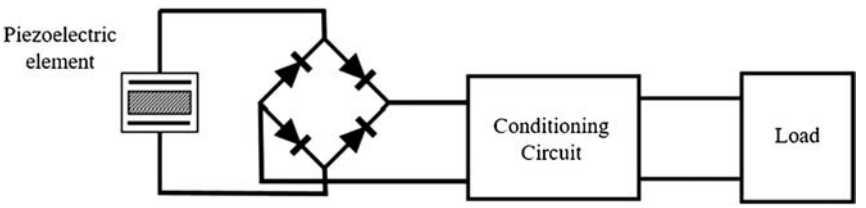

Figure 4.2 Basic collection and conditioning circuit (AC to DC).

Downloaded From: https://www.spiedigitallibrary.org/ebooks/ on 07 Mar 2022
Terms of Use: https://www.spiedigitallibrary.org/terms-of-use

the transducer output is oscillatory or pulsed. Since most loads require a DC voltage (or current), a CC circuit with a four-diode bridge rectifier followed by a conditioning circuitry to bridge the load have been routinely used. Integrated circuits have even become commercially available to serve this purpose (for example, IC number LTC3588-1 from Linear Technology Corp.). These circuits have been used in many commercial systems, such as emergency beacons, which may need only to power a light or transmit a single-tone.

It is appreciated that in certain applications, for example, when powering heating filaments, there is no need for rectification and conditioning circuitry. In such cases the collected energy may be transferred directly to the filament.

4.2.2 Circuits to maximize harvested energy

When the output energy of the transducer does not leave enough margin for losses that are inevitable in any CC circuitry, then the circuits have to be designed to maximize the amount of energy that is transferred to the load. A few such circuit designs are described in this section. However, to better describe the circuit designs and their logic and functionality, it is helpful to first illustrate the physics of the mechanical-to-electrical energy conversion process in piezoelectric transducers.

A piezoelectric transducer designed for energy harvesting is poled such that when properly strained, electrical charges accumulate on its electrodes for collection. These charges result in the development of a voltage difference between the two electrodes.

Consider the case in which a sinusoidal strain is applied to a piezoelectric element in the direction of its poling (Fig. 4.3). The open-circuit voltage continues to build up proportionally in response to the increasing applied strain, as illustrated in Fig. 4.3. In the case of an

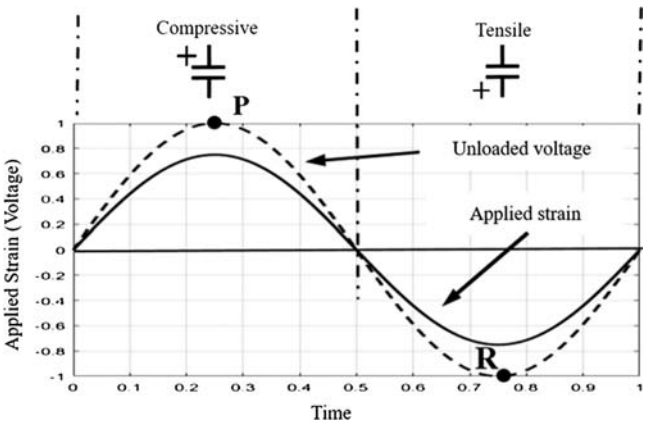

Figure 4.3 The open-circuit voltage (dashed line) generated by a piezoelectric transducer with an applied oscillatory strain (solid line). Points P and R indicate the extremum values of the voltage, corresponding to the points of maximum electrical PE.

Downloaded From: https://www.spiedigitallibrary.org/ebooks/ on 07 Mar 2022
Terms of Use: https://www.spiedigitallibrary.org/terms-of-use

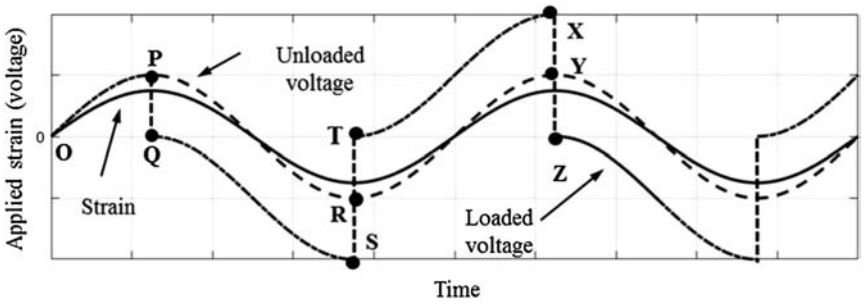

Figure 4.4 Energy-harvesting cycle for a piezoelectric transducer. The solid curve is the applied strain, the dashed curve is the unloaded voltage profile (no energy harvested), and the dash-dotted curve is the voltage profile with energy-harvesting points P, S, and X.

oscillatory applied strain, the voltage polarity reverses as the applied strain transitions from compressive to tensile, and vice versa.

The maximum electrical energy becomes available when the extrema of generated open-circuit voltage levels have been reached, as illustrated in Fig. 4.3 by the points P and R. Figure 4.4 shows the ideal energy-harvesting cycle that maximizes the harvested electrical energy. Here, to present the basic concept of maximizing the extracted electrical energy from the piezoelectric transducer, an idealized sinusoidal strain is applied to the transducer.

Referring to Fig. 4.4, the energy-harvesting cycle begins from the zero strain point indicated by O. The open-circuit voltage follows the unloaded voltage profile in response to the applied compressive strain until it reaches the extremum value indicated by point P. At this point, energy is extracted from the transducer by momentarily connecting it to the load. Immediately, the open-circuit voltage drops to zero (point Q). Subsequently, the load is disconnected as the compressive strain cycle begins to decrease toward zero, however, with a reversal of the polarity of the voltage. Consequently, the unloaded open-circuit voltage increases with negative polarity. As the strain cycle switches from compressive to tensile, a new extremum in the unloaded open-circuit voltage is reached (point S). It should be noted that the new voltage extremum (point S) is twice the magnitude of the extremum value of the unloaded voltage cycle, indicated by point R. At the extremum point S, energy is extracted from the transducer in the same fashion as indicated above for point P. Subsequently, the open-circuit voltage goes to zero at point T. As a tensile strain is applied to the transducer, the open-circuit voltage is increased, reaching a new extremum point X, which has twice the magnitude of the corresponding point Y of the unloaded open-circuit cycle. The above discussion shows that the open-circuit voltage during the energy harvesting cycle is twice that predicted by the unloaded voltage/strain response. This means that quadruple the amount of energy is ideally

Downloaded From: https://www.spiedigitallibrary.org/ebooks/ on 07 Mar 2022
Terms of Use: https://www.spiedigitallibrary.org/terms-of-use

available for collection if the harvesting process is synchronized with the extremum points of the open-circuit voltage.

It is noted that the input from the host system to the piezoelectric transducer can rarely be considered to be a strain, and that it is not affected by the extraction and/or accumulation of generated charges. In most practical implementations, the transducer input is force, and the collection and accumulation of charges greatly affect the amount of mechanical strain that the piezoelectric transducer can undergo, as described in detail in Chapter 2. Selection of a sinusoidal strain input in the example of Figs. 4.3 and 4.4 idealizes the process of energy harvesting for the purpose of simplifying the discussion. In this way the effects of the generated charges in the piezoelectric transducer on the generated mechanical strain can be ignored. However, the process is similar even when the transducer input is force; thus, maximum electrical energy should be extracted at the extremum values of the open-circuit voltage by momentarily closing a switch that connects the transducer output to the collection circuit to maximize the harvested electrical energy. It is appreciated that since the electrical energy is proportional to the square of the voltage, it is prudent to extract energy very close to the extremum open-circuit voltage. In addition, the electrical energy must be collected rapidly before the open-circuit voltage has significantly dropped. The design of the CC circuitry must therefore consider the transducer input and the resulting open-circuit voltage time profile for maximum energy collection.

In the following sections the various collection circuit techniques that have been used for efficient harvesting of generated electrical energy are discussed. The section on specific collection circuits begins by highlighting the salient features of the energy-harvesting process for oscillatory strain through the use of simple resistive and capacitive loads. This discussion establishes the need for elaborate switching circuits when the amount of energy to be harvested is to be maximized.

4.2.3 Collection circuits

In the above discussion, it was noted that the collection of the generated electrical energy (or charge) from a piezoelectric transducer is accompanied by an immediate drop in the load voltage to zero. In practice, the dynamics of the collection process is dependent on the nature of the load or the collection circuit. For example, the harvested energy may be used to drive a resistive load as illustrated in Fig. 4.5. At the extremum voltage points of the transducer output, a switch S is closed to deliver the electrical energy to a resistive load R_L such as a heating filament. In this simple example, the energy transfer time is $(R_L C_P)$, where C_P is the equivalent piezoelectric capacitance. In the case of a heating element, this time is relatively fast since the resistance of the filament R_L is usually taken to be very low. This simple example further illustrates that the piezoelectric energy harvester is not close to being an ideal

Downloaded From: https://www.spiedigitallibrary.org/ebooks/ on 07 Mar 2022
Terms of Use: https://www.spiedigitallibrary.org/terms-of-use

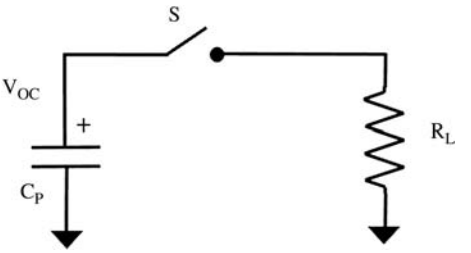

Figure 4.5 Energy transfer to a resistive load.

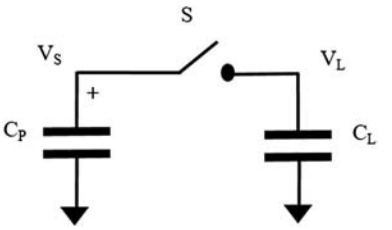

Figure 4.6 Electrical energy collection circuit using a load capacitor C_L.

current or voltage source, and the reader should exercise caution when using circuit models of piezoelectric transducers with equivalent current and voltage sources.

In the case of capacitive loads, the generated energy can be transferred to the load capacitor by closing switch S as indicated in Fig. 4.6. In this situation, the energy is transferred from the piezoelectric capacitance to the load capacitance until their voltages are equal. If the ratio of the two capacitances is $\gamma = C_L/C_P$, then using basic circuit analysis and conservation of charge, the final voltage for the two connected capacitors is

$$V_S^{\text{final}} = V_L^{\text{final}} = \frac{1}{1+\gamma} V_S^{\text{initial}} \tag{4.1}$$

Since the stored energy in the capacitor is proportional the product CV^2, the following equations express the initial and final energy values of the system:

$$E_S^{\text{final}} = \frac{1}{(1+\gamma)^2} E_T^{\text{initial}},$$
$$E_L^{\text{final}} = \frac{\gamma}{(1+\gamma)^2} E_T^{\text{initial}},$$
$$E_T^{\text{final}} = \frac{1}{1+\gamma} E_T^{\text{initial}},$$

where E_S is the generated electrical energy stored in the piezoelectric element with capacitance C_P, E_L is the electrical PE in the load capacitor, and E_T represents the total energy of the system, i.e., both capacitors. For the

Downloaded From: https://www.spiedigitallibrary.org/ebooks/ on 07 Mar 2022
Terms of Use: https://www.spiedigitallibrary.org/terms-of-use

symmetrical case, with $C_L = C_P$, 25% of the initial energy remains in C_P and 25% is transferred to C_L, while 50% of the stored energy is lost during the transport of charges from the storage capacitor to the load capacitor.

An explanation for the missing energy cannot be found by considering only the steady state conditions described by the above equations. Fundamentally, in the absence of circuit inductance, the circuit resistance becomes dominant. Therefore, attainment of steady state conditions requires losses in the circuit in the form of joule heating and radiation as the charges are transferred from one capacitor to the other.[45] In the presence of appreciable inductance, charges will oscillate between the two capacitors until steady state is reached.

The above analysis illustrates the need for additional circuitry for maximizing the transfer of generated electrical energy from piezoelectric transducers. Additionally, as illustrated in the example of Figs. 4.3 and 4.4, the collection circuits must also contend with the issue of polarity reversal. This voltage polarity reversal is of no consequence for a resistive load, such as a heating filament. However, in the case of capacitive (or inductive) loads, the collection circuit of Fig. 4.6 requires additional circuitry to handle the polarity reversal of the open-circuit voltage. One possible solution, illustrated in Fig. 4.7, uses a set of four switches to control the flow of current so that the stored charge can be transferred to the load capacitor at both extremum points of the open-circuit voltage. For example, at one of the two alternating extremum voltage points, switches S_1 and S_2 are open while S_3 and S_4 are closed, and at the next extremum point of opposite polarity the switching sequence is reversed.

A second solution, illustrated in Fig. 4.8, uses two load capacitors C_{L1} and C_{L2} for charge transfers when the energy harvester is in one of the two voltage extremum states. For example, for a positive-polarity voltage extremum, S_1 is closed and S_2 is open, and for the next voltage extremum (negative polarity),

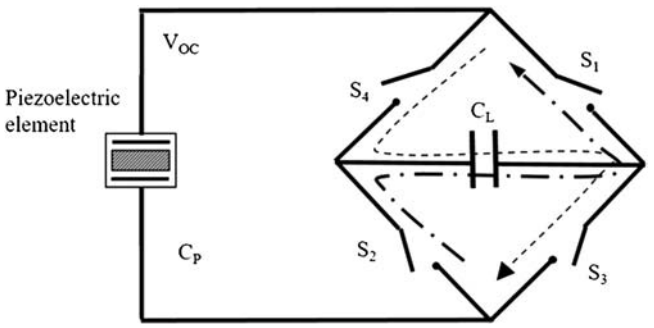

Figure 4.7 Energy transfer to a capacitive load during both extremum points of open-circuit voltage. The dashed path provides charge transfer when V_{OC} is positive, and the dot-dashed path provides charge transfer when V_{OC} is negative.

Downloaded From: https://www.spiedigitallibrary.org/ebooks/ on 07 Mar 2022
Terms of Use: https://www.spiedigitallibrary.org/terms-of-use

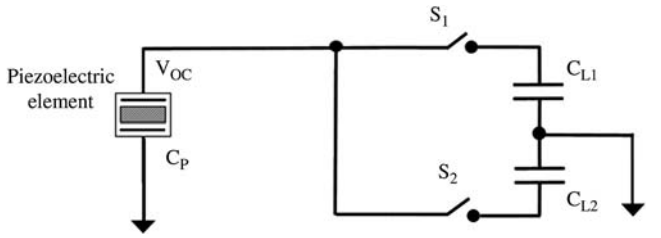

Figure 4.8 Energy transfer to a capacitive load during both extremum points of open-circuit voltage: S_1 when V_{OC} is positive and S_2 when V_{OC} is negative.

S_1 is open and S_2 is closed. In this configuration the two load capacitors can either supply electrical energy to two independent downstream circuits or be combined to accumulate the energy in a single capacitor.

As discussed above, a capacitor-to-capacitor transfer of energy is inefficient. However, 100% of the PE stored in the electrostatic field can be transferred to a load capacitor through the use of a switched inductive element as described below.

The collection circuit of Fig. 4.6 is modified to include an inductor L with switches S_1 and S_2, as illustrated in Fig. 4.9. At the extremum voltage points, collection of the stored charge in the piezoelectric element begins by closing S_1 with S_2 in the open position, forming a LC_P tank circuit (a harmonic oscillator). The initial value of the inductor current is the highest and begins to decrease as the back electromotive force (emf) in the inductor increases. After some time, all of the energy from the piezoelectric capacitor C_P is transferred to the inductor but at this point the current in the inductor is not flowing in the desired direction for energy transfer to the load capacitor. However, one half-period later, maximum energy is stored in the inductor again, and the inductor current is flowing in the correct direction for the next phase of the collection circuit operation. At this time, S_1 is opened as S_2 is closed, connecting the fully charged inductor to C_L. Subsequently, all of the energy from the inductor is dumped to the load capacitor C_L. Upon completion of

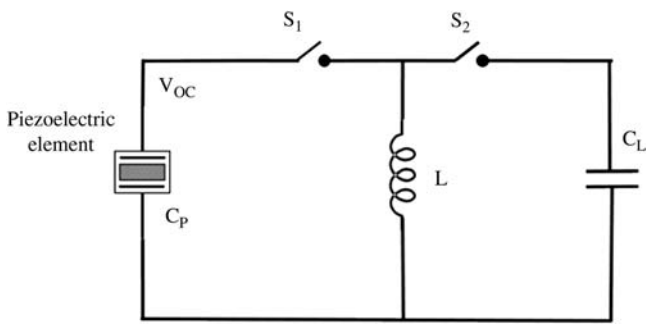

Figure 4.9 Switched-inductor collection circuit.

Downloaded From: https://www.spiedigitallibrary.org/ebooks/ on 07 Mar 2022
Terms of Use: https://www.spiedigitallibrary.org/terms-of-use

the energy transfer, S_2 is opened to isolate the load capacitor from the piezoelectric element. The two (LC_P) and (LC_L) loops formed by closing the switches S_1 and S_2 in Fig. 4.9 have different characteristic time periods that are proportional the square-root of the (LC) product. It is appreciated that timing is critical to proper and efficient operation of these collection circuits. In general, the effective transfer time of the electrical PE from C_P to the inductor must be faster than any effective mechanical time period, in other words, transfers must take place rapidly at the extremum voltage points as discussed in the above sections.

In the above collection circuit descriptions, a generic ideal switch has been used to illustrate the circuit concepts, i.e., zero resistance. For practical circuits, several switching options are available. A diode has been extensively utilized as a passive switching device, and various low-voltage solutions exist. For better performance and lower loss, active switches based on diode-transistor, MOSFET (metal–oxide–semiconductor field-effect transistor), and comparator-synchronized MOSFET may be used. Furthermore, the speed of a switch may also affect performance of the CC circuit.

4.2.4 Conditioning circuits

Typically, there is a mismatch between the output voltage of the collection circuits and the voltage requirements of the load. For example, a piezoelectric energy harvester may produce a DC voltage of over one-hundred volts at the output of the collection circuit, while the load may be a 5-V rechargeable battery. In such cases, a conditioning circuit is needed to provide the necessary electronics for translating voltage levels to satisfy the voltage requirements of the load. Ideally, the conditioning circuit would be a buffer circuit that isolates the load from the collection circuit. For some harvesters, as discussed below, DC-to-DC buck–boost switching regulators are sufficient, while in others, a flyback transformer implementation may be a better solution. The following section describes some of the proposed CC circuit solutions that have been published for collecting and conditioning the output of piezoelectric transducers subjected to a sinusoidal strain profile. This is not an exhaustive review of the literature but is rather a synopsis and comparison of the proposed circuit solutions using an electromechanical figure of merit[10] that they have defined as a measure of the effective volume of piezoelectric material required to achieve the same level of output power as the standard AC-to-DC circuit.

4.2.4.1 Standard AC–DC interface

As an illustrative example, the CC circuit in Fig. 4.10 has been used to harvest electrical energy from piezoelectric energy harvesters driven near resonance.[1] Consequently, the output of the transducer is modeled by a sinusoidal current source shunted by an equivalent piezoelectric capacitance C_P, generating an AC voltage at the output of the piezoelectric transducer. The AC voltage is

Downloaded From: https://www.spiedigitallibrary.org/ebooks/ on 07 Mar 2022
Terms of Use: https://www.spiedigitallibrary.org/terms-of-use

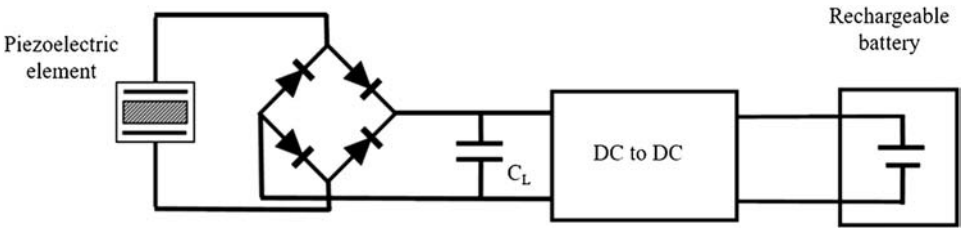

Figure 4.10 Standard CC circuit for harvesting electrical PE from a piezoelectric transducer with a sinusoidal strain profile.[1,11]

converted to a DC voltage using a four-diode bridge rectifier and a large smoothing capacitor C_L. As the generated DC voltage is likely to be different from that required by a load, such as a rechargeable battery, a DC-to-DC regulator[46] is used to perform the needed voltage-level transformation. The circuit of Fig. 4.10 has come to be known as the "standard" interface as it provides the simplest method for harvesting electrical PE from piezoelectric harvesters driven near resonance.

Under steady state conditions, this standard CC circuit has been used to establish a benchmark for comparison with other CC circuits used for harvesting electrical PE from piezoelectric transducers assumed to be generating an AC voltage. This standard circuit has been extensively analyzed[6,12,47,48] to determine optimal power transfer conditions, which are valid only near resonance.

While the standard CC circuit has utility when large circuit losses may be acceptable, it is not a preferred solution in practical energy harvesters with limited output energy. More efficient designs using inductor switching and synchronized energy exchange have been designed and are briefly described below.

4.2.4.2 Synchronized switch harvesting on inductor

Various versions of the switch inductor technique described in Section 4.3.3 have been used in piezoelectric harvesting systems.[8,49–52] Two approaches implement these concepts using an inductor in either a parallel or series configuration.

The parallel configuration of the synchronized switch harvesting on inductor (SSHI) technique is illustrated in Fig. 4.11(a).[6,53] Circuit operation is divided into three discontinuous operating phases. The corresponding voltage/strain waveforms are illustrated in Fig. 4.11(b). In the conductive phase, the rectifier passes the current from the piezoelectric element to the storage circuit element C_L, while the piezoelectric voltage remains clamped at its extremum value. During the next phase, the load is isolated from the piezoelectric, and the inductor L is connected to the piezoelectric element, creating the LC_P tank circuit.

Downloaded From: https://www.spiedigitallibrary.org/ebooks/ on 07 Mar 2022
Terms of Use: https://www.spiedigitallibrary.org/terms-of-use

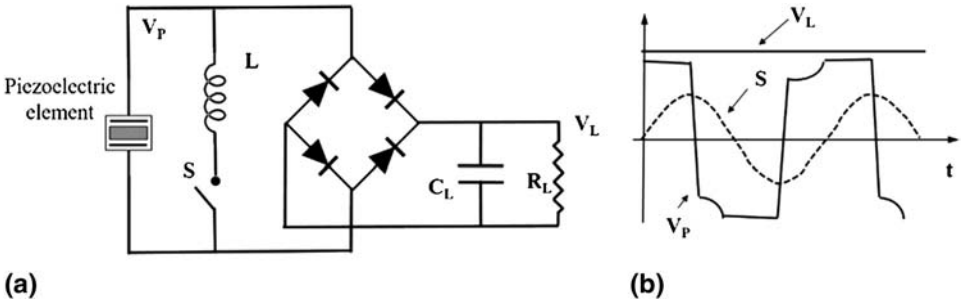

Figure 4.11 Parallel SSHI CC circuit: (a) circuit schematic and (b) corresponding waveforms of the applied strain (or deflection) S, the piezoelectric terminal voltage V_P, and the load voltage V_L.[6]

The switching inductor causes a rapid reversal of the piezoelectric voltage. After a further half-cycle, the inductor switch is opened again. The switching phase duration, determined by the resonance frequency of the electrical oscillator formed by the piezoelectric element capacitance and the shunt inductor L, must be much faster than the resonance frequency of the applied strain.

The series SSHI circuit sketched in Fig. 4.12 places the switch and inductor in series with the piezoelectric element.[54] The operation of this CC circuit is similar to that of the parallel circuit; i.e., the electrical PE is extracted at the voltage extremum points, corresponding to the extremum points of the applied strain in Fig. 4.11.

It should be noted that most often [including in Fig. 4.12(b)], a sinusoidal strain profile is used and the effect of extracting the generated charges on the strain profile is neglected. This is done mainly to simplify the description of the energy-harvesting process without affecting the basic method of operation of the corresponding CC circuitry. In the simulation of the actual CC circuits, the effects of this coupling should be included.

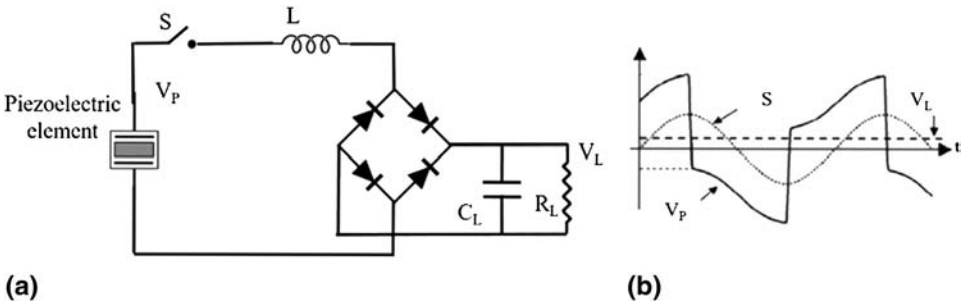

Figure 4.12 Series SSHI: (a) schematic and (b) corresponding waveforms of the applied strain S, the piezoelectric terminal voltage V_P, and the load voltage V_L.[53]

Downloaded From: https://www.spiedigitallibrary.org/ebooks/ on 07 Mar 2022
Terms of Use: https://www.spiedigitallibrary.org/terms-of-use

4.2.4.3 Synchronous electric charge extraction (SECE)

The CC circuits described in the previous section are designed to supply power to a resistive load. Under the assumption of oscillatory applied strain at the resonant frequency of the interfacing mechanisms, loading conditions for maximum power transfer are employed.[10] However, for general and nonresonant applied strain, a buffer circuit is the preferred method of isolating the load from the source. One type of active CC circuit that achieves the buffering function uses synchronous electric charge extraction (SECE), as illustrated in Fig. 4.13(a). A transformer M provides the isolation function and is commonly used in DC-to-DC converters when combined with an active MOSFET switch T on the primary side of the transformer (the buffering circuit known as a flyback transformer).

When the piezoelectric voltage reaches an extremum of the piezoelectric transducer voltage, the transistor T is turned ON, and the stored electric energy in C_P is transferred to the primary side of transformer M. As the piezoelectric voltage V_P passes zero, all of the energy has been transferred to the primary winding of the transformer, and the transistor is switched OFF. The value of the inductor is chosen so that the resonance period of the LC_P tank is much shorter than the period of the applied strain. The switching ensures that the piezoelectric element is in the open-circuit configuration during the energy transfer. As illustrated in Fig. 4.13(b), the piezoelectric voltage is a discontinuous piecewise function of the applied strain S.

The SECE technique achieves very good isolation between the load and the transducer output, thereby power delivery does not require any optimization strategy. It should be noted that the turns ratio of the secondary to the primary windings of the transformer may be selected to provide any charging voltage V_B. For detailed analysis and methods for selecting inductors to ensure correct timing, the reader is referred to Ref. 55.

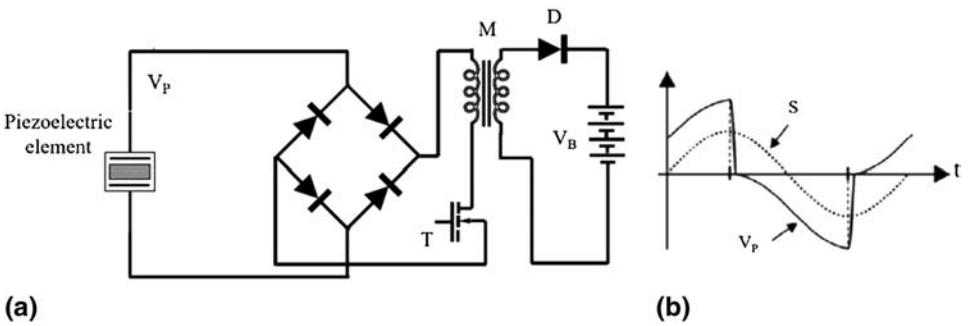

Figure 4.13 Schematic of the SECE operation: (a) circuit schematic, where T is a MOSFET switch, M is a transformer, and D is a high-speed diode; and (b) corresponding waveforms of the applied strain S and the piezoelectric terminal voltage V_P. (Reprinted with permission from Ref. 53.)

Downloaded From: https://www.spiedigitallibrary.org/ebooks/ on 07 Mar 2022
Terms of Use: https://www.spiedigitallibrary.org/terms-of-use

4.2.4.4 Comparison of synchronized switch harvesting techniques

The four synchronized switch harvesting (SSH) techniques discussed were developed for harvesters operating at resonance. Figure 4.14 shows a comparison of the normalized output power as a function of the electromechanical figure of merit,[10] which is expressed as the product of the square of the coupling coefficient and the electromechanical quality factor. It is proportional to the square of the piezoelectric coefficient and inversely proportional the resonant frequency. The output power of each conditioning circuit is normalized to the output power of the standard circuit.

Figure 4.14 shows that all conditioning circuits reach the same asymptotic value of the normalized power; the difference between the various techniques is the value of the electromechanical figure of merit M (defined in Ref. 10), which is a direct measure of the amount of piezoelectric material used. Thus, lower values, which correspond to smaller transducers, are preferable for space-constrained applications. It can be ascertained from Fig. 4.14 that SECE techniques lead to three-fold reduction in the amount of piezoelectric material needed to generate the same amount of power as is generated by the standard technique. However, as they require active switches, the CC circuit will need to be powered by a button battery or the like.

The original SSH techniques are suitable for resonant structures with a narrowband frequency spectrum. These techniques have been extended for use with pulsed operation[56] to include energy harvesters excited by mechanical shocks and impacts. As discussed in Ref. 50, the efficiency of energy conversion for pulsed operation is strongly dependent on the speed of conversion of the mechanical energy to electrical energy. The authors have experimentally confirmed that parallel SSHI configuration is the CC circuit design of choice, giving a five-fold improvement in comparison with other techniques discussed above.

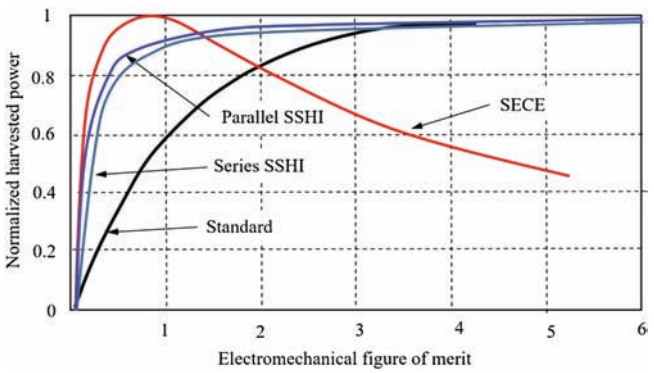

Figure 4.14 Comparison of normalized harvested power for SSHI techniques.[10]

Downloaded From: https://www.spiedigitallibrary.org/ebooks/ on 07 Mar 2022
Terms of Use: https://www.spiedigitallibrary.org/terms-of-use

Standard and SSH techniques may be used to harvest energy from broadband excitation using multimodal resonant mechanical structures.[11] However, the SECE techniques exhibit two major advantages. Firstly, the SECE techniques do not require load optimization, which has no utility for broadband sources of mechanical energy, as the optimal load is dependent on the resonant frequency. Secondly, SECE circuits are said to harvest 4 times more energy compared with the standard circuit, with a figure of merit below 2.

Other evolutionary implementations of the SSH technique for use with low piezoelectric voltages and practical electromechanical figures of merit are discussed in detail in Ref. 10. Piezoelectric transducers with output powers below a few microwatts present a challenging problem for the switching circuits, as most transducer power is dissipated in these circuits. Such systems are prevalent in MEMS-based devices with open-circuit voltages of a few volts, which may be below the threshold voltage of commonly available diodes. One approach to mitigate the low-voltage issue is to replace the full-wave rectifier (four diodes) by a half-wave rectifier (two diodes), resulting in the development of half-bridge SSH circuits.[7,57] Further reduction of collection circuit losses is possible through the use of a single diode, or active diodes emulated using a comparator/switch combination. A collection circuit consisting of a transformer and dual inductive switching (Fig. 4.15) is referred to as a SSHI-MR (SSHI magnetic rectifier) and is a preferred configuration.

In the SSHI-MR collection circuit of Fig. 4.15, a transformer T with two primary windings and one secondary winding replaces the diodes and the series inductor of a SSHI circuit. The transformer is used as a voltage up-converter, so that the voltage coupling factor is much larger than unity. Consequently, the ohmic losses in the transformer are lower due to the reduced current. An added benefit is the higher output voltage, which can be matched to the desired logic device voltage levels. These circuits have harvested energy in low levels of vibration, producing a transducer output voltage at 20-mV levels.[58]

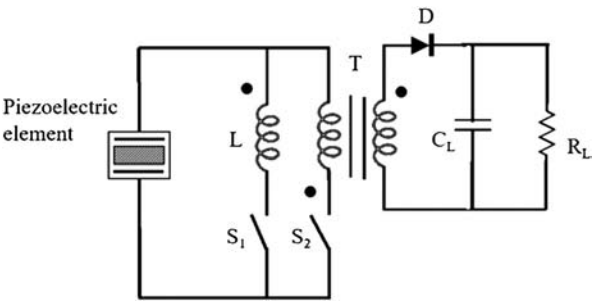

Figure 4.15 SSHI-MR collection circuit.[58]

Downloaded From: https://www.spiedigitallibrary.org/ebooks/ on 07 Mar 2022
Terms of Use: https://www.spiedigitallibrary.org/terms-of-use

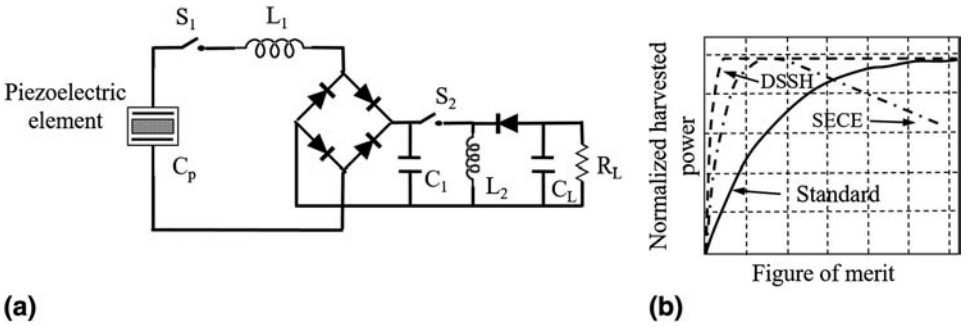

Figure 4.16 (a) DSSH circuit schematic and (b) graphical representation of normalized harvested power versus figure of merit.[10]

Further evolutionary changes in SSH circuit architecture to double synchronized switch harvesting (DSSH)[8] are enabling energy harvesting in the domain of weak electromechanical figures of merit. The DSSH circuit in Fig. 4.16 is a series combination of the series SSHI and a buck–boost DC-DC SECE circuit. The SECE section provides load isolation for the SSHI circuit, thereby, making the harvested energy independent of the resistive load; that is, the same performance results under all loading conditions.

The energy transfer can be described in four distinct steps. During the first step, both switches (S_1 and S_2) remain open until the piezoelectric voltage reaches one of its extremum values. At that point the circuit enters the second step by momentarily closing switch S_1, allowing the generated electrical energy to be dumped into the intermediate storage capacitor, C_1. The resonance time of the (L_1C_1) tank is much faster than the mechanical time constant. The third step begins by opening switch S_1 and closing switch S_2 to transfer the stored energy to the inductor L_2. The fourth and final step in the cycle transfers the energy stored in L_2 to the reactive load modeled by resistor R_L and capacitor C_L.

The DSSH configuration synchronizes the switching cycles at the extremum values of the piezoelectric transducer output voltage. According to Lallart et al.,[8] the energy conversion is optimal when the shunt capacitance C_1 is much larger than the piezoelectric element capacitance C_P for the case of weak values of the figure of merit; otherwise, an appropriate value has to be calculated.[10] Figure 4.16(b) shows a comparison of normalized power harvested as a function of the figure of merit for the DSSH, SECE, and the standard circuit.

The energy-harvesting circuit designs presented above are predominantly for piezoelectric devices driven by narrowband oscillatory motion. For all other mechanical motions, these circuits are far from optimal, but the concept of synchronizing electrical PE energy harvesting with the applied strain cycle is applicable to all harvester types. The primary concern with the above designs is their inherent dependence on the resonance condition. If resonance

Downloaded From: https://www.spiedigitallibrary.org/ebooks/ on 07 Mar 2022
Terms of Use: https://www.spiedigitallibrary.org/terms-of-use

synchronization cannot be maintained, the result is the loss of a significant portion of the available energy. A delayed-switching approach has been proposed to mitigate some of the losses due to mistuning.[59]

4.2.5 CC circuits for pulsed piezoelectric loading

Pulsed loading of piezoelectric transducers occurs in many applications, such as those in munitions firing or when a mechanical system is subjected to impact-type loading. In such cases, the charges generated by the piezoelectric transducer are typically short lived, and the CC circuits have to be designed to capture the maximum amount of electrical energy.

The generated electrical energy may be dumped directly to a load, as described in Section 4.2.5.1, or provided by a properly designed CC circuitry for storage in a capacitor, as described in Section 4.2.5.2. The latter circuitry may be provided with shock-loading event detection logic as described in Section 4.2.5.3. Key differences in the conditioning circuits and their detailed descriptions are provided in Refs. 25 and 27. These types of generators are referred to as one-shot power sources. In almost all such energy-harvesting devices, the piezoelectric transducer is considered to be loaded in compression and in the 33 mode. In certain applications, added mass may be required to achieve the desired level of transducer compressive loading.

Design of efficient CC circuits is particularly challenging in applications such as gun-fired munitions, which require additional safety features to prevent accidental powering of the load. In general, the CC and the safety and event detection circuits have to be passive and use minimal amounts of the generated electrical energy to allow the use of relatively small piezoelectric elements.

4.2.5.1 CC circuits for event detection and direct transfer of generated electrical energy to the load

Self-powered conditioning circuits for one-shot piezoelectric generators that are used as event-detection sensors with integrated safety electronics for initiation and switching in munitions have been reported.[25,27–30] Figure 4.17 shows the schematic of a passive CC circuit for shock-loading event detection with safety logic and direct transfer of the generated electrical energy to the load, in this case a bridge wire.

The circuitry shown in Fig. 4.17 is designed to differentiate firing setback induced shock loading (of the order of one to tens of thousands of $G = 9.8$ m/s^2) from all other no-fire accelerations such as high-G but with much shorter duration pulse(s), or relatively low-G but with long-term vibration loading such as those experienced during transportation and the like.

In the safety and all-fire event detection circuitry of Fig. 4.17, electrical energy (charge) is provided by the piezoelectric element via its compressive loading due to an experienced acceleration event. The all-fire setback

Downloaded From: https://www.spiedigitallibrary.org/ebooks/ on 07 Mar 2022
Terms of Use: https://www.spiedigitallibrary.org/terms-of-use

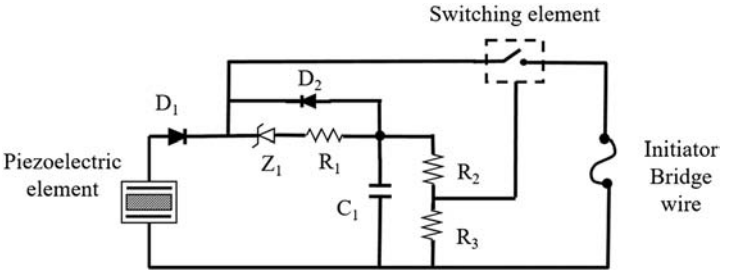

Figure 4.17 The safety and all-fire detection circuit with a switching circuit.

condition is detected by the voltage level of the capacitor C_1, while the circuitry prevents the charging of the capacitor C_1 to the prescribed voltage level if the generated piezoelectric charges are due to any of the aforementioned no-fire conditions, as described below. Diode D_1 has a low forward voltage drop and a very fast switching action. Diode D_1 also needs a high backward leakage, which is used as a safety feature for discharging collected charges in the capacitor C_1 when the voltage of the piezoelectric element drops below the prescribed all-fire voltage level.

The current due to the charges generated by the piezoelectric element passes through diode Z_1 (preferably a Zener or a similar diode) and resistor R_1 to charge capacitor C_1, and also passes through resistors R_2 and R_3 to the ground. During this time, diode D_2 is under reverse bias, thereby passing a very small amount of current. The resistance of resistor R_1 is selected to be very high and the capacitance of the capacitor C_1 very low to minimize the amount of electrical energy that is drained from the piezoelectric transducer. This is generally necessary to minimize the required size of the piezoelectric transducer.

The CC circuit is designed to detect acceleration profiles that generate piezoelectric voltage amplitudes that are of a sufficiently high and long duration to correspond to the all-fire event and be detected. All other generated voltage pulses not satisfying both constraints are considered to be no-fire events. The discussion below describes the operation of the basic CC circuit design shown in Fig. 4.17.

When a device using the circuitry shown in Fig. 4.17 is subjected to a relatively short-duration shock loading such as that due to accidental dropping, the piezoelectric element generates relatively high voltage pulses with very short duration. The generated voltages may even be higher than the voltage levels that are generated as the device is subjected to a prescribed all-fire setback acceleration, but the duration of such pulses is significantly shorter than those of the all-fire setback acceleration pulses. For example, an all-fire acceleration may be around 1000 Gs with 10 ms of duration, while an accidental drop may cause a shock loading of up to 2000 Gs but for a very short duration of less than 0.5 ms.

Downloaded From: https://www.spiedigitallibrary.org/ebooks/ on 07 Mar 2022
Terms of Use: https://www.spiedigitallibrary.org/terms-of-use

The passive circuit of Fig. 4.17 performs the needed event detection functions through an innovative circuit configuration that allows the voltage threshold and charging time constant of C_1 to be changed, while minimizing the energy consumption of the components. A typical implementation of the CC circuit requires the determination of suitable values for the components R_1, R_2, R_3, and C_1 for detection of the intended shock-loading event. Firstly, resistor R_1 and capacitor C_1 are selected such that a very small amount of generated electrical energy is consumed. As previously described in Section 4.2.3, the fractional energy extracted from the piezoelectric element is proportional to the load capacitance; thus, a value of C_1 that is much smaller than the equivalent capacitance of the piezoelectric element is required. The time constant of the CC circuit is a function of R_1, R_2, R_3, and C_1, while the required threshold voltage is determined by the values of R_2, R_3, and the voltage across capacitor C_1.

It is noted that leakage through resistors R_2 and R_3 is generally used to vary the time constant of the CC circuit. This capability provides a simple tool to readily adjust ("program") the device to the desired all-fire condition. The leakage through resistors R_2 and R_3 would also provide additional means of ensuring that the aforementioned high-voltage and short-duration pulses do not accumulate charge in capacitor C_1 to trigger a false all-fire detection signal. In addition, vibration loading such as that experienced during transportation—even if it is accompanied by high-G but short-duration shock-loading pulses—is similarly rejected by diode Z_1 and leaking resistors R_2 and R_3. Vibration-related loading usually has significantly lower peak G levels than that of accidental drops.

Several applications of the basic CC circuit of Fig. 4.17 for event detection are described in Chapter 5.

4.2.5.2 CC circuits for efficient transfer of generated electrical energy to a storage device

A CC circuit used for one-shot harvesting of electrical energy and storage in a capacitor is illustrated in Fig. 4.18. This passive circuit is ideally suited for micro-energy harvesters. In this circuit, when the piezoelectric element is subjected to a shock loading such as during impact or munitions firing, it generates charge Q. As illustrated in Fig. 4.19, the piezoelectric element may be modeled as a current source I_1 that is shunted by the piezoelectric element equivalent capacitance C_P. In response to the increasing strain, the voltage V_P increases, resulting in an equivalent current source I_1, which divides into three components as indicated at node M. The majority of the initial current flows into the piezoelectric capacitor C_P. The initial inductor current I_2 is comparatively small as is proportional to the integral of the voltage. Current

Downloaded From: https://www.spiedigitallibrary.org/ebooks/ on 07 Mar 2022
Terms of Use: https://www.spiedigitallibrary.org/terms-of-use

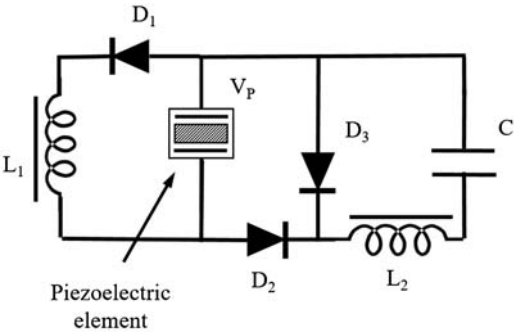

Figure 4.18 Charge collection and storage circuit for one-shot energy-harvesting devices. (Reprinted with permission from Ref. 27.)

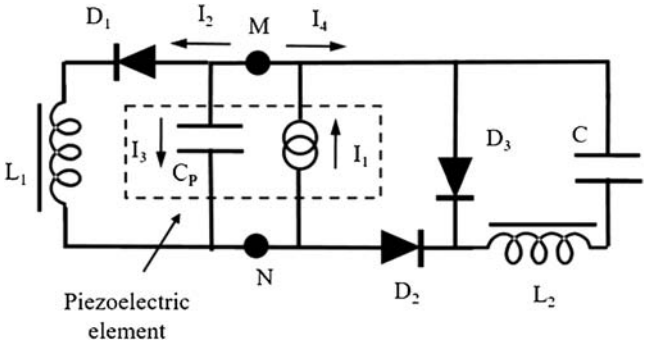

Figure 4.19 Equivalent circuit for the charge collection and storage circuit of the one-shot energy-harvesting device shown in Fig. 4.18.

I_4 is negligible because diode D_2 presents a very high impedance path. As applied strain increases toward the maximum value, the rate of change of voltage decreases, while the voltage increases. Thus, capacitor current I_3 decreases, while inductor current I_2 increases. The (L_1C_P) configuration is described as a tank circuit. The corresponding rise time of the tank circuit should be smaller than the rise time of the applied loading pulse. At the point of maximum strain, the open-circuit voltage is maximum and the inductor current will be maximum. As the strain begins to reverse, there is also a reversal in the voltage polarity at the node M. At this point the directions of current flow are reversed. Now the generated current flows into node N, through diode D_2 and inductor L_2, through storage capacitor C, and returns through diode D_3, forming a second (L_2C) tank. It should be noted that the generated current is prevented from flowing through the piezoelectric capacitor C_P by diode D_2. Furthermore, it should be noted that the energy stored during the first half of the pulse is also recovered from inductor L_1. Due to the reversal of the polarity, inductor L_1 discharges and dumps its stored

Downloaded From: https://www.spiedigitallibrary.org/ebooks/ on 07 Mar 2022
Terms of Use: https://www.spiedigitallibrary.org/terms-of-use

energy into the (L_2C) tank via diode D_3, which presents a very low impedance path compared with the piezoelectric capacitor C_P. In this way, the maximum electrical energy is harvested from the short-duration pulsed loading of a piezoelectric element.

4.2.5.3 CC circuits for event detection and efficient transfer of generated electrical energy to a storage device

In certain applications the event detection circuit of Fig. 4.17 may be combined with the collection and storage circuit of Fig. 4.18 to transfer the generated electrical energy to a holding storage capacitor once the intended all-fire event is detected.[25] Such circuits may be designed to serve various functions such as event sensing and switching, several of which are described in some detail in Chapter 5.

4.3 Collection and Conditioning Circuits for Electromagnetic Energy Harvesters

Generation of electrical energy based on Faraday's electromagnetic induction is perhaps the most established method of generating electrical energy from the microwatt to the gigawatt scale. Fundamentally, rotary or linear kinetic energy in the presence of a magnetic field produces an electromotive force (emf) within the conductor. The induced emf, as described in Chapter 2, is proportional to the rate of change of the magnetic flux linked by a conducting loop. In this section, some of the CC circuit techniques that are applicable to micro-generators that produce DC outputs compatible with integrated circuits (ICs) are briefly highlighted, and the reader is referred to the vast body of commercial and research literature on the general subject matter. A basic description of electromagnetic generators is followed by a brief description of particular techniques such as synchronous magnetic flux extraction and active full-wave rectifier systems.

Collection and conditioning circuits for micro-electromagnetic energy harvesters with energy output of a few micro-joules require the use of low-loss active-switching components for rectification and voltage level amplification, either through the use of voltage doublers/quadruplers on the AC side or a separate DC-DC boost circuit. Some of these conditioning circuit designs are based on active AC-DC rectification, transfer window alignment,[60] synchronous magnetic flux extraction (SMFE),[61] or a feedforward and feedback DC-DC pulse-width-modulated boost converter.[62]

Typically, conditioning circuits are designed to produce a DC output voltage that is compatible with a buffer capacitor for storage. The harvester has a charging phase that adds energy to the reservoir capacitor during each cycle. The charge can either be delivered to the load during each cycle, or be accumulated to a desired level needed for the load and transferred

Downloaded From: https://www.spiedigitallibrary.org/ebooks/ on 07 Mar 2022
Terms of Use: https://www.spiedigitallibrary.org/terms-of-use

asynchronously (event triggered). In all cases, the switching circuits need a start-up time that is determined by the voltage requirements of some components of the conditioning circuit. Several application-driven conditioning circuits are in use. As discussed in the beginning of the chapter, the complexity of the conditioning circuit is determined by the output energy of the transducer and the load demand. These circuits use the fundamental principles of switched capacitors and inductors. All circuits require rectification, which is implemented either using diodes, or using electronic switches or active diodes.

4.3.1 Synchronous magnetic flux extraction

Synchronous magnetic flux extraction (SMFE) is a switching technique used for vibration-based harvesters with electromagnetic transducers.[61] It is, in principle, equivalent to a synchronous electric charge extraction technique used for harvesting energy from piezoelectric transducers, as discussed in Section 4.2.4.3. SMFE is also referred to as a split-capacitor rectification[63] or as the flux-shaping method.[60] A schematic of a typical circuit, along with the corresponding waveforms, is provided in Fig. 4.20. The transducer output is described by an equivalent sinusoidal voltage source V_{EM} in series with the winding resistance R_S and inductance L_S. The method is similar to switching techniques used for piezoelectric harvesters discussed earlier. Charging current to the two capacitors with the extremum of the magnetically induced current, as illustrated in Fig. 4.20(b). The commutation gives a full-wave rectification of the sinusoidal signal from the transducer. Another shunting capacitor (not shown) may be used to further reduce the load voltage ripple. This is a simple solution that does not require complex switching circuits. However, a DC-DC boost converter is still needed to obtain voltages larger than the rectified voltage.

The above discussion of CC circuits for electromagnetic generators is applicable for vibration-based sources of mechanical energy. CC circuit

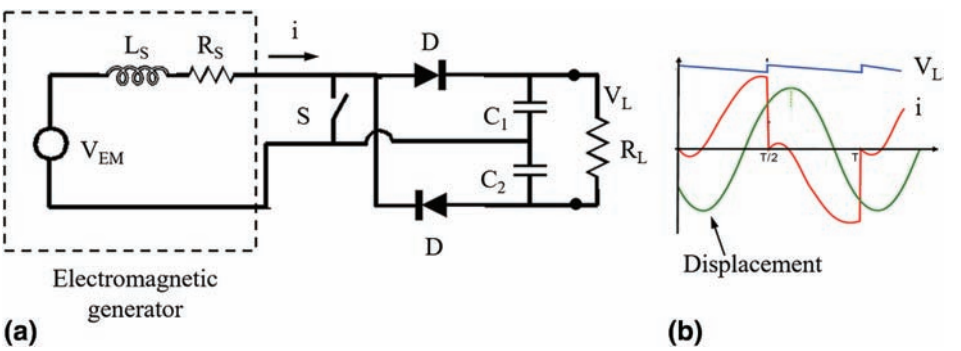

Figure 4.20 (a) SMFE circuit and (b) corresponding waveforms: displacement of the mass, current i, and output voltage V_L. (Reprinted with permission from Ref. 61.)

Downloaded From: https://www.spiedigitallibrary.org/ebooks/ on 07 Mar 2022
Terms of Use: https://www.spiedigitallibrary.org/terms-of-use

techniques are well established for energy-harvesting devices with continuously rotating electromagnetic transducers; the reader is referred to appropriate references on this subject matter, which are easily accessible.

4.3.2 Active full-wave rectifier

To overcome the above loss limitations, an active full-wave (AFW) rectifier (Fig. 4.21), comprising a cross-coupled transistor rectifier (CCTR) and an active diode (pCGAD) that prevents reverse saturation current flow, is preferred to the SMFE technique described above.

The active diode operates over a wide input voltage range from 0.48 V to 3.3 V, with efficiencies over 90%. This design uses a low-power solution gain-stage as a pseudo-comparator, producing more efficient and stable solutions as compared to typical active rectifier circuits. These circuits generally include a self-start feature that allows the CC circuit to reach full functional capability without the need for external voltage sources to power up the active transistor switches.[64]

4.4 Collection and Conditioning Circuits for Electrostatic Energy Harvesters

Electrostatic energy harvesters (eEHs) are characterized by open-circuit voltages that can reach hundreds of volts, but with a small sourcing current, of a few hundred nano-amperes. An electrostatic energy harvester is primarily a low-energy source, producing electrical output power less than a few 100 μW. Subsequently, CC circuits have to be low loss. As discussed for harvesting energy from piezoelectric devices, the most efficient extraction techniques are based on switched-mode operation. However, simpler passive designs with electret-based eEHs are attractive for certain low-energy-demand applications.

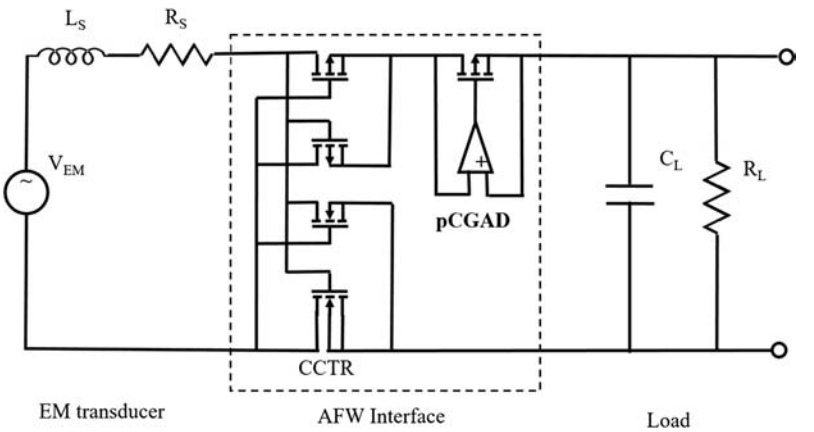

Figure 4.21 Active full-wave (AFW) rectifier CC circuit.[64] (Reprinted with permission from Ref. 64).

Downloaded From: https://www.spiedigitallibrary.org/ebooks/ on 07 Mar 2022
Terms of Use: https://www.spiedigitallibrary.org/terms-of-use

As discussed in Chapter 2, electrostatic transducers are capacitor-based devices in which relative movement between the electrodes causes a change in capacitance, resulting in the generation of electric charges. Two transducer designs are possible: (1) an electret-free design that requires an external voltage source to create the charge/discharge cycles and (2) an electret-based design that has permanent charges stored in the electret material. The former requires active electronic circuits that provide synchronization of the mechanical charge/discharge cycle with the changes in capacitance, while directly converting mechanical energy to electrical energy. The changes in capacitance are obtained by both in-plane and out-of-plane gap closing and in-plane and out-of-plane area overlap of the charged electrodes.[35,65]

In order for the electrostatic transducer to function as an energy harvester, two methods of establishing an initially charged capacitor are in use. The first uses an external voltage source to provide the initial charge on the electrodes of the capacitor, while a second approach uses a charged dielectric, known as an electret, sandwiched between the capacitor plates. The remainder of this section is divided into an introductory section followed by discussions on CC circuit designs for the electret-based and the electret-free configurations. Electret-based eEHs are operated either as passive devices suitable for direct use as sources in low-power applications such as wireless sensor networks, or as active energy harvesters providing 100-fold more power. In the latter mode, the eEH can be configured for energy transfer on the voltage extremum or with a pre-storage capacitor.

4.4.1 Electret-based eEHs

Electret-based energy harvesters are typically used to power MEMS-based devices[66] using resistive flyback[67,68] or inductive flyback.[46] However, the energy cycles are independent of how the initial voltage is supplied. In the case of electret-free construction, the external voltage is supplied through a battery, and since this voltage is typically not high enough, DC-DC charge pumps are needed to boost the bias voltage from 3 V to, e.g., the 100 V needed for an operational eEH.[35]

Electret-based harvesters offer a low-cost solution that can be exploited in certain applications when losses in the conditioning circuits are not of concern. These harvesters do not require the charge/discharge cycles associated with electret-free eEHs to be described in Section 4.4.2.

Figure 4.22 shows an equivalent circuit model comprising an equivalent fixed-voltage source V_S, corresponding to the electret charge density, in series with a variable capacitance C(t), which is dependent on the motion of one of the electrodes.

As illustrated in Fig. 4.22, eEHs can directly drive resistive or capacitive loads, provided that load current demand is on the order of nano-amperes. Since typical eEH capacitances are small, consideration of parasitic circuit

Downloaded From: https://www.spiedigitallibrary.org/ebooks/ on 07 Mar 2022
Terms of Use: https://www.spiedigitallibrary.org/terms-of-use

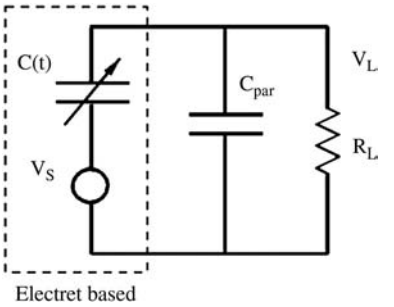

Figure 4.22 Equivalent circuit model for an electret-based electrostatic transducer, where V_S is the electret equivalent voltage, C(t) is the variable capacitor, R_L is the load resistor, C_{par} is the parasitic capacitance, and V_L is the load voltage.

capacitance C_{par} should be included in any design analysis. The conditioning circuit can be configured to be either passive or active. This provides the simplest means for converting the AC high-voltage, low-current eEH output into a 3-V DC power supply source, which is suitable for most system applications such as wireless sensor networks. A simple diode-based rectifier circuit such as that discussed in Section 4.2.1 can be used.

4.4.2 Active conditioning circuits

Active eEHs are needed to step down the high AC open circuit to match the operating voltage of the capacitor. Common configuration of these circuits include the use of step-down buck converters and flyback conditioning circuits to generate a 3-V DC voltage. While a number of designs are possible, two accepted approaches are described here. The first uses energy transfer based on maximum voltage detection, and the second uses energy transfer based on a pre-storage capacitor, which keeps an optimal voltage across the eEH.

4.4.2.1 Energy transfer at maximum voltage detection

The conditioning circuit designed to transfer power at maximum voltage detection is illustrated in Fig. 4.23. Closing switch S_1 on the primary side of

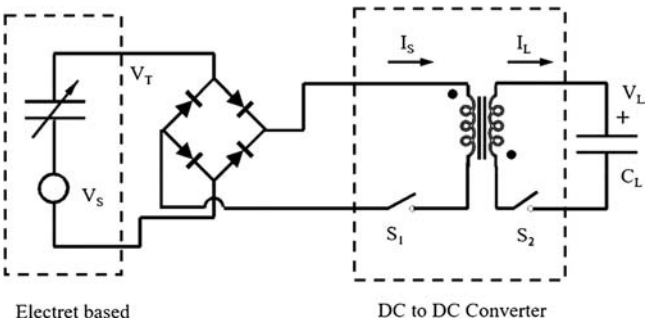

Figure 4.23 Energy transfer at maximum voltage detection.[35]

Downloaded From: https://www.spiedigitallibrary.org/ebooks/ on 07 Mar 2022
Terms of Use: https://www.spiedigitallibrary.org/terms-of-use

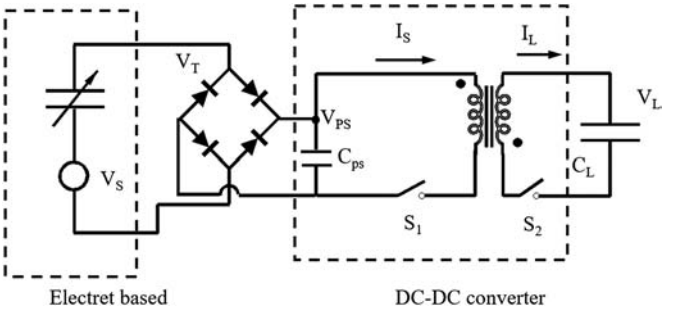

Figure 4.24 eEH energy transfer with pre-storage capacitor C_{PS}.

the transformer after detection of the eEH voltage maximum initiates energy flow to the magnetic circuit on the primary side. As the primary current reaches its maximum value, the voltage goes to zero, indicating that the primary inductor is fully charged and all of the energy from the eEH has been stored in the magnetic field. At this time point, switch S_2 is opened and S_1 is closed to magnetically couple energy to the secondary coil and into the storage capacitor C_L.

Due to the small capacitance of the eEH, parasitic capacitances of the transformer winding can cause increased conversion losses. These are reduced by using a pre-storage capacitor C_{PS} at the output of the diode bridge rectifier as illustrated in Fig 4.24. Although not explicitly shown, the precise switching action is achieved through the use of digitally controlled electronic switching devices such as MOSFETs, BJTs (bipolar junction transistors), and IGBTs (insulated-gate bipolar transistors).

4.4.2.2 Energy transfer with a pre-storage capacitor

In this mode, C_{PS} essentially maintains an optimal voltage across the diode bridge, which maximizes the energy extraction from the eEH. The conditioning circuit maintains the voltage V_{PS} within $\pm 10\%$ ripple as illustrated in Fig. 4.24. When V_T exceeds the upper limit, energy from C_{PS} is sent to C_L through the flyback capacitor in order to maintain a constant rectifier output voltage.

4.4.3 Electret-free eEHs

For the present discussion on CC circuits, most of the contemporary CC circuit designs are based on the SECE techniques described in Section 4.2.4. In particular, two switching configurations based on maintaining either constant charge or constant voltage during energy conversion are preferred.[35,36,65] Electret-free eEHs have three phases of operation—charging, harvesting, and pre-charge—while the charge/discharge phases are not needed for electret-based devices. Precise timing knowledge of these distinct time events is critical to the design of an efficient CC circuit, which is typically analyzed using the

Downloaded From: https://www.spiedigitallibrary.org/ebooks/ on 07 Mar 2022
Terms of Use: https://www.spiedigitallibrary.org/terms-of-use

steady state equivalent for each of the phases of the energy cycle. Harvesting cycles can be triggered by internal voltage/current swings or through the use of external sensors attached to the mechanical system. The time-dependent state of the variable capacitor may be determined using the charge–voltage diagrams described in Ref. 69.

Electret-free eEHs need sophisticated timing circuits to charge/discharge the capacitor at the appropriate time. As discussed in Chapter 2, there are two possible operational modes that are either the voltage constrained or charge constrained.

4.4.3.1 Voltage-constrained conditioning circuits

Figure 4.25 is a schematic of the conditioning circuit used to implement the voltage-constrained cycle. This conditioning circuit requires two switched inductor networks to maintain constant voltage during the energy conversion phase. The constant voltage V_L is achieved through the use of the capacitor C_L. A rechargeable battery V_{ext} charges the variable capacitor C(t) using switches S_1 and S_2 of the magnetic core M_1. The switching time is much faster than the period of the mechanical input motion. Closing of S_1 is synchronized with the time at which the variable capacitance is at its maximum value. A charge $\Delta Q = V_L \Delta C(t)$ is transferred to the constant voltage capacitor C_L. When the voltage V_L is higher than the threshold voltage, a quantity of energy is transferred from the constant voltage capacitor to the rechargeable battery by closing switch S_4 and then S_3. At the end of the conversion cycle, when the variable capacitor reaches its minimum value, the remaining stored energy is transferred back to the rechargeable battery by closing switches S_2 and S_1. Variations of this circuit using a charge pump and transformer-based switching circuit have been proposed.[70] In practice, due to the difficulty of operation, few practical systems use the constant-voltage-cycle conditioning circuit.

4.4.3.2 Charge-constrained conditioning circuit

Compared to the voltage-constrained cycle, the charge-constrained cycle (Fig. 4.26) is easier to implement as the charging step (1) takes place at the

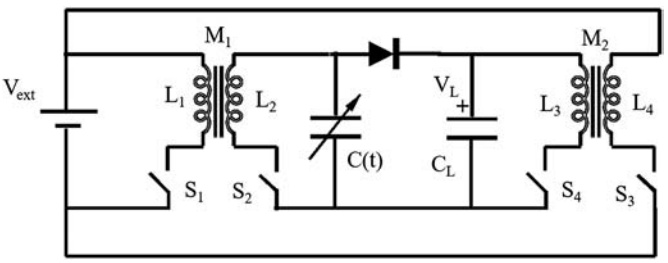

Figure 4.25 Example of a voltage-constrained conditioning circuit.[35]

Downloaded From: https://www.spiedigitallibrary.org/ebooks/ on 07 Mar 2022
Terms of Use: https://www.spiedigitallibrary.org/terms-of-use

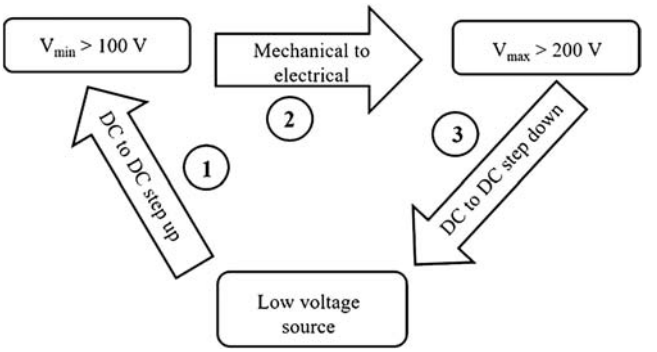

Figure 4.26 Electret-free energy conversion steps for the charge-constrained configuration.

maximum value of the capacitance. During the energy conversion phase (2), the variable capacitor is open-circuit as its capacitance decreases to its minimum value, resulting in an increase in the voltage across the variable capacitor. The discharge phase (3) takes place at minimum capacitance as the energy is returned to the storage element. As the polarizing voltages are on the order of several hundred volts, bidirectional DC-DC buck–boost converters or bidirectional flyback converter designs are needed for the conditioning circuit. The former requires bidirectional transistors for operation, but the latter do not. Figure 4.27 shows the flyback implementation, and Fig. 4.28 illustrates the corresponding voltage–current waveforms.

Charging of the variable capacitor C(t) [step (1) in Fig. 4.26] is initiated by closing S_1 for time t_1 to charge the inductor L_1 with sufficient energy to polarize the energy harvester. S_1 is opened and S_2 is closed until current I_2 goes to zero, indicating completion of the charging of the variable capacitor of the eEH. Transfer of the energy from the magnetic core M to the C(t) is accomplished in time interval t_2. During step 2 mechanical energy is converted to electrical energy. Both switches S_1 and S_2 are open to allow the voltage across the eEH to vary freely as the capacitance changes to its minimum value. Step 3 of the energy-harvesting cycle illustrated in Fig. 4.26 discharges the variable capacitor by transferring the energy back to the voltage source via

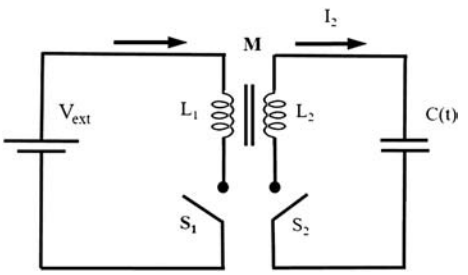

Figure 4.27 Bidirectional flyback CC circuit design for the electret-free eEH.

Downloaded From: https://www.spiedigitallibrary.org/ebooks/ on 07 Mar 2022
Terms of Use: https://www.spiedigitallibrary.org/terms-of-use

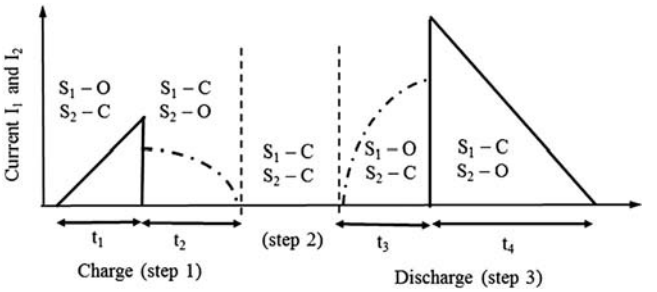

Figure 4.28 Current waveforms of the bidirectional flyback converter energy-harvesting cycle illustrated in Fig. 4.26[35] (O – switch open, C – switch closed).

the magnetic core. At the end of step 3, the variable capacitor is in its uncharged state. Step 3 is initiated by closing S_2 for a time t_3 to transfer energy to inductor L_1 and then opening S_2 and closing S_1 until current I_1 goes to zero.

4.5 Conditioning Circuits for Vibration-based Magnetostrictive Energy Harvesters

The electrical circuit equivalent of a vibration-based magnetostrictive energy harvester is similar to that of the electromagnetic energy harvester; namely, the time-varying strain generates a time-varying voltage according to Faraday's law. However, because the AC voltage is typically less than 1 V, conditioning circuits include a DC voltage multiplication stage as a part of the passive diode rectification. Figure 4.29 shows a rectifier with a quadruple multiplier. These conditioning circuits usually employ low-loss Schottky diodes and have been used in other high-voltage DC-to-DC applications.

This chapter has described the fundamental electrical circuit concepts for collecting and conditioning electrical energy generated from mechanical sources of kinetic and/or potential energy. While there are common design principles such as the universal use of switching devices across the various transducer types, some specific features are unique to a particular transducer; for example, the charge/voltage-constraint energy-harvesting cycles are specific to electrostatic energy harvesters. In the above discussion the

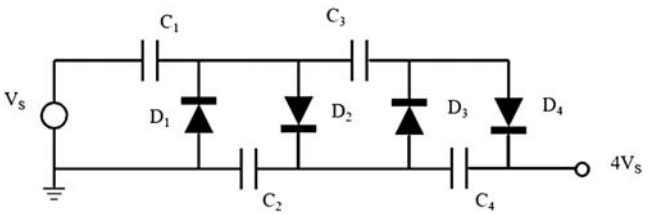

Figure 4.29 AC rectification and voltage quadrupler for a magnetostrictive energy harvester.

Downloaded From: https://www.spiedigitallibrary.org/ebooks/ on 07 Mar 2022
Terms of Use: https://www.spiedigitallibrary.org/terms-of-use

emphasis has been on principles rather than detailed analysis and simulation of particular designs. In general, collection and conditioning circuits are nonlinear and are typically analyzed by separating the design into linear regions in the time domain. For an in-depth discussion of the related topics, the reader is referred to Ref. 46.

References

1. G. K. Ottman, H. F. Hoffman, A. C. Bhatt, and G. Lesieutre, "Adaptive piezoelectric energy harvesting circuit for wireless remote power supply," *IEEE Transactions on Power Electronics* **17**(5), 669–676 (2002).
2. E. E. Aktakka and K. Najafi, "A micro inertial energy harvesting platform with self-supplied power management circuit for autonomous wireless sensor nodes," *IEEE Solid-State Circuits* **49**(9), 2017–2029 (2014).
3. E. E. Aktakka, R. L. Peterson, and K. Najafi, "A self-supplied intertial piezoelectric energy harvester with power-management IC," *IEEE International Solid-State Circuits Conference*, 120–121 (2011).
4. R. Calio, U. B. Rongala, D. Camboni, M. Milazzo, C. Stefanini, G. de Petris, and C. M. Oddo, "Piezoelectric energy harvesting solutions," *Sensors* **14**, 4755–4790 (2014).
5. K. A. Cook-Chennault, N. Thambi, and A. M. Sastry, "Powering MEMS portable devices – a review of non-regenerative and regenerative power supply systems with special emphasis on piezoelectric energy harvesting systems," *Smart Materials and Structures* **17**(4), 1–33 (2008).
6. D. Guyomar, E. Badel, E. Lefeuvre, and R. Richard, "Toward energy harvesting using active materials and conversion improvement by nonlinear processing," *IEEE Transactions on Ultrasonics, Ferroelectrics and Frequency Control* **52**, 594–595 (2005).
7. M. Lallart, E. Lefeuvre, C. Richard, and D. Guyomar, "Self-powered circuit for broadband, multimodal piezoelectric vibration control," *Sensors and Actuators A: Physical* **143**, 377–382 (2008).
8. M. Lallart and D. Guyomar, "An optimized self-powered switching circuit for nonlinear energy harvesting with low voltage output," *Smart Materials and Structures* **17**, 1–8 (2008).
9. M. Lallart, L. Garbuio, L. Petit, C. Richard, and D. Guyomar, "Double synchronized switch harvesting (DSSH): A new energy harvesting scheme for efficient energy extraction," *IEEE Transactions on Ultrasonics, Ferroelectrics and Frequency Control* **55**(10), 2119–2130 (2008).
10. E. Lefeuvre, M. Lallart, C. Richard, and D. Guyomar, "Piezoelectric Material-based Energy Harvesting Devices: Advances of SSH Optimization Techniques (1999–2009)," in *Piezoelectric Ceramics*, E. Suaste-Gomez, Ed., InTech Open Access Publisher, Rijeka, Croatia, pp. 165–184 (2010).
11. E. Lefeuvre, D. Audiger, C. Richard, and D. Guyomar, "Buck–boost converter for sensorless power optimization of piezoelectric energy

Downloaded From: https://www.spiedigitallibrary.org/ebooks/ on 07 Mar 2022
Terms of Use: https://www.spiedigitallibrary.org/terms-of-use

harvester," *IEEE Transactions on Power Electronics* **22**(5), 2018–2025 (2007).
12. E. Lefeuvre, A. Badel, C. Richard, L. Petit, and D. Guyomar, "A comparison between several vibration-powered generators for standalone systems," *Sensors and Actuators A: Physical* **126**(2), 405–416 (2006).
13. E. Lefeuvre, A. Badel, C. Richard, and D. Guyomar, "Piezoelectric energy harvesting device optimization by synchronous charge extraction," *Journal of Intelligent Material Systems and Structures* **16**, 865–876 (2005).
14. Y.-P. Liu and D. Vasic, "Self-Powered Electronics for Piezoelectric Energy Harvesting Devices," in *Small-Scale Energy Harveseting*, M. Lallart, Ed., InTech Open Access Publisher, Rijeka, Croatia, Chapter 14 (2012).
15. P. D. Mitcheson, E. M. Yeatman, G. K. Rao, A. S. Holmes, and T. C. Green, "Energy harvesting from human and machine for wireless electronic devices," *Proc. IEEE* **96**(9), 14577–1486 (2008).
16. Y. C. Shu and I. C. Lien, "Efficiency of energy conversion for a piezoelectric power harvesting system," *Journal of Micromechanics and Microengineering* **16**, 2429–2438 (2006).
17. G. D. Szarka, B. H. Stark, and S. G. Burrow, "Review of power conditioning for kinetic energy harvesting systems," *IEEE Transactions on Power Electronics* **27**(2), 803–815 (2012).
18. T. G. Engel, J. E. Becker, and W. C. Nunnally, "Energy conversion and high power pulse production using miniature magnetic flux compressors," *IEEE Transactions on Plasma Science* **28**(5), 1342–1346 (2000).
19. T. G. Engel, C. Keawboonchuay, and W. C. Nunnally, "Energy conversion and high power pulse production using miniature piezoelectric compressors," *IEEE Transactions on Plasma Science* **28**(5), 1338–1341 (2000).
20. T. G. Engel, W. C. Nunnally, J. Becker, R. Rahman, and C. Keawboonchuay, "Research progress on compact kinetic-to-electrical energy convertors," *IEEE International Pulsed Power Conference*, 1287–1290 (1999).
21. J. L. Gonzalez, A. Rubio, and F. Moll, "Human powered piezoelectric batteries to supply power to wearable electronic devices," *International Journal of the Society of Materials Engineering for Resources* **10**(1), 34–40 (2002).
22. J. L. Gonzalez, A. Rubio, and F. Moll, "A prospect of the use of piezoelectric effect to supply power to wearable electronic devices," *Proc. of the Fourth International Conference on Materials Engineering for Resources* **1**, 202–207 (2001).
23. C. Keawboonchuay and T. G. Engel, "Maximum power generation in a piezoelectric pulse generator," *IEEE Transactions on Plasma Science* **31**(1), 123–128 (2003).

Downloaded From: https://www.spiedigitallibrary.org/ebooks/ on 07 Mar 2022
Terms of Use: https://www.spiedigitallibrary.org/terms-of-use

24. J. Kymissis, C. Kendall, J. Paradiso, and N. Gershenfield, "Parasitic power harvesting in shoes," *IEEE International Symposium on Wearable Computers*, 132–139 (1998).
25. J. Rastegar, D. Feng, and C. Pereira, "Piezoelectric energy-harvesting power source and event detection sensors for gun-fired munitions," *Proc. SPIE* 9493, 94930H (2015) [doi: 10.1117/12.2176879].
26. J. Rastegar and D. Feng, "Inertially operated electrical initiation devices," U.S. Patent Number 9,097,502 (2015).
27. J. Rastegar, D. Feng, and C. Pereira, "Efficient methods of harvesting energy from ultra-short duration shock loading," *ASME 2014 Conference on Smart Materials, Adaptive Structures and Intelligent Systems* SMASIS2014-7657, V002T07A020, Newport, Rhode Island (2014).
28. J. Rastegar, D. Feng, and C. Pereira, "Piezoelectric-based event sensing and energy-harvesting power sources for thermal battery initiation in gun-fired munitions," *Proc. SPIE* **9115**, 911509 (2014) [doi: 10.1117/12.2053205].
29. J. Rastegar, D. Feng, and C. Pereira, "Self-powered event detection sensors with integrated safety electronics for initiation and switching in munitions," *ASME 2014 Conference on Smart Materials, Adaptive Structures and Intelligent Systems* SMASIS2014-7693, V002T04A025, Newport, Rhode Island (2014).
30. J. Rastegar, C. Pereira, M. Ervin, and D. Feng, "Piezoelectric-based electrical energy harvesting and storage methods and electronics for munitions," *Proc. SPIE* **9059**, 905909 (2014) [doi: 10.1117/12.2045257].
31. J. Rastegar, R. Murray, C. Pereira, and H.-L. Nguyen, "Novel piezoelectric-based energy-harvesting power sources for gun-fired munitions," *Proc. SPIE* 6527, 65270Y (2007) [doi: 10.1117/12.715009].
32. N. A. Shenck and A. Paradiso, "Energy scavenging with shoe mounted piezoelectrics," *IEEE Micro Magazine* **21**, 30–42 (2001).
33. N. A. Shenck, "A Demonstration of Useful Electrical Energy Generation from Piezoelectrics in a Shoe," M.S. thesis, Massachusetts Institute of Technology, Cambridge (1999).
34. M. Umeda, K. Nakamura, and S. Ueha, "Analysis of transformation of mechanical impact energy to electrical energy using a piezoelectric vibrator," *Japanese Journal of Applied Physics* **35**(5B), 3267–3273 (1996).
35. S. Boisseau, G. Despesse, and B. A. Seddik, "Electrostatic Conversion for Vibration Energy Harvesting," in *Small-Scale Energy Harvesting*, M. Lallart, Ed., InTech Open Access Publisher, Rijeka, Croatia, Chapter 5 (2012).
36. V. Janicek, M. Husak, J. Jakovenko, and J. Formanek, "Design and fabrication of 3D electrostatic energy harvester," *Radio Engineering* **21**, 231–238 (2012).

Downloaded From: https://www.spiedigitallibrary.org/ebooks/ on 07 Mar 2022
Terms of Use: https://www.spiedigitallibrary.org/terms-of-use

37. A. Cadei, A. Dionisi, E. Sardini, and M. Serpelloni, "Kinetic and thermal energy harvesters for implantable medical devices and biomedical autonomous sensors," *Measurement Science and Technology* **25**, 1–14 (2014).
38. C. Cepnik and U. Wallrabe, "Approaches for a fair comparison and benchmarking of electromagnetic vibration energy harvesters," *Micromachines* **4**, 286–305 (2013).
39. W. C. Chye, Z. Dahan, O. Sidek, and M. A. Miskam, "Electromagnetic micro power generator—a comprehensive survey," *IEEE Symposium on Industrial Electronics and Applications*, 376–382 (2010).
40. Y. J. Wang, C. D. Chen, and C. K. Sung, "System design of a weighted-pendulum-type electromagnetic generator for harvesting energy from a rotating wheel," *IEEE/ASME Transactions on Mechatronics* **18**(2), 754–762 (2013).
41. T. Fan and Y. Yamamoto, "Vibration-induced energy harvesting system using Terfenol-D," *IEEE International Conference on Mechatronics and Automation*, 2319–2324 (2015).
42. T. Ueno and S. Yamada, "Performance of energy harvesting using iron-gallium alloy in free vibration," *IEEE Transactions on Magnetics* **47**(10), pp. 2407–2409 (2011).
43. B. Yan, C. Zhan, and L. Li, "Design and fabrication of high efficiency magnetostrictive energy harvester for high impact vibration systems," *IEEE Transactions on Magnetics* **51**(11), 8205404 (2015).
44. M. Zucca, O. Bottauscio, C. Beatrice, A. Hadadian, F. Fiorillo, and L. Martino, "A study on energy harvesting by amorphous strips," *IEEE Transactions on Magnetics* **50**(11), 8002104 (2014).
45. D. H. Staelin, A. W. Morgenthaler, and J. A. Kong, *Electromagnetic Waves*, Prentice Hall, Upper Saddle River, New Jersey (1994).
46. D. W. Hart, *Power Electronics*, McGraw-Hill, New York (2011).
47. G. A. Lesieutre, G. K. Ottman, and H. F. Hofmann, "Damping as a result of piezoelectric energy harvesting," *Journal of Sound and Vibration* **269**, 991–1001 (2004).
48. G. K. Ottman, H. F. Hoffman, and G. Lesieutre, "Optimized piezoelectric energy harvesting circuit using step-down converter in discontinuous conduction mode," *IEEE Transactions on Power Electronics* **18**(2), 696–703 (2003).
49. A. Badel, M. Lagache, D. Guyomar, E. Lefeuvre, and C. Richard, "Finite element and simple lumped modelling for flexural nonlinear semi-passive damping," *Journal of Intelligent Material Systems and Structures* **18**, 727–742 (2007).
50. A. Badel, G. Sebald, D. Guyomar, M. Lallart, E. Lefeuvre, C. Richard, and J. Qiu, "Piezoelectric vibration control by synchronized switching on

Downloaded From: https://www.spiedigitallibrary.org/ebooks/ on 07 Mar 2022
Terms of Use: https://www.spiedigitallibrary.org/terms-of-use

adaptive voltage sources: Towards wideband semi-active damping," *Journal of the Acoustical Society of America* **119**, 2815–2825 (2006).
51. H. Ji, J. Qiu, and P. Xia, "Analysis of energy conversion in two-mode vibration control using synchronized switch damping approach," *Journal of Sound and Vibration* **330**, 3539–3560 (2011).
52. H. Shen, J. Qiu, H. Ji, K. Zhu, M. Balsi, I. Georgi, and F. Dell'Isolla, "A low-pass circuit for piezoelectric vibration control by synchronized switching on voltage sources," *Sensors and Actuators A: Physical* **161**, 245–255 (2010).
53. E. Lefeuvre, A. Badel, C. Richard, and D. Guyomar, "High-performance piezoelectric vibration energy reclamation," *Proc. SPIE* **5390**, 379–387 (2004) [doi: 10.1117/12.532709].
54. G. W. Taylor, J. R. Burns, S. M. Kammann, W. B. Powers, and T. R. Welsh, "The Energy Harvesting Eel: a small subsurface ocean/river power generator," *IEEE Journal of Ocean Engineering* **26**, 539–547 (2001).
55. P. H. DeJong, "Power Harvesting using Piezoelectric Materials—Applications in Helicopter Rotors," Ph.D. thesis, Universiteit of Twente, Enchede, The Netherlands (2013).
56. A. Badel, D. Guyomar, E. Lefeuvre, and C. Richard, "Efficiency enhancements of a piezoelectric energy harvesting device in pulsed operation by synchronous charge inversion," *Journal of Intelligent Material Systems and Structures* **16**, 889–902 (2005).
57. K. Makihara, J. Onoda, and T. Miyakawa, "Low energy dissipation electric circuit for energy harvesting," *Smart Materials and Structures* **15**, 1493–1498 (2006).
58. L. Garbuio, M. Lallart, D. Guyomar, C. Richard, and D. Audigier, "Mechanical energy harvester with ultralow threshold rectification based on SSHI nonlinear technique," *IEEE Transactions on Industrial Electronics* **56**, 1048–1056 (2009).
59. P.-H. Hsieh, C.-H. Chen, and H.-C. Chen, "Improving the scavenged power of nonlinear piezoelectric energy harvesting interface at off-resonance by introducing switching delay," *IEEE Transactions on Power Electronics* **36**(6), 3142–3155 (2015).
60. J. Moon and S. B. Leeb, "Power electronic circuits for magnetic energy harvesters," *IEEE Transactions on Power Electronics* **30**(1), 270–279 (2016).
61. E. Arroyo, A. Badel, and F. Formosa, "Modeling and design of an electromagnetic vibration energy harvester and its dedicated energy extraction circuit," *IEEE Instrumentation and Measurement Technology Conference* I2MTC, 425–430 (2012).
62. X. Cao, W. J. Chiang, Y.-C. King, and Y.-K. Lee, "Electromagnetic energy harvesting circuit with feedforward and feedback DC-DC PWM

Downloaded From: https://www.spiedigitallibrary.org/ebooks/ on 07 Mar 2022
Terms of Use: https://www.spiedigitallibrary.org/terms-of-use

boost converter for vibration power generation system," *IEEE Transactions on Power Electronics* **22**(2), 679–685 (2007).
63. D. Dayal and L. Parsa, "Low power implementation of maximum energy harvesting scheme for vibration-based electromagnetic microgenerators," *IEEE Applied Power Electronics Conference and Exposition* (APEC), 1949–1953 (2011).
64. D. Maurath, P. F. Becker, D. Spreemann, and Y. Manoli, "Efficient energy harvesting with electromagnetic enrgy transducer using active low-voltage rectification and maximum power point tracking," *IEEE Journal of Solid-State Circuits* **47**(5), 1369–1380 (2012).
65. A. Dudka, D. Galayko, E. Blokhina, and P. Basset, "Smart integrated conditioning electronics for electrostatic vibration energy harvesters," *Circuits and Systems, International Symposium*, 2600–2603 (2014).
66. D. Galayko, A. Dudka, A. Karami, E. O'Riordan, E. Blokhina, O. Feely, and P. Basset, "Capacitive energy conversion with circuits implementing a rectangular charge-voltage cycle—Part I: Analysis of the electrical domain," *IEEE Transactions on Circuits and Systems* **62**(9), 1–12 (2015).
67. H. R. Florentino, D. Galayko, R. C. S. Freire, B. A. Luciano, and C. Florentino, "Energy harvesting circuit using variable capacitor with higher performance," *Journal of Integrated Circuits and Systems* **6**(1), 66–74 (2011).
68. H. R. Florentino, R. C. S. Raimundo, C. S. Freire, S. Y. C. Catunda, A. V. S. Sa, and D. Galayko, "Energy harvesting using variable capacitor for power systems," *IEEE Instrumentation and Measurement Technology Conference* I2MTC, 1–4 (2011).
69. S. Meninger, J. Mur-Miranda, J. Lang, A. Chandrakasan, A. Slocum, M. Schmidt, and R. Amirtharajah, "Vibration to electric energy conversion," *IEEE Transactions on Very Large Scale Integration (VLSI) Systems* **9**, 64–76 (2001).
70. B. C. Yen and J. H. Lang, "A variable capacitance vibration-to-electric energy harvester," *IEEE Transactions on Circuits and Systems* **53**(2), 288–295 (2006).

Downloaded From: https://www.spiedigitallibrary.org/ebooks/ on 07 Mar 2022
Terms of Use: https://www.spiedigitallibrary.org/terms-of-use

Chapter 5
Case Studies

5.1 Introduction

This chapter highlights some of the mechanical potential and kinetic energy-harvesting technologies that have infiltrated or are on the verge of reaching the commercial marketplace, or are currently under development. Energy harvesters are enabling technologies that are driving a number of diverse applications. These include the direct replacement of batteries (as supplemental power sources), self-powered devices, and for vibration damping to dissipate the potentially damaging energy from a structure or system, in the process of which they may also serve as power sources. In certain applications, energy-harvesting devices may serve as power sources as well as self-powered event-detection sensors with integrated logic circuitry.

As discussed in previous chapters, several transduction methods are available to convert mechanical kinetic and potential energy into electrical energy. There is a long history of such energy-harvesting systems. Dynamos, which convert mechanical energy into electrical energy via electromagnetic transduction, are popular with bicyclists and have been around since the late nineteenth century, and are still in use today.[1] In fact, one of the contemporary commercial success stories is the regenerative braking system, which is based on the same energy-harvesting principle. Push-button piezoelectric igniters generating a few thousand volts have been used as ignition sources in gas appliances. These piezoelectric ignition systems are small, simple, long lasting, and require little maintenance.[2]

The academic literature as well as manufacturers' data sheets often characterize and compare the output of energy harvesters in terms of power. The use of power is somewhat misleading in many cases since it implies that the energy harvester is to serve as a source of continuous power at a certain prescribed voltage, similar to chemical batteries. However, in many applications, the host system cannot be considered to be a continuous source of mechanical energy to the energy harvester and may provide the energy for intermittent harvesting. In fact, in many applications the provided mechanical energy may be

Downloaded From: https://www.spiedigitallibrary.org/ebooks/ on 07 Mar 2022
Terms of Use: https://www.spiedigitallibrary.org/terms-of-use

in the form of shock-loading events that may be far apart or occur randomly. In the case of a remote-emergency-event-detection sensor powered by an energy-harvesting device, the events may occur very infrequently and far apart. In the case of an impact shock-loading detection device, the event may even occur only once, such as in the case of a remote sensor used to detect catastrophic failure of a system or sensors used to detect firing in gun-fired in munitions.

In general, an energy-harvesting-based electrical power source should be considered as two separate subsystems that are properly designed for integration to satisfy the requirements of each specific application. The first subsystem is the electrical energy generator that converts mechanical potential and/or kinetic energy from a host system to electrical energy. In the second subsystem, an appropriate CC circuitry would then collect, condition, and transfer the generated electrical energy directly to power the load and/or to be stored in an electrical energy storage device. The primary function of the first subsystem is to generate enough electrical energy to satisfy the total electrical energy requirement of the application at hand, considering its energy demand profile over time. All energy losses in the CC circuitry, storage devices, etc., must also be considered. The primary function of the second subsystem is to efficiently collect the generated electrical energy and condition it for direct transfer to the application electronics and/or for storage in an electrical energy storage device that would serve as a power source for later use.

As discussed in the previous chapters, the designer of the energy-harvesting solution is faced with a number of critical choices before embarking on the actual design solution. The process begins by identifying the required energy demand of the load and the available source(s) of the mechanical energy to be harvested. The designer should do a critical analysis of the energy demands of the expected load, as the demand is likely to be very event (time) dependent. Additionally, the designer has to be cognizant of the size and environmental requirements of the host system, as this will dictate the complexity of the interfacing mechanisms, as well as the design of the CC circuit.

Several vibration energy-harvesting power sources are becoming available to consumers, such as the Volture™ and Perpetuum products.[3,4] Semiconductor manufacturers such as Cypress Semiconductor Corp., Linear Technology Corp., and Maxim Integrated Products, Inc., have complementary ICs that are generally suitable for conditioning continuous and narrowband harvester outputs, producing a regulated output voltage.

The following sections highlight a number of mechanical-energy-harvesting systems and their components. Section 5.2 describes some commercial vibration energy harvesters. Section 5.3 describes current developments for wireless tire-pressure-monitoring solutions. Section 5.4 presents discussion of an energy-harvesting power source for gun-fired munitions. Sections 5.5 and 5.6 describe self-powered shock-loading event detection with a safety logic circuit and its applications.

Downloaded From: https://www.spiedigitallibrary.org/ebooks/ on 07 Mar 2022
Terms of Use: https://www.spiedigitallibrary.org/terms-of-use

5.2 Commercial Vibration Energy Harvesters

Energy-harvesting solutions are being offered by some of the large electronic distributors. For example, the Volture™ [Fig. 5.1(a)] is a vibration energy-harvesting module that consumers can integrate into their mechanical vibration energy source. It is based on the Midé Technology Corp.[3] proprietary Piezo Protection Advantage (PPA) manufacturing process that creates hermetically sealed and electrically insulated transducers [Fig. 5.1(b)]. PPA products are said to be capable of being tuned to a wide range of frequencies from a few hertz to 500 Hz, to match the resonant frequency of the source of mechanical vibration. Output powers of 60 mW at a resonant frequency of 60 Hz, using a 2.0-g tip mass have been reported on the manufacturer's data sheets.[3]

Another commercial vibration energy harvester, the Perpetuum PMG/C,[4] is offered by the manufacturer Perpetuum Ltd. It is based on electromagnetic transduction to convert vibration energy to electrical energy. Figure 5.2(a) is a photograph of a commercial device that can produce an output power of 27 mW at two output voltages of 5 V and 8 V. Figure 2(b) is a schematic

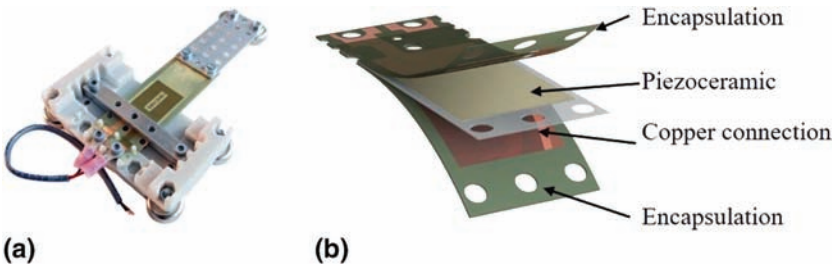

Figure 5.1 (a) The Volture™ power module and (b) Piezo Protection Advantage (PPA).[3]

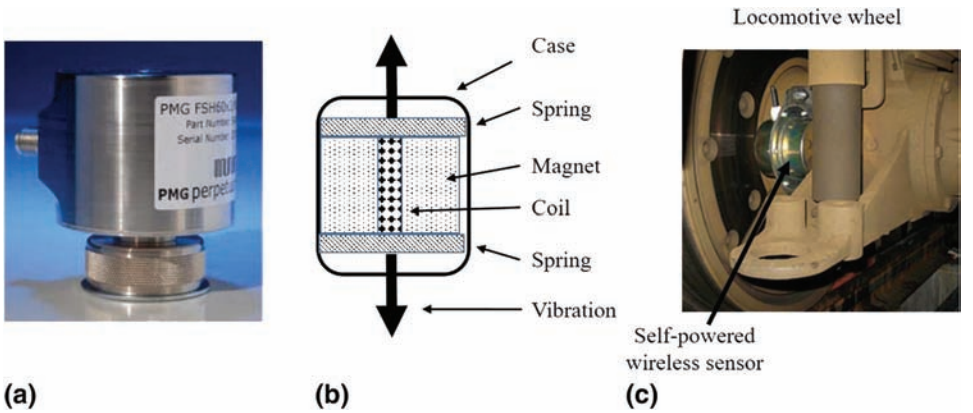

Figure 5.2 (a) Electromagnetic vibration energy harvester shown (b) as a schematic and (c) installed on a train wheel for wireless vibration monitoring. (Reprinted with permission from Ref. 5.)

Downloaded From: https://www.spiedigitallibrary.org/ebooks/ on 07 Mar 2022
Terms of Use: https://www.spiedigitallibrary.org/terms-of-use

showing the internal components. The vibration input has maximum limits of 10 G in the resonant frequency range of 100 Hz to 10 kHz. These power sources are integrated into self-powered wireless sensors, which transmit real-time data back to the asset owner. They have been installed on train wheels to report bearing, wheel, and track vibrations [Fig. 5.2(c)], and have been deployed in other industrial applications.[5]

There are also some novelty and hobbyist products that exploit energy-harvesting solutions. For example, several manufacturers sell electromagnetic flashlights. Basically, shaking the flashlight moves a magnet up and down inside a conducting coil, generating a small amount of electrical energy that is stored in a capacitor until powering an LED (light-emitting diode). Generally, such generators produce a very small amount of electrical energy by the shaking action. A properly designed generator using a vibratory mass and spring element should constitute a significantly more efficient means of transferring mechanical energy from the shaking action to the mass and spring element as potential and/or kinetic energy.

5.2.1 IC products for energy-harvesting devices

Some semiconductor manufacturers have developed ICs for collection and conditioning of generated electrical energy by piezoelectric-based energy-harvesting devices. These ICs are generally designed for energy-harvesting devices used in mechanical systems with a nearly continuous vibratory motion. For example, Linear Technology Corp.'s LTC3588-1 IC[6] has been used by Midé Technology Corp.[3] to develop the MIDE V2 1BL piezoelectric energy harvester (Fig. 5.3) that can be programmed to output voltage levels of 1.8 V, 2.5 V, 3.3 V, and 5 V, and can source up to 100 mA.

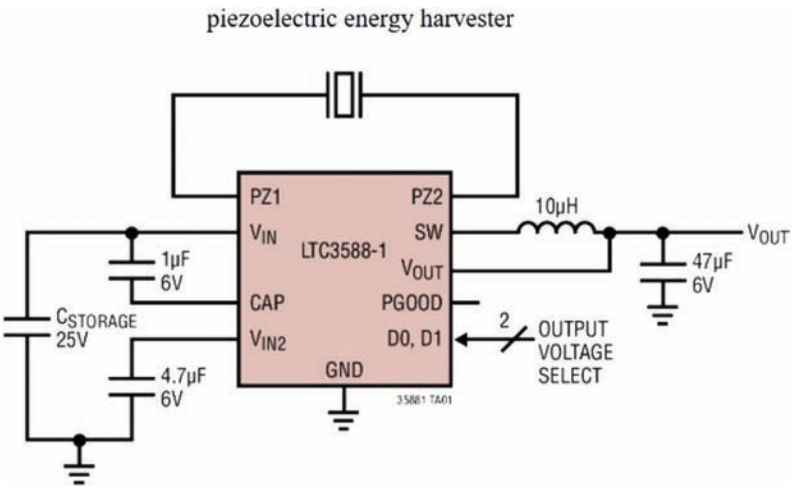

Figure 5.3 Collection and conditioning IC #LTC3588-1 for use in a piezoelectric energy harvester with generated AC electrical energy. (Reprinted with permission from Ref. 6.)

Downloaded From: https://www.spiedigitallibrary.org/ebooks/ on 07 Mar 2022
Terms of Use: https://www.spiedigitallibrary.org/terms-of-use

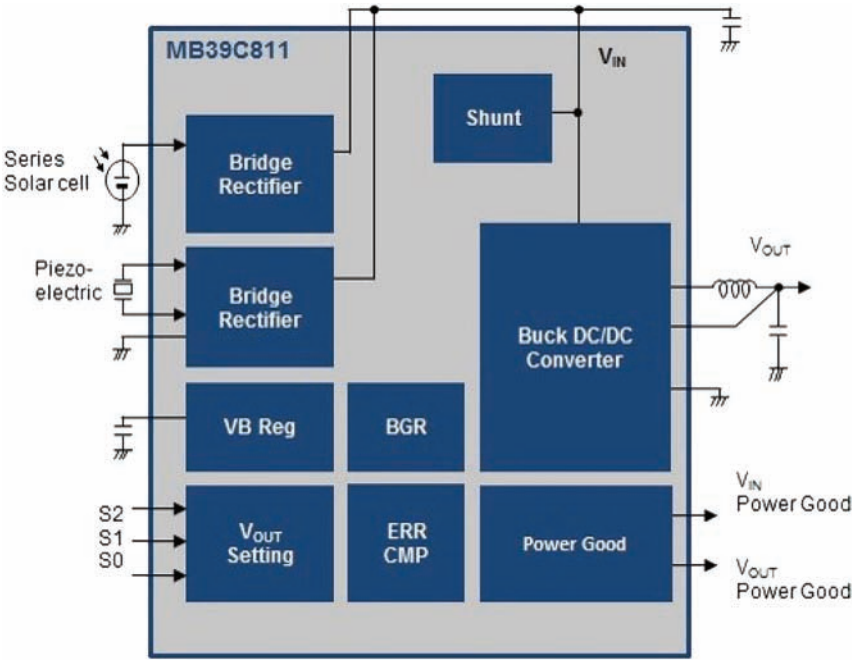

Figure 5.4 Collection and conditioning Cypress Semiconductor Corp.'s IC MB39C811 for piezoelectric energy harvesters and solar cells.[7]

Other semiconductor manufacturers have similar ICs for providing electrical energy collection and conditioning in energy harvesters. For example, Cypress Semiconductor Corp.'s MB39C811 (Fig. 5.4)[7] has a single IC solution for use with either a piezoelectric or a solar harvester. The IC contains a simple bridge rectifier and DC/DC regulation. The reader is cautioned that as discussed in Chapter 4, the ICs of Figs. 5.3 and 5.4 do not provide the maximum generated-to-harvested electrical energy efficiency. However, these circuits are very simple to use and are applicable when the amount of electrical energy that is needed by the load is significantly less than the amount of energy that the host system can provide. Detailed discussion is provided in Chapter 4.

5.3 Tire Pressure Monitoring System

Tire pressure monitoring systems were first employed by European manufacturers in the late 1980s. Subsequent to hundreds of fatalities related to vehicle roll-over as a result of tread separation, the U.S. Congress passed legislation known as the Transportation Recall Enhancement, Accountability and Documentation Act (TREAD Act) in November 2000.[8] The "Early Warning" reporting of low tire pressure is the central mandate of the Act. Vehicles manufactured after 2007 are equipped with wireless tire pressure

Downloaded From: https://www.spiedigitallibrary.org/ebooks/ on 07 Mar 2022
Terms of Use: https://www.spiedigitallibrary.org/terms-of-use

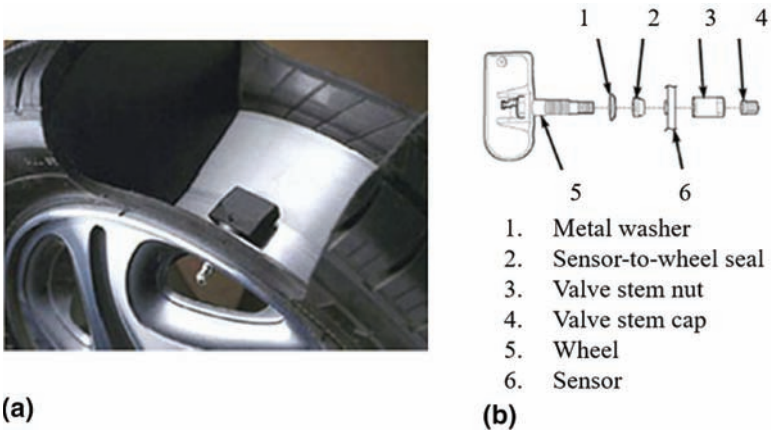

Figure 5.5 Example of a wireless TPMS: (a) mounted inside the tire and (b) components of the TPMS. (Reprinted with permission from Ref. 9.)

monitoring systems that are an integral part of the valve in each tire. Since the TREAD Act legislation, there has been a proliferation of the wireless tire pressure monitoring systems (TPMSs) for retrofitting to pre-2007 vehicles.

Figure 5.5 illustrates an example of a typical wireless TPMS used in automobiles to monitor the air pressure inside pneumatic tires.[9] The system comprises a direct air pressure sensor with the necessary electronics and transmitter mounted inside the tire, while the receiver unit is in the car. The system provides real-time status of individual tires while the vehicle is in motion and alerts the driver when the pressure falls below a pre-determined safe level. The system is powered by lithium ion batteries with a design life of 7 to 10 years.

While existing systems have been effective, a consensus among automobile manufacturers to replace the battery by a perpetual energy source has been a driving force in the development of energy-harvesting solutions that harvest mechanical energy from the rotating wheel or road vibrations.[10–12]

No commercial battery-less TPMS solutions are currently on the market. However, several companies have ongoing efforts that are closer to reaching the market. These include Honeywell (Weybridge, UK), Michelin (Greenville, South Carolina, USA), Visityre (East Killara, Australia), ASTRI (Hong Kong), Perilli (Milan, Italy), Goodyear Tire and Rubber Co. (Akron, Ohio, USA), and Siemens VDO (Regensburg, Germany). These ongoing efforts include energy harvesting based on piezoelectric and electromagnetic transducers, and the details of the systems are proprietary.

While there are many potential sources of energy that can be harvested from a vehicle in motion, for the TPMS, it is generally desired that the energy harvester be an integral part of the air valve or at least be located in the interior region of the tire. Thus, the effects of vehicle acceleration and deceleration, as well as road-induced and other sources of vehicle vibration are excluded as sources of mechanical energy for harvesting.[9,13–15]

Downloaded From: https://www.spiedigitallibrary.org/ebooks/ on 07 Mar 2022
Terms of Use: https://www.spiedigitallibrary.org/terms-of-use

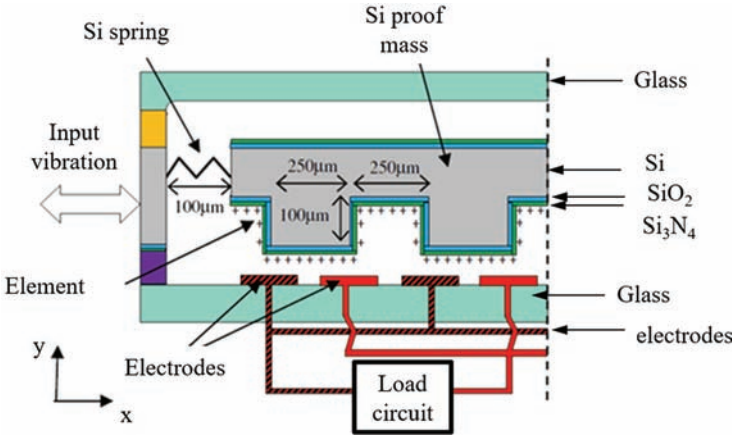

Figure 5.6 Schematic of the proposed MEMs electrostatic energy harvester being developed for TPMS. (Reprinted with permission from Ref. 16.)

Due to the potentially large market generated by mandated regulations, several developments are under way in search for a commercially viable TPMS that uses energy harvesters as its power source. One such solution (Fig. 5.6), a MEMS energy harvester using an electret-based electrostatic transducer, is reported to generate up to 50 μW of electrical power under normal road conditions.[16] As illustrated in the figure, the device consists of a central wafer that is a mechanical resonator made of a proof mass and springs etched into silicon. A corrugated electret, which is obtained by corona charging a SiO_2/Si_3N_4 stack, is supported by the proof mass. The bottom wafer is made of glass and has two metallic electrodes connected to a load. The top glass allows hermetic sealing of the device.

This particular arrangement of electret/electrode is referred to as slit or slot effect. In this configuration, both electrodes are attached to the "stator," while the electret is attached to the "rotor." Operation of these types of electrostatic energy harvesters is described in Chapter 2. For a detailed description of this particular device, see Ref. 16. Another solution uses an electromagnetic transducer to harvest the kinetic energy of the rotating tire.[17]

5.4 Self-Powered Wireless Sensors

A typical self-powered wireless sensor (SPWS) comprises an energy-harvesting module; sensors for measuring (for example) temperature, pressure, and acceleration; and a wireless communication capability to connect to a monitoring station or to another SPWS. These sensors can be deployed rapidly on existing infrastructure and can remain functional almost indefinitely. A SPWS can provide vital asset-monitoring capability to operators of large industrials plants, transportation systems, and many other similar applications requiring remote sensing, monitoring, and emergency-event-detection and

Downloaded From: https://www.spiedigitallibrary.org/ebooks/ on 07 Mar 2022
Terms of Use: https://www.spiedigitallibrary.org/terms-of-use

warning systems. Its real value is realized in applications where wired sensors are not practical and where battery replacement is not an option or is costly. In those scenarios, a SPWS can reduce operational costs for large industrial concerns by providing event-driven alerts and by monitoring the health of critical components that can be serviced prior to catastrophic breakdown.

SPWSs are under development both in academic institutions[18–21] as well as in the commercial sector.[6,7,22] One such SPWS that incorporates the Perpetuum PMG/C energy harvester has been deployed on the wheels of trains [Fig. 5.2(c)] operated by the Southeastern Railway of the United Kingdom.[5] The SPWS provides real time monitoring to the health of the asset to its operator. In particular, the SPWS reports on the vibrational activity of the wheel and the bearing as well as that of the track. Among several other deployments, Fig. 5.7 shows the SPWS mounted on large industrial machinery.[23]

Figure 5.8 shows another example of a SPWS: a MEMS-based vibrational energy harvesting micro-power generator (MPG).[24] These generators use

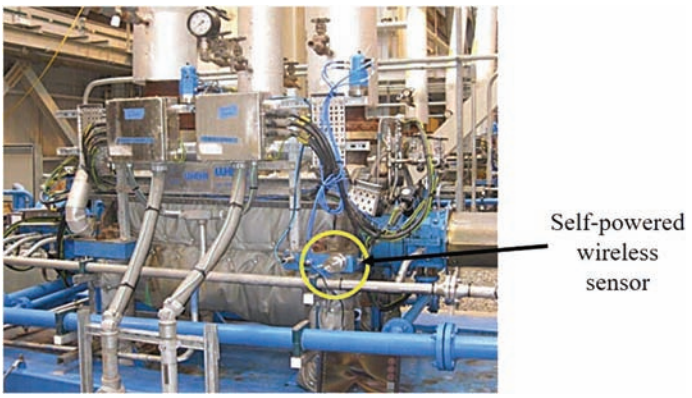

Figure 5.7 Self-powered wireless sensor mounted on power plant machinery. (Reprinted with permission from Ref. 23.)

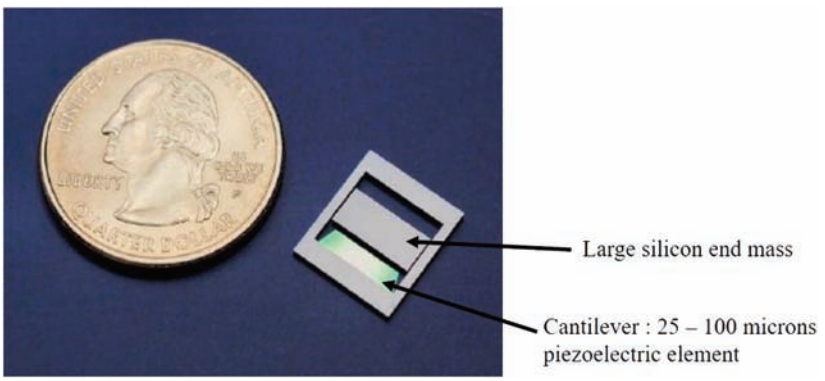

Figure 5.8 Piezoelectric MEMS vibration energy harvester. (Reprinted with permission from Ref. 24.)

Downloaded From: https://www.spiedigitallibrary.org/ebooks/ on 07 Mar 2022
Terms of Use: https://www.spiedigitallibrary.org/terms-of-use

MEMS technology to implement a cantilevered vibration harvesting generator (Fig. 5.8). Operation of such energy harvesters is based on the assumption of continuous oscillation at the resonant frequency. The generated electrical energy is regulated and stored in a super-capacitor. The semiconductor manufacturer Linear Technology Corp. has incorporated these energy harvesters into the DC9003A-B Smart-Mesh™ wireless mote for constructing self-powered remote sensors with built-in networking capability.[25]

5.5 Piezoelectric Energy-Harvesting Power Sources for Gun-Fired Munitions and Similar Applications

Piezoelectric-based energy-harvesting power sources have been developed for gun-fired munitions and other similar applications.[26–36] Energy-harvesting devices for gun-fired munitions in which the piezoelectric transducer is also used for firing or impact acceleration event detection are described in Refs. 37–45. Self-powered electrical initiation devices for thermal reserve batteries and the like with event-detection and safety electronic and logic circuitry that use piezoelectric transducers to harvest energy from a firing acceleration event are described in Refs. 46–54. These piezoelectric-based self-powered devices may also be used as stand-alone firing or impact-event-detection sensors.

Piezoelectric-based energy harvesters with stored potential energy have also been used to develop reserve-type power sources that are activated by various events such as impact and are described in more detail in Section 3.2.5.[55]

For munitions applications, the developed power sources are designed to harvest mechanical energy primarily from the firing acceleration, but may also be designed to harvest mechanical energy from in-flight vibration and oscillatory motions, and convert it to electrical energy.

One class of such energy-harvesting devices may be represented by the schematic of Fig. 3.13. The device uses a mass–spring type of interfacing mechanism and is aligned with the direction of munitions firing. During the munitions firing, the mass–spring element reacts to the firing (setback) acceleration, deforming and storing mechanical energy primarily in the form of potential energy. After the projectile exits the muzzle, the mass–spring element is free to vibrate, and the energy of vibration is harvested using piezoelectric transducers. The energy-harvesting device may similarly be used to generate electrical energy upon target impact.

Such piezoelectric-based energy-harvesting devices have been shown to produce enough electrical energy for many applications (such as for certain fuzing) and may be able to eliminate the need for chemical batteries in some applications. When employed in fuzing applications, the developed power sources have the added advantage of providing augmented safety, since the fuzing electronics are powered only after the projectile has exited the muzzle and has traveled a safe distance from the weapon platform. In addition, the

Downloaded From: https://www.spiedigitallibrary.org/ebooks/ on 07 Mar 2022
Terms of Use: https://www.spiedigitallibrary.org/terms-of-use

piezoelectric output can be used as the means of detecting firing, muzzle exit and target impact events, and the corresponding acceleration and deceleration magnitude profiles.

Energy-harvesting devices using mass–spring interfacing mechanisms to store mechanical energy from short-duration acceleration and deceleration pulses such as those shown schematically in Fig. 3.13 are described in Section 3.2.5. This section describes two design variations of such energy-harvesting devices for use in munitions, including methods of hardening the power sources for high-G firing accelerations primarily to protect the piezoelectric element. One of the described designs is modular in the sense that its mass–spring element can be readily changed to vary its natural frequency (i.e., the rate at which it produces power) and the total mechanical energy that it can store when subjected to a certain firing acceleration level. Several of such piezoelectric-based energy harvesters have been prototyped and tested in the laboratory by air gun firing, and test fired at over 45,000 Gs.

In almost all devices for mounting in gun-fired munitions, one of the main problems facing the designer is the high and very rapidly varying acceleration and deceleration that such devices are subjected to during the firing process. The solid model of one high-G-resistant piezoelectric-based energy-harvesting device with a cut-away to show the various elements of the unit is shown in Fig. 5.9. The energy harvester is designed to be mounted into the projectile such that the firing acceleration is in the longitudinal (upward) direction. This design is particularly resistant to high-G firing accelerations since the piezoelectric element is positioned such that the firing acceleration does not cause loading of the element by the mass–spring assembly of the generator. This design can be considered to be modular in the sense that it can be

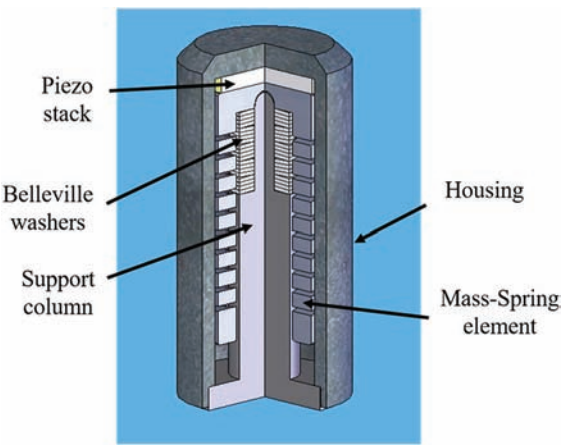

Figure 5.9 The solid model of a high-G-hardened piezoelectric-based energy-harvesting device for munitions applications.[45]

Downloaded From: https://www.spiedigitallibrary.org/ebooks/ on 07 Mar 2022
Terms of Use: https://www.spiedigitallibrary.org/terms-of-use

assembled with a wide range of mass–spring units and piezoelectric element preloads to match the requirements of the munitions powering.

As shown in Fig. 5.9, each device consists of a mass–spring element that rests against the piezoelectric stack positioned inside the device housing. A set of Belleville washers provides a preloading force, pressing the base of the mass–spring element against the piezoelectric stack. The preloading is achieved by the support column, which also serves as the means of positioning the spring centered inside the housing. This energy-harvesting device has been shown in finite element simulations to be capable of withstanding firing accelerations on the order of 100,000 Gs. The piezoelectric stack is attached to the housing with epoxy. During the firing, the firing acceleration causes the mass–spring element to elongate, thereby storing the desired amount of potential energy in the spring. The gap provided between the bottom surface of the mass–spring element and the support column base serves to limit the amount of elongation of the spring. The spring element is constructed with three helical strands so that during vibration, the mass–spring element undergoes minimal lateral displacement.

The fabricated prototype of the energy-harvesting device of Fig. 5.9 is 20 mm in diameter and 45 mm in length. The spring rate is $k = 168 \times 10^3$ N/m with an equivalent mass of about $m = 7.6 \times 10^{-3}$ kg, yielding a natural frequency of approximately 750 Hz. The spring is designed such that a firing acceleration of about 18,000 Gs would fully extend the end of the spring to the bottom of the assembly. The spring stores about 2 J of potential energy for conversion into electrical energy.

The assembly drawing and cross-sectional view of another developed piezoelectric-based energy-harvesting device for munitions applications is shown in Fig. 5.10. This design is also modular in the sense that the piezoelectric element is packaged as one unit to which various mass–spring elements can be attached to match the application power requirements. The

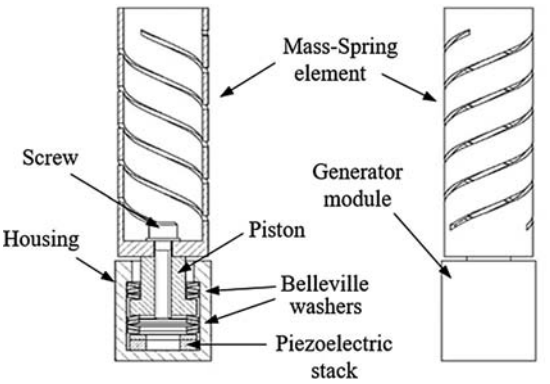

Figure 5.10 Drawing of a modular high-G-hardened piezoelectric-based energy-harvesting device for munitions applications.[56]

Downloaded From: https://www.spiedigitallibrary.org/ebooks/ on 07 Mar 2022
Terms of Use: https://www.spiedigitallibrary.org/terms-of-use

harvesters are designed to be mounted in the projectile aligned with the direction of firing acceleration.

Each generator consists of a mass–spring element (module) that is fastened to the generator module by a screw. The generator module is designed to withstand very high firing (setback) accelerations and set-forward decelerations. The generator module has a housing inside to which the piezoelectric stack is attached with epoxy. A load-distributing flat ground washer is attached to the top surface of the piezoelectric stack, over which Belleville washers are positioned. The piston head is positioned between the aforementioned set of Belleville washers and another set of upper Belleville washers. During assembly, the Belleville washers are compressed to preload the piezoelectric stack in compression and are locked in place by a retaining ring (to simplify the drawing in Fig. 5.10, the retaining ring is shown as a step inside the housing). For very high-G applications, a cylindrical spacer is placed around the piston to fill the gap between the retaining ring and the cylinder to prevent the retaining ring from being released during the firing. The gap between the mass–spring element and the top surface of the housing is provided to limit the maximum compressive force on the piezoelectric stack. The retaining ring in turn limits the maximum upward movement of the piston, thereby preventing loss of contact with the piezoelectric stack.

A number of the aforementioned designs of high-G-hardened piezoelectric-based energy-harvesting power sources have been prototyped and successfully tested for survivability in shock-loading machines, air gun firing, and actual munitions firing at up to 45,000 Gs. High-strength aluminum and stainless steel are primarily used to construct the mass–spring units. The basic design rules include keeping the frequency of the natural mode of vibration of the mass–spring unit as low as possible, preferably less than 300 Hz, since at higher frequencies the amount of stored mechanical energy that is lost due to internal damping of the spring material becomes increasingly large and quickly passes 50–75% levels. The efficiency of converting the stored mechanical energy to electrical energy can then rapidly drop to 5–10% or less. The amount of electrical energy that such energy-harvesting devices can produce is obviously dependent on the size of the device, the firing shock acceleration level, and the amount of oscillatory motions during the flight. As an example and just from the indicated size and firing acceleration levels for the harvester shown in Fig. 5.9, harvested electrical energy levels in the range of 20–50 mJ have been shown to be possible.

5.6 Self-Powered Shock-Loading-Event Detection with Safety Logic Circuit and Applications

Piezoelectric generators that are self-powered for one shot and have shock-loading-event detection and integrated safety logic for initiation and switching

Downloaded From: https://www.spiedigitallibrary.org/ebooks/ on 07 Mar 2022
Terms of Use: https://www.spiedigitallibrary.org/terms-of-use

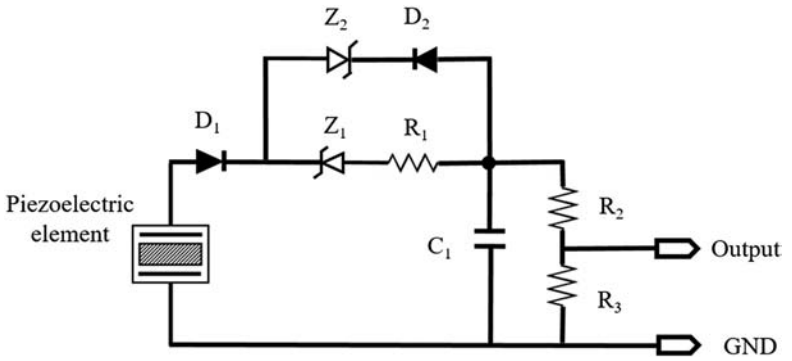

Figure 5.11 The basic safety and shock-loading-event-detection portion of the self-powered circuit of Fig. 4.17 (GND is ground).

in munitions are presented in Refs. 27, 37, 47, 57, and 58. Figure 4.17 shows the schematic of such a passive CC circuit for shock-loading event detection with safety logic and direct transfer of the generated electrical energy to the load. The circuit operation is described in Section 4.3.5.1.

The piezoelectric-based, self-powered circuit of Fig. 4.17 functions as a shock-loading-event detection sensor, the output of which is typically a voltage signal that can be either used to initiate direct transfer of the generated electrical energy to the load, or be the input to a passive or active logic circuitry that controls the flow of the generated electrical energy. Two such applications are described in this section.

The basic safety and all-fire detection portion of the circuit of Fig. 4.17 is shown in Fig. 5.11 with the addition of a Zener diode Z_2. In certain applications, as when the piezoelectric voltage drops, the amount of discharge through diode D_2 needs to be limited to a certain voltage threshold. The voltage threshold may be required, for example, to prevent the voltage at the circuit output from dropping below a certain limit. This goal can be readily achieved by, for example, the addition of a Zener diode Z_2 between diodes D_1 and D_2 as shown in Fig 5.11. As a result, when the piezoelectric voltage drops, the charge accumulated in capacitor C_1 is discharged through diode D_2, but only to the breakdown voltage level of diode Z_2 instead of dropping to essentially the voltage level of the piezoelectric element. Integrated event-detection and energy-harvesting devices using electromagnetic transducers have also been developed and are described in Refs. 59 and 60.

5.6.1 Self-powered shock-loading-event-detection and initiation device

The safety and all-fire detection circuitry of Fig. 5.11 is an essential front-end for constructing passive initiators for pyrotechnic materials as shown in Fig. 5.12. In such a device, when the prescribed all-fire voltage threshold is

Downloaded From: https://www.spiedigitallibrary.org/ebooks/ on 07 Mar 2022
Terms of Use: https://www.spiedigitallibrary.org/terms-of-use

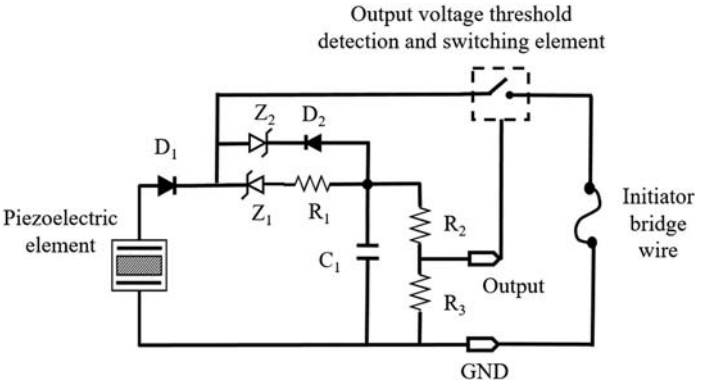

Figure 5.12 The circuit diagram of a piezoelectric-based, self-powered electrical initiator with safety and all-fire detection logic.

detected, the output-voltage-threshold-detection-and-switching element would close the indicated circuit and allow for direct flow of current from the piezoelectric element through the initiator bridge wire to the ground. The initiator bridge wire (usually around 1–3 Ω) is then heated by the passing current and ignites the pyrotechnic material. Initiator bridge wires of different types and different primary pyrotechnic materials may be used.

The output-voltage-threshold-detection-and-switching element may be designed in a number of ways. In the munitions applications, however, one of the main objectives is safety, i.e., the elimination of any chances that initiation occurs in the absence of all-fire detection. Other objectives in munitions applications include: passive circuitry, i.e., the initiator circuitry not requiring external power; and miniaturization, which requires very low-power circuitry that can be powered with very small piezoelectric elements. Some of these designs, while being passive, can include additional logic circuitry for munitions or the like applications and are described in Ref. 37.

In the passive initiator of Fig. 5.13, the safety and all-fire detection circuitry is provided with the output-voltage-threshold-detection-and-switching element designed with a circuitry shown in a box drawn with dashed lines. In the circuitry of Fig. 5.13, by proper selection of its component parameters, when the voltage at the OUTPUT of the safety and all-fire detection circuitry reaches the prescribed all-fire threshold, the N-MOS (Q_1) is switched on. During this switching-on process, the voltage on resistor R_4 increases and produces a current on an NPN transistor (Q_3) in the direction of the arrow at B. NPN transistor Q_3 amplifies the current and introduces the current on a PNP transistor Q_2, while the PNP transistor Q_2 amplifies the said current and sends it back to NPN transistor Q_3. This positive-feedback configuration of transistors Q_2 and Q_3 saturates the two transistors, making them act as a "switch" that has been closed between the nodes N_1 and N_2 in the circuit, thereby allowing the charges generated by the piezoelectric element

Downloaded From: https://www.spiedigitallibrary.org/ebooks/ on 07 Mar 2022
Terms of Use: https://www.spiedigitallibrary.org/terms-of-use

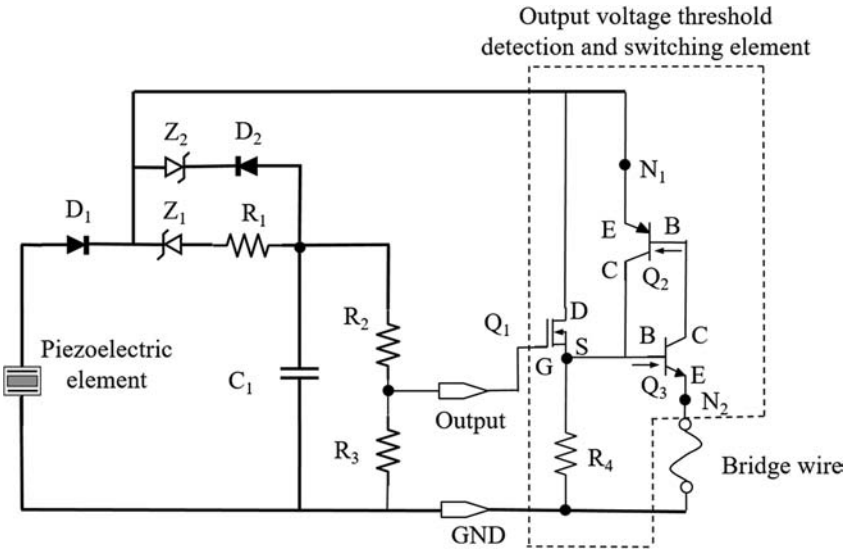

Figure 5.13 The self-powered initiation device with all-fire-event-detection and safety logic circuit.

to be discharged through the indicated bridge wire to the ground. The very low-resistance initiator bridge wire is then heated by the passing current, which then ignites the provided pyrotechnic material.

It should be noted that once the conduction path from the piezoelectric element through the bridge wire is established, transistors Q2 and Q3 remain latched in the saturated state (ON) until the bridge wire has been completely expended. However, in the absence of the latching action of Q2 and Q3, the conduction path from the piezoelectric element, through the bridge wire to the ground, is not sustainable, as the detected all-fire signal voltage at the "output" node drops below the threshold voltage, thereby shutting down transistor Q1. While the switching action of Q1 alone could be used to provide a current path through the bridge wire, the utilization of transistors Q2 and Q3 ensures 100% device initiation upon detection of the all-fire signal.

5.6.2 Shock-loading-event-detection switching applications

This section describes the design of a shock-loading-event-detection switching device that uses a self-powered event-detection sensor with the integrated safety logic circuit of Fig. 5.11. Here, the detection of shock loading is selected as a typical application for describing such event-detection devices. The shock-loading event may be induced by, for example, munitions firing setback, set-forward acceleration pulse, or impact. As can be seen, the present event-detection devices may be used for detecting one or more shock-loading events as well as the level of each experienced shock loading as a function of time.

Downloaded From: https://www.spiedigitallibrary.org/ebooks/ on 07 Mar 2022
Terms of Use: https://www.spiedigitallibrary.org/terms-of-use

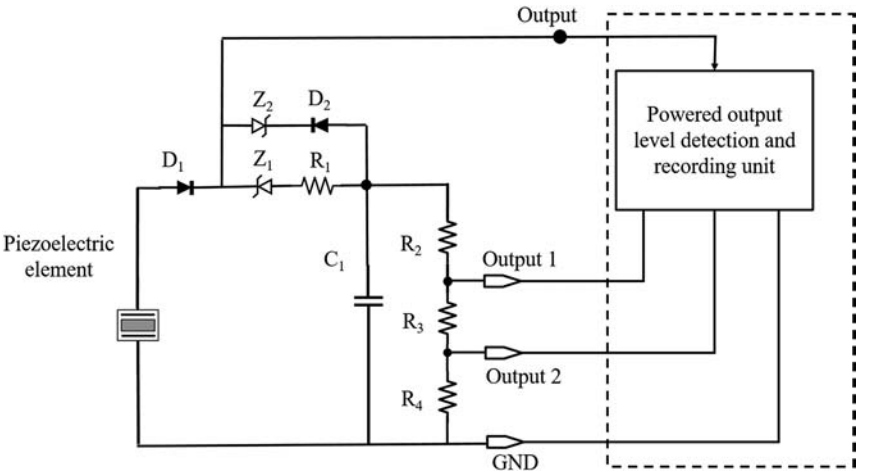

Figure 5.14 The self-powered shock loading sensor for detection and recording of one or more events.

The basic method for implementing the present self-powered event-detection sensor is described using the schematic of Fig. 5.14. In Fig. 5.14, the shock-loading-event-detection sensor circuitry portion of the sensor is shown enclosed by dashed lines. In this method, the safety and shock-loading-event-detection circuitry of Fig. 5.11 is used to detect the shock-loading events, and a powered output-level-detection-and-recording unit records the level and time history of the detected shock loadings. The shock-loading sensor of Fig. 5.14 can be used to detect one or more of such events while rejecting all aforementioned non-event loadings. The shock-loading events are detected as described for the initiator device of Fig. 5.12 by the voltage level of capacitor C_1. The circuitry similarly prevents the charging of the capacitor C_1 to the prescribed voltage levels if the generated piezoelectric charges are due to the aforementioned non-event conditions. Once a shock-loading condition is detected, the provided powered output-level-detection-and-recording-unit of the sensor can record or register the event as a function of time.

In Fig. 5.14, the safety and event-detection circuitry portion of the sensor is shown to be provided with two voltage detection levels: OUTPUT1 and OUTPUT2. By using such multiple output-voltage detection levels, the shock-loading profile can be detected as a function of time with the desired accuracy. It is also appreciated that the circuitry output(s) may be similarly used to provide logic signal flags when the intended shock-loading-event levels and durations are encountered. As such, the described logic signal flags require minimal detection electronics and computational capability, and can also function as switches that can be triggered by the detection of the prescribed shock-loading event. It is also appreciated that the output voltage of the safety and event-detection device of Fig. 5.14 may be monitored directly by

Downloaded From: https://www.spiedigitallibrary.org/ebooks/ on 07 Mar 2022
Terms of Use: https://www.spiedigitallibrary.org/terms-of-use

externally powered electronics and possibly certain processing units for various purposes, such as for certain switching or event triggering.

References

1. http://www.velogical-engineering.com/rim-dynamo-en-1 (last accessed June 20, 2016).
2. https://www.americanpiezo.com/piezo-theory/generators.html (last accessed June 20, 2016).
3. http://www.mide.com/collections/vibration-energy-harvesting-with-protected-piezos (last accessed June 20, 2016).
4. http://www.perpetuum.com/ (last accessed June 20, 2016).
5. http://www.perpetuum.com/rail/ (last accessed June 20, 2016).
6. http://www.linear.com/solutions/1221 (last accessed June 20, 2016).
7. http://www.cypress.com/ (MB39C811, last accessed June 20, 2016).
8. http://www.nhtsa.gov/cars/rules/rulings/TPMSfinalrule.6/TPMSfinalrule.6.html (last accessed Nov 28, 2015).
9. Y. J. Wang, S. H. Chen, and C. D. Chen, "Wideband electromagnetic energy harvesting from a rotating wheel," in *Small-Scale Energy Harvesting*, M. Lallart, Ed., InTech Open Access Publisher, Rijeka, Croatia, Chapter 7 (2012).
10. E. S. Leland, C. T. Sherman, P. Minor, and P. K. Wright, "A new mems sensor for ac electric current," *IEEE Sensors Conference*, 1177–1182 (2010).
11. R. Matsuzakim and A. Todoroki, "Wireless monitoring of automobile tires for intelligent tires," *Sensors* **8**, 8123–8138 (2008).
12. S. Roundy, "Energy harvesting for tire pressure monitoring systems: design considerations," *Technical Digest Power*, Sendai, Japan, 1–6 (2008).
13. APOLLO, "Final Report: Intelligent tyre for accident-free traffic," *Technical Research Center of Finland* (VTT), Tampere, Finland, 2001–2343 (2005).
14. D. A. V. D. Ende, H. J. V. D. Wiel, W. A. Groen, and S. V. D. Zwag, "Direct strain energy harvesting in automobile tires using piezoelectric PZT-polymer composites," *Smart Materials Structures* **21**, 1–11 (2011).
15. N. Makki, "Piezoelectric power generation in automotive tires," *Proc. Smart Material and Structures/NDT in Aerospace*, Montreal, Canada (2011).
16. M. Renaud, G. Altena, M. Goedbloed, C. de Nooiher, S. Matova, Y. Naito, T. Yamakawa, H. Takeuchi, K. Omishi, and R. van Schaijk, "A high performance electrostatic MEMS vibration energy harvester with corrugated inorganic SiO_2-Si_3N_4 electret," *IEEE Conference*, 693–696 (2013).
17. Y. J. Wang, C. D. Chen, and C. K. Sung, "System design of a weighted-pendulum-type electromagnetic generator for harvesting energy from a rotating wheel," *IEEE/ASME Transactions on Mechatronics* **18**(2), 754–762 (2013).

Downloaded From: https://www.spiedigitallibrary.org/ebooks/ on 07 Mar 2022
Terms of Use: https://www.spiedigitallibrary.org/terms-of-use

18. E. E. Aktakka and K. Najafi, "A micro inertial energy harvesting platform with self-supplied power management circuit for autonomous wireless sensor nodes," *IEEE Solid-State Circuits* **49**(9), 2017–2029 (2014).
19. D. Clayton, H. A. Andrews, Jr., and R. Lenarduzzi, "Power harvesting practices and technology gaps for sensor networks," Oak Ridge National Laboratory, ORNL/TM-2012/442, September (2012).
20. E. Mournier, "MEMS market and applications," *dMEMS* 2012, Besancon, France (2012).
21. G. Zhou, L. Huang, W. Li, and Z. Zhu, "Harvesting ambient environmental energy for wireless sensor networks: A survey," *Journal of Sensors*, 1–20 (2014).
22. http://omnitekpartners.com/ (last accessed June 20, 2016).
23. http://www.perpetuum.com/appsaction.asp/ (last accessed June 20, 2016).
24. https://www.microgensystems.com/content/MicroGen_BOLT-INDUSTRIAL_Jun2013.pdf (last accessed June 20, 2016).
25. http://www.linear.com/solutions/1837 (last accessed June 20, 2016).
26. J. Rastegar, "Energy harvesting from input impulse with motion doubling mechanism for generating power from mortar tube firing impulses and other inputs," U.S. Patent Number 8,912,710 (2014).
27. J. Rastegar, C. Pereira, M. Ervin, and D. Feng, "Piezoelectric-based electrical energy harvesting and storage methods and electronics for munitions," *Proc. SPIE* **9059**, 905909 (2014) [doi: 10.1117/12.2045257].
28. J. Rastegar and R. Murray, "Generators for very-high-G energy harvesting," U.S. Patent Number 8,525,392 (2013).
29. J. Rastegar, R. Murray, and M. Bridge, "Energy harvesting device for power generation onboard gravity-dropped weapons," *Proc. SPIE* **8341**, 83411C (2012) [doi: 10.1117/12.915404].
30. J. Rastegar, R. Murray, R. Tillinghast, C. Pereira, and H.-L. Nguyen, "Energy-harvesting from mortar tube firing impulse to supplement fire-control electronics battery," *Proc. SPIE* **7977**, 79770R (2011) [doi: 10.1117/12.880476].
31. J. Rastegar and R. Murray, "Development and commercialization strategy for piezoelectric energy-harvesting power sources for gun-fired munitions," *Proc. SPIE* **7645**, 764502 (2010) [doi: 10.1117/12.847759].
32. J. Rastegar, R. Murray, C. Pereira, and H.-L. Nguyen, "Energy-harvesting power sources for very-high-G gun-fired munitions," *Proc. SPIE* **7643**, 76430D (2010) [doi: 10.1117/12.847777].
33. J. Rastegar and T. Spinelli, "Piezoelectric generators for munitions fuzing and the like," U. S. Patent Number 7,701,120 (2010).
34. J. Rastegar, R. Murray, C. Pereira, and H.-L. Nguyen, "Novel piezoelectric-based energy-harvesting power sources for gun-fired munitions," *Proc. SPIE* **6527**, 65270Y (2007) [doi: 10.1117/12.715009].

Downloaded From: https://www.spiedigitallibrary.org/ebooks/ on 07 Mar 2022
Terms of Use: https://www.spiedigitallibrary.org/terms-of-use

35. J. Rastegar and D. Haarhoff, "Mass–spring unit for generating power by applying a cyclic force to a piezoelectric member due to an acceleration of the mass–spring unit," U.S. Patent Number (2007).
36. J. Rastegar and T. Spinelli, "Power supplies for projectiles and other devices," U.S. Patent Number 7,231,874 (2007).
37. J. Rastegar, D. Feng, and C. Pereira, "Piezoelectric energy-harvesting power source and event detection sensors for gun-fired munitions," *Proc. SPIE* **9493**, 94930H (2015) [doi: 10.1117/12.2176879].
38. J. Rastegar, R. Pereira, and C. Dratler, "Energy harvesting power sources for detecting target impact of a munition," U.S. Patent Number 8,701,559 (2014).
39. J. Rastegar and R. Murray, "Miniature safe and arm (S and A) mechanisms for fuzing of gravity dropped small weapons," U.S. Patent Number 8,701,558 (2014).
40. J. Rastegar, "Miniature safe and arm mechanisms for fuzing of gravity dropped small weapons," U.S. Patent Number 8,646,386 (2014).
41. J. Rastegar, R. Pereira, and C. Dratler, "Munition having detonation time-out circuitry," U.S. Patent Number 8,635,956 (2014).
42. J. Rastegar and T. Spinelli, "Methods and apparatus for integrated energy harvesting power sources and inertial sensors for gun-fired munitions," U.S. Patent Number 8,266,963 (2012).
43. J. Rastegar, "Methods and devices for enabling safe/arm functionality within gravity dropped small weapons resulting from a relative movement between the weapon and a rack mount," U.S. Patent Number 8,245,641 (2012).
44. J. Rastegar, C. Pereira, and R. Dratler, "Energy harvesting power sources for accidental drop detection and differentiation from firing," U.S. Patent Number 7,762,191 (2010).
45. J. Rastegar, R. Murray, C. Pereira, and H.-L. Nguyen, "Integrated event sensing and energy-harvesting power sources for gun-fired munitions," *Proc. SPIE* **7288**, 72880Z (2009) [doi: 10.1117/12.815513].
46. J. Rastegar and D. Feng, "Inertially operated electrical initiation devices," U.S. Patent Number 20,120,180,680 A1 (2015).
47. J. Rastegar, D. Feng, and C. Pereira, "Self-powered event detection sensors with integrated safety electronics for initiation and switching in munitions," *ASME 2014 Conference on Smart Materials, Adaptive Structures and Intelligent Systems* SMASIS2014-7693, V002T04A025, Newport, Rhode Island (2014).
48. J. Rastegar and D. Feng, "Inertially operated electrical initiation devices," U.S. Patent Number 9,021,955 (2015).
49. J. Rastegar, "Electrically initiated inertial igniters for thermal batteries and the like," U.S. Patent Number 8,776,688 (2014).

Downloaded From: https://www.spiedigitallibrary.org/ebooks/ on 07 Mar 2022
Terms of Use: https://www.spiedigitallibrary.org/terms-of-use

50. J. Rastegar, "Inertially operated electrical initiation devices," U.S. Patent Number 8,677,900 (2014).
51. J. Rastegar, "Inertially operated electrical initiation devices," U.S. Patent Number 8,601,949 (2013).
52. J. Rastegar, "Inertially operated electrical initiation methods," U.S. Patent Number 8,596,198 (2013).
53. J. Rastegar, "Electrically initiated inertial igniters for thermal batteries and the like," U.S. Patent Number 8,286,554 (2012).
54. J. Rastegar and T. Spinelli, "Electrically initiated inertial igniters for thermal batteries and the like," U.S. Patent Number 8,042,469 (2011).
55. J. Rastegar, "Methods and apparatus for mechanical reserve power sources for gun-fired munitions, mortars, and gravity dropped weapons," U.S. Patent Number 8,183,746 (2012).
56. J. Rastegar, D. Haarhoff, C. Pereira, and H.-L. Nguyen, "Piezoelectric-based energy harvesting power sources for gun-fired munitions," *Proc. SPIE* **6174**, 61740W (2006) [doi: 10.1117/12.657441].
57. J. Rastegar, D. Feng, and C. Pereira, "Efficient methods of harvesting energy from ultra-short duration shock loading," *ASME 2014 Conference on Smart Materials, Adaptive Structures and Intelligent Systems* SMASIS2014-7657, V002T07A020, Newport, Rhode Island (2014).
58. J. Rastegar, D. Feng, and C. Pereira, "Piezoelectric-based event sensing and energy-harvesting power sources for thermal battery initiation in gun-fired munitions," *Proc. SPIE* **9115**, 911509 (2014) [doi: 10.1117/12.2053205].
59. J. Rastegar and R. Murray, "Dynamo-type lanyard operated event detection and power generators," U.S. Patent Number 9,112,390 (2015).
60. J. Rastegar and R. Murray, "Miniature safe and arm (S and A) mechanisms for fuzing of gravity dropped small weapons," U.S. Patent Number 8,443,726 (2013).

Downloaded From: https://www.spiedigitallibrary.org/ebooks/ on 07 Mar 2022
Terms of Use: https://www.spiedigitallibrary.org/terms-of-use

Index

Downloaded From: https://www.spiedigitallibrary.org/ebooks/ on 07 Mar 2022
Terms of Use: https://www.spiedigitallibrary.org/terms-of-use

Downloaded From: https://www.spiedigitallibrary.org/ebooks/ on 07 Mar 2022
Terms of Use: https://www.spiedigitallibrary.org/terms-of-use

Downloaded From: https://www.spiedigitallibrary.org/ebooks/ on 07 Mar 2022
Terms of Use: https://www.spiedigitallibrary.org/terms-of-use

Downloaded From: https://www.spiedigitallibrary.org/ebooks/ on 07 Mar 2022
Terms of Use: https://www.spiedigitallibrary.org/terms-of-use

Downloaded From: https://www.spiedigitallibrary.org/ebooks/ on 07 Mar 2022
Terms of Use: https://www.spiedigitallibrary.org/terms-of-use

Downloaded From: https://www.spiedigitallibrary.org/ebooks/ on 07 Mar 2022
Terms of Use: https://www.spiedigitallibrary.org/terms-of-use

Downloaded From: https://www.spiedigitallibrary.org/ebooks/ on 07 Mar 2022
Terms of Use: https://www.spiedigitallibrary.org/terms-of-use

Dr. J. Rastegar received his B.S. from SMU in 1969 and his M.S. and Ph.D. Degrees from the Mechanical Engineering Department of Stanford University in 1972 and 1977. He then joined the General Engineering and Bioengineering faculty at the University of Illinois at Urbana-Champaign, and after several years of work in the industry, he joined the Mechanical Engineering Department at Stony Brook University in 1987. He has published over 240 journal and conference articles. He holds 194 issued and over 90 pending U. S. patents in the fields of sensors; actuation devices; medical systems and devices; safety and accident prevention devices; power sources and components; mechanical tools, devices, and structural elements; military products and components; and optical and electronic devices. He served as Associate Editor of ASME Journal of Mechanical Design and Journal of Medical Devices. He is a Fellow of the American Society of Mechanical Engineers (ASME) and recipient of its "2010 Machine Design Award" for "eminent achievements as an inventor and scholar in the field of machine design, particularly in the area of smart actuation and control." He is a fellow of the National Academy of Inventors.

Dr. Harbans Dhadwal received his B.Sc. and Ph.D. degrees from the Electrical Engineering Department of Queen Mary College of the University of London in 1976 and 1980. He then took the position of Higher Science Officer at the Royal Aircraft Establishment in Farnborough, England. In 1982 he took a post-doctoral position in the Department of Chemistry at Stony Brook University, and in 1984 he joined the faculty in the Electrical and Computer Engineering Department. He has had visiting appointments at IBM Thomas Watson Research Center in New York and at the NASA Glen Research Center. He has published over 100 journal and conference articles, and holds 13 U.S. patents. His research has spanned multidisciplinary fields of electronics, polymer physics, and marine sciences through the use integrated fiber optics, optoelectronics, photon correlation spectroscopy, fluorescence spectroscopy, light scattering and RF sensor systems. He is a senior member of the Institute of Electrical and Electronics Engineers (IEEE), and a member of the Optical Society of America and SPIE.

Downloaded From: https://www.spiedigitallibrary.org/ebooks/ on 07 Mar 2022
Terms of Use: https://www.spiedigitallibrary.org/terms-of-use